SOLAR INDUCED VENTILATION IN THE ALGERIAN AND SIMILAR CLIMATES

by

Ammar BOUCHAIR

Submitted in Accordance With the Requirements
for the degree of
Doctor of Philosophy (Ph.D)

Department of Civil Engineering
The University of Leeds
October 1989.

ABSTRACT

In hot climates ventilation can be a useful means of cooling dwellings, if the outside air be cooler than that inside the dwelling. Often, in hot regions the outside air is so hot during the day that cooling by ventilation is of no benefit until the evening when the outside air gets cooler. Ventilation can then be beneficial, and can be promoted by a sun-warmed cavity or 'solar chimney' added to a building on the sunward side. The cavity may be of any material of high thermal capacity. Heat from the sun is stored within the walls forming the cavity and heats the air within. The cavity is closed at the top and bottom by dampers. These, when opened in the evening, allow the buoyant hot air contained within to rise, drawing cooler outside air into the building. This process continues until the stored energy is consumed.

The performance of a typical cavity to induce ventilation into a house is studied experimentally and theoretically. The measurements are made on a full-scale model in the steady state. Cavity width and air inlet area to the cavity are important parameters in this study. Measurements are made on the temperature and velocity of the air. Observations on air flow patterns in the room and the cavity are made. A steady state analysis is compared with the measurements. A dynamic model is developed based on a finite difference technique, and used to examine the performance of the cavity in various circumstances.

The results show that air movement can be produced by a sun-warmed cavity if the dimensions of inlet and cavity width are kept at certain values.

TABLE OF CONTENTS

ACKNOWLEDGEMENTS

I would like to express my sincere gratitude to Dr. D. Fitzgerald and Dr W. Houghton Evans, for their supervision and help during the course of this work.

I extend my thanks to Dr J. A. Tinker for his comments and help.

I am grateful to the Algerian Government for financial support throughout this work.

I would like also to thank all member of staff who contributed to building my apparatus.

Finally, a very special thanks to my father Tahar, mother Fatma, all member of my familly and to my wife to whom I dedicate this work.

NOMENCLATURE

Symbol	Description	Units
A	area	m^2
b	boundary layer thickness	m
c	specific heat capacity	J/kgK
C_v	ventilation conductance	m^2K/W
D_h	hydraulic diameter	m
g	gravitational acceleration	$9.8m/s^2$
Gr	Grashof number	–
h_c	convection heat transfer coefficient	W/m^2K
h_r	radiation heat transfer coefficient	W/m^2K
M	mass flow rate	kg/s
N	Nusselt number	–
Q	heat loss	W
P	pressure	$Pascal$
Pr	Prandtl number	–
R	thermal resistance	m^2K/W
t	time	s
T	temperature	$°C$
x	distance from the wall	m
v	velocity	m/s
V	volume	m^3
W	cavity width	m
Y	cavity length	m

Z	height	m

Greek Symbols

β	volume coefficient of expansion of air	K^{-1}
ε	surface emissivity	–
ρ	density	kg/m^3
σ	Stefan-Boltzmann constant	$5.67 \times 10^{-8} W/m^{2o}K^4$
λ	thermal conductivity	W/mK
υ	air kinematic viscosity	$1.5 \times 10^{-5} m^2/s$
μ	air dynamic viscosity	$2 \times 10^{-5} kg/ms$
Δ	difference	–

Subscripts

a	air
ac	cavity air
ai	inlet air
ao	outside air
ar	room air
eo	outside environment
g	gas
gr	ground
out	outlet air
si	inside surface
sm	mean surface
so	outside surface
v	ventilation
s	surface
ve	vent
wm	middle of a wall
mr	mean radiant
res	resultant

CHAPTER ONE

INTRODUCTION

1.1 General

Thermal comfort in buildings is the most important factor for builders and designers to achieve. Unlike in cold climates such as Northern Europe, where heat conservation is most required to combat cold weather, in hot arid climates heat causes discomfort and cooling is the major need. In hot arid climates, day air temperatures often reach 45°C, while at night they may drop to 5°C. Humidity is low and there is little rain. The absence of cloud cover leads to intensive solar radiation, which heat up the surfaces to 70°C at midday, while at night the rapid loss of heat by longwave radiation can cool them to 15°C or less. The cool nights offer an opportunity to use cold air as a natural cooling source.

In warm climates, cooling a dwelling during summer may be achieved by cross ventilation through doors or windows because the outside air is not very hot. However, this cannot be the case for hot climates because the air outside is too hot for such use. In the evening and during the night, the temperature of the outside air drops, and thus it can be used for cooling ventilation. Golneshan and Yagoubi (1984) showed that encouraging night ventilation and discouraging it during the day, could be a useful way of achieving comfort in hot summers. A rate of 12 air changes per hour could be achieved by cross ventilation using wind towers. However, in urban areas air movement may be very restricted by building layout so that wind towers may be of benefit only if built high enough and this may be too expensive. Moreover, there are cases where the wind speed at night is very low, and thus cooling by ventilation is limited. It is of interest therefore to study ways in which night ventilation could be improved by simple and low cost means, by

taking advantage of day and night conditions as experienced in hot arid climates. The comfort temperature or 'Resultant Temperature' in a hot arid climate suggested by the CIBSE (1986) is of the order of 28 $°C$ with low air movement but Nicol (1975) has shown that thermal comfort can be achieved with warmer conditions if the air velocity is in the order of $0.25 m/s$. He observed in India and Baghdad, that 80% of people were comfortable at a resultant temperature up to 36 $°C$.

1.2 Climate of El-Oued

El-Oued is one of the hot places in Algeria and it is given here as an example. El-Oued, latitude 33°30'N, and longitude6°47'E, is in the SE of Algeria. It has hot summers and cold winters. The outside air temperature reaches its peak in July and its minimum in January. In June, July and August, the monthly mean outside air temperatures are, 29.7, 32.5 and 31.7°C respectively. In winter the air temperature is low. In December, January and February the mean temperatures are 11.3, 11.0 and 13.2°C respectively (figure 1.1). The hottest month is July, the maximum hourly air temperature being 40°C at 1500 hours falling to 25°C at about 0600 hours (figure 1.2).

Humidity is low in summer with a mean of 37 %, and high in winter with a mean of 65 %. Figure 1.3 shows the monthly means of relative humidity. Figure 1.4 shows the variation of mean hourly relative humidity against time for the summer months. It can be seen that the humidity rises to a maximum of about 55 % at 0600 hours with a minimum of about 18 % at 1500 hours.

The sky is almost clear. There is little rain and a high rate of evaporation.

In general, wind speeds are recorded at 10m height above the ground to avoid obstacles. In El-Oued the wind speed has an average of 4m/s in summer. It increases during the day and decreases at night as it is shown in figure 1.5. The wind speed values plotted on the graph are recorded at 10m height, and the CIBSE Guide suggests that they should be reduced to take account of the type of terrain and the location. At 1m height, in urban

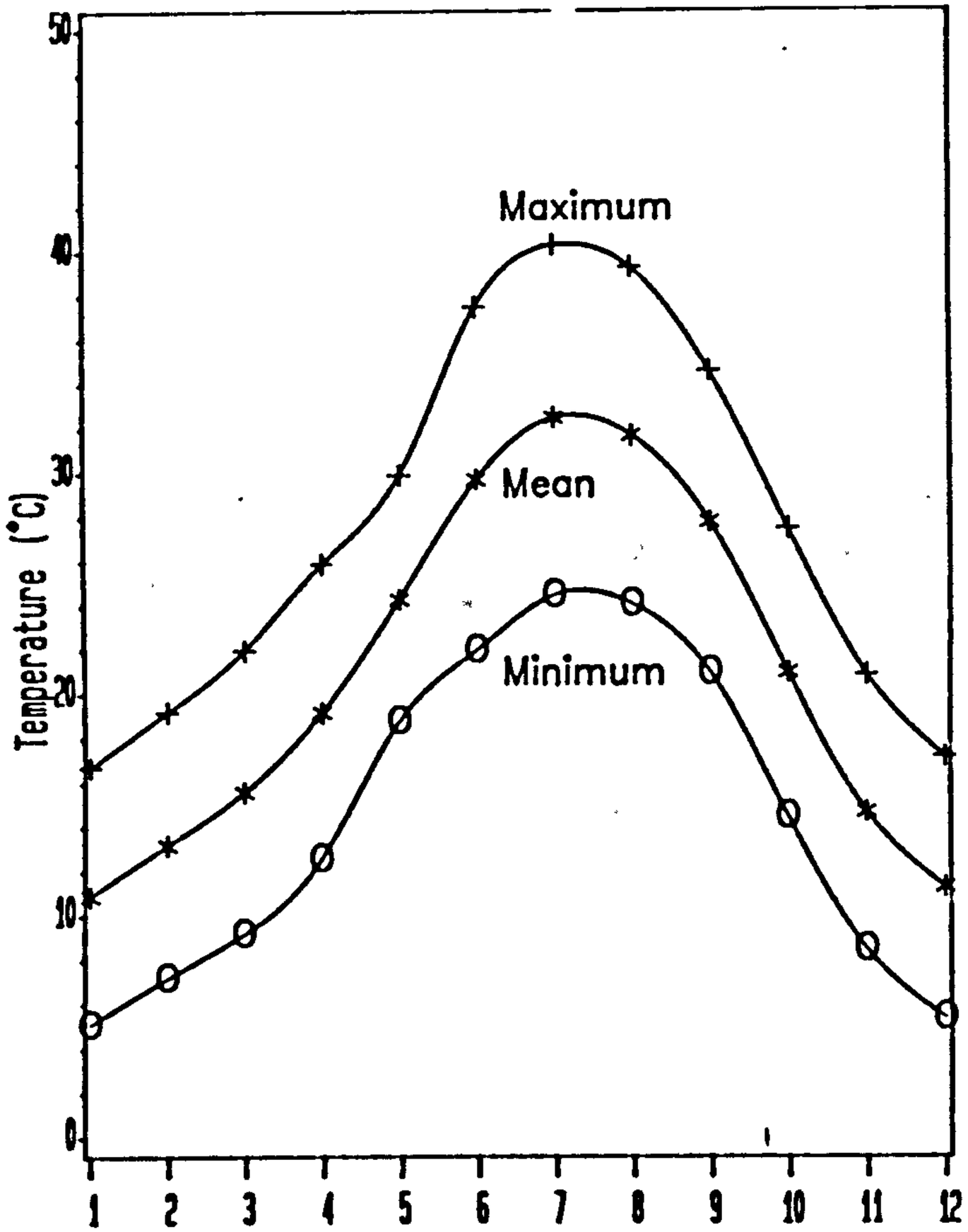

Figure 1.1 Monthly outside air temperature
for El-Oued (33.3 N)

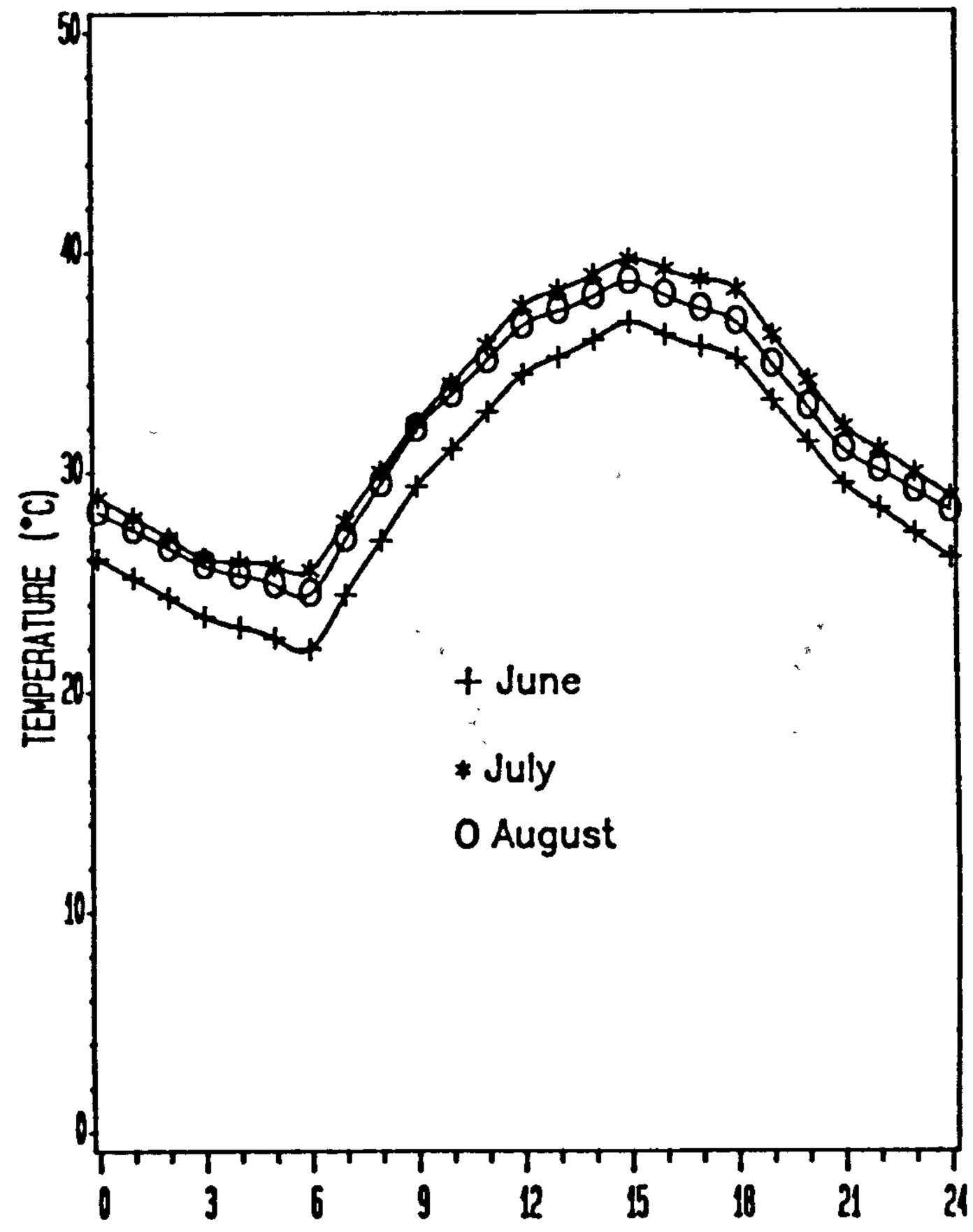

Figure 1.2 Mean hourly outside air temperature
for El-Oued (33.3 N)

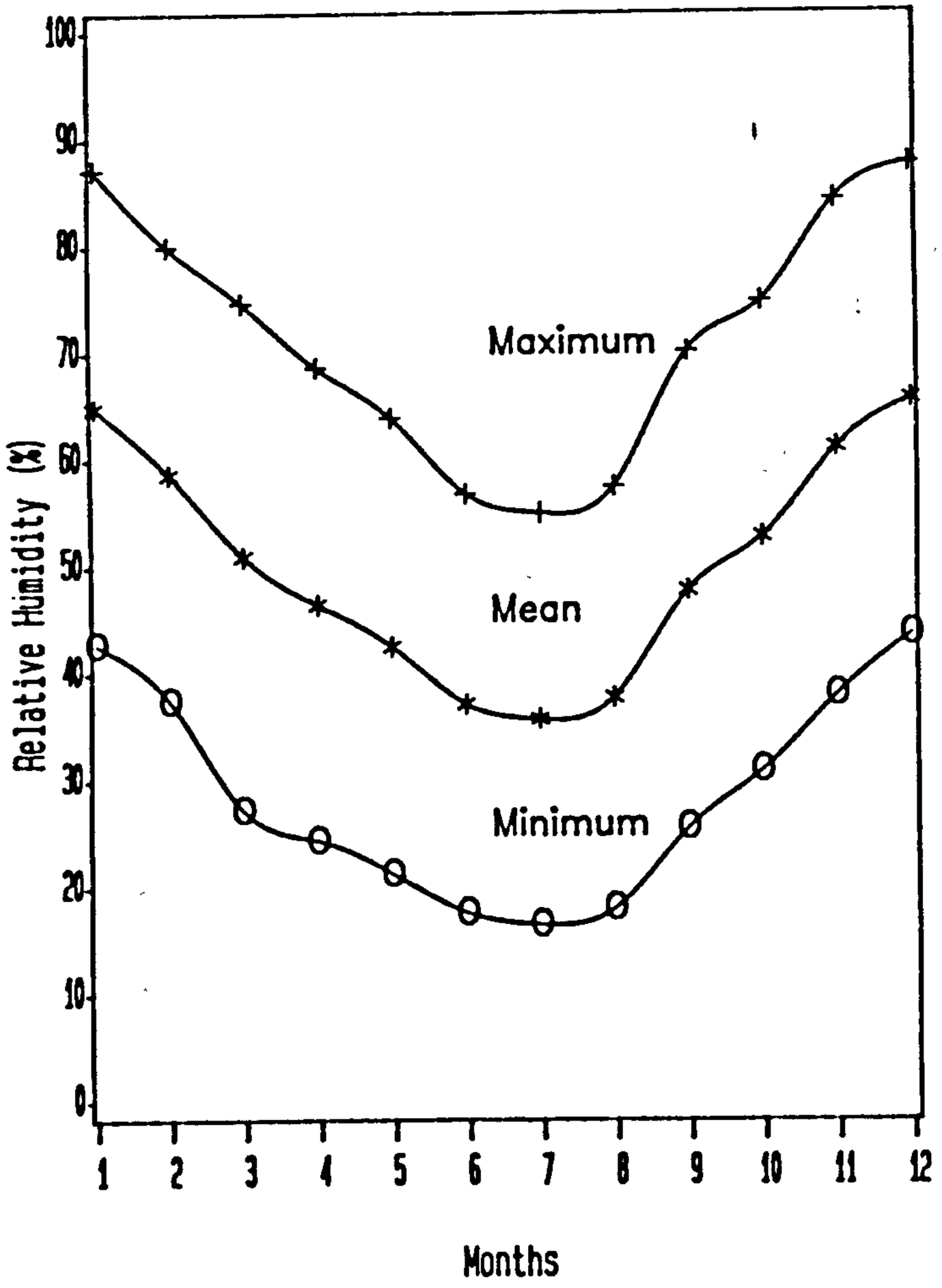

Figure 1.3 Monthly relative humidity
for EL-Oued (33.3 N)

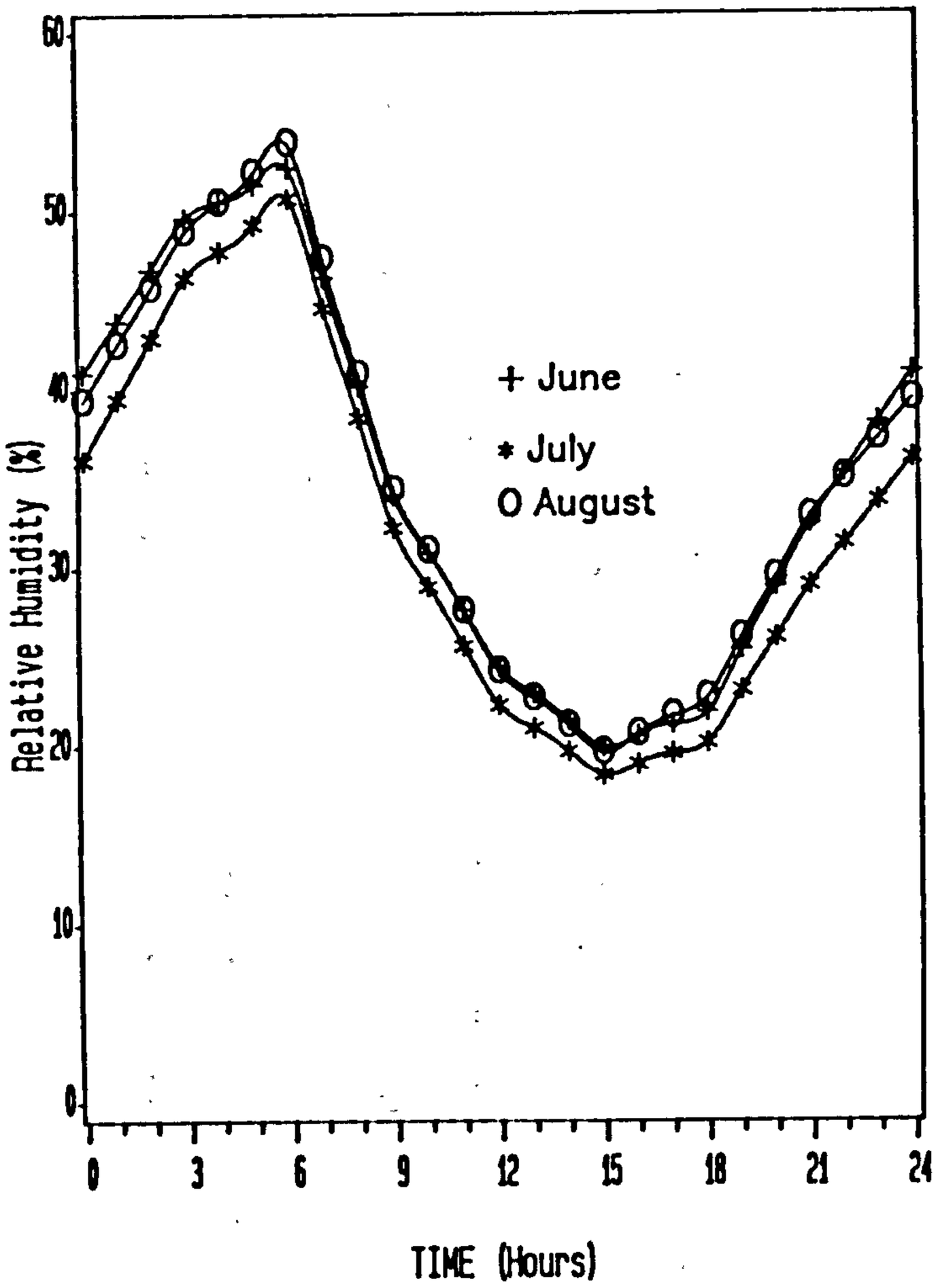

Figure 1.4 Mean Hourly Relative Humidity
for El-Oued (33.3 N)

areas, a reduction factor of 0.35 is recommended; and for cities a factor of 0.21. The wind speeds given in figure 1.5 may thus be reduced by at least 65%. Wind speeds in El-Oued are higher than in many hot climates and prevail from the east.

Solar radiation data for many countries are not available due to lack of instrumentation and theoretical estimation is necessary. For El-Oued, estimates were made using the CIBSE Guide (1986), supported with some actual climatic data. Total solar radiation, for both horizontal and vertical surfaces, was calculated for cloudless days and this illustrated the variation in solar radiation intensity over a 24 hours period during summer.

Figure 1.6 shows total solar irradiance on the horizontal. The peaks appear at noon during June and July when they are about 1100 W/m^2, and for August slightly less at 1030 W/m^2.

Figure 1.7 shows total solar irradiance on an east facade. As can be seen it is greater before noon because the sun's elevation at this time is low and thus much of solar radiation strikes an east facade. The peak value of about 885 W/m^2 appears at around 0800h.

Figure 1.8 shows total solar irradiance on a south facade. These lower than those on the East. The peaks appear at noon and their magnitudes depend on the month. The South receives more solar radiation in August than in June and July. In August the peak is 670 W/m^2; in June, 500 W/m^2; and in July, about 545 W/m^2.

Figure 1.9 shows total solar radiation on a west facade. This is a mirror image of the east facade. The only difference is that peaks appear at 1500h. The peaks for June and July are about 885 W/m^2 and for August slightly lower at 865 W/m^2.

Figure 1.10 shows the total solar radiation on a north facade, which is much lower than that on the others. Peaks appear at 0600h, at noon and at 1800h. The highest peak is in June which is about 325 W/m^2.

It can be seen from the above that in summer at latitude 33.3 °N, the north and south facades receive less solar radiation than west and east ones. The comparison of these is presented in figure 1.11.

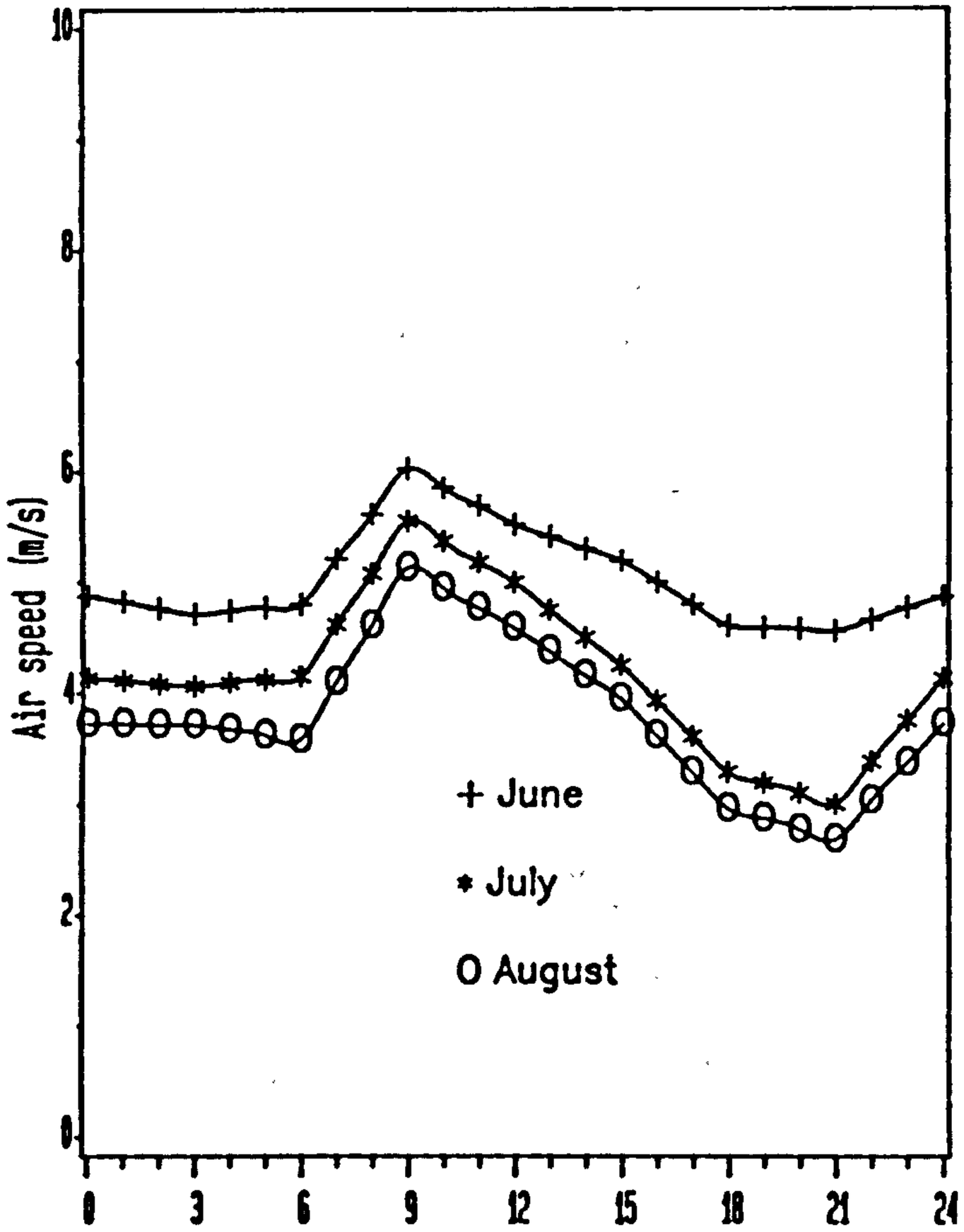

Figure 1.5 Mean hourly air speed
for El-Oued (33.3 N)

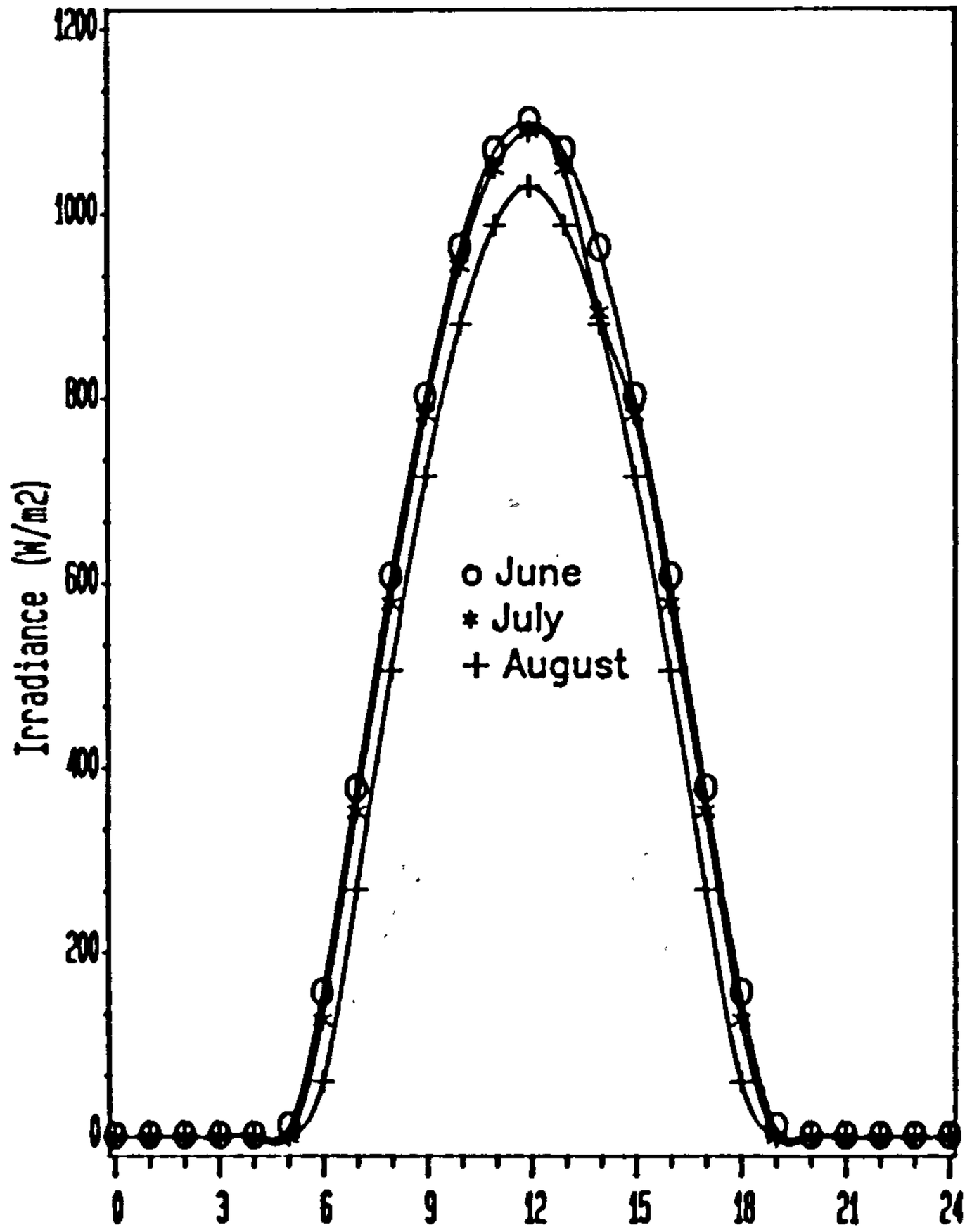

Figure 1.6 Total solar irradiance on the horizontal
for El-Oued (33.3 N)

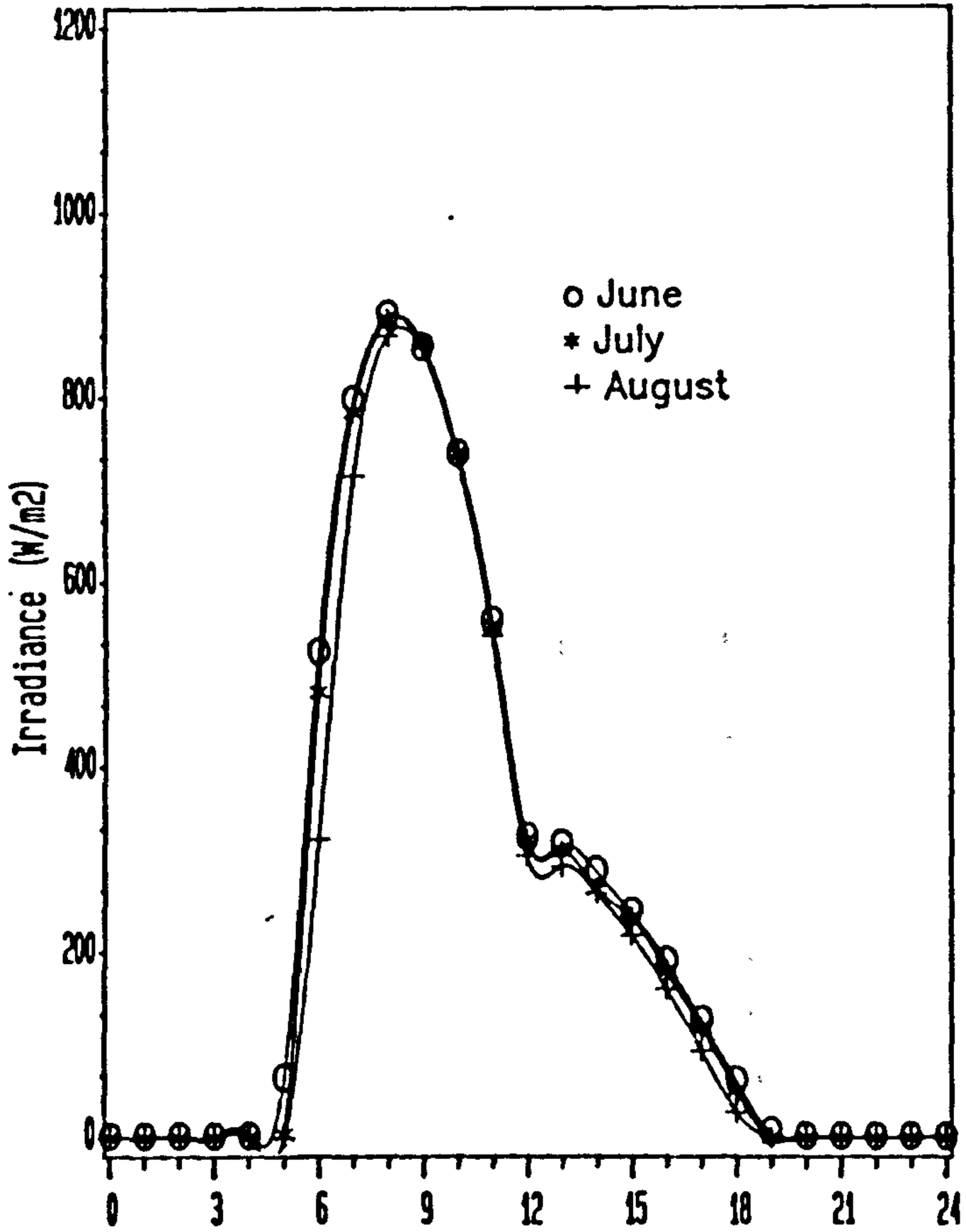

Figure 1.7 Total solar irradiance on an east wall
for El-Oued (33.3 N)

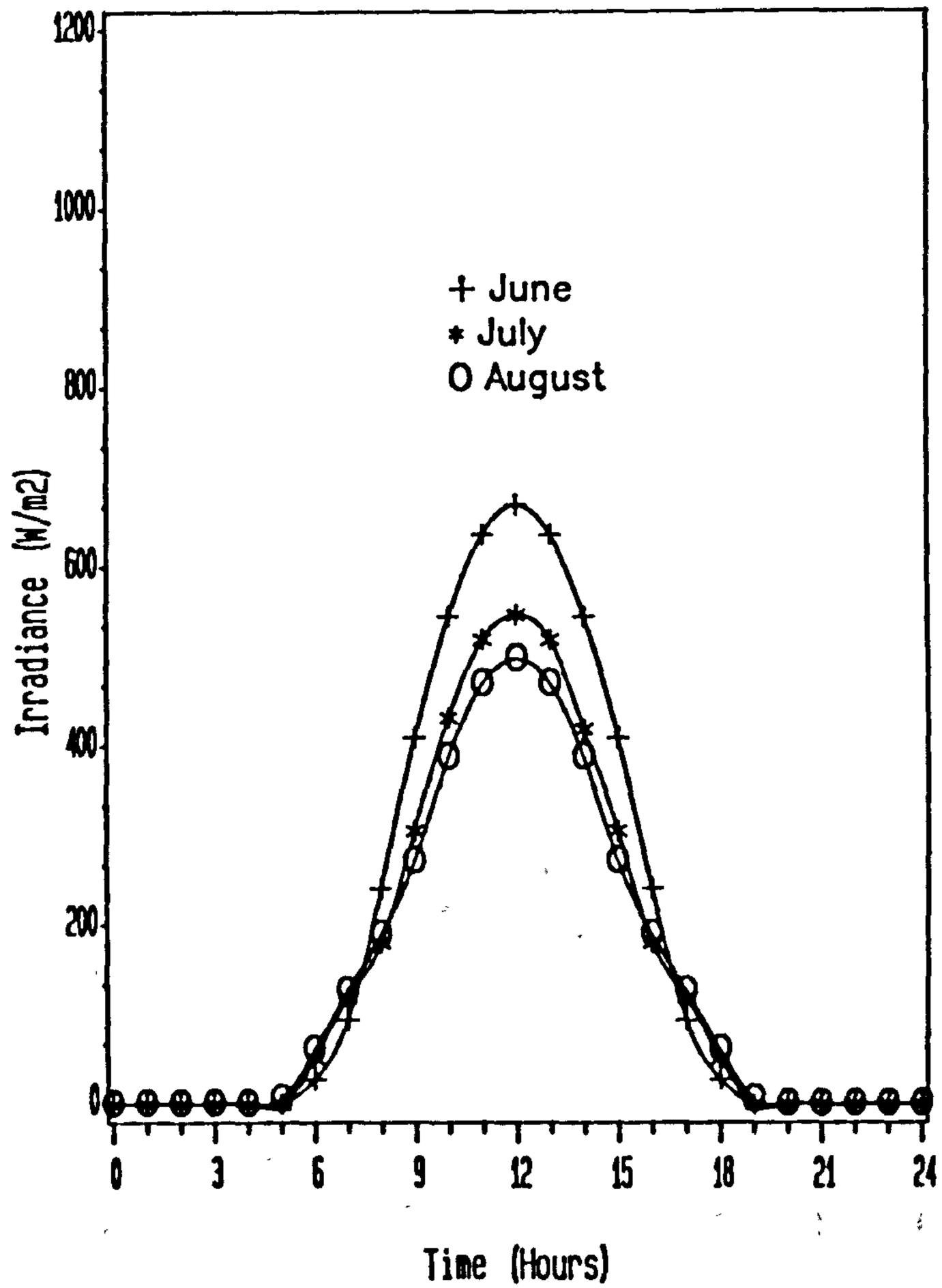

Figure 1.8 Total solar irradiance on a south wall
for El-Oued (33.3 N)

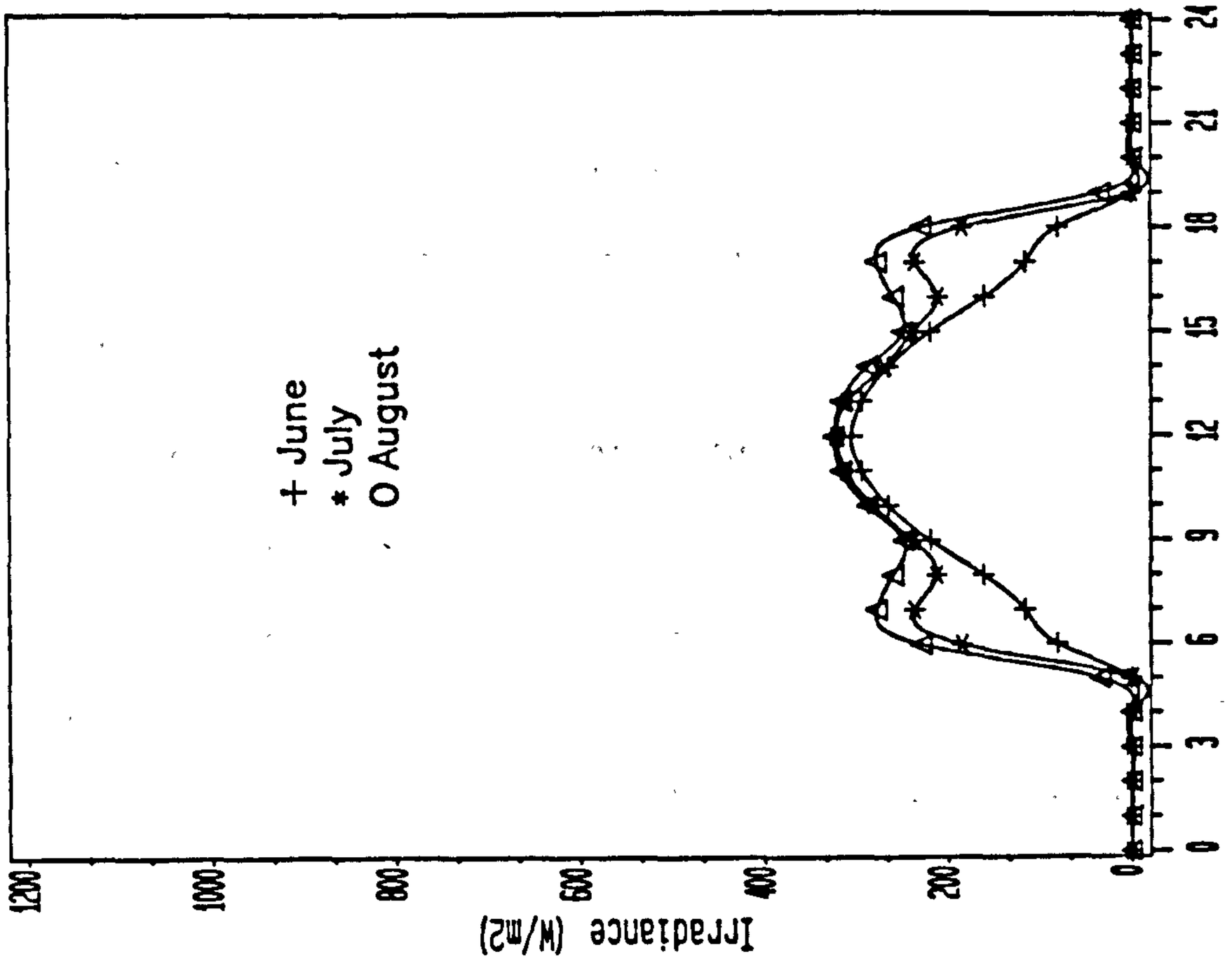

Figure 1.10 Total solar irradiance on a north wall for El-Oued (33.3 N)

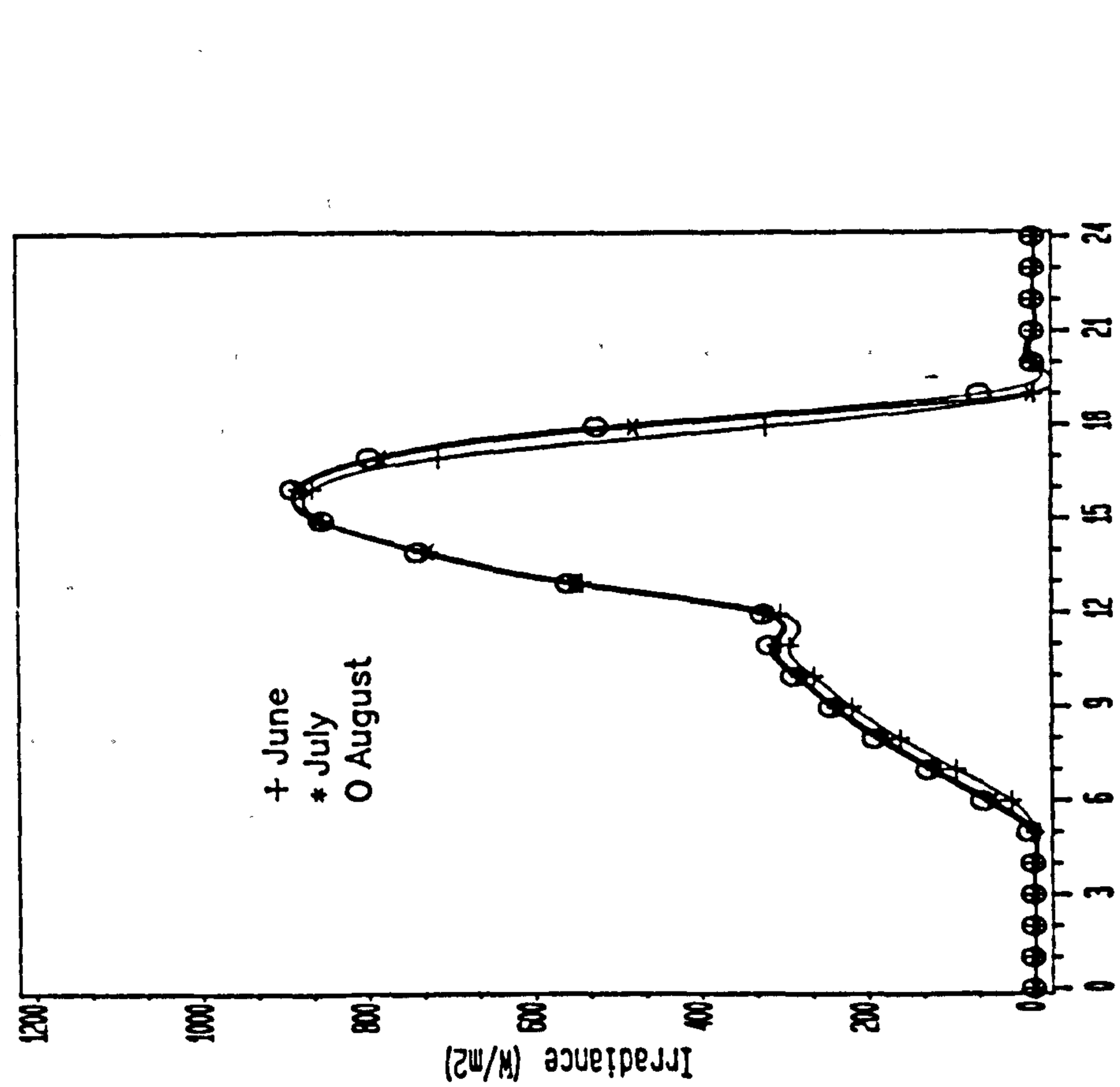

Figure 1.9 Total solar irradiance on a west wall for El-Oued (33.3 N)

It is evident that the west facade receives higher solar radiation in the afternoon than the South, this makes this orientation more important than a South one for the purpose of heat collection. For more details on the above climatic data (see appendix 1).

1.3 Comfort in Southern Algerian housing

Thermal comfort in dwellings depends upon various environmental factors such as; air temperature, mean radiant temperature, relative humidity and air movement. The range of conditions within which the majority of people would feel comfortable is called the "Comfort Zone" (Koenigsberger *et al.* 1974). Various thermal index scales have been developed to express the base conditions. These indices are discussed in details in references such as Evans (1980). Olgay (1963) constructed a bio-climatic chart (figure 1.12) from which the comfort zone is defined in terms of relative humidity and air temperature. The lower and upper limits of thermal comfort in still air being 20 °*C* to 30 °*C* respectively, within this temperature range, the relative humidity lies between 20% to 50%. As relative humidity increases, above 50%, the upper limit of the comfort zone decreases. Thus the maximum air temperature for comfort appear to be less than 30 °*C*. In places where the air temperature is higher than 30 °*C*, thermal comfort can be improved by improving the air movement as shown in figure 1.12.

In hot climates such as El-Oued, the relative humidity in summer goes up to 50% in the early hours of the morning (figure 1.4) which is within the comfort zone. At night and early morning, the air temperature is low (figure 1.2) and is within the comfort zone, consequently, ventilation at night to improve thermal comfort would be desirable. However, the bio-climatic chart does not include the mean radiant temperature which is an important environmental factor that affects thermal comfort. The CIBSE Guide (1985) suggests an index to express thermal comfort which takes into account air velocity, mean radiant temperature and air temperature. It is called "Resultant Temperature", it is usually

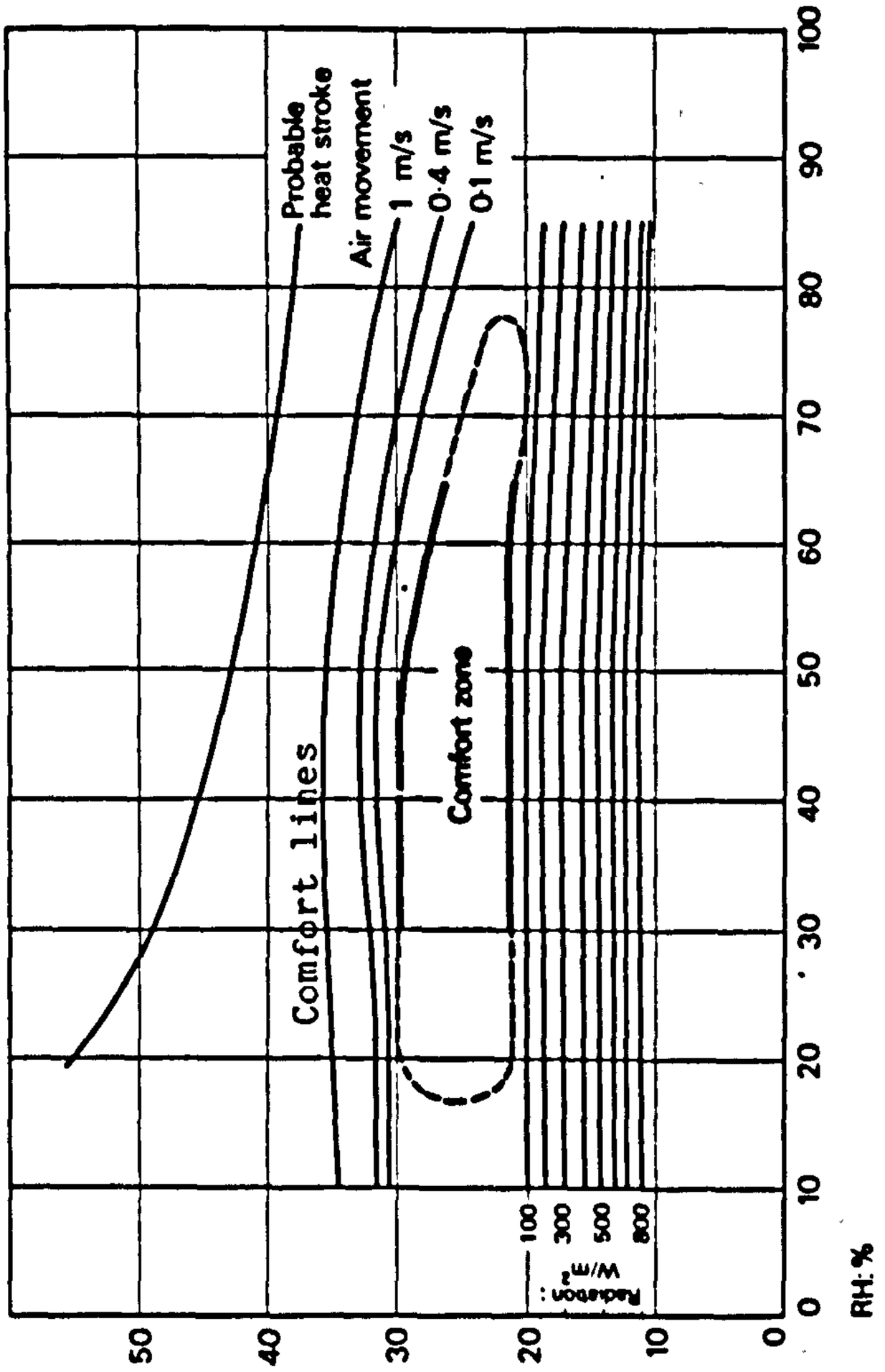

Figure 1.12 Bioclimatic chart showing the effect of air movement on comfort zone lines

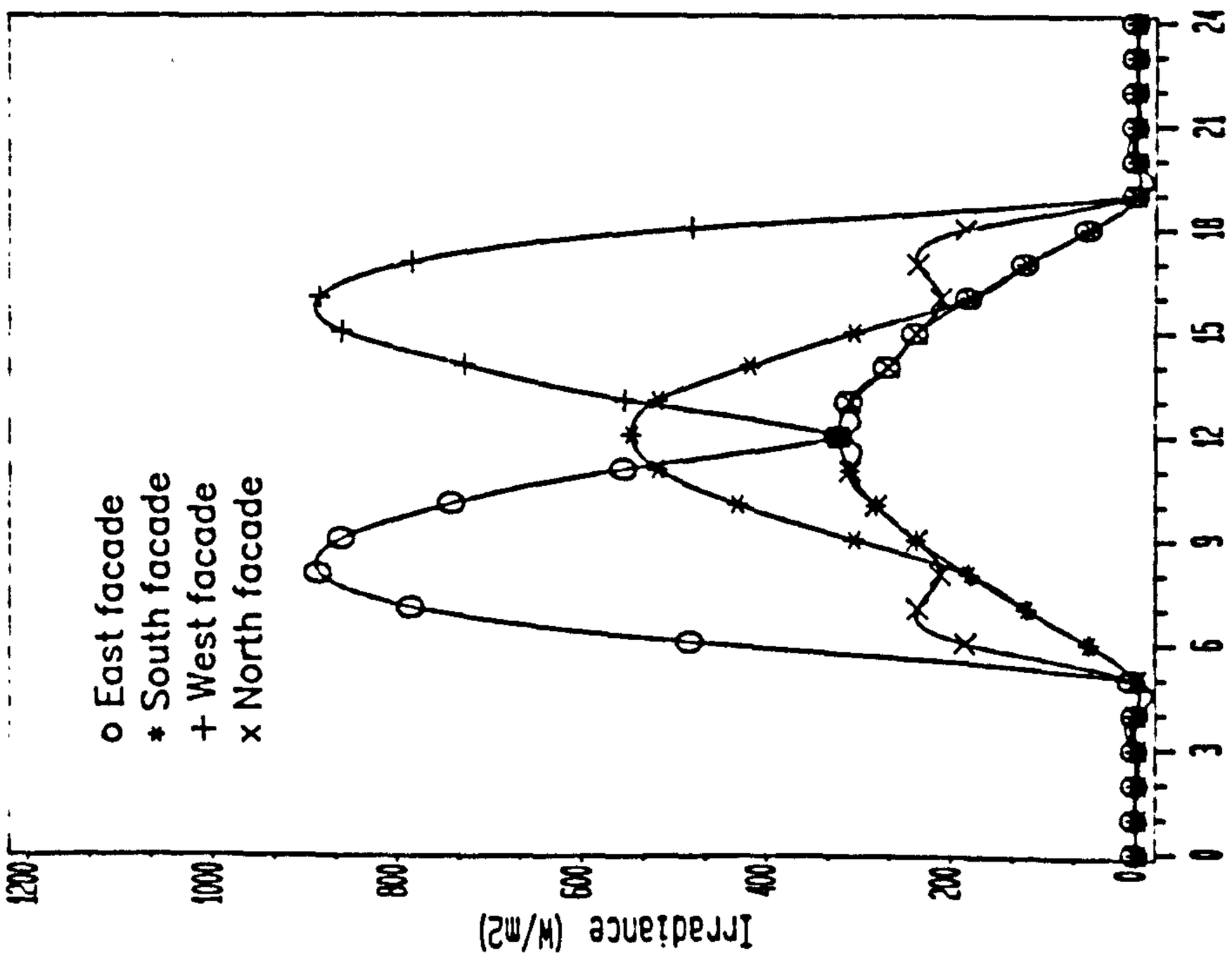

Figure 1.11 Total solar irradiance on different facades in July for El-Oued (33.3 N)

recorded by a globe thermometer placed in the centre of a room. The resultant temperature is used as index to indicate comfort in cold climates but it also suitable for hot climates (CIBSE 1986). The resultant temperature is given by:

$$T_{res} = \frac{T_{mr} + T_a(10v)^{0.5}}{1 + (10v)^{0.5}} \qquad (1.1)$$

T_{res} = resultant temperature °C

T_{mr} = mean radiant temperature °C

T_a = air temperature °C

v = air velocity m/s

At an indoor air velocity of $0.1 m/s$, the resultant temperature simplifies to:

$$T_{res} = 0.5T_{mr} + 0.5T_a \qquad (1.2)$$

For higher air velocities, say $v = 0.3$m/s, the resultant temperature becomes:

$$T_{res} = 0.37T_{mr} + 0.63T_a \qquad (1.3)$$

Comparison of the terms in the latter two equations shows that air movement lowers the mean radiant temperature term but increases the air temperature. However since comfort is influenced to a greater extent by the radiant component, increasing air velocities is beneficial.

Conditions in southern Algeria are very hot and without air conditioners or other means of cooling, thermal discomfort is experienced. Thick walls may protect the building from high resultant temperature during the day, but later in the evening, heat stored in the fabric of the walls is released to the interior. This results in uncomfortably high resultant temperatures. There are no studies of the range of resultant temperatures people in southern

Algeria can tolerate. Webb (1964) studied thermal comfort in hot dry ones, and found that acclimatized subjects, with sedentary conditions and normal clothing, were comfortable in much warmer conditions than in hot humid conditions. The CIBSE (1986) states that a comfortable resultant temperature, with low air movement for the U.K is from 20 to 22 $°C$ but for hot climates it is 28 $°C$. Nicol (1975) shows that the comfort temperature for temperate and cold climates ranges from 20 to 25 $°C$, whereas for hot dry climates this range is much higher: in the order of 28 to 36 $°C$, with air velocities up to 0.25 m/s. This difference is attributed to habituation and acclimatisation. Clothing also has an effect on the preferred temperature because it insulates the skin from the environment. In the hot dry climate of Algeria, people usually wear white, light weight clothes called "Kamiss". These allow air to move over the skin which in turn evaporates the sweat.

1.4 Existing methods of achieving comfort in Southern Algerian housing

Comfort in Algerian housing is generally achieved by air conditioning for the high income population, and by traditional means for the low income population Traditional ways of achieving comfort are:

-Evaporative cooling using pools or water sprinkled upon blinds and floors. The ambient air is cooled by evaporation as it passes over wet surfaces. Usually the water is kept in pools inside courtyards, in porous pots at windows, or by wet fabric hung at windows. The disadvantage of cooling by evaporation is the increase in relative humidity and the associated reduction in evaporation of sweat. The second disadvantage is that evaporative cooling requires water where it may be scarce.

-Building underground, the underground temperature at about 3m depth is stable around 21$°C$. This offers desirable cool surroundings. However, building underground may be expensive and an underground building will not benefit from cross ventilation. Drainage from an underground building may be difficult.

-Using vegetation for shade. This reduces direct solar radiation to building surfaces.

Examples are found in the city of M'zab in Algeria. In some dry places however, plants cannot be easily grown.

-Building layouts with winding, narrow streets, built with thick walls from locally available material such as stone, brick and mud. Thick walls have the advantage of reducing and delaying heat transfer to living spaces. The walls are usually constructed with small openings to reduce heat. The disadvantage of thick walls is that they use more material.

-Ventilation through courtyards. The air in the courtyards is usually cooler due to the evaporation of water from pools or due to low surface temperatures within the courtyard.

-Using outside spaces, such as roofs for sleeping in order to catch night breezes, and radiant cooling due to long wave radiation loss to a clear sky.

These ways of adaptation are common in most hot dry climates and are discussed in greater depth in the literature survey in chapter two.

1.5 The present work

In some hot areas such as Southern Algeria, the temperature of the air during the day is high, humidity is low, and air movement through buildings during the day brings no benefit. The windows are usually closed during the day and opened for ventilation during the evening, when the outside air becomes cooler. Buildings with high thermal capacity take longer to heat and cool than the surrounding air. The inside of dwellings can remain comfortable for much of the day, whereas in early evening, when the outside air temperature passes its peak, the heat built-up in the walls is released into dwelling. The air temperature and surface temperatures tend to increase beyond the limits of comfort especially with low air movement at night, which is a characteristic of a hot climate. It is natural that people living in hot climates adjust their activities to suit the climate. Work begins early in the day while it is cool outside and continues till shortly after midday. People rest during the hottest part of the afternoon. During this time the internal air temperature is still well below

that outside. When activities restart later in the afternoon, the outside temperature is past its peak but the indoor air temperature is still rising due to the release of stored thermal energy consequently, people tend to move outdoors, spending time in courtyards, patios, and on roofs. However, sleeping outside may sometimes cause thermal discomfort due to the loss of long-wave radiation from the human body to a clear night sky.

It is intended in this study to investigate ways of improving thermal comfort inside dwellings by increasing ventilation in the evening so that people can continue their activities inside, rather than have to move conditions. One way of achieving this is by using a sun-warmed or "solar chimney" constructed of stone, concrete or any other material of high thermal capacity. It can be added to an existing building or made by modifying a cavity wall such as is often used for thermal insulation. The cavity is to have dampers at the top and bottom which are closed throughout the day, so that it is passively heated. In the evening the dampers, and the windows of the room are opened to permit ventilation. The air within the cavity flows upward by buoyancy thus drawing cool outside air into the room through the windows. The air entering the cavity will take up heat stored from the walls to prolong the upward flow. This naturally, will cool the cavity and the design must ensure that the rate of cooling is such that ventilation will continue for as long as is required. The cavity design has a length Y, width W and a height Z (figure 1.13)

1.6 Purpose and scope of the study

This work was undertaken to investigate a technique to improve thermal comfort in low cost housing in hot climates by cooling ventilation, without relying upon electricity. It attempts to develop a sun-warmed cavity or a "solar chimney" which is used to encourage air speeds through a room of $0.25 m/s$ as suggested by Nicol (1975) to reduce the resultant temperature inside a building to a comfortable level. When the incoming air is cool and is moving, it will lower the air temperature and the mean radiant temperature of a room. The effect of air movement on the resultant temperature is shown by equation 1.1. Moving air will also cool the human body by evaporation of sweat.

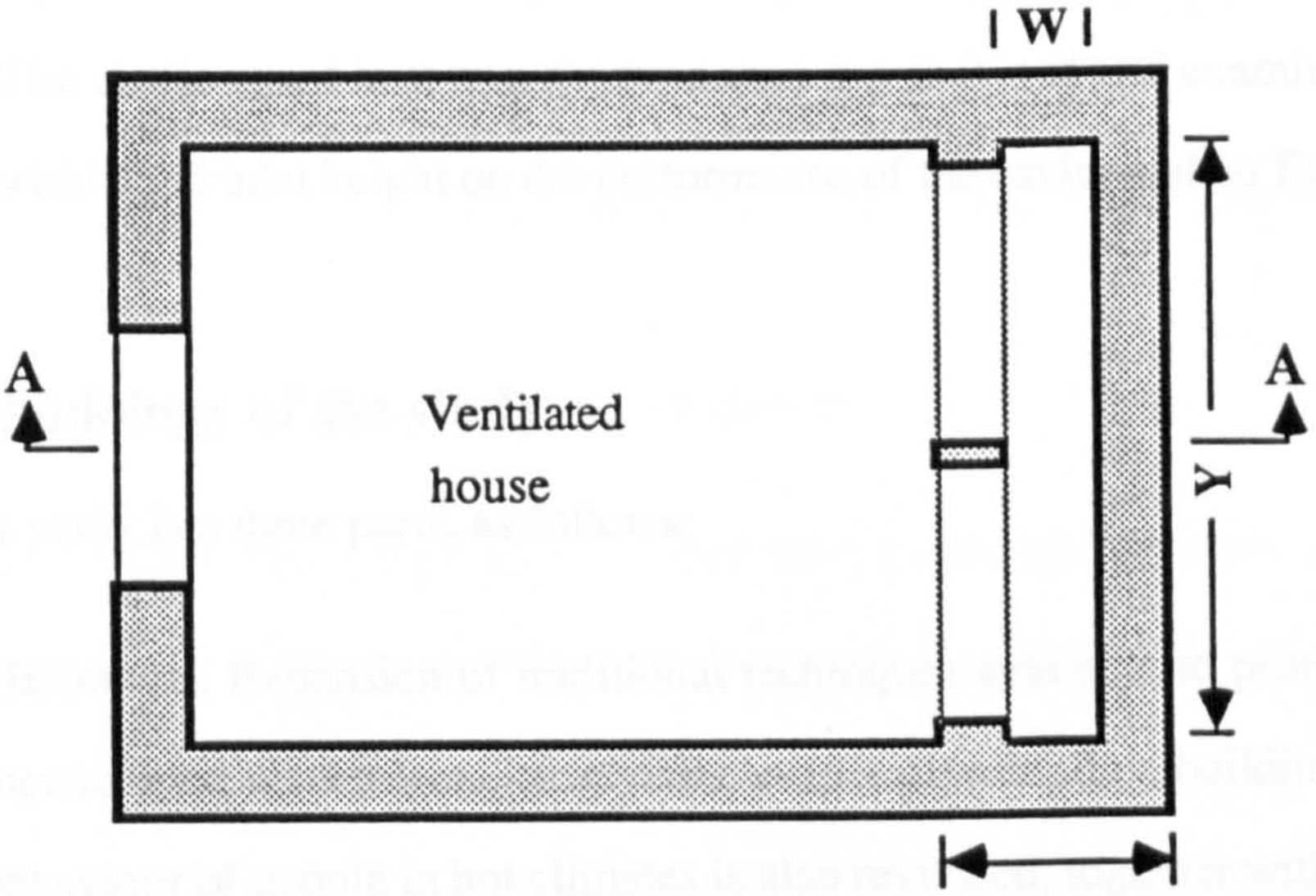

a) Plan of the proposed design

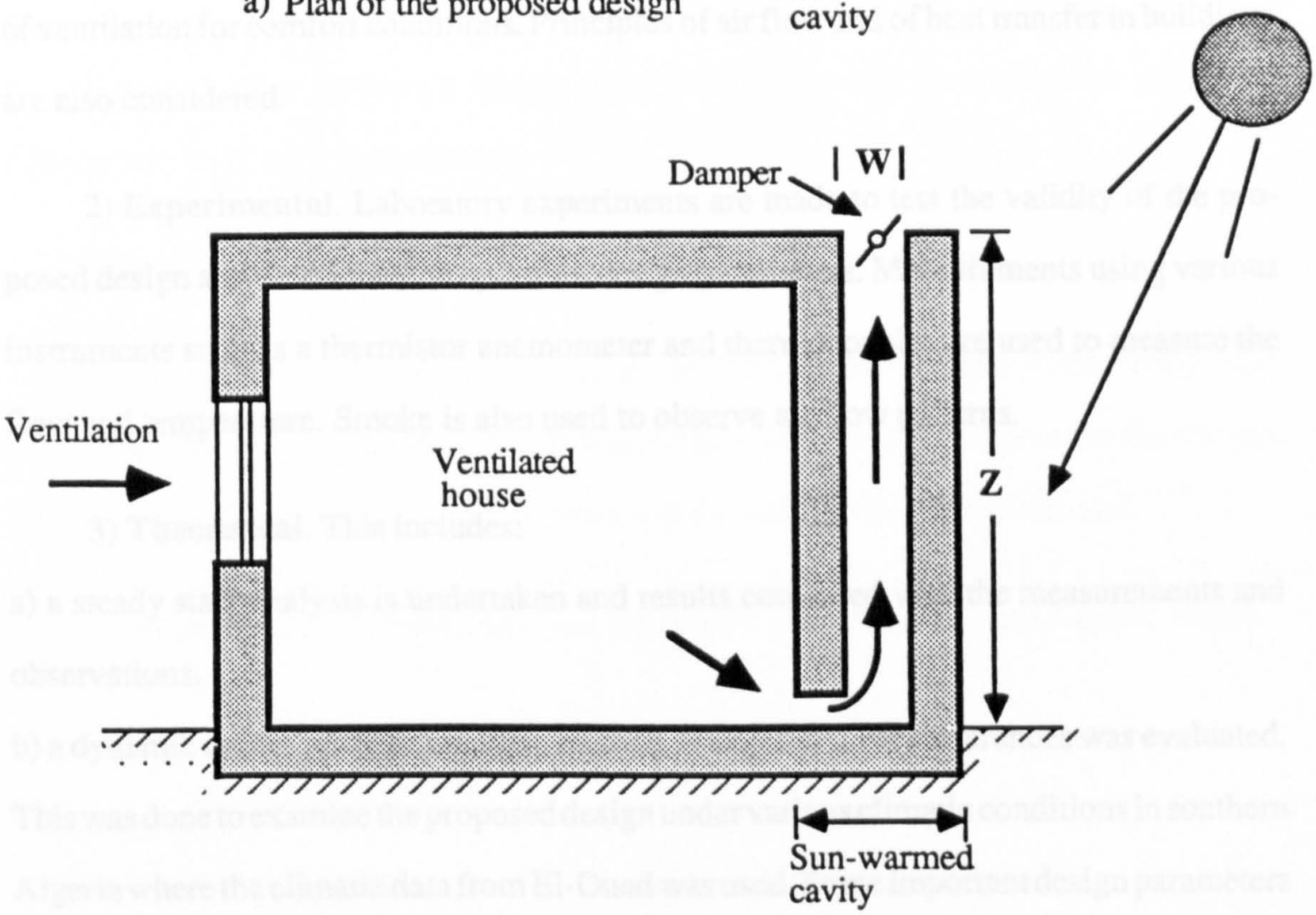

b) Section **A A** Through the proposed design

Figure 1.13 The proposed design

Air movement in a sun-warmed cavity is tested in the laboratory. The temperature of the cavity is varied to cover the possible range of temperature experienced in-hot dry climates. The air flow and heat transfer processes are analysed and examined. The effect of cavity width, and inlet height on the performance of the cavity and air flow patterns are assessed.

1.7 Methodology of the study

This study has three parts, as follows:

1) **Historical.** Expansion of traditional techniques available to promote cooling in hot climates such as: wind towers, courtyards, evaporative cooling, building underground. Special behaviour of people in hot climates is also reviewed, together with relevant areas of ventilation for comfort conditions. Principles of air flow and of heat transfer in buildings are also considered.

2) **Experimental.** Laboratory experiments are made to test the validity of the proposed design and determine the optimum design parameters. Measurements using various instruments such as a thermistor anemometer and thermocouples are used to measure the flow and temperature. Smoke is also used to observe air flow patterns.

3) **Theoretical.** This includes:

a) a steady state analysis is undertaken and results compared with the measurements and observations.

b) a dynamic model using a numerical method of implicit finite differences was evaluated. This was done to examine the proposed design under various climatic conditions in southern Algeria where the climatic data from El-Oued was used. Some important design parameters such as the optimum azimuth and the external wall thickness were difficult to determine by experimental techniques, so they are determined by a theoretical dynamic model.

1.8 Outline of the thesis

Chapter Two reviews the relevant literature in the following areas:

a) traditional passive ways of cooling,

b) ventilation in buildings, ventilation needs for comfort, and existing methods of moving air,

c) heat transfer mechanisms in building components.

Chapter Three describes the apparatus used for the observations, and how it was built, the conditions of the measurement, the instruments used, and the limitation and range of applicability of the apparatus as a whole.

Chapter Four presents and analyses the measurements and observations.

Chapter Five presents a steady state theoretical analysis which was used as a comparison with the measurements.

Chapter Six compares and discusses theory and measurements.

Chapter Seven presents a dynamic model for heat and air flow in the cavity, with reference to the magnitude of the flow produced by a sun-warmed cavity under the climatic changes. The best azimuth, wall thickness and time of operation are discussed.

Conclusions and recommendations for further work are given in **Chapter Eight.**

CHAPTER TWO

LITERATURE SURVEY

2.1 Introduction

This chapter presents knowledge gained from the existing literature related to the current study. The review is divided into:

-Traditional ways of achieving comfort

-Ventilation needs for comfort

-Ventilation theory

-Air moving devices

-Heat transfer mechanisms in buildings

-Heat transfer and air flow mechanisms in cavities

-Dynamic models

2.2 Traditional ways of achieving comfort

In most hot climates, people have few energy sources (fuel and animals) apart from the wind and the sun. They have learned from long experience various ways of maintaining comfort inside dwellings. Especially popular are:

-air movement using wind towers and courtyards,

-evaporation of water,

-use of high thermal capacity material,

-shading using plants and building layout.

2.2.1 Air movement

2.2.1.1 Traditional wind towers

Wind towers are traditionally used for cooling ventilation inside dwellings in the hot areas of Iran and the Middle East. They are attached to dwellings and are up to 10m high to catch breezes from any direction. The wind is directed down into the living quarters (figure 2.1). They have been described and studied thoroughly by Bahadori (1978, 1979, 1981, 1985, 1987) and are sometimes combined with stairs and a basement to improve their effectiveness.

Wind towers are mainly wind dependent, but, in the absence of wind, they might perform like a chimney and cool by stack effect. Hot surfaces of the tower warm the air within lowering its density. The air then flows upwards drawing hot air from the house to the outside.

2.2.1.2 Courtyards

In hot climates, a courtyard has many functions; it provides:

-security and privacy especially for children and women,

-light, since the house is inward looking provided with few and small openings on the external walls,

-protection from glare and sand storms,

-ventilation.

During the day, surfaces of the courtyard remain cool for long periods. Fountains, pools and plants promote the cooling of the courtyard. Air within cools by convection and evaporation, and will be used for ventilating the house (figure 2.2a). At night, the heat from the courtyard will partly be radiated to the clear nocturnal sky, and partly removed by convection by the cool outside air. Meanwhile, hot air in the courtyard moves upward drawing cool outside air through windows into the house (figure 2.2b).

A recent study on the performance of a courtyard was by Mohsen (1979).

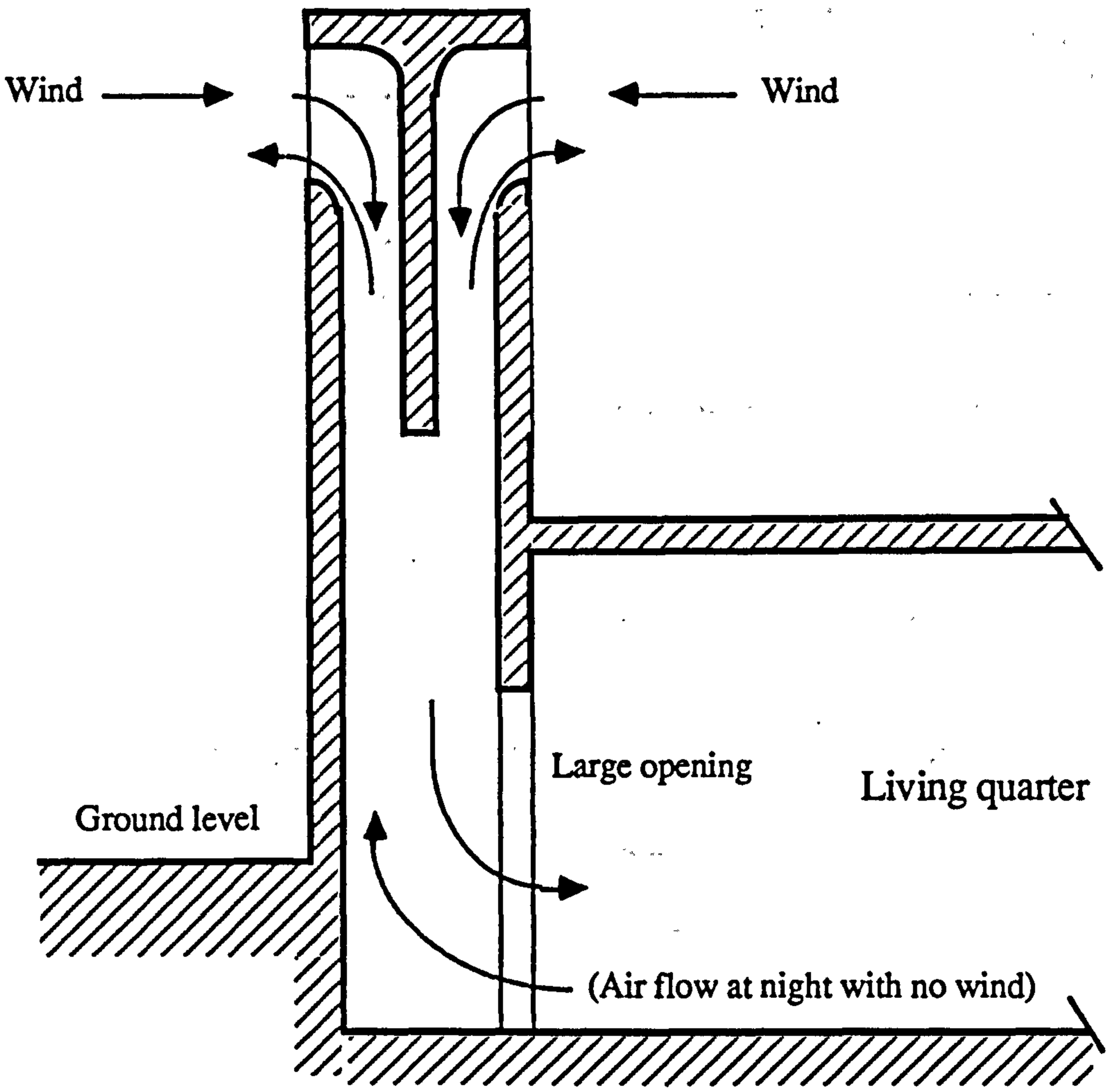

Figure 2.1 Performance of a traditional wind tower .

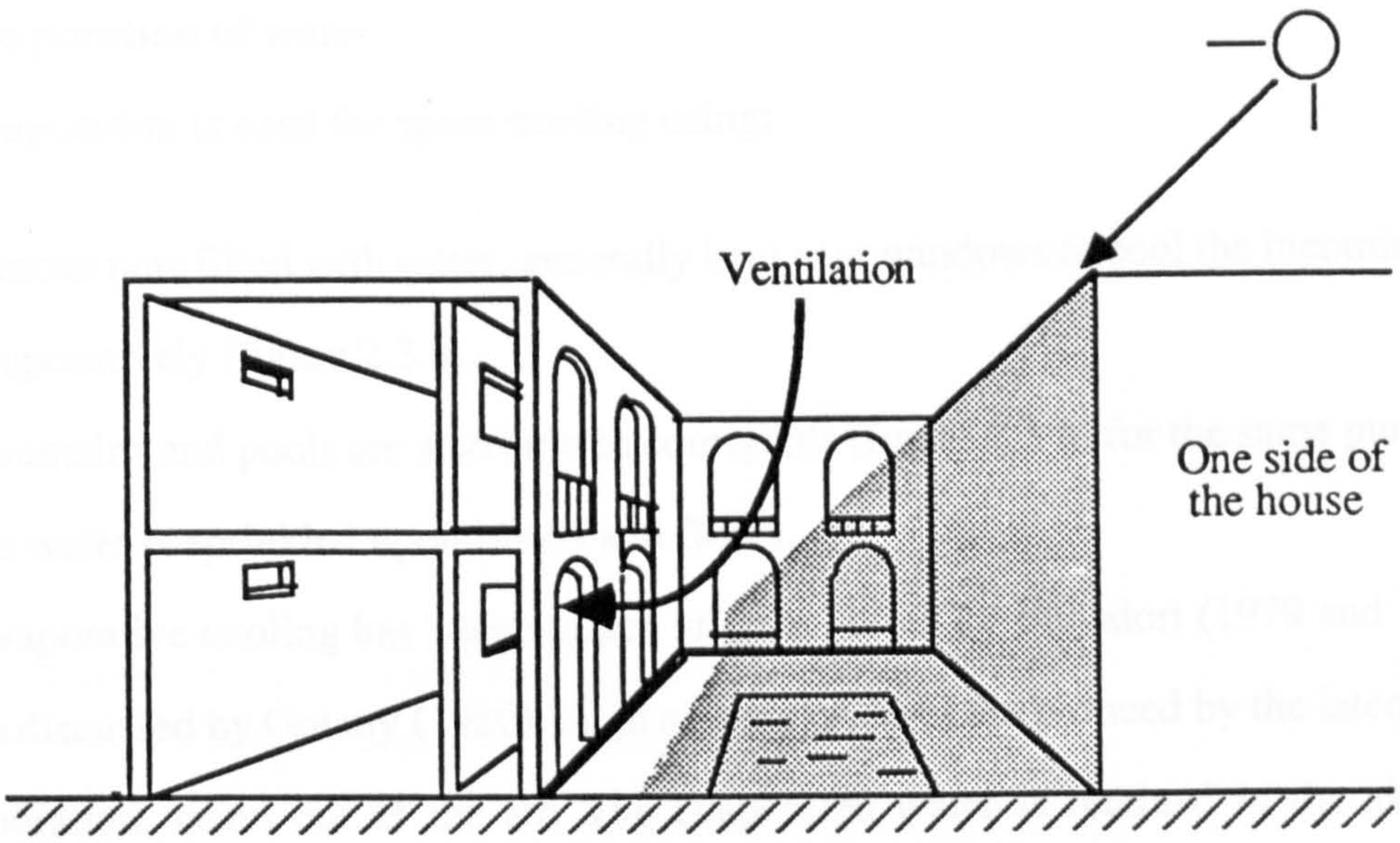

a) during the day a courtyard gives shade to the house,
and is used for ventilation.

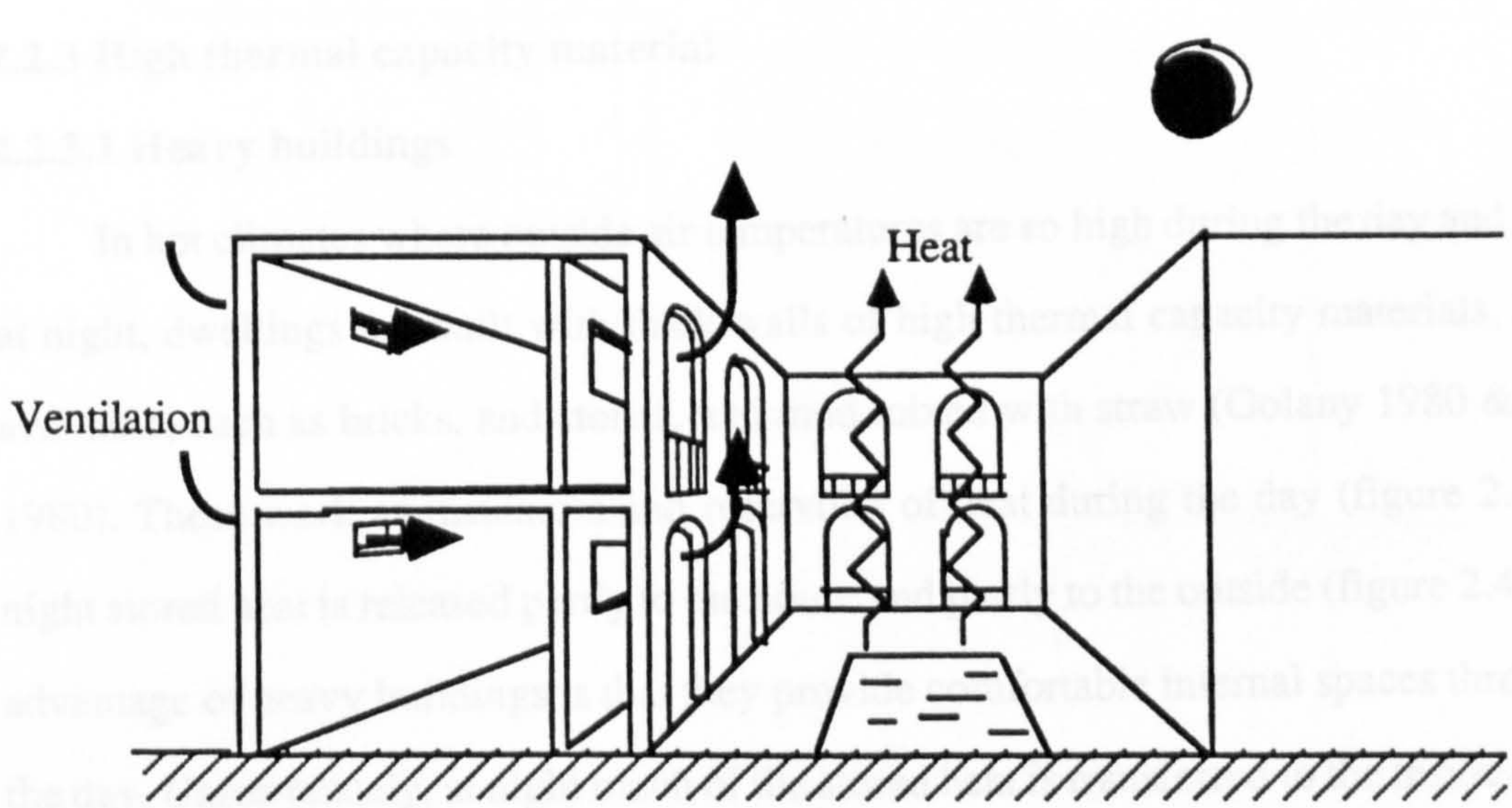

b) at night heat accumulated in the courtyard is dissipated to the clear sky,
hot air within courtyard flows upwards drawing outside air through .
the building.

Figure 2.2 Thermal performance of a courtyard in a hot dry climate.

2.2.2 Evaporation of water

Evaporation is used for space cooling using:

-porous pots filled with water, generally kept near windows to cool the incoming air evaporatively (figure 2.3 a),

-fountains and pools are also built in courtyards (figure 2.3 b) for the same purpose,

-or water is sprinkled upon blinds and floors.

Evaporative cooling has been studied at great length by Bahadori (1979 and 1985) and it is discussed by Golany (1980). High air temperatures are reduced by the latent heat of evaporation, taken out of the air. The evaporated water is retained in the air thus increasing its humidity, which may not be undesirable in-hot dry climates. Evaporative cooling may not be effective in the absence of air movement, because increasing of relative humidity decreases the evaporation of sweat. It also requires water where it may be scarce.

2.2.3 High thermal capacity material

2.2.3.1 Heavy buildings

In hot climates where outside air temperatures are so high during the day and so low at night, dwellings are built with thick walls of high thermal capacity materials, locally available, such as bricks, and stones, and mud mixed with straw (Golany 1980 & Evans 1980). These work as insulators and reservoirs of heat during the day (figure 2.4a). At night stored heat is released partly to the house and partly to the outside (figure 2.4b). The advantage of heavy buildings is that they provide comfortable internal spaces throughout the day. Unfortunately, at night much of the stored heat is transferred to the inside causing discomfort. This is why people in hot climates move outdoors at night to sleep on roofs and balconies.

2.2.3.2 Underground buildings

Building underground is an effective way of keeping dwellings cool and it is traditional in hot climates. Matmata in Tunisia and Cappadocia in central Turkey are examples (Golany 1980). The advantage of underground structures is that the temperature fluctuation

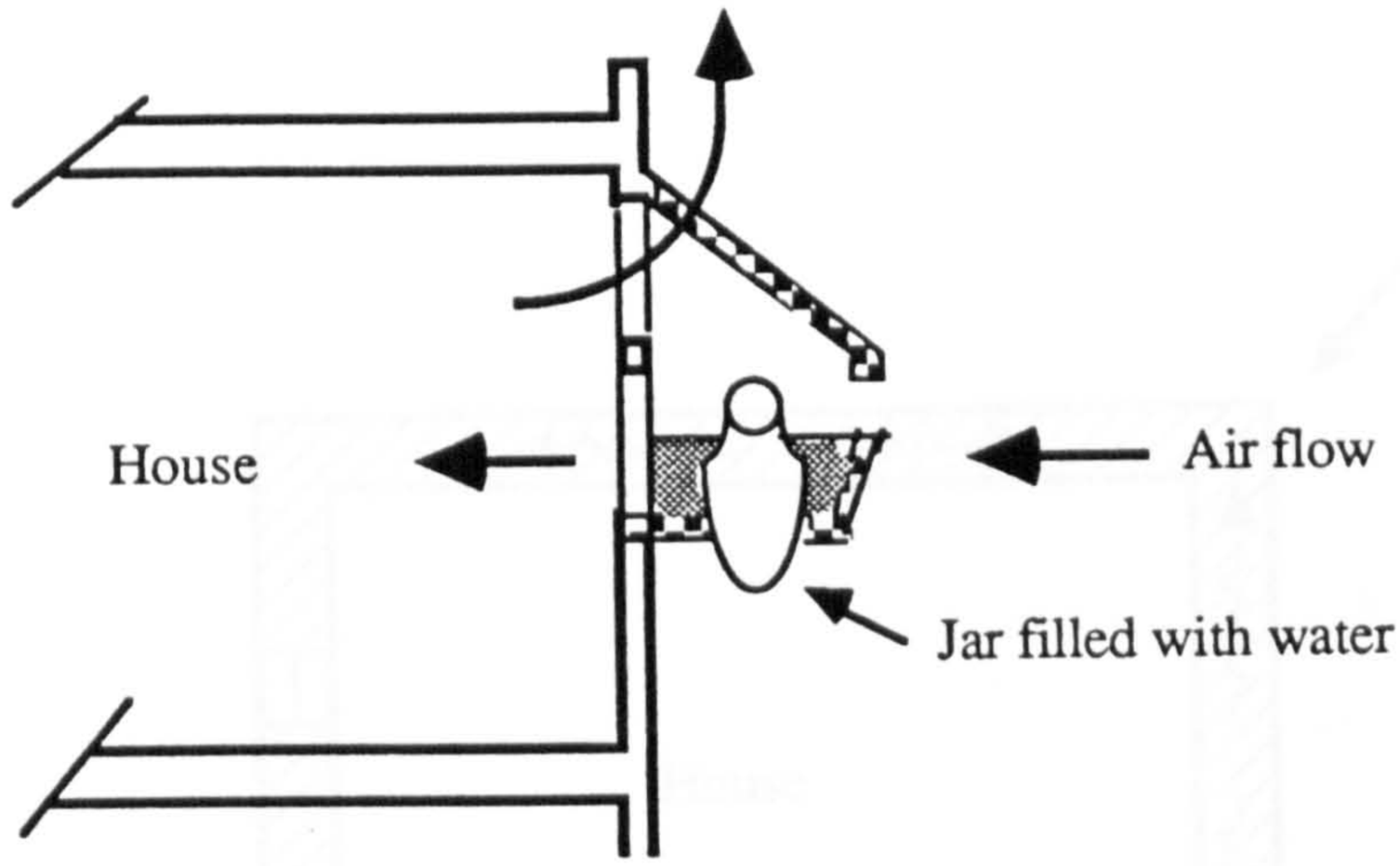

a) Jar filled with water fixed to a window to cool incoming outside air.by evaporation.

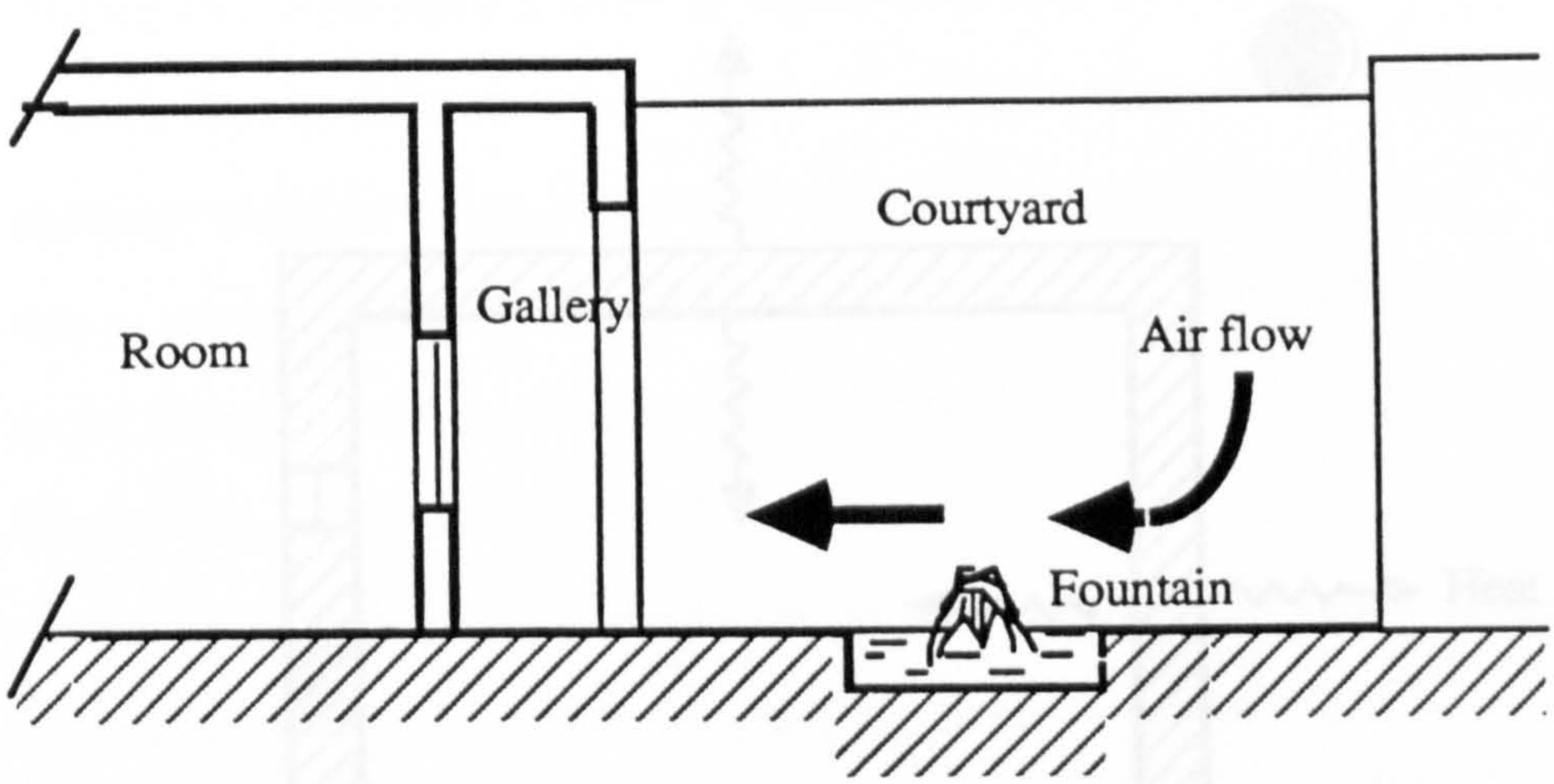

b) Pools and fountains are built in courtyards for evaporative cooling of the house.

Figure 2.3 Evaporative coolers used in hot dry climates

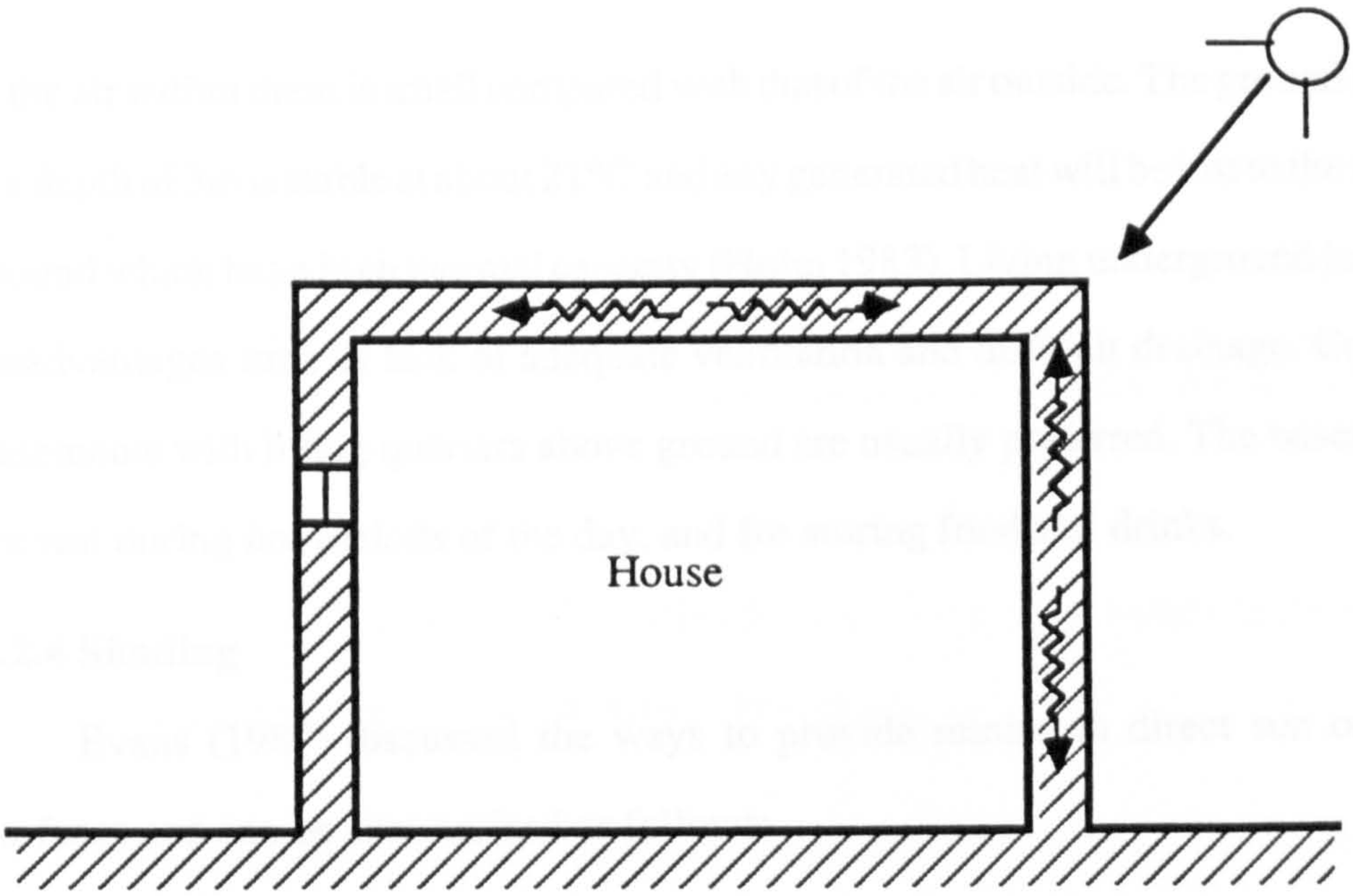

a) During the day thick walls and roofs perform as reservoirs of heat.

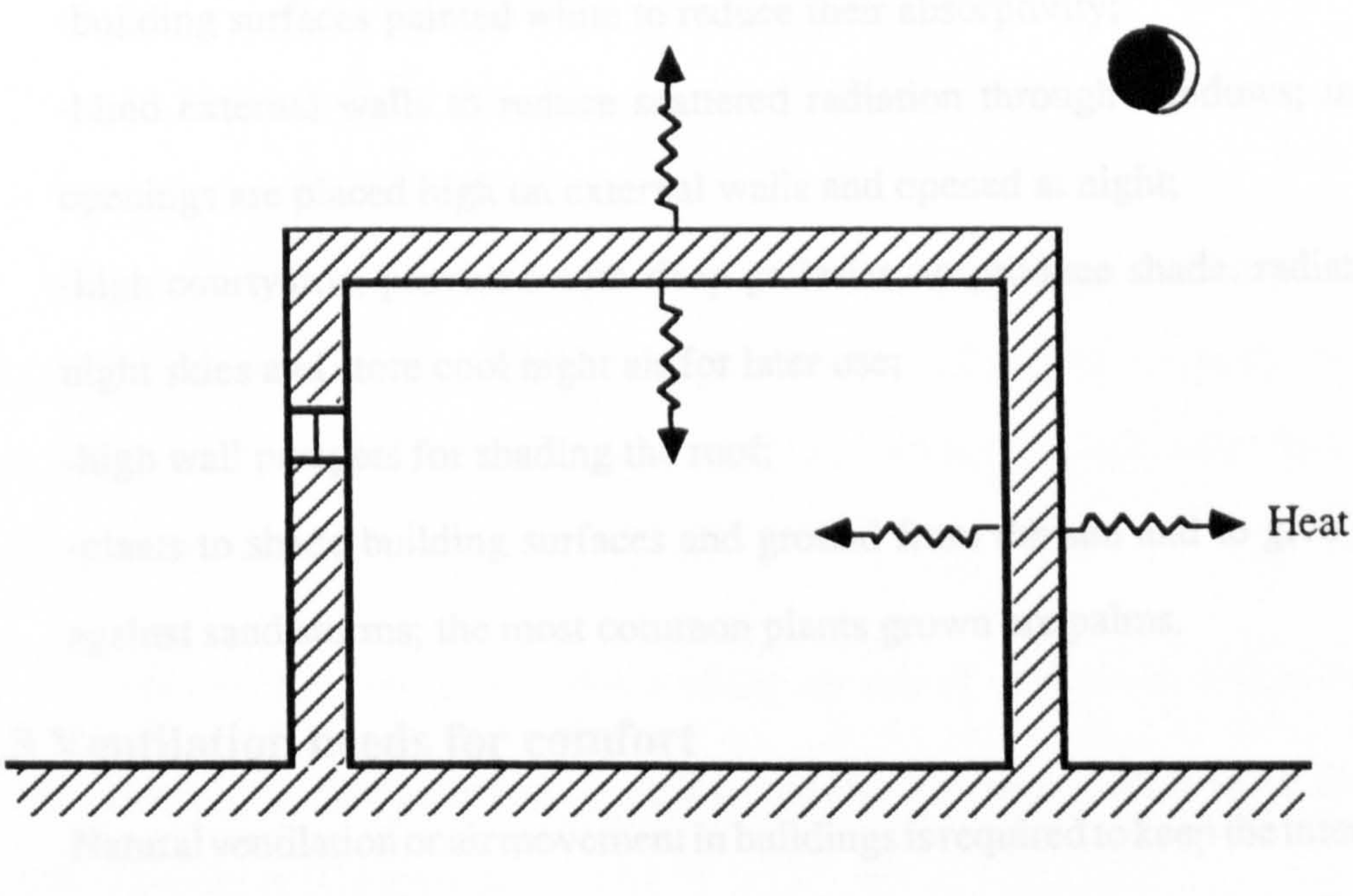

b) At night heat is partly transferred to the inner spaces and partly is dissipated to the clear nocturnal sky.

Figure 2.4 Thermal performance of a heavy building.

of the air within them is small compared with that of the air outside. The ground temperature at a depth of 3m is stable at about 21°C and any generated heat will be lost to the surrounding ground which has a high thermal capacity (Holm 1983). Living underground has numerous disadvantages such as lack of adequate ventilation and difficult drainage. Consequently, basements with living quarters above ground are usually preferred. The basement is used for rest during hot periods of the day, and for storing food and drinks.

2.2.4 Shading

Evans (1980) discussed the ways to provide minimum direct sun onto building surfaces and can be summarised as follows:

-compact buildings in cellular layouts with winding and narrow streets to reduce surface exposure to direct sun and to minimise heat build up on building surfaces,

-building surfaces painted white to reduce their absorptivity;

-blind external walls to reduce scattered radiation through windows; usually the openings are placed high on external walls and opened at night;

-high courtyards, provided with deep galleries, to produce shade, radiate to clear night skies and store cool night air for later use;

-high wall parapets for shading the roof;

-plants to shade building surfaces and ground from the sun and to give protection against sand storms; the most common plants grown are palms.

2.3 Ventilation needs for comfort

Natural ventilation or air movement in buildings is required to keep the internal spaces healthy, to cool the surrounding surfaces of a building, and for thermal comfort.

2.3.1 Health

Ventilation is needed to remove smells, carbon dioxide, products of combustion, pollutants generally, and to prevent condensation in dwellings. But the rate of ventilation

for health is rather small compared to the rate of ventilation required for cooling. Studies of the required rates of ventilation to keep a space healthy have produced different ventilation standards.

Evans (1980) suggested one air change per hour is the minimum rate of ventilation for odour removal.

Yaglou and Witheridge (1937) recommended that to keep human body odours down, a minimum rate of ventilation per person should be:

-$0.2m^3$/min for an air space of $40m^3$ volume occupied by three adults, or $0.07m^3$/min per person

-$0.45m^3$/min if the number of occupants increases to 7 adults, or $0.06m^3$/min per person

-and $0.7m^3$/min for 14 occupants, or$0.05m^3$/min per person. The differences between these are hardly significant.

Klauss *et al.* (1970) summarised work carried out by Tredgold (1836) who reported that the minimum air supply rate necessary to remove carbon dioxide, body moisture and to supply oxygen to candles and lamps is $0.1m^3$/min per person, little more than suggested by Yaglou and Witheridge.

ASHRAE (1985) recommended a minimum rate of ventilation of 0.14 m^3/min per person to keep the concentration of carbon dioxide low, again rather more than Yaglou and Witheridge or Klauss *et al.*

However, Klauss *et al.* (1970), on the other hand, stated that the concentration of carbon dioxide was not a very good indicator for ventilation rate requirements.

2.3.2 Structural cooling

As stated above, ventilation can help reduce the temperature of the air inside buildings if the outside air is cooler than that inside.

If a room at an air temperature T_{ar} is ventilated with outside air at temperature T_{ao}, the heat removed by ventilation is:

$$Q_v = Mc(T_{ar} - T_{ao}) \tag{2.1}$$

As the room air temperature drops, heat is transferred from the walls to the air by convection. Convective cooling is expressed by:

$$Q_c = Ah_c(T_{sm} - T_{ao}) \tag{2.2}$$

Evans (1980) suggested that a ventilation rate of 10 air changes per hour is enough to assist structural cooling.

Yagoubi and Golneshan (1986), presented a theoretical analysis of a effect of variable ventilation at night and during the day on the temperature of the basement using traditional wind towers. Ventilation at night was allowed from 2300 to 0600 hours. With one air change per hour the basement temperature remained constant. With ventilation increased up to 12 air changes per hour, the basement air temperature dropped $2K$ during the day. Increasing the ventilation rate from 12 to 30 air changes per hour did not make a significant difference to the basement temperature. By keeping night ventilation constant at 30 air changes per hour, and varying day-time ventilation from 1 to 3 air changes per hour, it was found that basement temperature remained high. They pointed out that ventilation in hot dry climates should be discouraged during the day and should only be allowed at night.

2.3.3 Ventilation and thermal comfort of the human body

Thermal comfort depends on several factors such as mean radiant temperature, air temperature, relative humidity and air movement. Over the last decade many studies have

shown the importance of air movement on improving thermal comfort. Air movement increases comfort because it increases heat loss by convection and evaporation from the human body. The amount of heat loss by convection depends on the speed and temperature of the air. van Straaten (1967) stated that at normal conditions i.e. air temperature 18°C, relative humidity from 40% to 60%, and air velocity less than 0.25m/s, a person engaged in sedentary work will dissipate 30% of heat by convection, 25% by evaporation and the rest by radiation.

Winslow *et al.* (1939) investigated the influence of air movement upon heat loss from a clothed human body. The convection heat transfer coefficient was:

$$h_c = 12v^{0.5} \tag{2.3}$$

for $v < 2.6m/s$

so that the cooling effect of air at 0.5m/s is about twice that of air at 0.1m/s, and if the air is at 2m/s the cooling effect is about four times greater.

Evans (1980) pointed out that air at a velocity up to 1 m/s is comfortable, but beyond that air movement is unpleasant and causes movement of dust and papers. He suggested 100 air changes per hour or more for cooling the human body. Heat loss by convection takes place if the air temperature is lower than skin temperature (usually between 31 °C and 34 °C). As air temperature approaches skin temperature, heat loss by convection will decrease. If the radiant temperature of the room equals or exceeds skin temperature, the only way to dissipate heat is by evaporation. Lack of air movement will decrease evaporation, as the air layer adjacent to the skin will become saturated (Koenigsberger *et al.* 1974). If the body is exposed to severe conditions, with the surrounding air saturated and warmer than skin temperature, and if the air speed is very low, heat gain will be positive and the deep body temperature will begin to rise, causing a heat stroke.

Fanger (1963) gave a general equation for human comfort where he includes:

-environmental variables such as air humidity, mean radiant temperature and air velocity,

-type of activity

-type of clothing.

He constructed comfort curves based on mean radiant temperature versus air velocity with activity level as a parameter. For a person wearing light clothing doing sedentary work, the comfort line ranges from 25 to 28 $°C$ for velocity up to 1.4 m/s. Discomfort might be possible because of draughts when the velocity of the air is more than 0.6m/s.

Olgyay (1963) constructed a bio-climatic chart for a man doing sedentary work wearing 1 clo. (a business man's suit in the U.S before 1940). He showed a comfort zone dependent on relative humidity, air temperature and velocity. His chart shows clearly how this comfort zone is increased by air movement. The upper comfort limit with still air for 50% RH is 30^oC but this limit goes to 36^oC with an air movement of 1 m/s. The only disadvantage of Olgyay's index is that he uses dry bulb temperature instead of mean radiant temperature which is an important parameter in comfort.

Missenard (1933) developed a comfort scale called "resultant temperature" $T_{res}°C$ in which the mean radiant temperature $T_{mr}°C$, the air temperature, $T_a°C$ and the air velocity, vm/s, were combined. The resultant temperature is usually recorded by a thermometer at the centre of a blackened globe 100mm in diameter. The resultant temperature is used as an index to indicate comfort in cold climates but it also suitable for hot climates (CIBSE 1986). It states that;

$$T_{res} = \frac{T_{mr} + T_a(10v)^{0.5}}{1 + (10v)^{0.5}} \qquad (2.4)$$

At an indoor air velocity of $0.1 m/s$, the resultant temperature simplifies to:

$$T_{res} = 0.5T_{mr} + 0.5T_a \tag{2.5}$$

Unfortunately indoor air is not always still, so that for higher air velocities, say v = 0.3m/s, the resultant temperature becomes:

$$T_{res} = 0.37T_{mr} + 0.63T_a \tag{2.6}$$

Recommended values of the resultant temperatures for comfort are summarised by the CIBSE Guide (1986). For arid climates the recommended resultant temperature is 28 $°C$.

Various studies have been carried out in temperate climates for sedentary work in normal clothing. The results showed that comfort temperatures lay between 20 and 24 $°C$ (Bedford 1936, Webb 1964 and Nicol 1975). However, Webb (1964) showed that subjects in the hot dry climates of Northern India and Iraq felt comfortable in much warmer conditions than were acceptable in hot humid conditions.

Nicol (1975) made a comparative study on several acclimatised subjects for England, Baghdad in Iraq and Roorkee in India. He used the resultant temperature as an index. He observed that English subjects were comfortably warm at globe temperature between 20 and 25 $°C$ whereas in the hot dry conditions of Baghdad and Roorkee they were most comfortable at a globe temperature of 32 $°C$. By increasing the air movement up to or above 0.25 m/s, the sedentary acclimatised subjects had little discomfort, not more 20% were uncomfortable until the globe temperature rose above 36 $°C$. The large difference in comfort conditions between cold and hot dry climates may be attributed to acclimatisation and habits of people.

2.4 Ventilation theory

Ventilation is generally necessary for purposes such as pollution control, and removal of excessive heat generated from occupants and hot weather. Ventilation may be achieved either mechanically, using fans and ventilators, or naturally using wind and/or stack effect. Mechanical equipment reduces internal pressures which induces air intake through openings in the building envelope. It may be affected by the action of wind and stack effect unless the building envelope is airtight, but this may reduce internal air quality (Liddament 1986). Totally controlled ventilation is expensive and has running costs which are generally not acceptable.

Natural ventilation results from winds and a temperature difference between external and internal air (stack effect). The presence of fireplaces, chimneys and wind towers enhances the ventilation of dwellings. The disadvantage of natural ventilation is that the rate of air flow cannot be readily controlled due to climatic changes. Wind and stack effect can act independently or be combined. Natural ventilation occurs through a wide variety of openings such as windows, doors, chimneys and cracks. If there is an applied pressure difference across an opening then a flow of air will take place. The magnitude of air flow will depend upon the dimensions and shape of the opening, which, according to CIBSE Guide (1986), can be expressed by the following equation;

$$Q_v = C_d A \left\{ 2\frac{(\Delta P)}{\rho} \right\}^{0.5} \tag{2.7}$$

where

Q_v = the rate of ventilation (m^3/s)

C_d = discharge coefficient which has a value equal to that for a sharp-edged opening which is 0.6.

ΔP = pressure difference across opening (Pa)

A = area of opening (m^2)

A typical building will have various openings differently placed, so that an effective area A_e is used to represent the openings. The effective area of a number of openings $A1$, $A2$ and so on, combined in parallel, across which the same pressure is applied, is given by CIBSE Guide (1986) as,

$$A_e = A1 + A2 + \ldots$$

For a number of openings combined in series the effective area may be obtained by adding the inverse squares and taking the inverse of the square root of the total as follows,

$$\frac{1}{A_e} = \frac{1}{A1^2} + \frac{1}{A2^2} + \ldots$$

The use of a discharge coefficient in the estimation of air flow rate is suitable for sharp edged orifices or sharp edged openings in a system. But in reality, the flow of air may take place within a system of complicated configuration whereby the discharge coefficient is not appropriate. For cracks around doors, windows and in the building envelope generally, with long flow paths, the nature of the flow is different and is dominated by the effect of viscosity (Liddament 1986). The flow through these cracks is generally laminar and is proportional to the applied pressure difference. A general equation known as the "power-law equation" is essentially given to approximate the air flow rates through any flow system configuration for both laminar and turbulent regimes. This is expressed as follows;

$$Q_v = K(\Delta P)^n \qquad (2.8)$$

where

K = flow coefficient, which depends on the configuration of the opening

n = flow exponent, which depends the type of flow. It ranges from 0.5 for turbulent flow to 1.0 for laminar flow.

Equation 2.8 comes from the fact that a driving total pressure such as stack effect, wind or any external applied pressure should be equal to the pressure losses throughout a system where a fluid flow is taking place (Cronvall 1980a, CIBSE 1986). If we assume for example a flow of air taking place from the outside into a duct and then out of the duct due to an applied pressure ΔP. If the duct has an area A_d vertical to the flow direction, with inlet area of A_ϵ and outlet area A_o, thus the driving pressure will be equal to the pressure losses due to inlet, friction along the duct and exit. These pressure losses are generally expressed in terms of velocity pressure as shown below,

$$\Delta P = \frac{1}{2}K_\epsilon \rho_\epsilon v_\epsilon^2 + \frac{1}{2}K_d \rho_d v_d^2 + \frac{1}{2}K_o \rho_o v_o^2 \qquad (2.9)$$

where

K_ϵ = inlet loss coefficient, equal to 0.5

K_d = loss coefficient along the duct which is dependent on friction factor and the dimensions of the duct, $K_d = 4fL/D_h$, where f is the friction factor, L is the length of the duct (m), and D_h is the hydraulic diameter of the duct (4 area/perimeter).

K_o = outlet loss coefficient, equal to 1.

Values of K for different system configurations are listed in the CIBSE Guide (1986) and Cronvall (1980).

The velocities in equation 2.9 can be converted in terms of volume flow Q_v giving,

$$\Delta P = \frac{1}{2}\sum_i^n \frac{K_i \rho_i}{A^2} Q_v^2 \qquad (2.10)$$

Equation 2.10 can be rearranged for Q_v which will then be in similar form as equation 2.8, with the exponent $n = 0.5$. Equation 2.10 is in fact a general fluid flow equation for a turbulent regime in pipes, ducts and flues and is applied in buildings (Cronvall 1980).

The air flow rate in ducts and chimneys will be then given by,

$$Q_v = A_d\left(2\frac{A_d}{PfL\rho}\right)^{0.5}(\Delta P)^{0.5} \qquad (2.11)$$

where

A_d = cross sectional area of opening (m^2)

P = cross sectional perimeter (m)

f = friction coefficient

ρ = air density in the duct (kg/m^3)

The pressure difference ΔP in natural ventilation is due to wind or to stack effect.

Wind pressure is generally expressed by Bernoulli's equation as,

$$\Delta P = (1/2)C_p\overline{v}^2 \qquad (2.12)$$

where

C_p = pressure coefficient which depends on the wind direction and height

$\overline{v}$ = mean wind speed (m/s)

The wind speed varies with height and the type of terrain and topography. Generally, the meteorological data for winds are recorded at 10m above the ground which should be corrected for design applications depending on the height and type of terrain (CIBSE Guide 1986, BRE Digest 1978).

A pressure difference may arise as a result of density differences between the air inside a building and the outside which will create air movement through openings. When the internal air temperature is higher than that outside, air enters through openings in the lower parts of the building and escapes through openings at higher level. The pressure difference due to temperature difference between the air inside and that outside may be given by;

$$\Delta P = gZ(\rho_{ai} - \rho_{ao}) \tag{2.13}$$

where, ρ_{ai} and ρ_{ao} are densities of inside air and the outside air (kg/m^3). From the gas law, the density of air at temperature T is given by its density at a reference temperature usually $0°C$ or $273°K$, where dry air has a density of 1.293 kg/m^3 (CIBSE 1986). This gives $\rho = 1.293(273/(273+T))$. So equation 2.13 becomes;

$$\Delta P = \frac{3463Z}{(T_{ao}+273)(T_{ai}+273)}(T_{ai} - T_{ao}) \tag{2.14}$$

where

T_{ai} = absolute temperature of air inside building ($°K$)

T_{ao} = absolute temperature of outside air ($°K$)

Z = the height difference between two openings (m)

2.5 Air moving devices

There are various ways for moving air passively inside buildings, those most relevant are solar heated chimneys and traditional open fire chimneys.

2.5.1 Thermal chimneys

Thermal chimneys have been used to eliminate smells from latrines, for drying and for the ventilation of buildings, especially parts below ground.

Ryan and Mara (1981) worked on the application of solar heated vent pipes to exhaust smells from traditional pits or "squat toilets" in Botswana and Zimbabwe. Vent pipes can exhaust odours from pits, but there are problems. They reported that in windy places, wind is the predominant factor in raising the rate of ventilation and sometimes works in the opposite direction to stack effect. Vent pipes might not be effective in wet seasons when cloud cover can be high. Their work was mainly concerned with a rather tinny devices without regard to their thermal capacity. The flow of air through the vent pipes was assumed fully upwards. Field measurements were not reported.

Zambrano and Alvarado (1984) reported a theoretical study on the use of a thermal chimney for drying. Agricultural products such as fruits can be over-dried with high solar radiation and low air velocity. Air movement using a chimney in the shape of a truncated inverted cone was reported to be greater than with a cylindrical one. The temperature decrease recorded was of the order of 12 K.

Underground structures usually do not benefit from cross ventilation. The inside air temperature of an underground building is lower than the ambient air temperature during the day, which will not help ventilation. Orlowski (1979) discusses the use of a thermal chimney projecting through the roof to the outside. Air movement may be increased by heating the air at the bottom using a solar collector with a hot water coil. That was in the form of a proposal and no results were reported.

Haisley (1981) reported a theoretical study on the use of a solar heated chimney combined with an evaporatively cooled one to provide cooling ventilation during hot days. In the solar chimney the air is heated using a solar heated plate at the bottom of the chimney, whereas in the evaporative shaft, the air is cooled by evaporation of water. No results on the rate of air flow were reported.

2.5.2 Open fire chimneys

A solar chimney and an open fire chimney differ in that in the former the heat needed to cause an upward flow does not come from a fire at the bottom, but from the sun. But in many respects they are similar. Experience in designing traditional flues may therefore be relevant.

The rate of air flow in a chimney in general depends on:

-the temperature difference between the hot gas in the chimney and the cold outside air,

-the height of the chimney,

-its internal resistances,

-external influences such as wind

Temperature difference creates a pressure difference (buoyancy pressure), which is equal to the difference between the pressure exerted by the weight of a column of gas in the flue at temperature T_g and that exerted by an equivalent column of outside air at temperature T_{ao}, given by:

$$\Delta P = gZ(\rho_g - \rho_{ao}) \qquad (2.15)$$

If the buoyancy pressure is not enough to exhaust the gas to the outside, smoke can go back into the house. The main factor that can cause low buoyancy pressure in a chimney is heat loss to the environment, especially in the presence of wind. Various recommendations dealing with this problem are given by BRE Digest (1973) which recommends the reduction of heat loss from a chimney by:

-incorporating thermal insulation in the chimney

-reducing the size of the flue

Page and Cheyney (1980), suggest that a chimney should be placed internally wherever possible.

Daws (1966) pointed out that heat loss is caused by a large secondary air flow through a fire front. A throat restrictor can be used to narrow the inlet so that secondary draughts will be reduced (Fox & Whittaker 1957).

The height of a chimney is also an important factor which increases the buoyancy pressure and thus the amount of air flow. It is well known that the higher a chimney, the greater is the rate of combustion.

The rate of air flow decreases as the resistance in the flue increases. This resistance is

caused by bends and the roughness of internal surfaces. Bends should be avoided whenever possible and be no greater than 45 ° as they will increase resistance (Page and Cheyney 1980). Rough surfaces with low flue diameters increase flow resistance if the flow is turbulent.

Wind can cause downdraught which can be modified by cowls etc. (Page & Cheyney 1980). However winds can help increase the flow rate of a flue by suction. This can only occur if the chimney top is placed away from obstructions, such as roof ridges and nearby objects (Daws 1966). Schmitt and Engahl (1948) suggested that a chimney should rise at least 0.3m above the ridge to avoid the region of turbulence.

2.6 Heat transfer mechanisms in buildings

Heat is transferred via the mechanisms of conduction, radiation and convection. Conduction of heat takes place in solid materials from points of higher to points of lower temperature. Radiation takes place between building surfaces of different temperatures. Convection takes place between a surface and the adjacent air. These mechanisms are explained in detail in the following sections.

2.6.1 Conduction

The rate of heat flow by conduction in a material depends on the following quantities:

-the thermal conductivity of the material,

-the area through which heat flows measured perpendicularly to the direction of the heat flow,

-and the temperature gradient at the section with respect to distance in the direction of flow.

The mathematical form to express heat by conduction is given by;

$$Q/A = -\lambda dT/dx \qquad (2.16)$$

The direction of increasing distance x is the direction of positive heat flow. Since according to the second law of thermodynamics heat will flow from points of higher temperature to points of lower temperature, heat will flow will be positive when the temperature gradient is negative. Where Q/A is the rate of heat flow expressed in W/m^2K, λ is the thermal conductivity of the material indicating the quantity of heat flow across a unit area if the temperature gradient is unity, it is expressed in W/mK.

Integrating equation 2.14 in respect to x, yields

$$Q/A = \frac{\lambda}{x}\Delta T \tag{2.17}$$

where, ΔT is the temperature difference between the hotter part and the cooler one, (K).

2.6.2 Radiation

The quantity of heat leaving a surface depends upon the absolute temperature and the nature of the surface. A surface of area $A\ m^2$ at absolute temperature $T°K$ and emissivity ε radiates energy at the rate of:

$$\sigma\varepsilon A T^4 \tag{2.18}$$

where σ is the Stephan-Boltzmann constant.

The radiation exchange between two surfaces at temperatures T_1 and T_2 $°K$ with emissivities ε_1 and ε_2 is given by:

$$C_{12}\sigma(T_1^4 - T_2^4) = h_r(T_1 - T_2) \tag{2.19}$$

Thus, the radiation coefficient is given by:

$$h_r = \frac{\sigma(T_1 + T_2)(T_1^2 + T_2^2)}{\frac{1}{\varepsilon_1} - 1 + \frac{A_1}{A_2}\left(\frac{1}{\varepsilon_2} - 1\right) + \frac{1}{F_{12}}} \tag{2.20}$$

where,

C_{12} = configuration factor which is given by:

$$C_{12} = \frac{1}{\frac{1}{\varepsilon_1} - 1 + \frac{A_1}{A_2}\left(\frac{1}{\varepsilon_2} - 1\right) + \frac{1}{F_{12}}} \tag{7.21}$$

F_{12} = relative shape factor.

The relative shape factors, F_{12} etc, for simple and complex shapes are presented in detail by Howell (1982) and Wong (1977).

2.6.3 Convection

Convective heat transfer occurs between a surface at a temperature T_s $°C$ of area A (m^2) with an adjacent fluid such as air at a temperature T_f $°C$. It depends on the temperature difference between the surface and the air, air movement over the surface, the roughness of the surface, and the orientation of the surface (horizontal, inclined or vertical). It is generally defined from the following equation:

$$Q/A = h_c(T_s - T_f) \tag{2.22}$$

where h_c is the convection heat transfer coefficient (W/m^2).

Various correlations for convective heat transfer coefficients used for various building components were found in the literature. Most of these were empirically derived for sizes smaller than those of building surfaces which are much larger. The magnitude of the convection heat transfer coefficient depends on the process involved. For still air or low velocities, natural convection takes place and the heat transfer coefficient depends on

the temperature difference between the air and the surface. The natural heat transfer coefficient over a vertical surface is calculated from empirically derived equations given in a general form by:

$$\frac{h_c Z}{\lambda_a} = C(GrPr)^n \tag{2.23}$$

where

C and n = constants whose values depend on whether the flow is laminar or turbulent. These are given by several authors such as McAdams (1954), and Eckert & Jackson (1950). For laminar flow $C = 0.55$ and $n = 1/4$, for turbulent flow $C = 0.13$ and $n = 1/3$.

Alamdari and Hammond (1983) have stated that one of the big problems in heat transfer by convection is the use of two part correlations, one for laminar and one for turbulent flow with an abrupt change in exponent. This can give rise to numerical instability in dynamic models. They have proposed an equation which fits both laminar and turbulent flows over vertical and horizontal surfaces. They point out that for horizontal surfaces, with downward heat flow, there will be no turbulence due to thermal stratification. Their correlations are given in SI units as follows:

a) for both vertical and horizontal surfaces,

$$h_c = \left\{\left(A\left(\frac{\Delta T}{Z}\right)^p\right)^m + (B(\Delta T)^q)^m\right\}^{\frac{1}{m}} \tag{2.24}$$

where A, B, p, q and m are empirical constants which depend on the heat flow direction, summarised as follows:

	A	B	p	q	m
Vertical surface	1.5	1.23	1/4	1/3	6

Horizontal surface flow upwards	1.4	1.63	1/4	1/3	6

b) for horizontal surfaces with downward heat flow,

$$h_c = 0.6\left(\frac{\Delta T}{Z^2}\right)^{0.2} \tag{2.25}$$

IHVE Guide (1970) states that the convection heat transfer coefficient,

-for a vertical surface $h_c = 3W/m^2K$

-for a horizontal surface with heat flow upwards $h_c = 4.5W/m^2K$

-for a horizontal surface with heat flow downwards $h_c = 1.5W/m^2K$

For moving air or high velocities, forced convection occurs and the heat transfer coefficient depends on the velocity.

In the case of air moving parallel to a vertical plate, the convective heat transfer coefficient, which was originally derived by Nusselt and Jurges (1922) and later was reported by McAdams (1954), is:

$$h_c = 5.8 + 4.1\overline{v} \tag{2.26}$$

where

$\overline{v}$ = air speed

McAdams merely requires $v < 5m/s$, but gives no lower limit.

Waters (1977) summarised most correlations in natural and forced convection. He found that the use of an average value of $6W/mK$ for the heat transfer coefficient for all internal surfaces of a room with an air speed of $0.36m/s$, showed much better agreement between measured and calculated values.

Examination of McAdams equation shows a weakness. If the velocity is very low, when the heat transfer coefficient is largely by natural convection, the value of the natural convection coefficient according to CIBSE Guide is3W/m^2K. This is about half of the value given by McAdams if v is taken as zero.

McAdams (1954) stated that both forced and natural convection should be calculated and the larger of the values used.

2.7 Heat transfer and air flow mechanisms in cavities

Several studies concern cavities in general. These mainly deal with heat transfer over small surfaces. However, there is a lack of information on the design of wall cavities for ventilation in buildings. Review of relevant work may be divided into two: wall cavities and Trombe walls.

Cavities are used in buildings for thermal insulation and moisture control. They may reduce the quantity of material used in a wall, but this is often offset by greater construction cost. A cavity wall may improve thermal performance because it reduces heat transfer to the inside due to the thermal resistance offered by the air gap (usually 50mm) (figure 2.5). The cavity may be wholly or partially filled with insulating material such as polystyrene, glass fibre or vermiculite. These materials may deteriorate from condensation and they may encourage water penetration. In wet climates, cavities are used to protect the house from wind driven rain and are sometimes ventilated and drained to remove water. In hot climates, cavities are always sealed.

Natural convection in a viscous fluid such as air, in an enclosure bounded by parallel vertical walls, has been widely studied (Jakob 1946, Batchelor 1954, Emery *et al.* 1965, MacGregor *et al.* 1969).

The most important parameters that affect heat transfer in enclosed cavities are:

-the aspect ratio (height to width ratio)

-the temperature difference between the two sides

-the nature of the flow (laminar or turbulent).

Jakob (1946) and Emery (1965) suggested that the aspect ratio has an effect on the heat transfer coefficient, but de Graaf reported no such effect (de Graaf 1953).

Batchelor (1954) studied heat transfer in a closed cavity between two vertical walls at different temperatures. Different values of height, width, and the Raleigh number were investigated. He observed that for cavities with widths less than 10mm, heat flow will be mostly by conduction. If the air gap is widened from 10mm to 25mm, the heat transfer by convection increases but that by conduction will decrease. With more than a 25mm wide gap, the heat transfer remains constant at a value proportional to the height.

Eckert and Carlson (1961) observed that the temperature of the central region of air in a cavity increases almost linearly in the vertical direction. This contradicts the assumption of an isothermal core suggested by Batchelor (1954). They found that for large Grashof numbers and lower height to thickness ratios, boundary layers appear along the surfaces of the enclosure and heat transfer is similar to that of a single plate. This agrees with Jakob's observations that if the aspect ratio of a cavity were less than two, the relation for the convective heat transfer coefficient over a single plate applies (Jakob 1949).

Jakob (1946) suggested that the transition from laminar to turbulent flow occurs at $Ra = 2 \times 10^5$ whereas Emery and Chu (1965) believed that laminar flow holds at least up to $Ra = 10^7$.

In general heat transfer in enclosures is given by:

$$\mathrm{N} = C Gr^m \left(\frac{Z}{W}\right)^n \qquad (2.27)$$

where

-for laminar flow

$C = 0.18, m = 1/4, n = -1/9$

-for turbulent flow

$C = 0.065, m = 1/3, n = -1/9$

In a Trombe wall the cavity is formed between external glazing, which may be double, and a massive wall. It is opened to the house by two vents, one at the top and one at the bottom. The air within is used for heating in winter (figure 2.6).

Little work has been done related to two parallel plates with open ends, because of the complexity of the problem.

Balcomb *et al.* (1977) studied convective heat transfer and air flow using a one dimensional, implicit thermal network analysis. A forced convective heat transfer coefficient over a vertical surface given by McAdams (1954) was used:

$$h_c = 5.7 + 4.1\bar{v} \tag{2.28}$$

The air flow rate was determined by equating the pressure caused by buoyancy with the losses in the cavity and the vents. The losses in the cavity were considered negligible as compared with the losses in the vents. The volume flow was given by:

$$V = C_d A_{ve} (2gZ\beta(T_{ac} - T_{ao}))^{0.5} \tag{2.29}$$

where

C_d = discharge coefficient of the two vents in series, of similar size = 0.6.

The temperature increase along the duct was assumed linear.

The heat balance for the flow in the duct was given by:

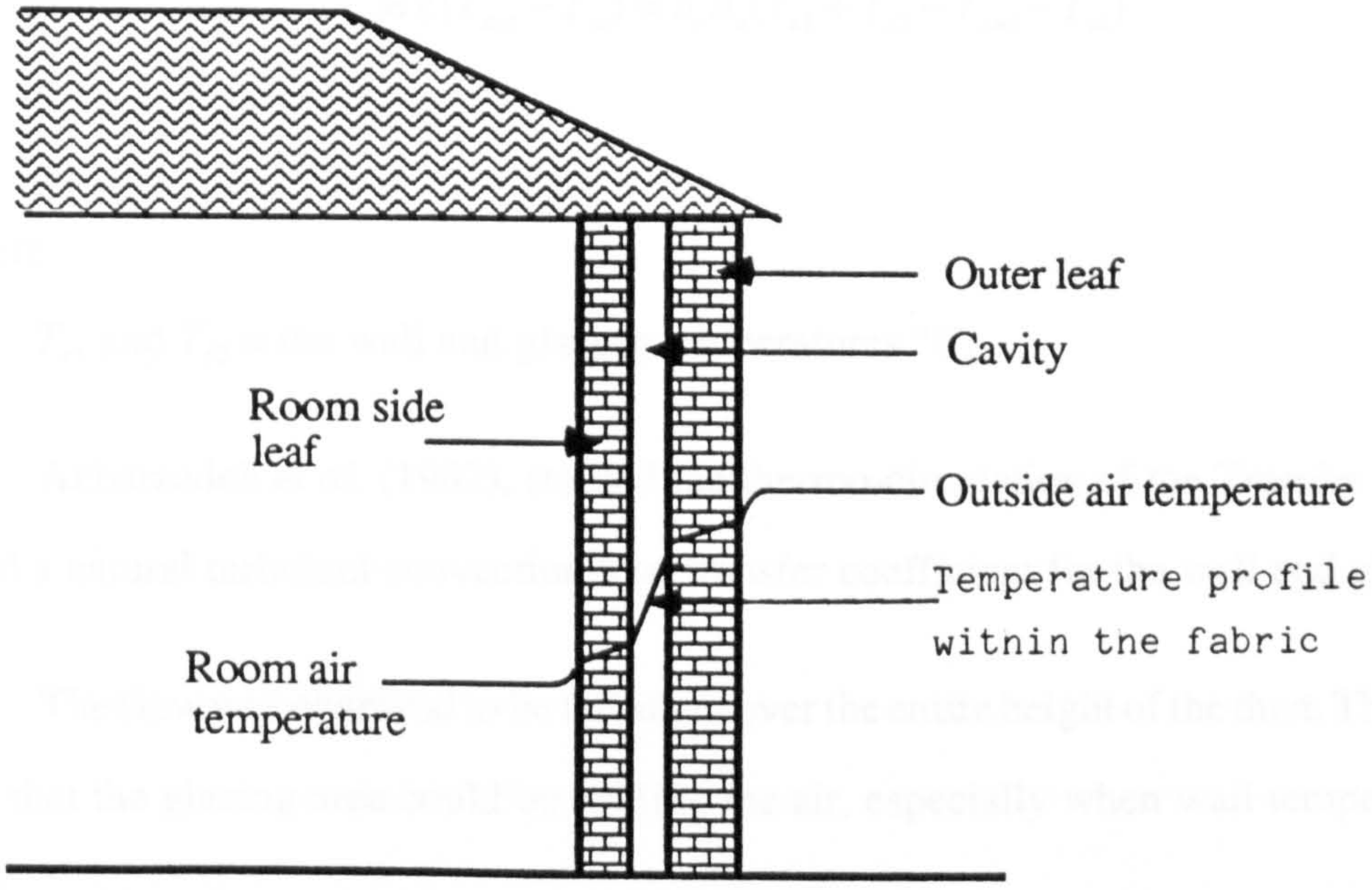

Figure 2.5 wall cavity

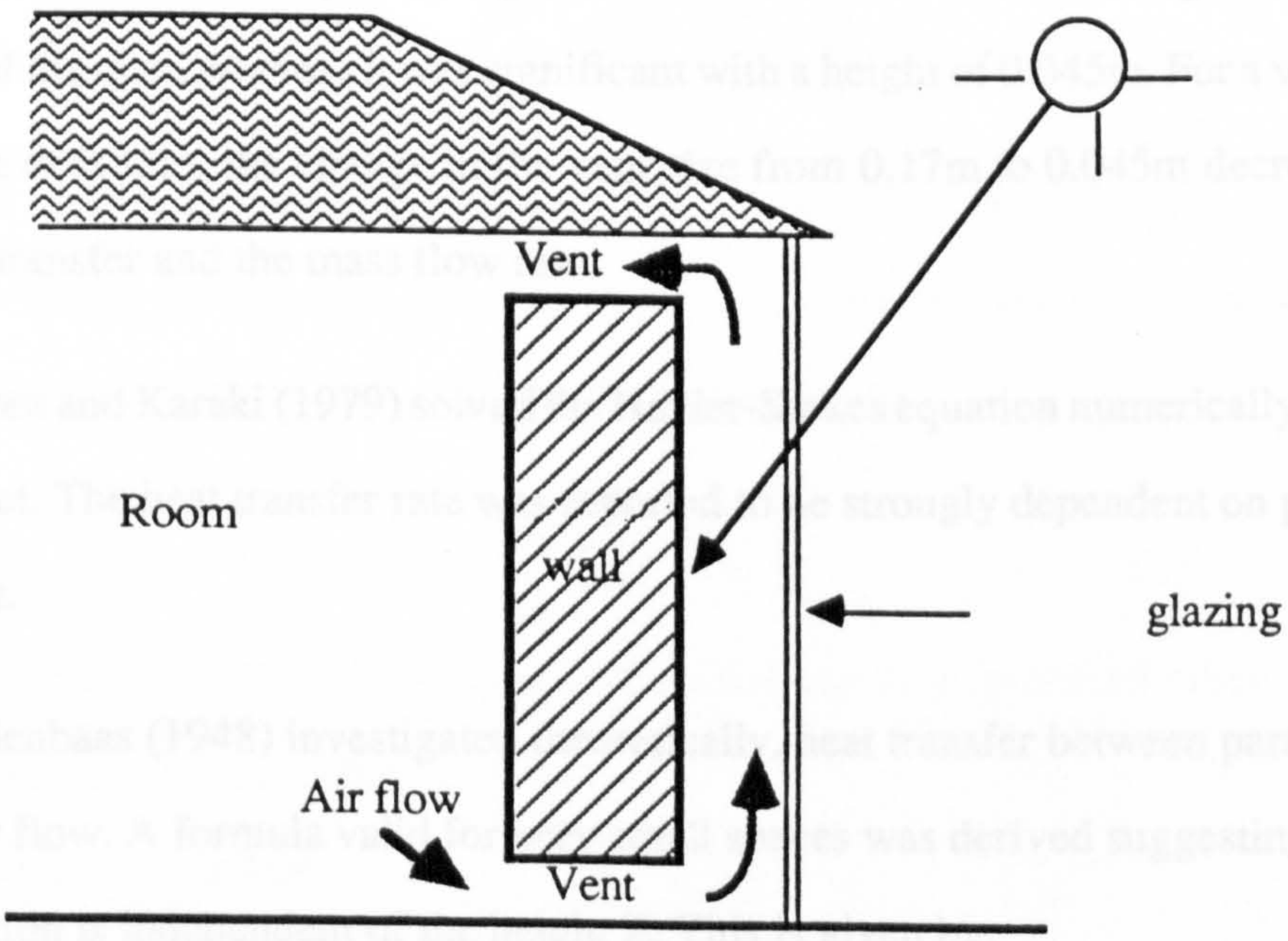

Figure 2.6 Trombe wall

$$Mc(T_{out}-T_{ai})=h_cA_s(T_{s1}+T_{s2}-T_{out}-T_{ai}) \tag{2.30}$$

where

T_{s1} and T_{s2} = the wall and glazing temperatures °C.

Akbarzadeh *et al.* (1982), studied the thermo-circulation of the Trombe wall. They used a natural turbulent convection heat transfer coefficient for the wall and glazing.

The flow was observed to be turbulent over the entire height of the duct. They pointed out that the glazing area could be cooling the air, especially when wall temperatures are low.

No significant difference in performance with gap widths between 0.1m and 0.35m was found. However, they found that performance was slightly better for a 0.25m duct width. The vent loss using vent heights of 0.17m and 0.095m was not significant in relation to that of the duct, whereas it was significant with a height of 0.045m. For a wall to glazing distance of 0.35m, the change in the vent size from 0.17m to 0.045m decreased the rate of heat transfer and the mass flow rate.

Pratt and Karaki (1979) solved the Navier-Stokes equation numerically for a Trombe wall duct. The heat transfer rate was reported to be strongly dependent on position along the duct.

Elenbaas (1948) investigated theoretically, heat transfer between parallel plates for laminar flow. A formula valid for very small spaces was derived suggesting that the heat dissipation is independent of the height Z. This is given by:

$$h_c=\frac{\lambda_a}{24Z}Ra \tag{2.31}$$

In spaces between plates, the temperature of the outflowing air is the same as that of the plates. With large separation the above formula is not applicable, as in that case the heat dissipation is considered to take place over a separate vertical heated plate. Using the above equation, he defined a relationship to determine the optimum spacing (b_o) to obtain the maximum dissipation of heat, viz:

$$b_o = \frac{50Z}{Ra_b} \tag{2.32}$$

2.8 Dynamic models

This review is intended to provide a basic understanding of the assumptions and limitations of dynamic models applicable to buildings.

Dynamic modelling methods were developed to solve Fourier differential equations for heat conduction. Heat conduction through a building fabric for three dimensional flow is written in the following general form:

$$\frac{\partial^2 T}{\partial x^2} + \frac{\partial^2 T}{\partial y^2} + \frac{\partial^2 T}{\partial z^2} = \frac{\rho c}{\lambda} \frac{\partial T}{\partial t} \tag{2.33}$$

where, x, y and z are space dimensions, t is time and T is temperature.

Generally, in building applications, a one dimensional heat flow is used for simplicity of the solution so that equation 2.33 will be reduced to;

$$\frac{\partial^2 T}{\partial x^2} = \frac{\rho c}{\lambda} \frac{\partial T}{\partial t} \tag{2.34}$$

The way in which the Fourier differential equation is solved takes several forms. Those best known are as follows:

-harmonic method

-response factor method

-numerical method

2.8.1 Harmonic methods

In the harmonic method, the climatic data are presented by a number of sinusoidal waves increasing in frequency and decreasing in amplitude. The total response of a building is the sum of the response to each of these energy cycles. In the CIBSE Guide, the same approach is used to solve the Fourier equation with some simplifications. These are features of the admittance procedure, which is the standard method for energy and temperature calculations in the UK. The simplification incorporated include:

-only the first harmonic (24 hours frequency) is used,

-three factors are suggested which simplify the heat transfer calculation (decrement factor, surface factor and admittance) with their associated time lags. They are expressed in terms of complex numbers and details for that are given by Milbank (1974).

-The actual climatic data is used in conjunction with the above factors obtained from the first harmonic.

-The environmental temperature model is used to represent the internal heat exchange between building elements. The details are given by Loudon (1970), Davies (1974) and chapters A5 and A8 of the CIBSE Guide (1986).

The basic equations given in the CIBSE Guide (A8) are;

The total mean heat gain $\overline{Q}_t$ is determined by adding the mean solar heat and the mean casual heat gains, which is given by;

$$\overline{Q}_t = \overline{Q}_s + \overline{Q}_c \qquad (2.35)$$

Having obtained Q_t, the mean internal environmental temperature can be determined from the following equation;

$$\overline{Q}_t = \Sigma(A_f.U_f)(\overline{T}_{ei} - \overline{T}_{eo}) + (\Sigma A_g U_g + C_v)(\overline{T}_{ei} - \overline{T}_{ao}) \qquad (2.36)$$

where

$\overline{Q}_t$ = mean total heat gain (W)

A_f = area of exposed opaque fabric (m^2)

A_g = area of glazed exposed surface (m^2)

U_f = thermal transmittance of exposed opaque fabric (W/m^2K)

$\overline{T}_{ei}$ = mean internal environmental temperature ($°C$)

$\overline{T}_{eo}$ = mean sol-air temperature $°C$

$\overline{T}_{ao}$ = mean outside air temperature $°C$

$\overline{Q}_s$ = mean solar heat gain = $S.A_g\bar{I}$ (W)

$\overline{Q}_c$ = mean casual heat gain (W)

The total swing in heat gain is obtained by;

$$\tilde{Q}_t = (\Sigma(A.Y) + C_v)\tilde{T}_{ei} \qquad (2.37)$$

which in turns $\tilde{Q}_t$ is equal to;

$$\tilde{Q}_t = \tilde{Q}_s + \tilde{Q}_c + \tilde{Q}_f + \tilde{Q}_a \qquad (2.38)$$

where

$\tilde{Q}_s$ = swing solar heat gain (W) = $\tilde{S}.A_g\tilde{I}$

$\tilde{Q}_f$ = swing fabric heat gain (W) = $f.A.U(\tilde{T}_{eo})$, where f is the decrement factor

Y = admittance of surfaces (W/m^K)

$\tilde{Q}_a$ = swing in effective heat input due to swing in outside air temperature (W)

The CIBSE Guide suggested that for low rates of ventilation (2 air changes per hour) the ventilation heat loss may be obtainable by,

$$C_v = \frac{1}{3} N.V \tag{2.39}$$

But for higher rates of ventilation, the ventilation heat loss should be given in the following form,

$$\frac{1}{C_v} = \frac{1}{0.33NV} + \frac{1}{4.8\sum A} \tag{2.40}$$

where

C_v = ventilation heat loss (W/K)

$\sum A$ = total area of internal room surfaces (m^2)

N = air change per hour

V = room volume

Unlike the response factor and the numerical methods, the admittance procedure assumes constant boundary conditions. It also assumes that outside climatic conditions could be represented as the first harmonic which might not be correct in some cases. The way it is presented by the Guide, it only provides the calculation of the mean and swing about the mean. It has the advantage of easy calculation which can be performed without a computer.

2.8.2 Response factor method

The response factor method suggested by ASHRAE solves the Fourier equation for unsteady heat conduction through slabs. It is based on the idea of the time series and response factors in which a continuous function of time such as the energy input to a building is presented by a series of consecutive triangular pulses, and the total response of a system is the sum of the response to each pulse. In this way, the climatic conditions do not need to be periodic as in the harmonic method. Its application in buildings for heat

transfer calculation is developed by Stephenson and Mitalas (1967 a, b). It is also recommended by ASHRAE for unsteady heat conduction. The heat flow by conduction in time series form is given by,

$$Q_{cd,t} = -\sum_{p=0}^{\infty} T_{(i,t-p)} x_p + \sum_{p=0}^{\infty} T_{(j,t-p)} y_p \qquad (2.41)$$

where

T_i and T_j = temperatures on two sides of a wall

x_p and y_p = response factors on each surface

t = time

p = number of response factor terms

In general, the values of response factor x_p and y_p tends to zero as the calculation proceeds in time, which they are a function of slabs structure characteristics. Kusuda (1976) demonstrated that the number of terms rarely exceeds 20.

A set of simultaneous heat balance equations for each time is performed of which equation 2.41 is the conduction part. A detailed discussion is given by Stephenson and Mitalas (1967 a, b), and Clarke (1985).

In its application, the response factor method is not different from numerical methods but unlike finite differences it cannot be applied to non-linear and variable systems (Clarke 1985). This is assumed not to cause severe restriction in its application in buildings (Mitalas 1965).

2.8.3 Numerical methods

Numerical methods are generally used when the geometry of the system and the boundary conditions are complicated and vary with time. The basis of a numerical method is to approximate the Fourier differential equation and the boundary conditions by a set of algebraic equations solved by digital computers.

The Fourier differential equation 2.34 could be approximated explicitly using the Taylor series expansion and thus it becomes,

$$\frac{T_{n+1}^{t}-2T_{n}^{t}+T_{n-1}^{t}}{(\Delta x)^2}=\frac{\rho c}{\lambda}\frac{T_{n}^{t+\Delta t}-T_{n}^{t}}{\Delta t} \qquad (2.42)$$

where

n = node to represent a finite slice or thickness from a wall

Δt = time increment

The numerical solution of a heat conduction problem is carried out by subdividing the system into a number of small sub-volumes each with a reference number (Kreith 1973). Each sub-volume is represented by a node at its centre with an assumed temperature. For N nodes, there must be N equations which will be solved using an explicit or implicit finite differences method.

Heat conduction through a wall is solved by dividing the wall into small layers or "thicknesses" Δx, each of which is represented by a node n, and a time increment Δt is set up.

For a wall with three nodes $n-1$, n and $n+1$, there will be three temperatures, T_{n-1}^{t}, T_{n}^{t} and T_{n+1}^{t}. During a time interval Δt, heat will be conducted between node n and the rest of nodes $n-1$ and $n+1$.

Equation 2.42 can be rearranged to the following form,

$$\left(\frac{T_{n-1}^{t}-T_{n}^{t}}{R_{n-1,n}}+\frac{T_{n+1}^{t}-T_{n}^{t}}{R_{n,n+1}}\right)\Delta t = c\rho\Delta x A(T_{n}^{t+\Delta t}-T_{n}^{t}) \qquad (2.43)$$

where, $R_{n-1,n}$ is the thermal resistance between node $n-1$ and n, which is $\Delta x/\lambda A$.

By rearranging equation (2.43) for the future temperature of node n yields;

$$T_{n}^{t+\Delta t}=T_{n}^{t}\left(1-2\frac{\lambda\Delta t}{c\rho\Delta x^2}\right)+\frac{\lambda\Delta t}{c\rho\Delta x^2}(T_{n-1}^{t}+T_{n+1}^{t}) \qquad (2.44)$$

where $1-2\lambda\Delta t/c\rho\Delta x^2$ is the stability criterion which should be positive for convergence and stability of the solution.

As can be seen from equation 2.44, the future temperature of the node n is expressed in terms of present temperatures of all nodes.

The accuracy and rapidity of solution depends on the size of layers and time increment. The larger the values of Δx and Δt, the more quickly the solution is obtained but on the contrary the accuracy will be less. The accuracy of the solution is increased by having smaller Δx and Δt.

The implicit method gives the future temperatures of the node n from future temperatures of the neighbouring nodes, so that equation 2.43 turns into,

$$\left(\frac{T_{n-1}^{t+\Delta t}-T_n^{t+\Delta t}}{R_{n-1,n}}+\frac{T_{n+1}^{t+\Delta t}-T_n^{t+\Delta t}}{R_{n,n+1}}\right)\Delta t = c\rho\Delta x A\,(T_n^{t+\Delta t}-T_n^t) \tag{2.45}$$

rearranging for future temperature of node n yields;

$$T_n^{t+\Delta t} = T_n^t + \alpha T_{n-1}^{t+\Delta t} + \beta T_n^{t+\Delta t} + \gamma T_{n+1}^{t+\Delta t} \tag{2.46}$$

where

$$\alpha = \frac{\Delta t}{c\rho\Delta x A R_{n-1,n}}$$

$$\beta = -(1/R_{n-1,n}+1/R_{n,n+1})\frac{\Delta t}{c\rho\Delta x A}$$

$$\gamma = \frac{\Delta t}{c\rho\Delta x A R_{n,n+1}}$$

Equation 2.46 can be applied to each existing node in the system. The result will be a set of simultaneous equations for the future temperatures at each node in terms of future temperatures at neighbouring nodes and the present temperature of node n. The set of

simultaneous equations is written in matrix form as $AX=B$ which may be solved by iteration, Gauss elimination or by matrix inversion for each time step. The advantage of using the implicit method is that the solution will be stable with any time or space increments (Clarke 1985).

One might come to the conclusion that each of the above mentioned methods can be regarded as a temperature predictor. However, the harmonic method has certain limitations in its application in buildings because on one hand it assumes the weather data periodic, which in many cases it may not be. On the other hand it uses constant boundary conditions whereas in reality the boundary conditions are time dependent. The response factor method is not different from numerical methods in handling periodic and non-periodic heat flow and temperatures, but it can only be applied to a system of equation which are linear and invariable. It is not applied for multidirectional heat flow especially for systems of complicated configuration. Mathematically the response factor method is complicated and it is a computer based method. The finite difference technique has certain advantages over the other existing methods, in that it allows direct application to buildings with various configurations. It can deal with time-dependent boundary conditions, can be also applied to non-linear systems and it is easy to use.

CHAPTER THREE

APPARATUS AND MEASUREMENTS

3.1 General description of the apparatus

The apparatus was designed to study the effect of different parameters such as inlet height and cavity width on air flow and heat transfer in the cavity. Because the thermal capacity of the material around a cavity (usually stone, brick or mud) may be large in relation to the thermal changes taking place in it, it was not considered necessary to model its thermal capacity: the heat removed by the air in the cavity is small in relation to the heat stored in the walls. The observations were made at "steady state" in a laboratory considered large enough (20m long, 10m wide and 5m high) to simulate a free environment. The cavity had two heated parallel walls of nearly equal size, one fixed in position on the room side, (1.9m high and 1.5m wide) and the other movable. The end walls were variable in width (0.1m, 0.2m, 0.3m, 0.5m and 1.0m wide), their heights were similar to the heated walls. They were constructed of insulation board with polished aluminium on their internal faces to reflect radiation from the heated plates. The end walls were not heated because their sizes were considered small in relation to the other walls, so heat loss or gain through them was negligible. Figure 3.1a shows the plan and figure 3.1b shows a vertical section through the apparatus and the room with the openings.

To simulate a real building, a wooden box or "room" of internal dimensions (1.8m long, 1.65m wide and 2m high) was constructed (figure 3.2a). The room was sealed apart from a 0.5m by 0.6m opening in the centre of one its faces, and a 1.40m wide inlet variable in height, on the opposite side open to the base of the cavity. An additional small window was made on one side to observe air flow patterns using smoke.

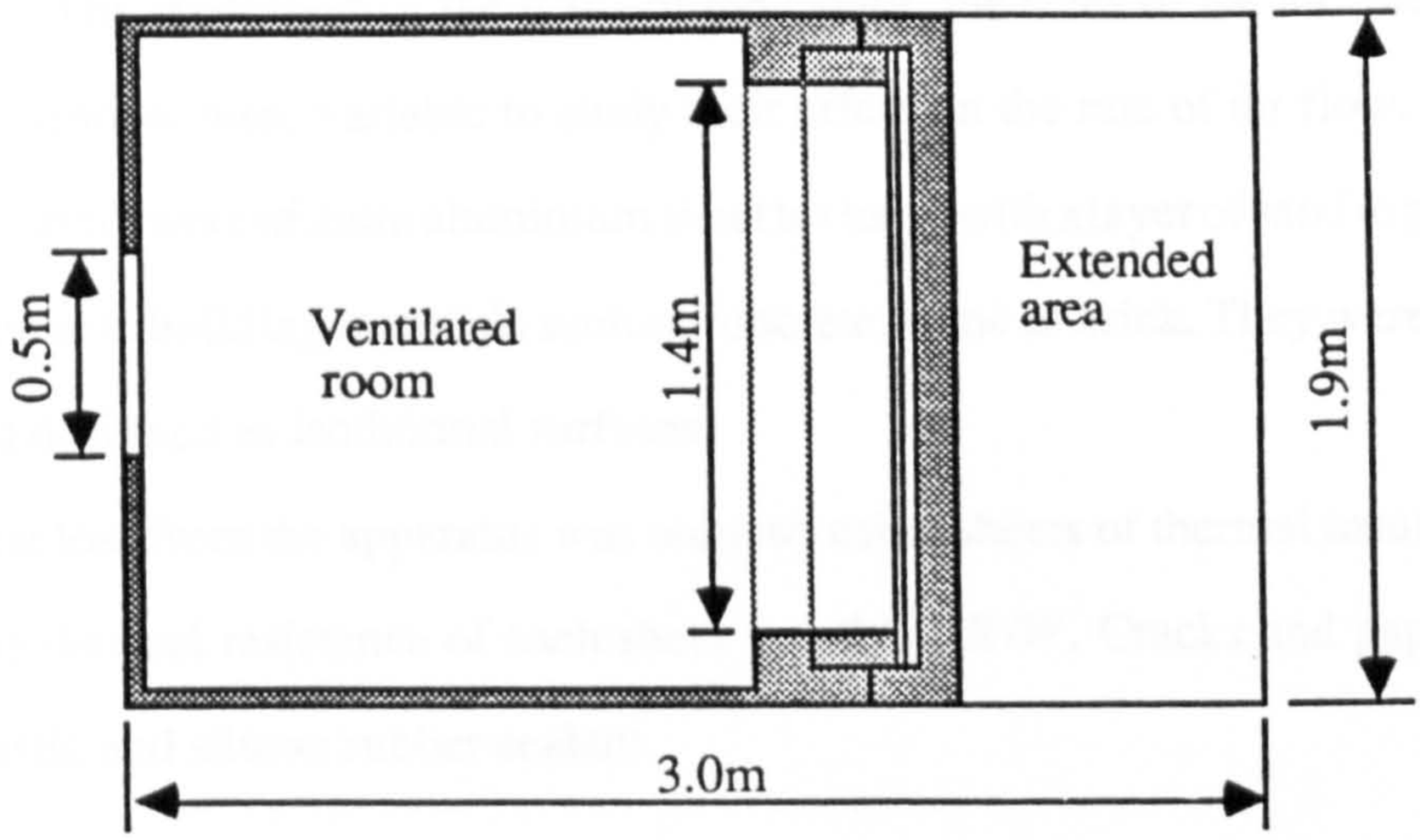

a) Plan of the apparatus

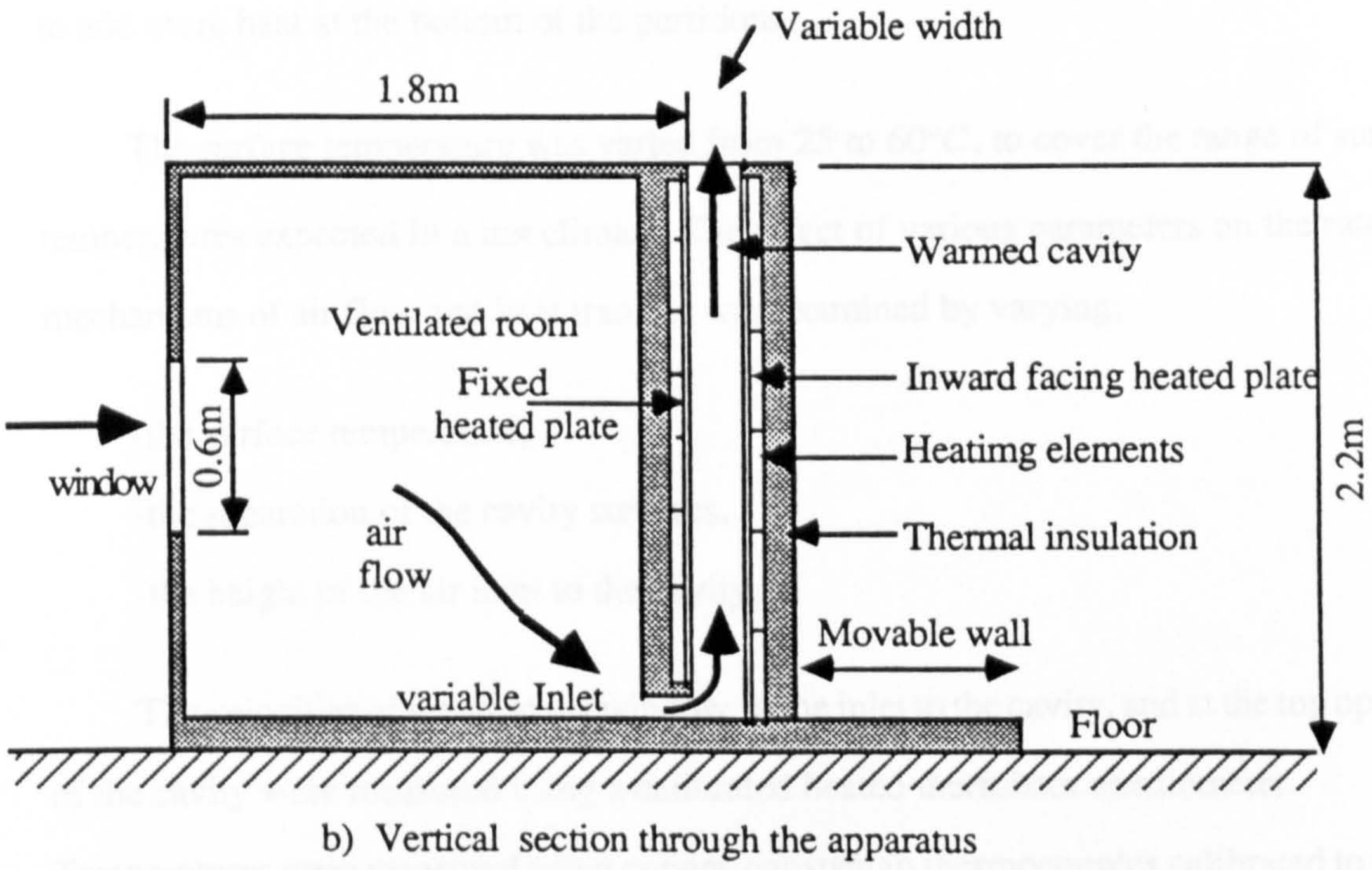

b) Vertical section through the apparatus

Figure 3.1 Plan and section of the apparatus

The separation of the walls of the cavity, the sizes of the air inlet to the cavity and the window were variable to study their effect on the rate of air flow. The walls forming the cavity were of 2mm aluminium sheet textured with a layer of sand to provide a roughness similar to building materials such as concrete, stone or brick. They were heated electrically and designed as isothermal surfaces.

Heat loss from the apparatus was reduced using sheets of thermal insulation, 50mm thick. The thermal resistance of each sheet was $2.5 m^2K/W$. Cracks and gaps were sealed with mastic and silicon rubber sealant.

The partitions were found to be cooler at the bottom because of radiation heat loss into the room. Attempts to deal with this by covering the room walls with polished aluminium sheets to reflect the radiation were found to be of little benefit and it was decided to add more heat at the bottom of the partitions.

The surface temperature was varied from 25 to $60°C$, to cover the range of surface temperatures expected in a hot climate. The effect of various parameters on the rate and mechanisms of air flow and heat transfer was examined by varying;

-the surface temperature,

-the separation of the cavity surfaces,

-the height of the air inlet to the cavity.

The velocities of the air at the window, at the inlet to the cavity, and at the top opening of the cavity were measured using a calibrated heated thermistor anemometer.

Temperatures were measured using copper-constantan thermocouples calibrated to tables presented in B.S. 4937 tables. Figure 3.2b shows the instrumentation used.

The thermistor anemometer gives air speeds but not the direction of air flow; to determine the air flow patterns, smoke was used.

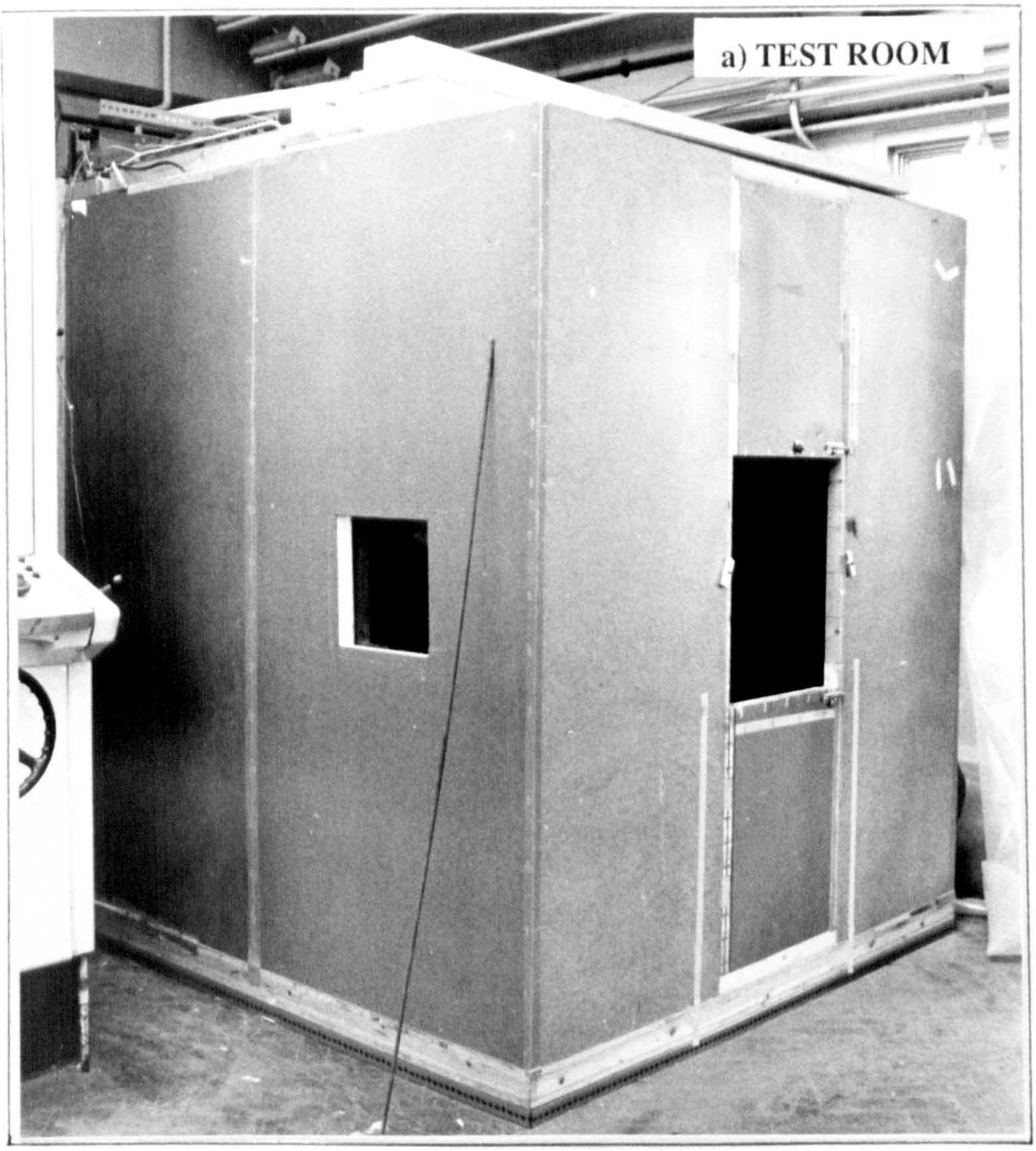

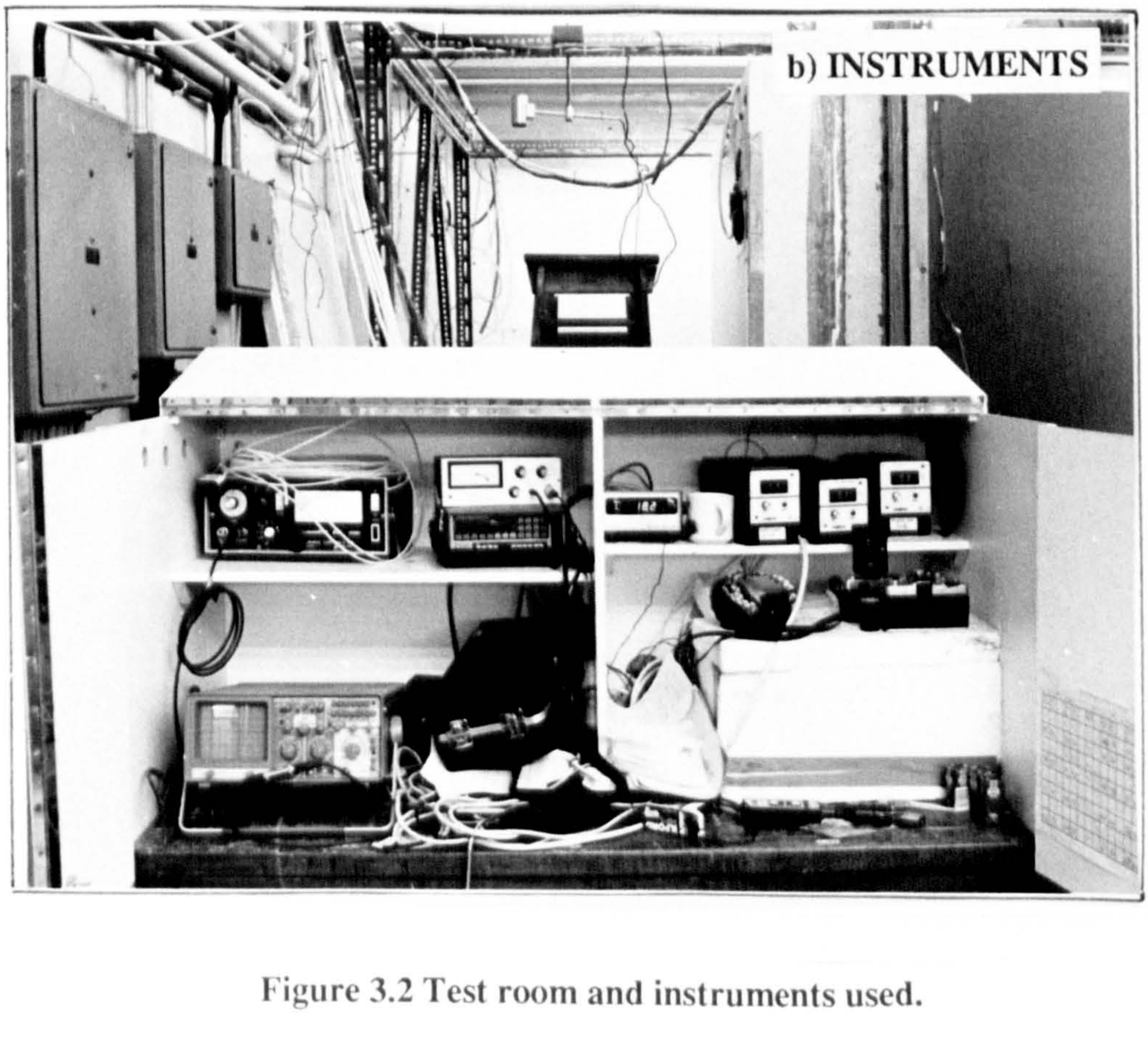

Figure 3.2 Test room and instruments used.

3.2 Measurement apparatus

3.2.1 Heating system

The inner surfaces of the cavity were heated by horizontal electrical heaters with the outer faces insulated. The electrical heaters were separated by horizontal partitions (baffles) to discourage air movement behind the heated surfaces, to help keep the temperature of the cavity surfaces nearly constant (figure 3.3). The heaters were mounted behind the plates at a distance of 50mm so that the radiation heat input was well distributed over the plates.

3.2.2 Temperature control

The surface temperature of the walls of the cavity was controlled by a number of time proportioning temperature controllers (Anglican DH series). The sensing elements of the controllers were thermocouples which were placed in the middle of each heated surface to be controlled. They have high sensivity and a short time response of the order of 2 seconds.

3.2.3 Flow visualisation

Thermistors and most air speed measuring instruments give no indication of the direction of air movement, so smoke was used for determining flow patterns in the room and in the cavity and to observe upflow and downflow of air within the cavity. It also helped to determine the boundary layer thickness. Smoke tubes were used that produced a dense white smoke (from hydrochloric acid fumes). The smoke was injected in the air streams within the room and the cavity and photographs of their traces were taken. One disadvantage of this smoke is that it was dangerous to breathe. The advantage of using it was that its temperature was the same as the air. If the smoke were warmer than the air, it would rise, but as it was at the same temperature it followed the air paths. The nature of the flow is important since the rate of heat transfer depends on whether the flow is laminar or turbulent. An oscilloscope (Gould OS1420) was used to observe the nature of fluctuations of air speed and temperature. The oscilloscope was attached to the thermistor anemometer via the air velocity meter (AVM).

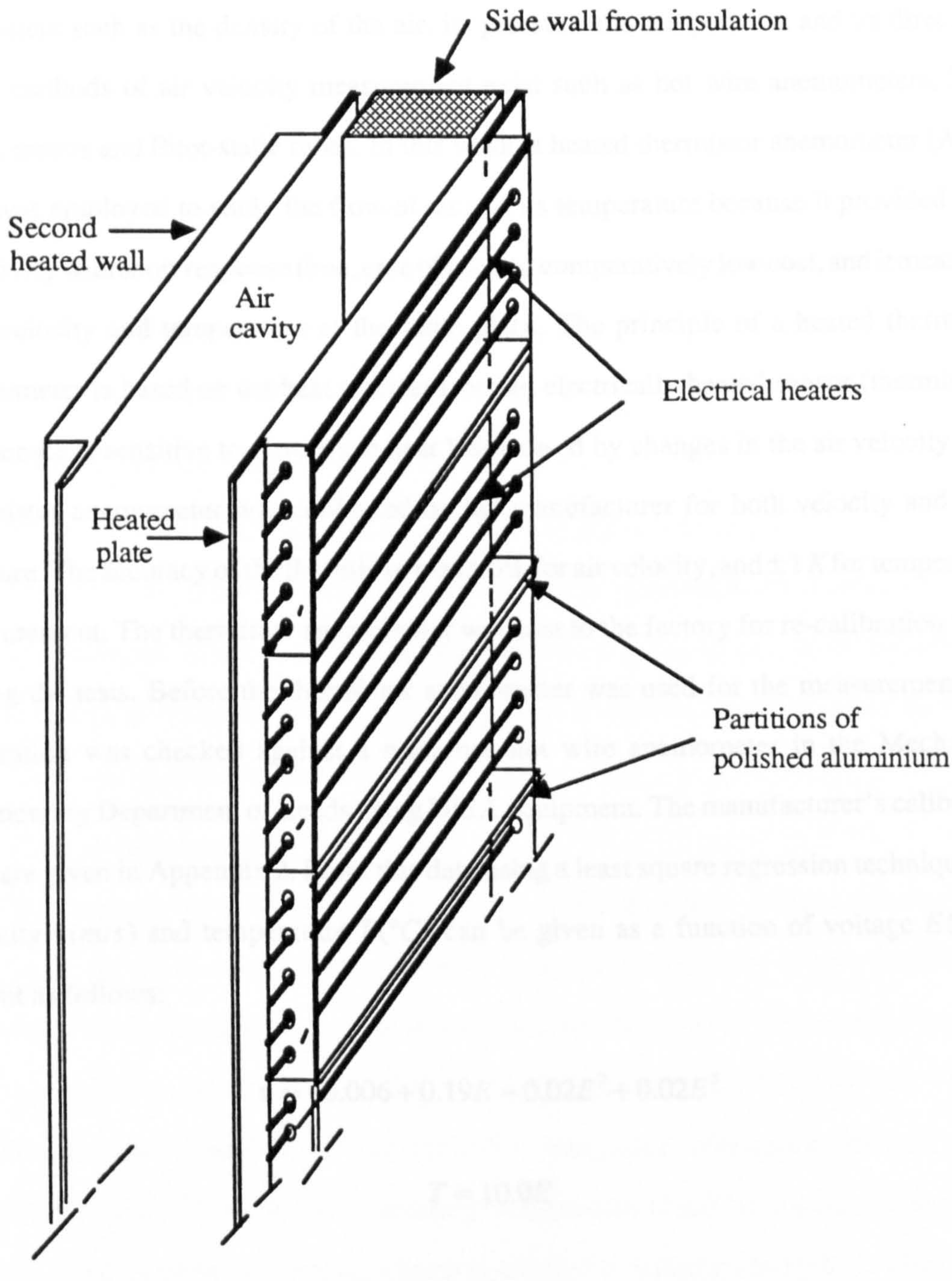

Figure 3.3 Arrangement of electrical heaters between partitions.

3.2.4 Air speed measurement

The accurate measurement of air velocity is a complex problem. It depends on various parameters such as the density of the air, its pressure and temperature and its direction. Other methods of air velocity measurement exist such as hot wire anemometers, laser anemometers and Pitot-static tubes. In this work, a heated thermistor anemometer (AVM 502) was employed to study the flow of air and its temperature because it provided high sensitivity with short response time, ease of use and comparatively low cost, and it measures both velocity and temperature at the same place. The principle of a heated thermistor anemometer is based on the heat transfer from an electrically heated sensor (thermistor). The sensor is sensitive to changes in heat loss caused by changes in the air velocity. The thermistor anemometer was calibrated by the manufacturer for both velocity and temperature. The accuracy of the thermistor was $\pm 5\%$ for air velocity, and $\pm 1\,K$ for temperature measurement. The thermistor anemometer was sent to the factory for re-calibration twice during the tests. Before the thermistor anemometer was used for the measurements, its calibration was checked against a reference hot wire anemometer in the Mechanical Engineering Department of Leeds using DISA equipment. The manufacturer's calibration data are given in Appendix 2. From this data using a least square regression technique, the velocity $v(m/s)$ and temperature $T(°C)$ can be given as a function of voltage $E(volts)$ output as follows:

$$v = -0.006 + 0.19E - 0.02E^2 + 0.02E^3 \tag{3.1}$$

$$T = 10.0E \tag{3.2}$$

E = voltage output (volts)

The sensor of the probe was screened with a cylindrical polished aluminium shield to avoid errors caused by radiation exchange with the surrounding surfaces, and to protect the sensing element from damage. Reading the data directly from the meter was not

practicable because of fluctuations. The problem was solved by connecting a digital voltmeter (Thurlby) to the air velocity meter to give the mean value of a set of reading data over a length of time.

Although the thermistor anemometer is a reliable instrument to measure air velocity and temperature, it has a limited range of applicability in that:

-it is calibrated to measure velocities more than 0.2m/s,

-it has certain inaccuracies when measuring downward air currents because of the upward convection currents generated from the heated thermistor,

-it cannot indicate the direction of the air currents.

3.2.5 Air temperature measurement

Air temperature at the inlet and outlet of the chimney was required to study the rate of heat transfer. The thermistor anemometer and copper-constantan thermocouples "Type T" were employed. The thermocouples were always screened from thermal radiation by hollow cylinders 30mm diameter by 70mm long, of polished aluminium to eliminate radiation from the surrounding surfaces.

3.2.6 Surface temperature measurement

The surface temperatures of the cavity were measured using calibrated copper-constantan thermo-couples monitored by a digital thermometer (*Comark* 5000). The calibration of the thermocouples was in accordance to B.S. 4937. The reference junction of the couples was kept at 0 $^{\circ}C$, using melting ice made from distilled water. The hot junction temperature was varied from 0 to 100$^{\circ}C$ using a thermocouple calibrator (Techne DB-40L/DB-35L). The readings were taken in microvolts (e.m.f) using a digital voltmeter (Data Precision-3500). The readings were close those in tables given by B.S. 4937, within $\pm 0.2\,K$. After calibration the thermocouples were also checked against a mercury in glass thermometer. The thermocouples and the mercury in glass thermometer were inserted into a large bath of distiled water. Readings were taken at the freezing and at the boiling points. The maximum difference obtained between the thermocouples and the mercury in glass

thermometer was about $\pm$ 0.3 K.

The thermocouples were carefully attached to the surfaces of the cavity using Araldite of high thermal conductivity. The wires were placed along the surfaces for a minimum distance of 200mm to avoid reading errors due to heat conduction along the connecting wires. Thermocouples were placed in 20 places on the internal surfaces of the cavity walls (figure 3.4a and figure 3.4b) and were connected to a multi-channel selection switch. The switch board was thermally insulated with 50mm polystyrene foam to reduce heat loss from the couple junctions.

3.3 Measurements procedure

The apparatus was built to measure the speed and temperature of the air, so that a heat and mass balance could be established, as follows:

The wall surfaces of the cavity were heated to various constant temperatures, 25, 30, 35, 40, 50 and 60°C which cover the range of likely surface temperatures of the cavity in a hot-dry climate. After the temperature of the wall surfaces and the air of the laboratory was stable, the probe was placed in position. The signals received by the air velocity meter were read. The air velocity meter had no storage capacity and no way of obtaining a mean velocity or temperature. It was therefore connected to a digital voltmeter (Thurlby 1905 intelligent multimeter) which stored, for later recall, the running average and extreme values. About three readings per second were taken. Fluctuations were high due to the variability of the flow, but reliable mean values for both velocity and temperatures were obtained during 90 seconds.

Data collected from the voltmeter were analysed by computer.

Mean values over the measuring points, at the window, inlet and top openings of the cavity were obtained. Figure 3.5 illustrates the grid of measurement points for the window and the inlet, and figure 3.6 shows measurement points at the top opening of the cavity for different widths.

Obstructions were moved out of the path of the air to avoid disturbing its flow. Only one

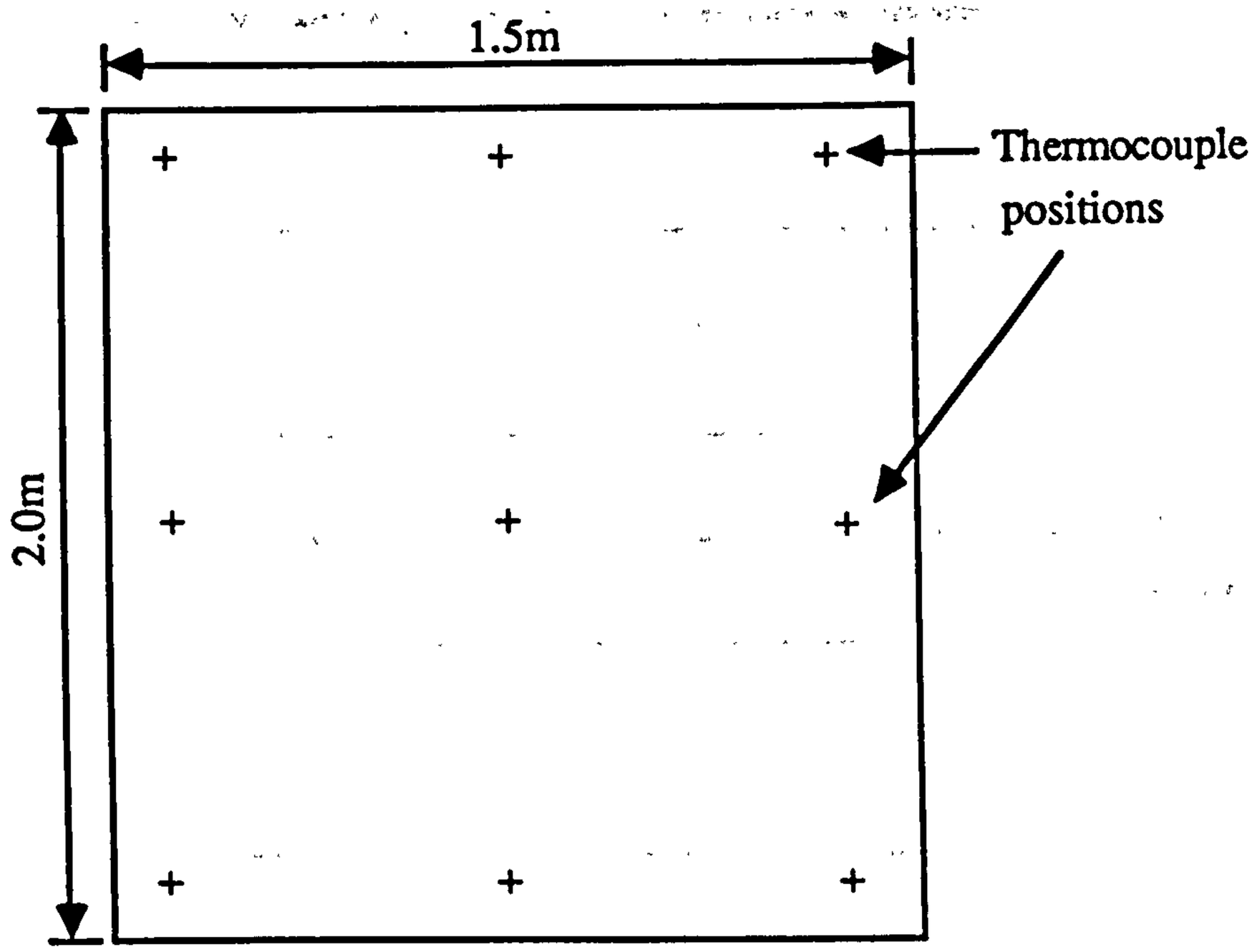

a) Elevation of the movable wall of the cavity

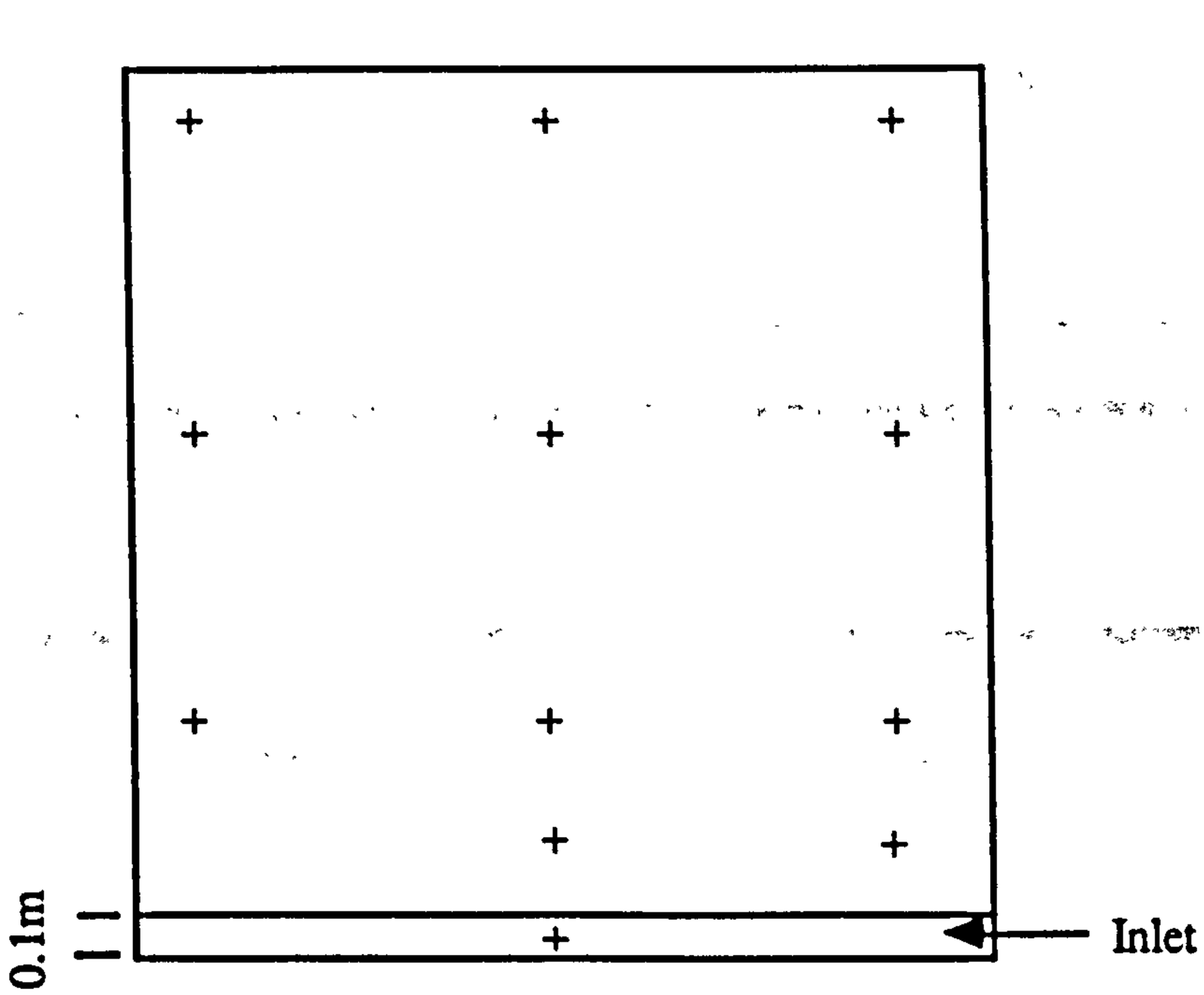

b) Elevation of the fixed wall of the cavity

Figure 3.4. Thermocouples layout on the inner faces of the cavity.

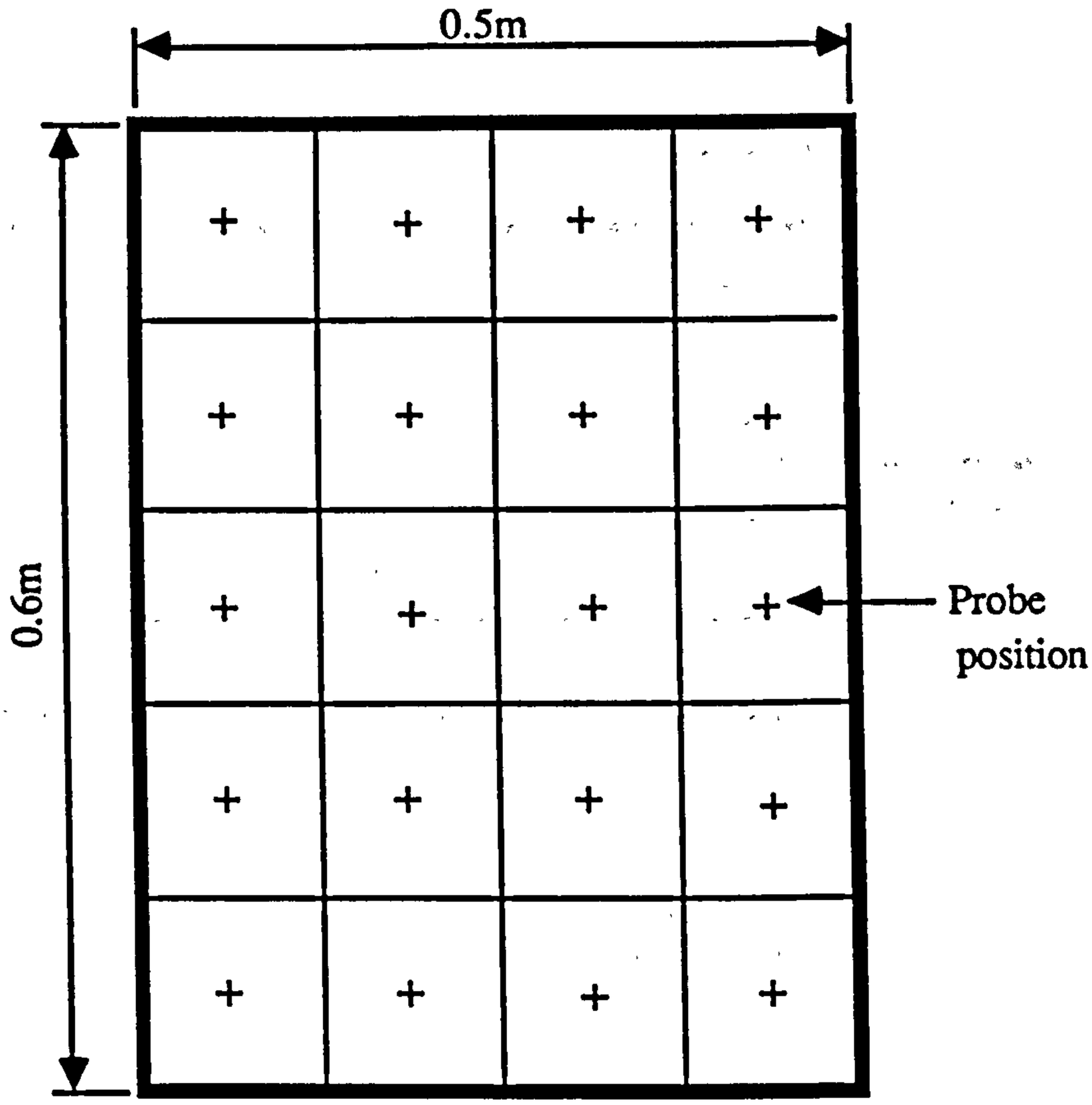

a) Elevation of the window into the room

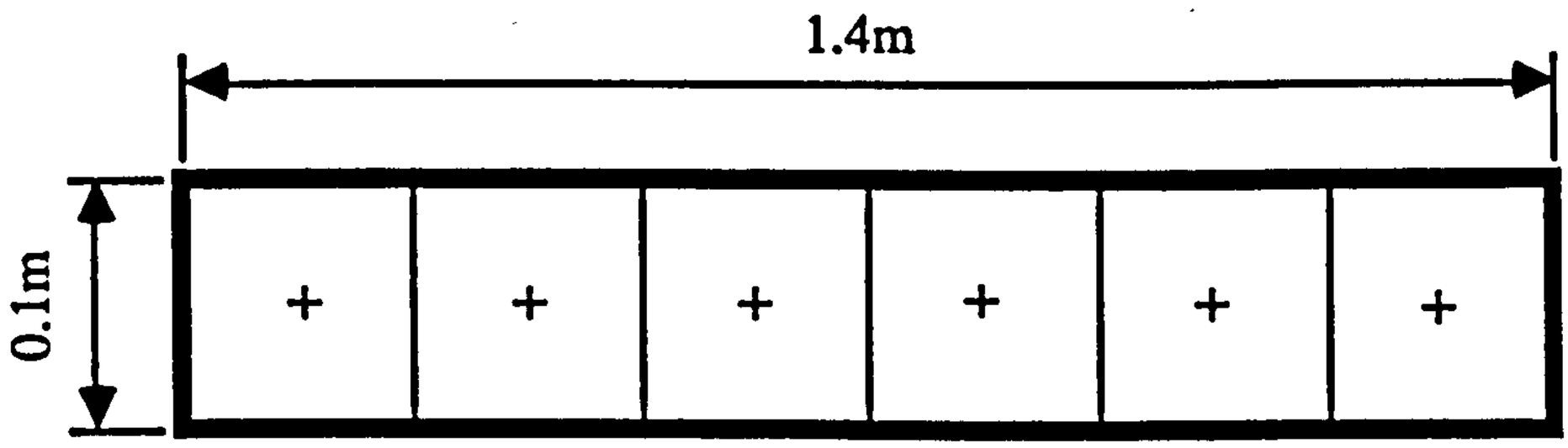

b) Elevation of the air inlet into the cavity.

Figure 3.5 Measuremnt points for the air temperature and its velocity. at the window and the inlet.

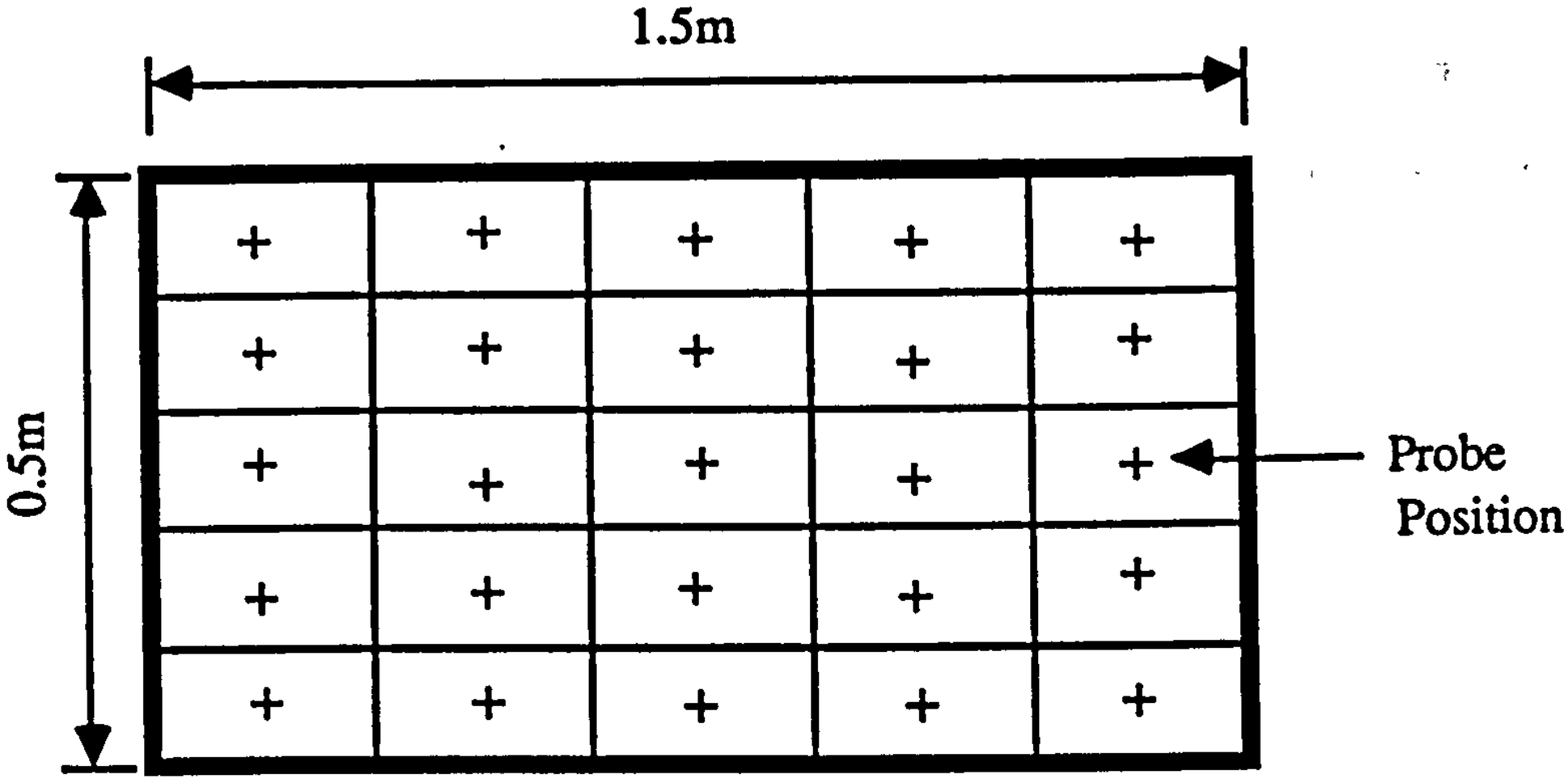

a) Plan of top opening for 0.5m wide cavity.
(0.3m has similar number of measuring points).

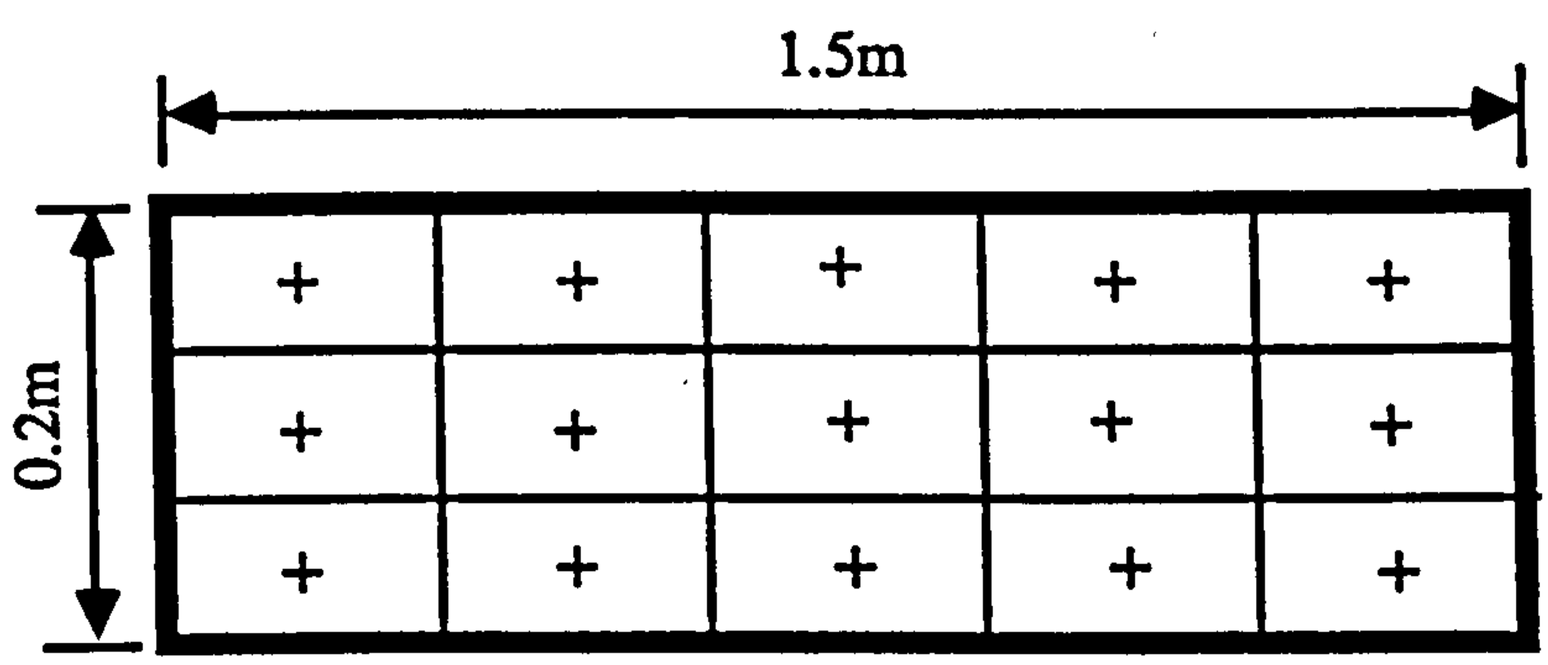

b) Plan of top opening for 0.2m wide cavity.
(0.1m has similar number of measuring points).

Figure 3.6 Measurement points for the air temperature and its velocity at the top opening of the cavity.

probe was used for all measurements to avoid interference with the air flow.

The tests were in two stages, the first was with an inlet height of 0.1m, the second was with an inlet height of 0.4m. The cavity width for both series of tests was varied between from 0.1 to 0.2, 0.3, 0.5 and 1m.

In all tests the following parameters were kept constant:

-length of the cavity 1.50m

-height of the cavity 2.00m

-length of the inlet 1.40m

-ambient air temperature 20°*C*

3.4 Limitation and range of applicability of the apparatus

The measurement apparatus was made in a laboratory away from any influence of changes of weather and winds, however it had certain limitations which can be summarised under the following points:

-air currents from nearby doors and movement of people in the laboratory affected some measurements. At times, measurements had to be postponed until the laboratory was unoccupied,

-fluctuations in ambient air temperature especially at night when the outside weather is colder. Measurements were sometimes postponed to the next day,

-the thermistor anemometer has certain limitations in that it measures air speeds but does not give indication of the direction of the air movement,

-non-homogeneity of the material used, due to the sand on the two heated plates, whereas shining aluminium on the other. Although their areas are small in respect to the heated plates. The room walls and floor were of wood of different roughness from a real building material,

-the temperature of the heated plates were not completely uniform due to a temperature gradient between the bottom and top of the cavity. Although this was reduced

to a minimum by adding more electrical bars to the bottom partition,

-the sealing of the edges of the movable plate was imperfect, although this did not really affect the flow because the air was allowed to move through a larger inlet. It may be important to take it into account in future measurements,

-The use of a single anemometer is advantageous in having the same accuracy. The disadvantage with only one anemometer is that it has to be moved manually to all measurement points, which make the readings take longer,

-screening the sensing element of the thermistor anemometer was imperfect, so that sometimes radiation from the heated plates may reach the sensor, which may affect the readings.

-The thermistor anemometer was not calibrated for velocities less than 0.2m/s, consequently the accuracy of these measurements is uncertain. However, in this experiment there were few points where the air velocity was less than 0.2m/s.

CHAPTER FOUR

EXPERIMENTAL RESULTS

4.1 Introduction

The apparatus described in chapter three was used to observe the flow of air produced by a heated cavity. Tests were performed to study the effect on air mass flow and heat transfer, to do this, changes in the following parameters within the cavity were made:

-space between the surfaces was varied from 0.1 to 1.0m

-inlet height changed from 0.1m to 0.4m

-surface temperature of walls changed from 25 $°C$ to 30 $°C$ and then from 30 $°C$ to 60 $°C$ at 10 K intervals.

The upward flow of air was found to be affected by the spacing between the walls of the cavity and the inlet height. Air mass flow rates reduced as the spacing between the surfaces of the cavity widened. When the cavity width exceeded more than 0.3m wide, there was air flowing downwards through the top. Reduction of mass flow also occurred if the cavity was narrowed to less than 0.15m, probably due to increased friction. The inlet height also affected the rate of mass flow; as the height of the inlet was increased the rate of mass flow increased.

In all the tests, the ambient air temperature was kept at 20 $°C$, whereas the mean temperature (T_{sm}) of the heated surfaces was varied.

A statistical analysis of the results was made using SAS (Statistical Analysis System), one of the statistical packages available on the main frame computer at the University of Leeds. This package gives most of the statistical parameters required such as best fit

regression equations, coefficients of correlation, standard deviation and so on.

To give a deeper insight to the results an errors analysis was performed (see section 4.4), error bars were plotted on graphs when required.

4.2 Air flow

4.2.1 Effect of cavity width

To study the effect of cavity width on the rate of mass flow, the cavity width was varied at the following intervals; 0.1m, 0.2m, 0.3m, 0.5m and 1.0m. The surface temperature of the cavity walls was varied between 30 $°C$ and 60 $°C$ at 10 K intervals and at each spacing and the mass flow rates were monitored and calculated for a unit length of the cavity width. Mass flow rates were determined by multiplying the following parameters measured at the air inlet: average air velocity $\bar{v}(m/s)$, air density$\rho(kg/m^3)$ and the area of the inlet $A(m^2)$). To determine the mass flow rate per unit length, the value obtained was simply divided by the length of the cavity. For each surface temperature, cavity width and inlet height a mass flow rate per unit length was calculated. The results are given in tables 4.1 and 4.2 for a 0.1m and 0.4m high inlet respectively. The tabulated data are plotted in figure 4.1. Statistically, it can be observed that the mass flow rate maximises when the cavity width is between 0.2m and 0.3m. Increasing the cavity width from 0.3m to 1.0m shows a decline in the mass flow rates which suggests that increasing the cavity width above 0.3m may not be beneficial. However considering the error bars, the changes in mass flow rate may not be as significant as it appears.

The graphs also show that increasing the surface temperature increases the mass flow rate. This can be explained by the fact that with high surface temperatures, the air within the cavity gets hotter thereby reducing its density and increasing the buoyancy pressure. However, considering the error bars, the results suggest that as the surface temperature is increased above about 35 $°C$ the increase in mass flow rate may not be significant as it appears on the graphs. This will be discussed again in section 4.2.4.

Table 4.1 Effect of cavity width on air mass flow with 0.1m high air inlet.

	Mass flow (kg/ms)				
Cavity width (m)	0.1	0.2	0.3	0.5	1.0
Surface temperature °C					
30	0.049	0.060	0.059	0.055	0.053
40	0.065	0.082	0.080	0.080	0.068
50	0.080	0.099	0.097	0.091	0.083
60	0.087	0.110	0.109	0.103	0.091

Table 4.2 Effect of cavity width on air flow rate with 0.4m high air inlet

	Mass flow (kg/ms)				
Cavity width (m)	0.1	0.2	0.3	0.5	1.0
Surface temperature °C					
30	0.046	0.064	0.067	0.073	0.066
40	0.067	0.094	0.097	0.083	0.080
50	0.080	0.103	0.107	0.108	0.096
60	0.086	0.118	0.121	0.124	0.105

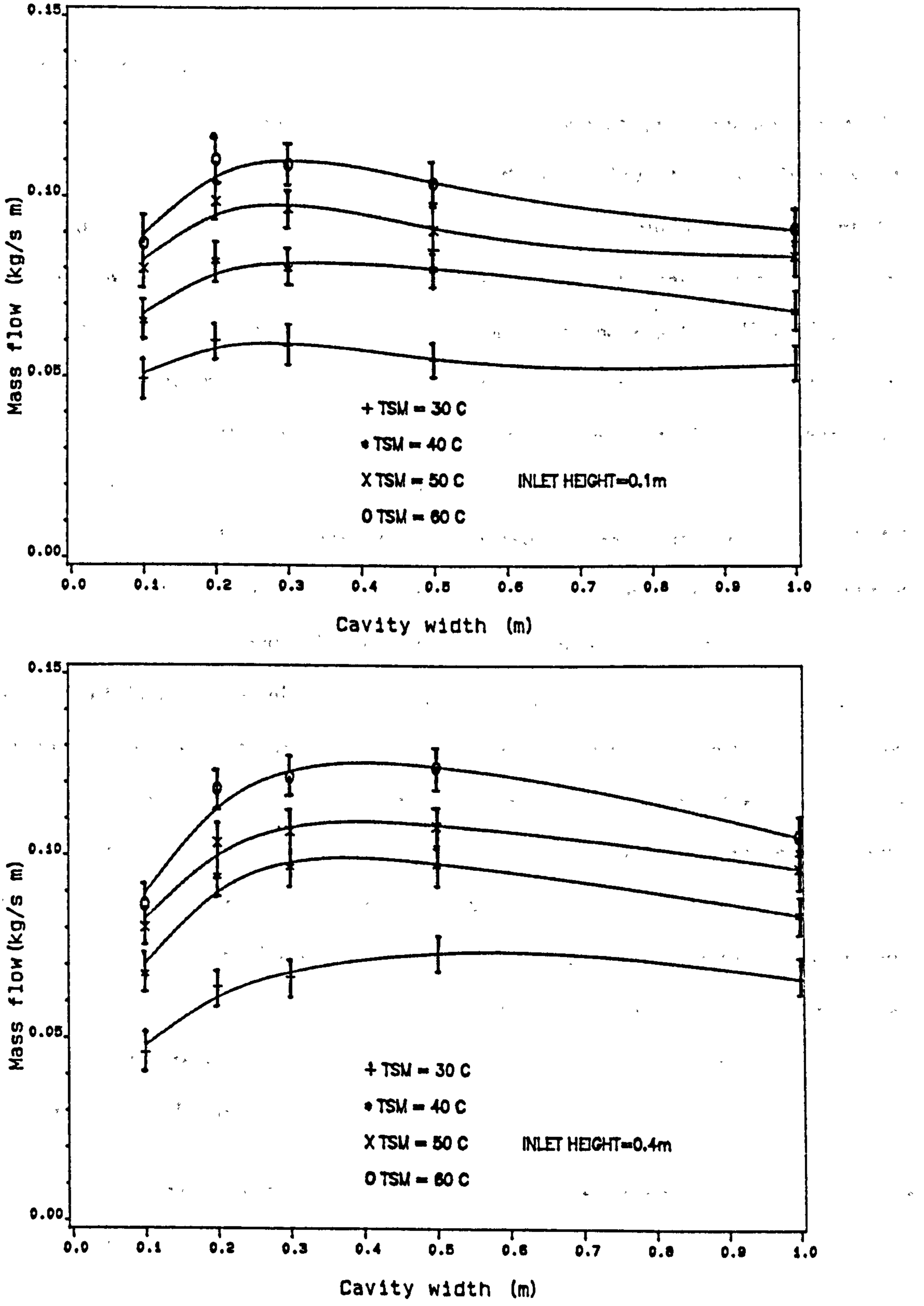

Figure 4.1 Effect of cavity width on air flow rate

4.2.1.1 Mass balance

The above observations were based on measurements taken at the air inlet to the cavity. For continuity through the whole system, the mass flow of air must be constant. Mass balances were carried out at the window and the inlet and the outlet to the cavity for each cavity width and surface temperature value. To do this the cavity width was varied from 0.1m, 0.2m, 0.3m to 0.5m and surface temperatures increased by 5K to 40K above the ambient air temperature at each width. The ambient air temperature was kept constant at 20 °*C*. The inlet height was initially 0.1m and then increased to 0.4m. The results are given in tables 4.3 to 4.10 and plotted in figures 4.2 to 4.5.

Statistical analysis of the data shows that the regression lines plotted in figures 4.2, 4.3 and 4.4 are close to one another. The error bars of the data overlap to such an extent that the curves could be assumed to be the same. This closeness of fit suggests that the mass flow rates of the air at the inlet, window and outlet are the same. Comparing the figures with one another for widths of 0.1m, 0.2m and 0.3m suggest that the mass flow rates are about the same. For a cavity with width of 0.5m, the statistics show that the mass flow rate at the outlet was higher than at the inlet and window (see figure 4.5). The mass flow at the inlet and the window are similar. The reason why the mass flow rates are higher at the outlet than those at the inlet and window is due to additional air entering the system. Knowing that the thermistor anemometer used in these measurements indicates the speed of air but not its direction, it was necessary to use smoke to identify the flow patterns and to see where the additional air came from.

Statistical analysis showed that the best regression equations for the data in figures 4.2 to 4.5 were third power polynomials represented by the general form:

$$M = a + bX + cX^2 + dX^3 \tag{4.1}$$

where

X is the variable $(T_{sm} - 20)\ K$

Table 4.3 Mass balance for 0.1m wide cavity with 0.1m high inlet.

$(T_{sm}-20)$ K		5	10	15	20	30	40
Mass flow (kg/sm)	at Inlet	0.036	0.049	0.059	0.065	0.080	0.085
	at Window	0.035	0.048	0.057	0.063	0.077	0.083
	at Outlet	0.037	0.050	0.060	0.067	0.082	0.087

Table 4.4 Mass balance for 0.1m wide cavity with 0.4m high inlet.

$(T_{sm}-20)$ K		5	10	15	20	30	40
Mass flow (kg/sm)	at Inlet	0.035	0.046	0.056	0.067	0.080	0.086
	at Window	0.033	0.048	0.053	0.065	0.079	0.084
	at Outlet	0.036	0.047	0.057	0.067	0.082	0.088

Table 4.5 Mass balance for 0.2m wide cavity with 0.1m high inlet.

$(T_{sm}-20)$ K		5	10	15	20	30	40
Mass flow (kg/sm)	at Inlet	0.043	0.060	0.073	0.082	0.099	0.113
	at Window	0.041	0.062	0.074	0.080	0.099	0.112
	at Outlet	0.041	0.059	0.070	0.084	0.099	0.115

Table 4.6 Mass balance for 0.2m wide cavity with 0.4m high inlet.

$(T_{sm}-20)$ K		5	10	15	20	30	40
Mass flow (kg/sm)	at Inlet	0.045	0.064	0.079	0.094	0.103	0.118
	at Window	0.044	0.065	0.078	0.096	0.105	0.120
	at Outlet	0.047	0.062	0.081	0.092	0.100	0.115

Table 4.7 Mass balance for 0.3m wide cavity with 0.1m high inlet.

$(T_{sm}-20)$ K		5	10	15	20	30	40
Mass flow (kg/sm)	at Inlet	0.041	0.059	0.071	0.080	0.097	0.110
	at Window	0.039	0.057	0.068	0.081	0.095	0.107
	at Outlet	0.040	0.060	0.072	0.082	0.098	0.112

Table 4.8 Mass balance for 0.3m wide cavity with 0.4m high inlet.

$(T_{sm}-20)$ K		5	10	15	20	30	40
Mass flow (kg/sm)	at Inlet	0.047	0.067	0.086	0.097	0.107	0.121
	at Window	0.044	0.065	0.085	0.095	0.105	0.118
	at Outlet	0.048	0.069	0.089	0.099	0.109	0.124

Table 4.9 Mass balance for 0.5m wide cavity with 0.1m high inlet.

		$(T_{sm}-20)$ K	5	10	15	20	30	40
Mass flow		at Inlet	0.040	0.055	0.069	0.080	0.093	0.109
(*kg/sm*)		at Window	0.041	0.056	0.071	0.082	0.092	0.107
		at Outlet	0.060	0.073	0.091	0.104	0.130	0.133

Table 4.10 Mass balance for 0.5m wide cavity with 0.4m high inlet.

		$(T_{sm}-20)$ K	5	10	15	20	30	40
Mass flow		at Inlet	0.052	0.073	0.093	0.103	0.113	0.128
(*kg/sm*)		at Window	0.050	0.072	0.092	0.101	0.112	0.126
		at Outlet	0.064	0.085	0.103	0.111	0.127	0.140

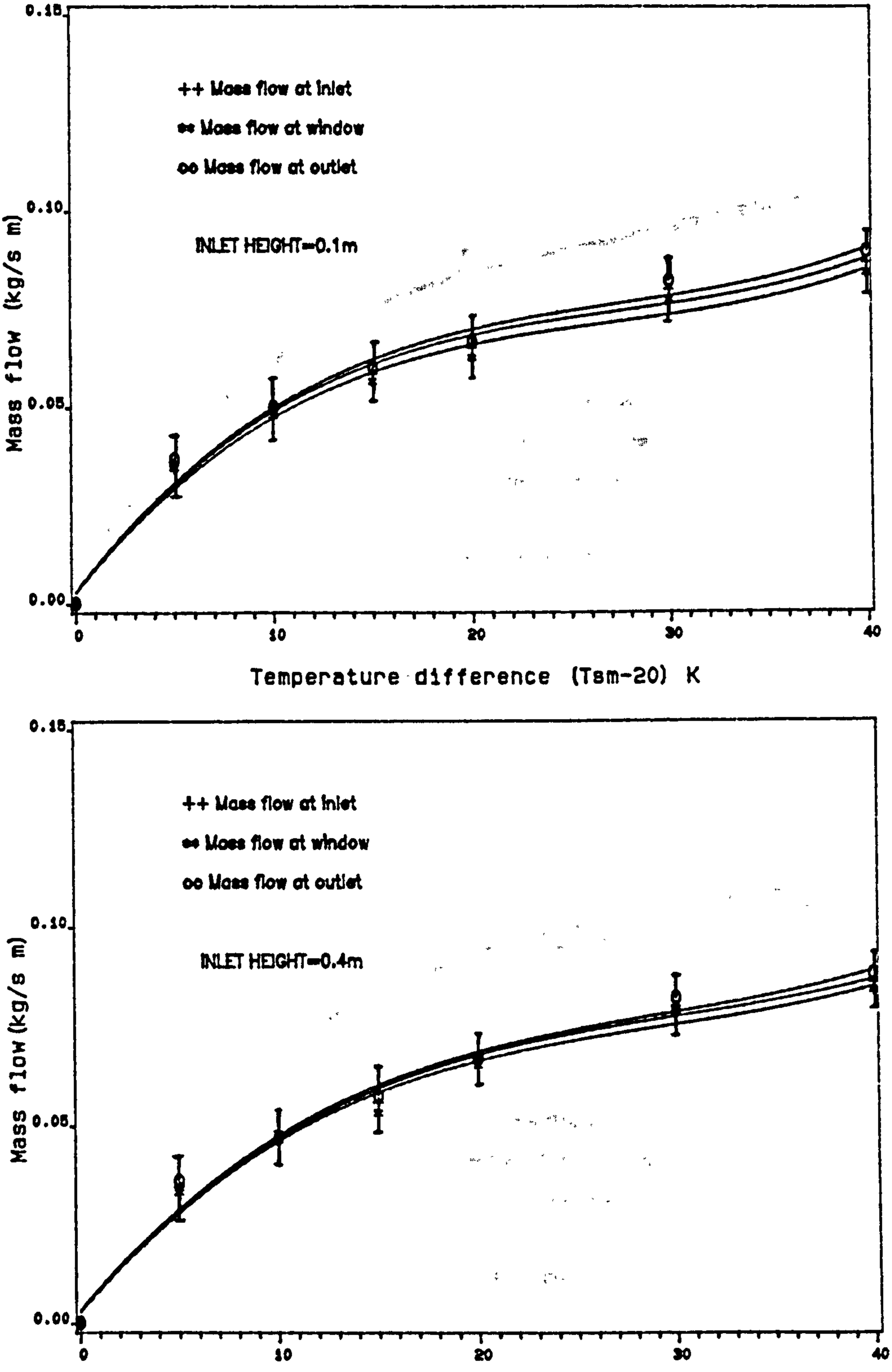

Figure 4.2 Mass balance for 0.1m wide cavity

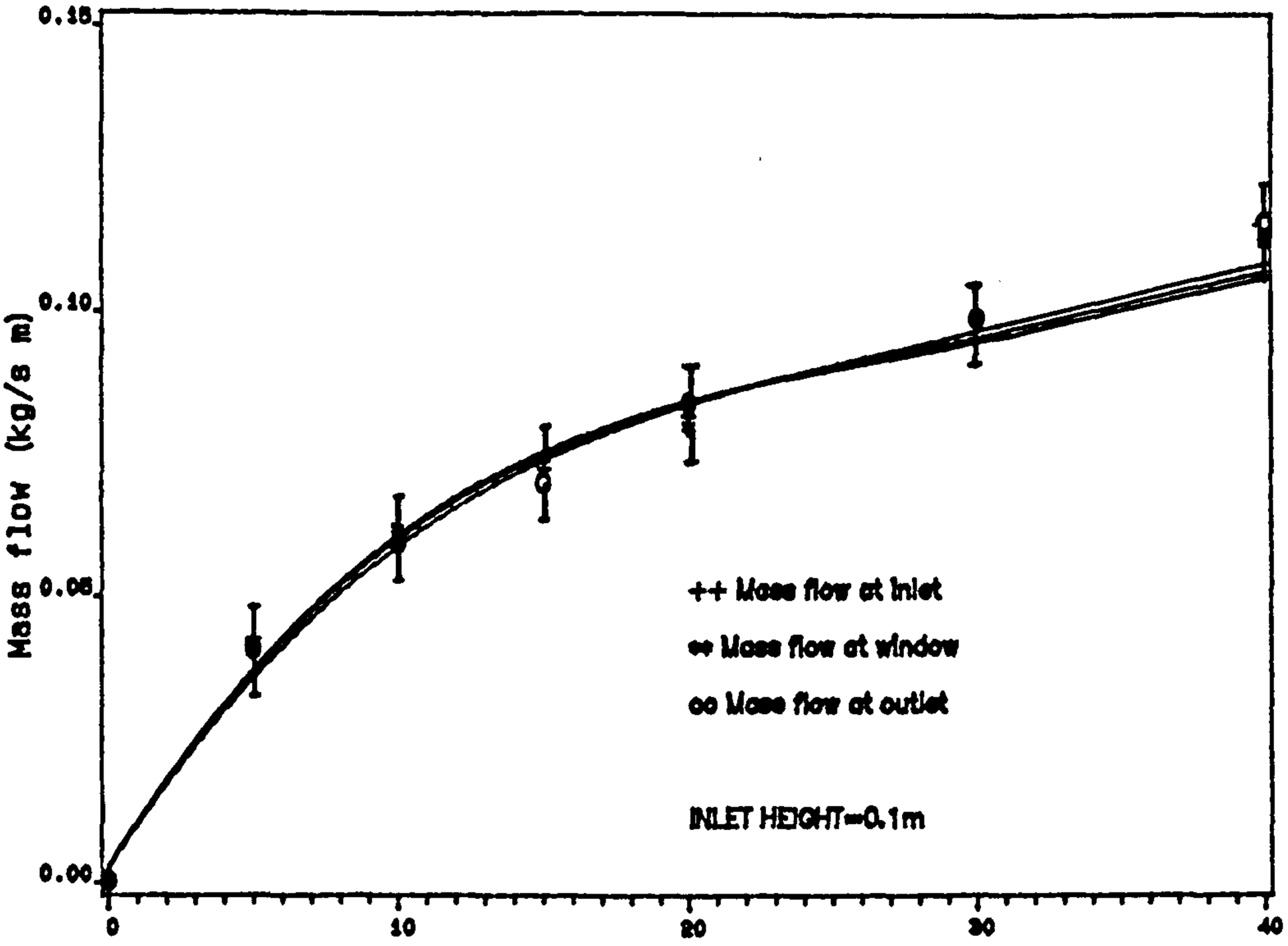

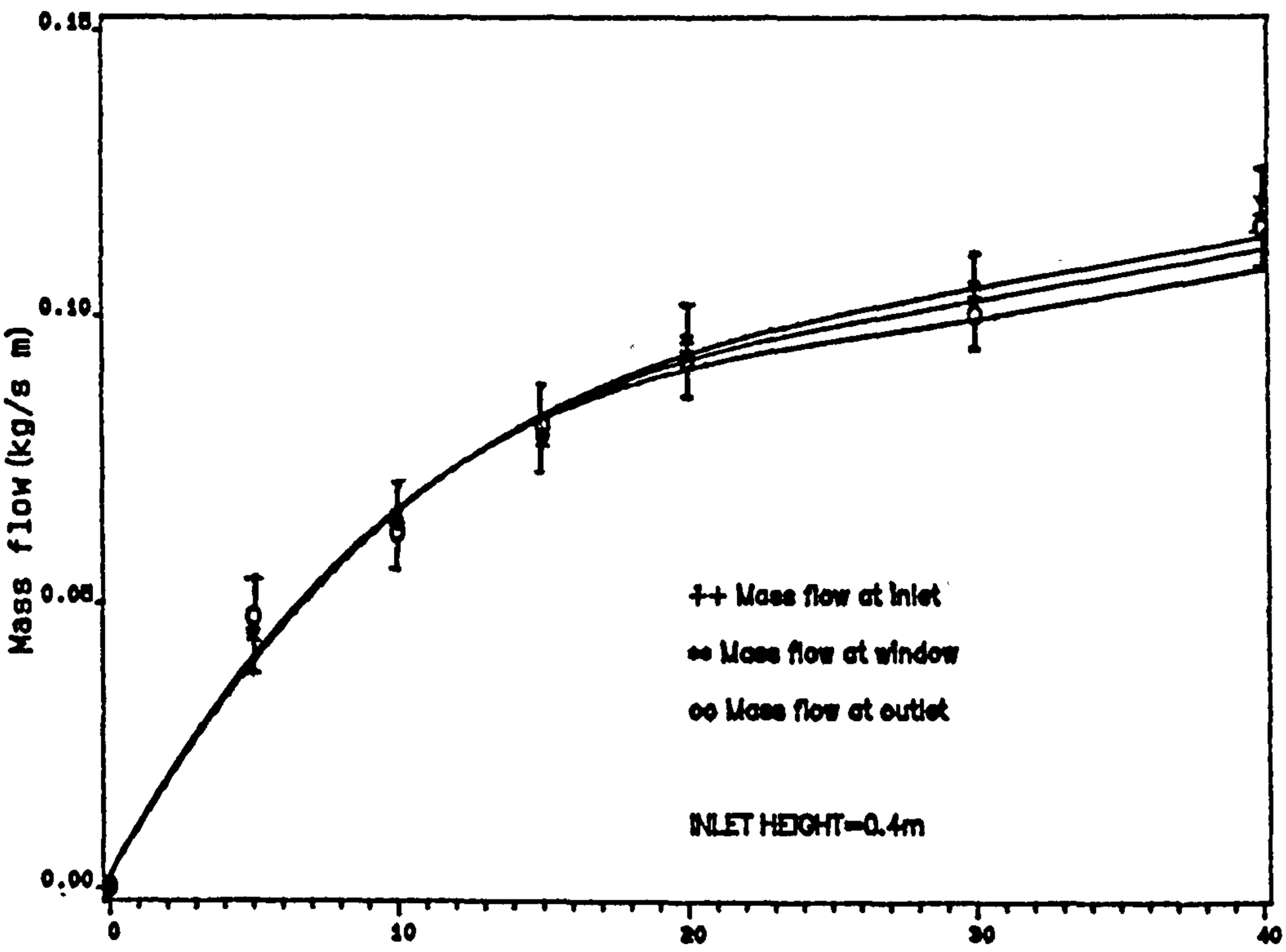

Figure 4.3 Mass balance for 0.2m wide cavity

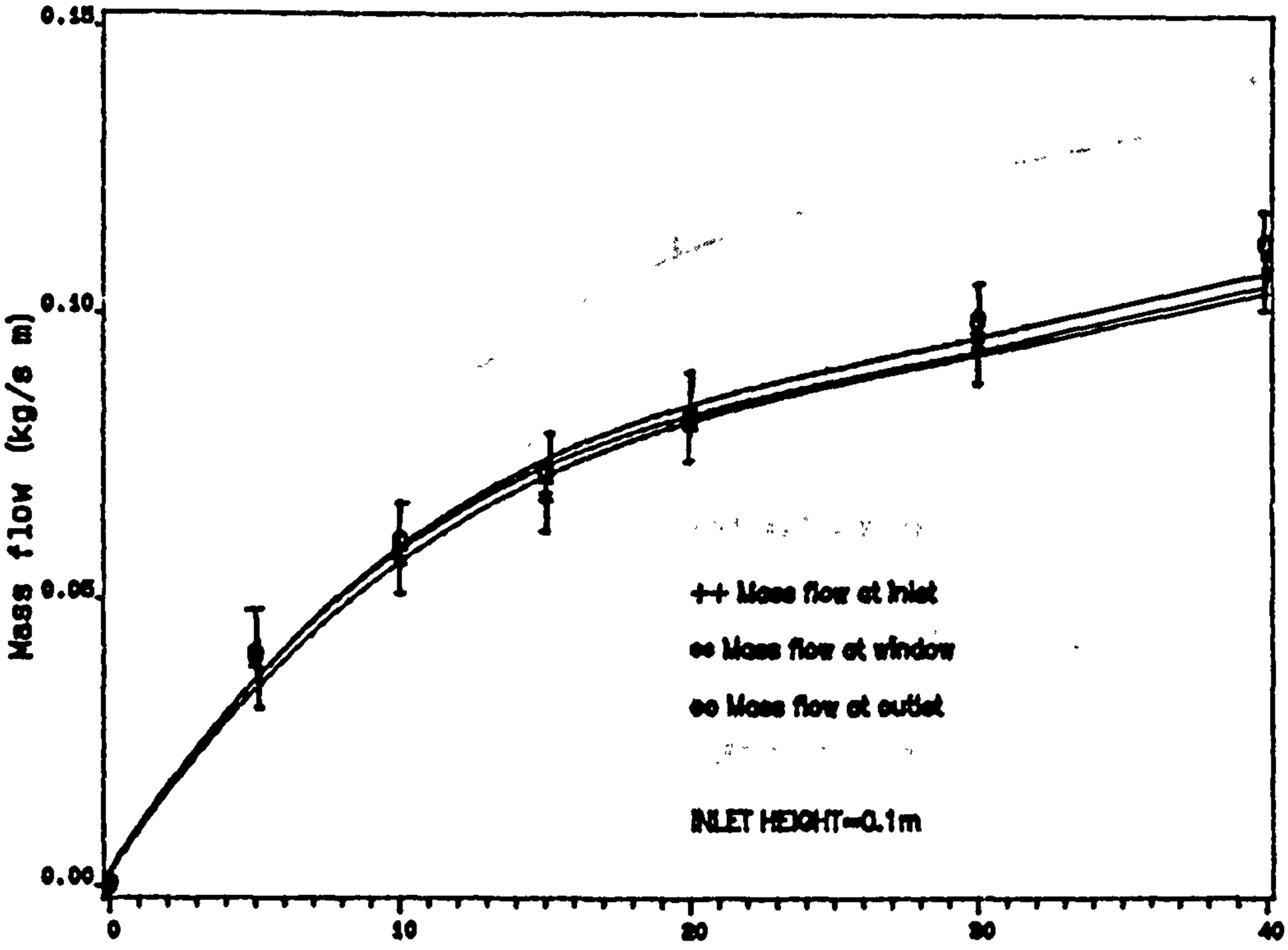

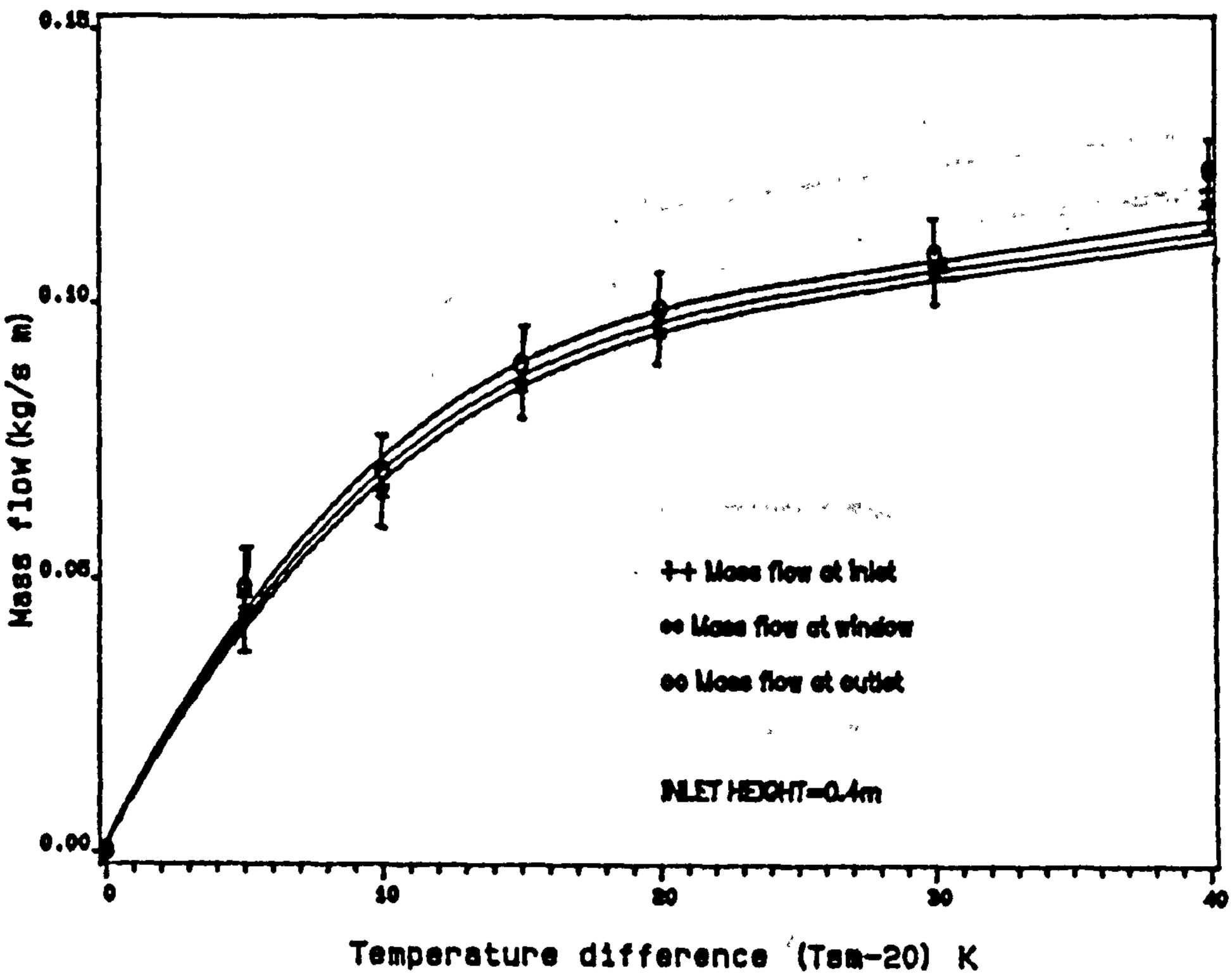

Figure 4.4 Mass balance for 0.3m wide cavity

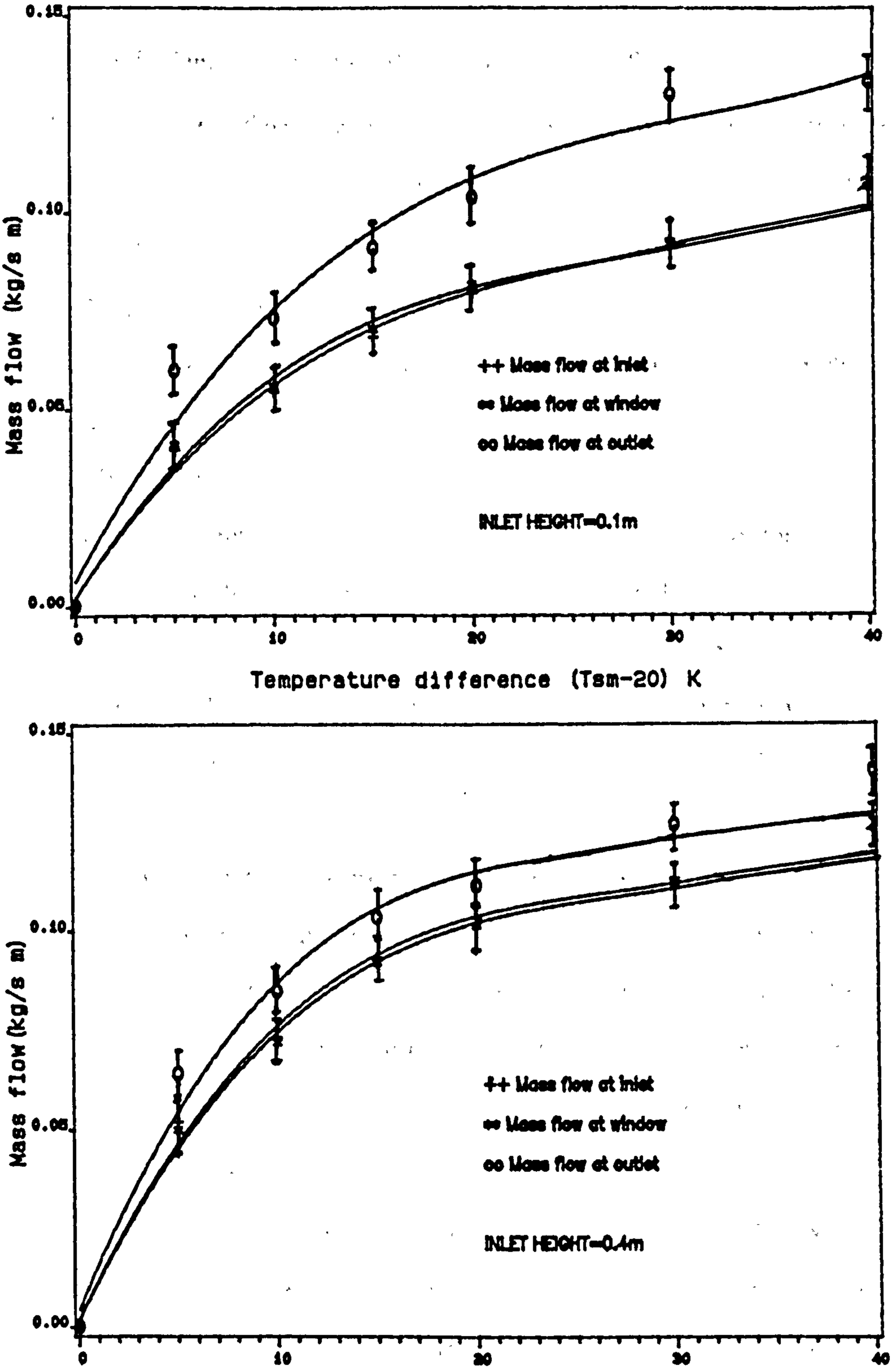

Figure 4.5 Mass balance for 0.5m wide cavity

The coefficient of correlation R of the data was 0.99 with a coefficient of rejection $P < 0.05$. The values of parameters a, b, c, d and R are summarised for each curve in tables 4.11 to 4.18. It is seen from these that the parameters c and d are negligible in relation to b and a.

4.2.1.2 Air flow patterns

The use of smoke enabled the air flow patterns in the cavity and in the room to be traced at various places.

4.2.1.2.1 In the cavity

Smoke was injected horizontally in various places at the top of the cavity. If there is no up or down flow, the smoke will move slowly, horizontally. If there is up or down flow then the smoke will migrate respectively. The cavity was varied in width from 0.1m, 0.2m, 0.3, to 0.5m. For 0.1m, 0.2m and 0.3m wide cavities the smoke trace was observed to be entirely upwards (figure 4.6). This in fact confirms the mass flow results reported in section 4.2.1.1.

With a 0.5m wide cavity, the smoke was downwards in the central section of the cavity, whereas it was upwards within a section of about 125mm thick from each side of the cavity (figures 4.7 and 4.8). The upward air flow on either side was supplied from the room through the inlet, and partly from down flow in the centre of the cavity. Figure 4.9 shows a schematic diagram of the possible flow patterns in a 0.5m wide cavity.

4.2.1.2.2 In the room

Similar observations were made to check the direction of the flow of air through the room to see whether there was any reverse flow from the room to the outside via the window, and also to see how the air passed through the room into the cavity. Observations also made it possible to see whether the air filled the whole room before it migrated into the cavity or whether it goes in a stream line directly to the inlet. Smoke was injected initially through the window and then through the inlet. Figure 4.10 shows the smoke at various positions inside the room. As can be seen, air travels through the room in a stream

Table 4.11 Values of a, b, c, d and R for figure 4.2, for 0.1m wide cavity with a 0.1m high inlet.

Parameters	$a \times 10^{-5}$	$b \times 10^{-5}$	$c \times 10^{-5}$	$d \times 10^{-5}$	R
Inlet	304	638	-20	0.2	0.99
Window	291	622	-20	0.2	0.99
Outlet	313	647	-20	0.2	0.99

Table 4.12 Values of a, b, c, d and R for figure 4.2, for 0.1m wide cavity with a 0.4m high inlet.

Parameters	$a \times 10^{-5}$	$b \times 10^{-5}$	$c \times 10^{-5}$	$d \times 10^{-5}$	R
Inlet	294	590	-16	0.2	0.99
Window	289	586	-17	0.2	0.99
Outlet	334	596	-17	0.2	0.99

Table 4.13 Values of a, b, c, d and R for figure 4.3, for 0.2m wide cavity with a 0.1m high inlet.

Parameters	$a \times 10^{-5}$	$b \times 10^{-5}$	$c \times 10^{-5}$	$d \times 10^{-5}$	R
Inlet	285	808	-26	0.3	0.99
Window	236	831	-28	0.4	0.99
Outlet	244	785	-25	0.3	0.99

Table 4.14 Values of a, b, c, d and R for figure 4.3, for 0.2m wide cavity with a 0.4m high inlet.

Parameters	$a \times 10^{-5}$	$b \times 10^{-5}$	$c \times 10^{-5}$	$d \times 10^{-5}$	R
Inlet	213	896	-29	0.4	0.99
Window	192	885	-28	0.3	0.99
Outlet	240	914	-31	0.4	0.99

Table 4.15 Values of a, b, c, d and R for figure 4.4, for 0.3m wide cavity with a 0.1m high inlet.

Parameters	$a \times 10^{-5}$	$b \times 10^{-5}$	$c \times 10^{-5}$	$d \times 10^{-5}$	R
Inlet	278	781	-26	0.3	0.99
Window	222	747	-23	0.3	0.99
Outlet	225	791	-25	0.3	0.99

Table 4.16 Values of a, b, c, d and R for figure 4.4, for 0.3m wide cavity with a 0.4m high inlet.

Parameters	$a \times 10^{-5}$	$b \times 10^{-5}$	$c \times 10^{-5}$	$d \times 10^{-5}$	R
Inlet	172	959	-32	0.4	0.99
Window	119	935	-31	0.4	0.99
Outlet	164	1003	-34	0.4	0.99

Table 4.17 Values of a, b, c, d and R for figure 4.5, for 0.5m wide cavity with a 0.1m high inlet.

Parameters	$a \times 10^{-5}$	$b \times 10^{-5}$	$c \times 10^{-5}$	$d \times 10^{-5}$	R
Inlet	242	753	-24	0.2	0.99
Window	224	795	-27	0.3	0.99
Outlet	643	926	-26	0.3	0.99

Table 4.18 Values of a, b, c, d and R for figure 4.5, for 0.5m wide cavity with a 0.4m high inlet.

Parameters	$a \times 10^{-5}$	$b \times 10^{-5}$	$c \times 10^{-5}$	$d \times 10^{-5}$	R
Inlet	212	1064	-37	0.5	0.99
Window	184	1039	-35	0.4	0.99
Outlet	444	1206	-44	0.5	0.99

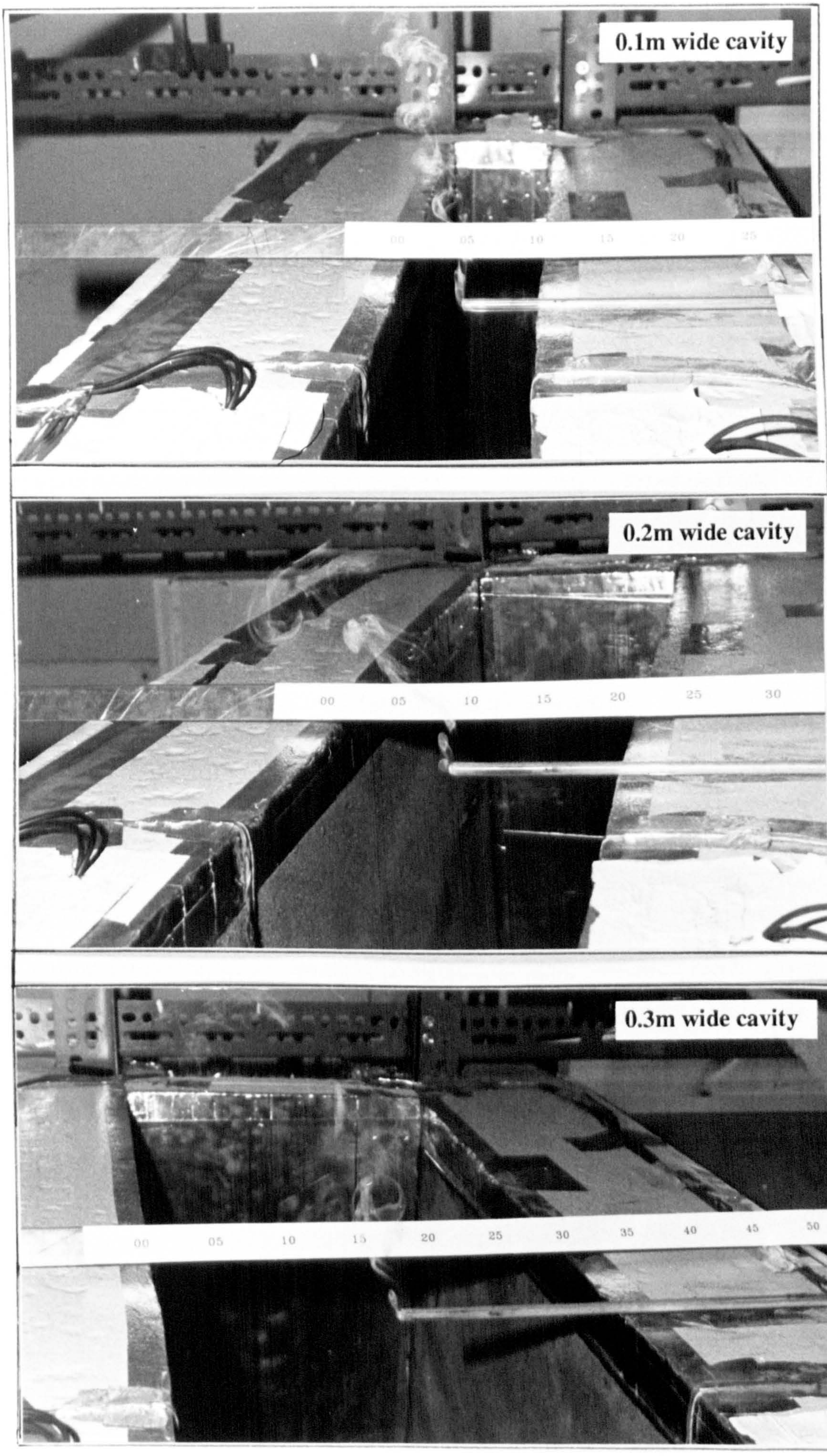

Figure 4.6 Air flow patterns at top of cavity.

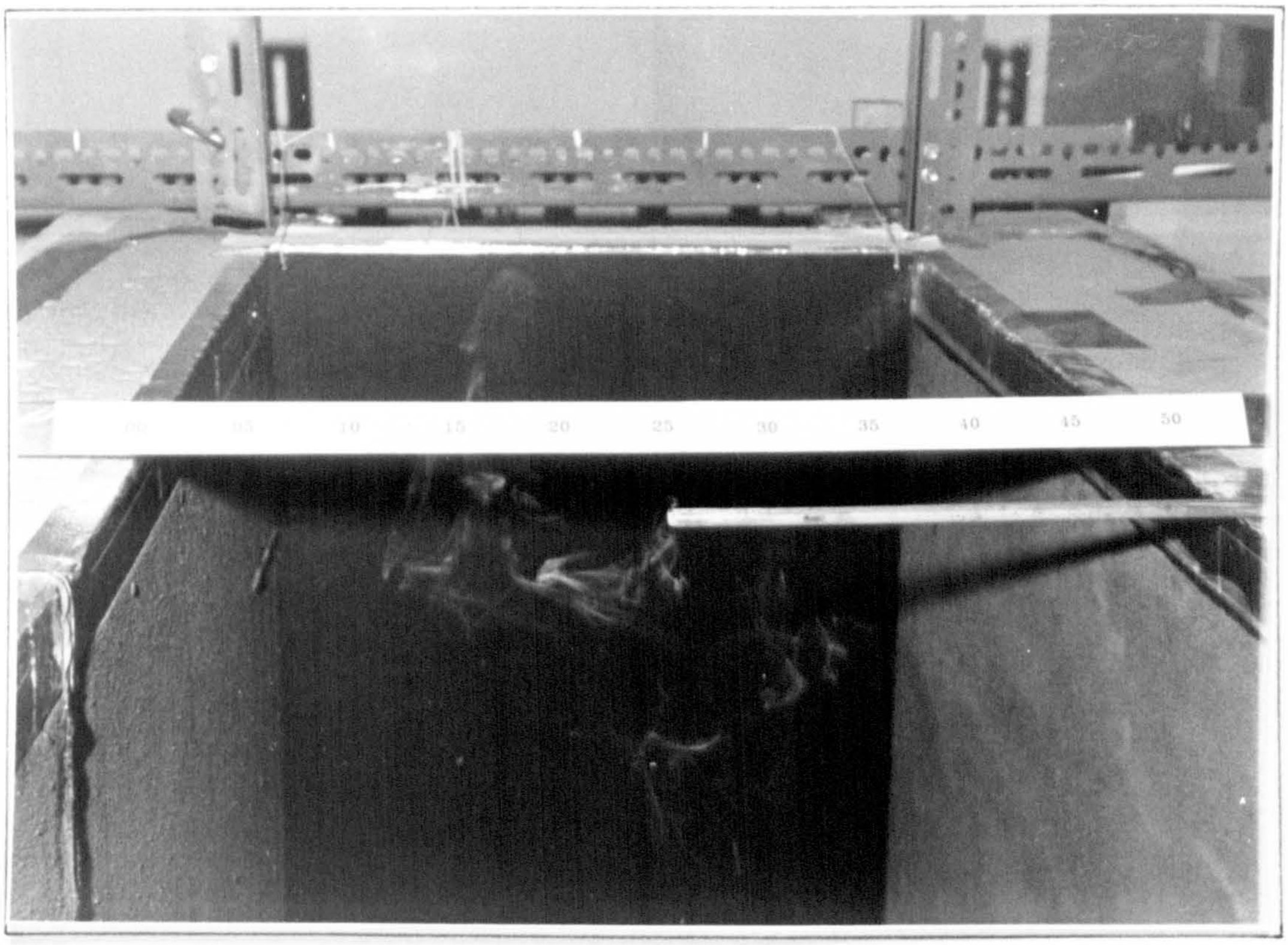

Figure 4.7 Downflow in the centre of a 0.5m wide cavity.

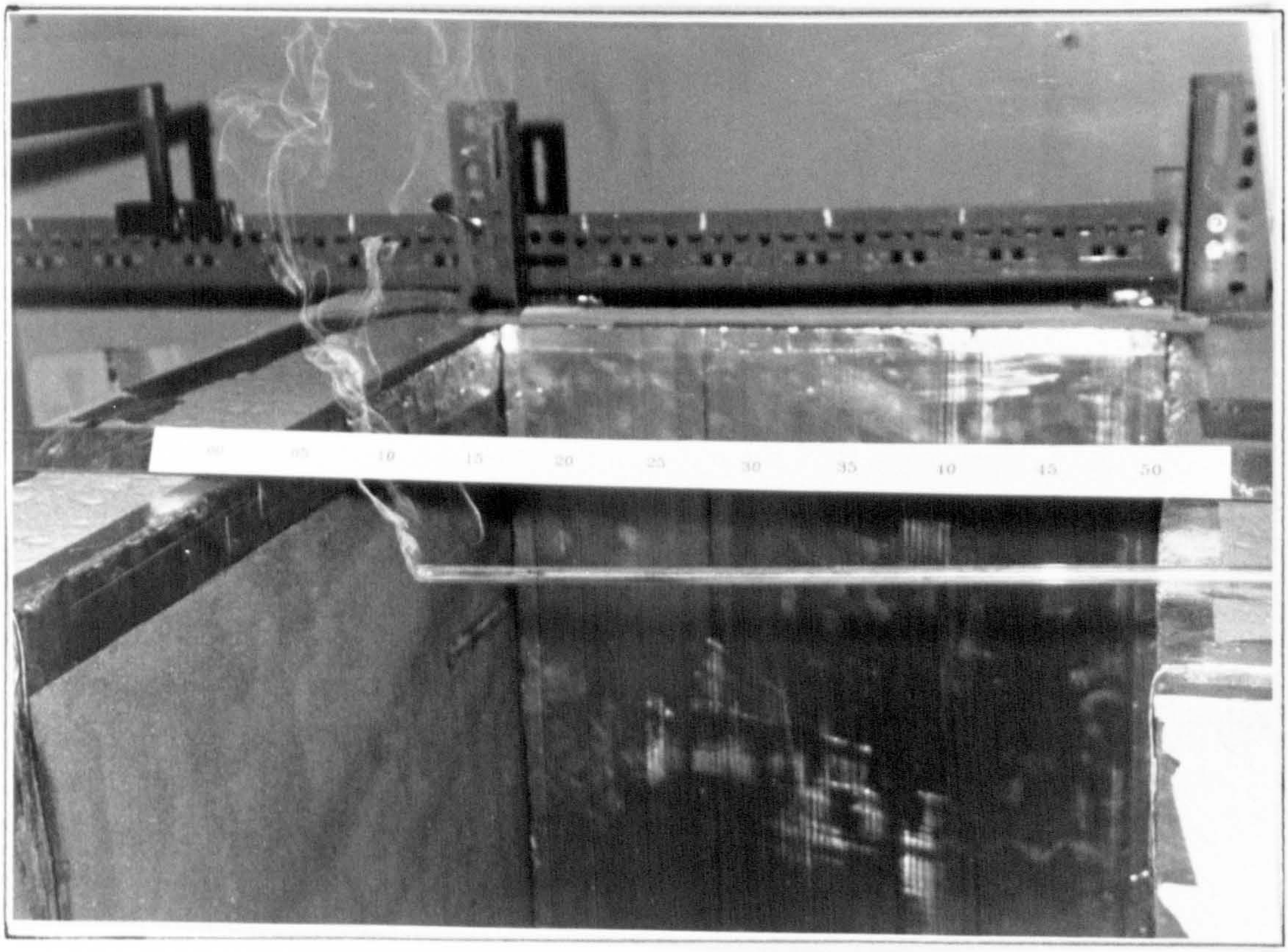

Figure 4.8 Upward flow near the surface of movable wall.

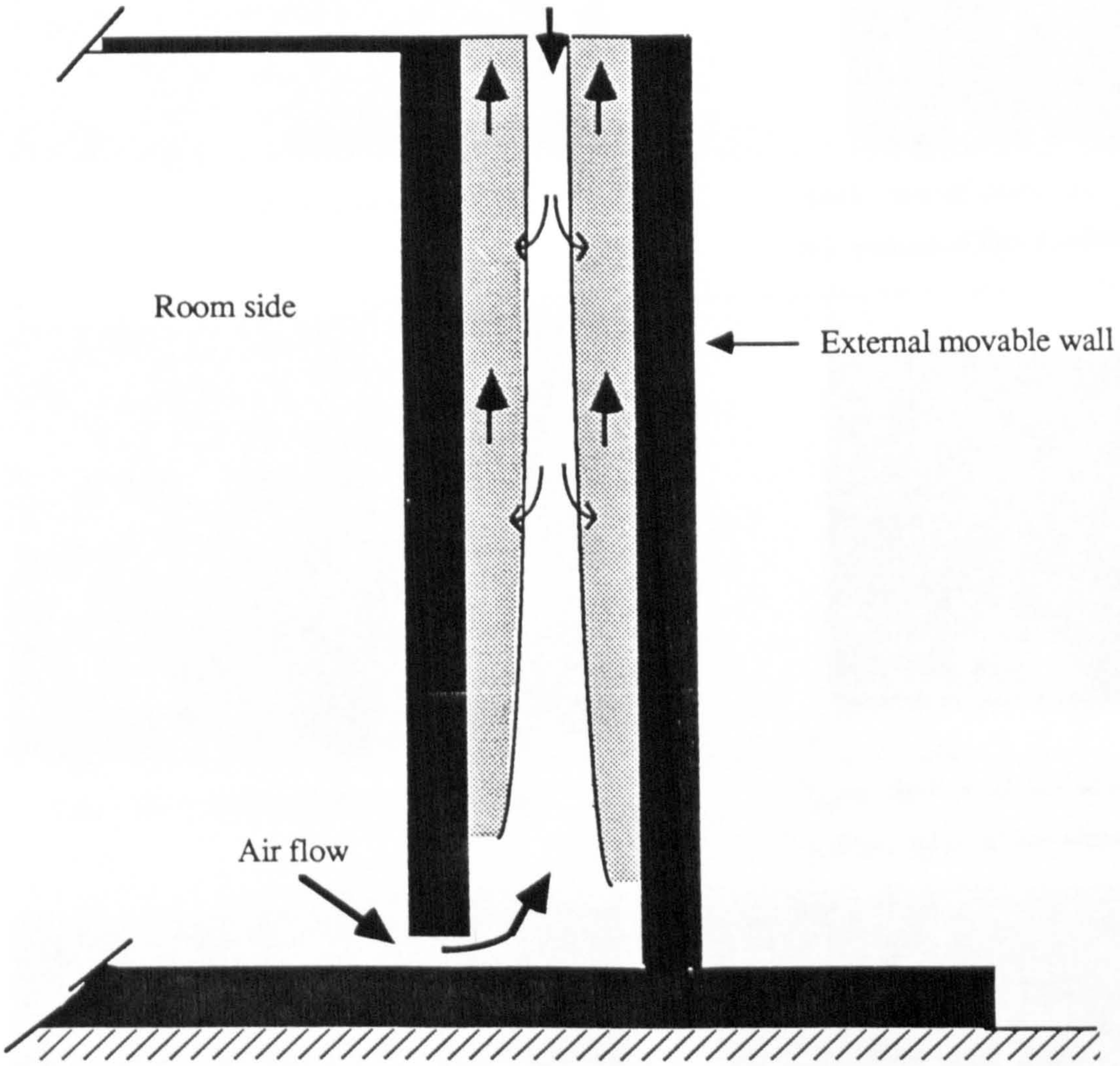

Figure 4.9 Schematic diagram of possible air flow patterns inside the cavity.

Side view of smoke across the room.

Back view of smoke at
the middle of the window.

Side view of smoke below the window.

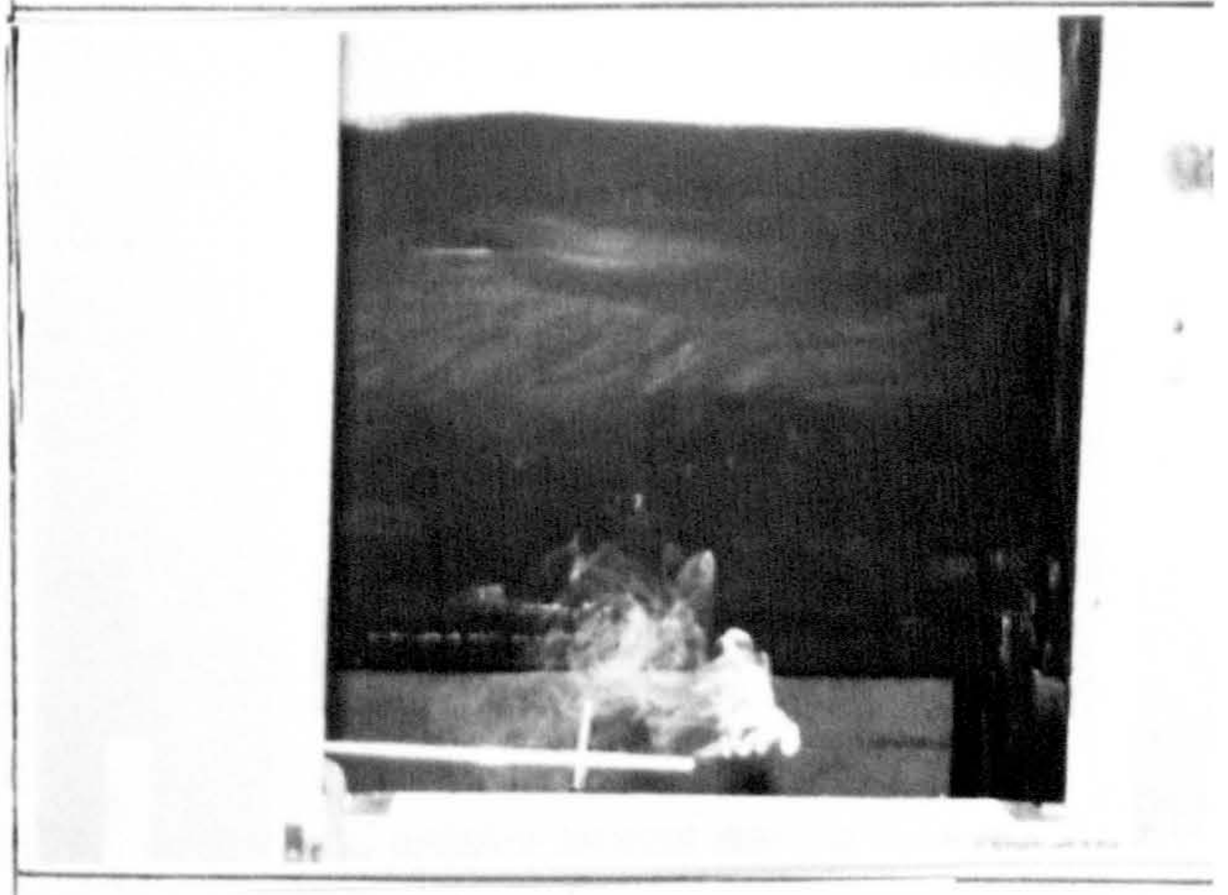

Back view of smoke at the
bottom edge of the window.

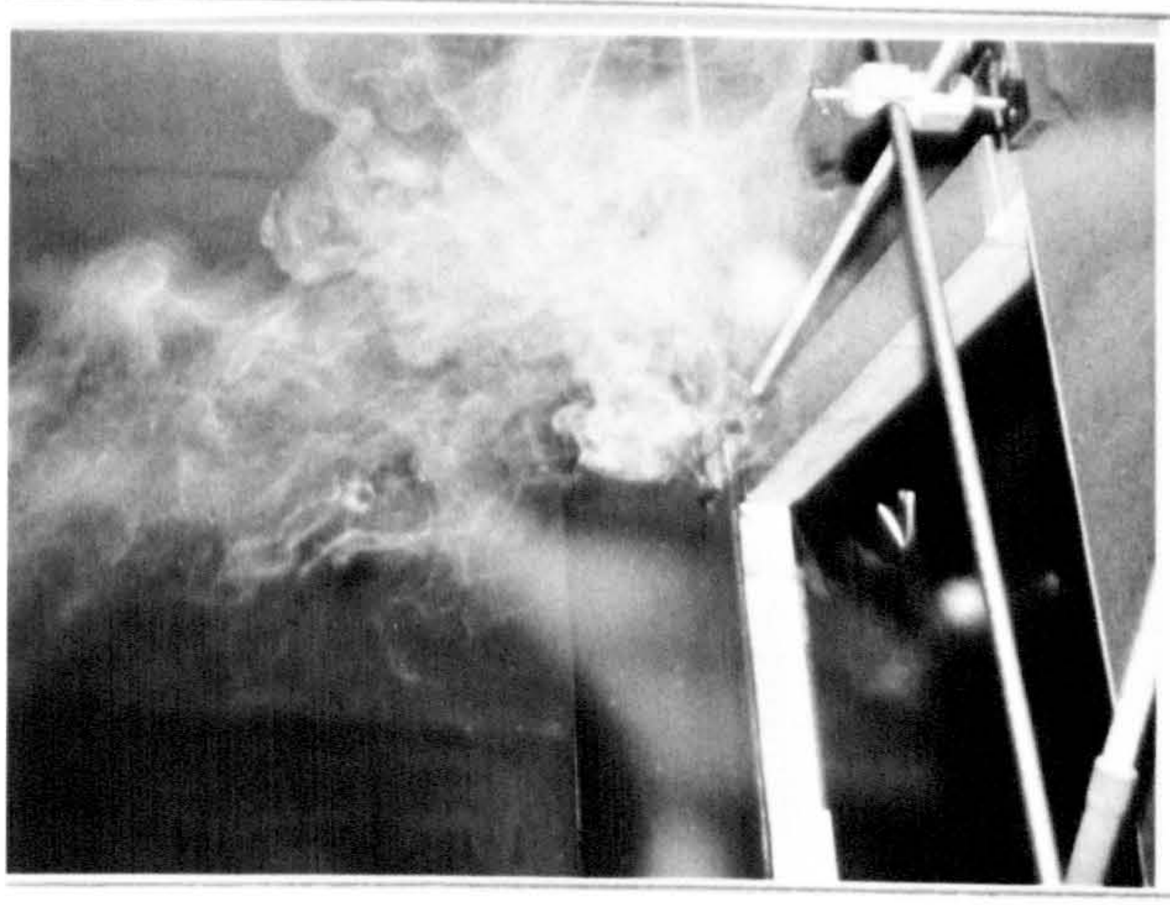

Side view of smoke above the window.

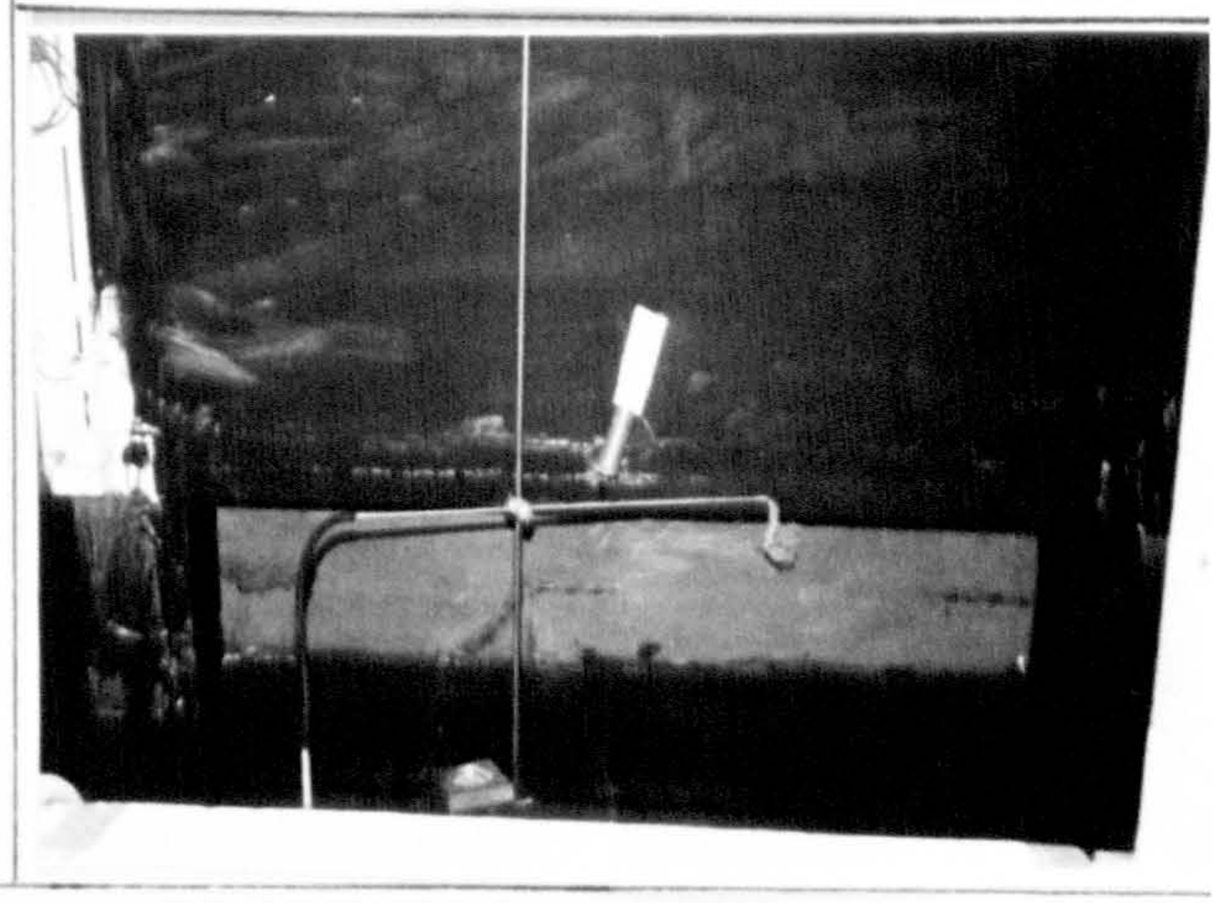

Smoke at the inlet to the cavity

Figure 4.10 Airflow patterns in the room.

line from the window towards the inlet and then to the heated cavity. There was no reverse flow. Smoke traces below and above the window were almost stagnant, indicating that the flow does not affect the whole of the air in the room. This indicates that the position of the windows should be chosen in such a way that ventilation can affect most of the internal space.

4.2.2 Effect of air inlet height

In order to know the effect of inlet height on the rate of mass flow, flows were monitored for 0.1m and 0.4m high inlets together with different cavity widths (0.1m, 0.2m, 0.3m and 0.5m). The surface temperature was increased from 5K to 40K above the ambient air temperature. Results are presented in tables 4.19 to 4.22 and plotted in figures 4.11 and 4.12 which show the mass flow rate as a function of temperature difference between surfaces and the entering air. Figure 4.11 shows that with a 0.1m wide cavity that, statistically, the curves for 0.1m and 0.4m high inlet are very close, suggesting that the inlet has no effect on the rate of mass flow, and the flow is dominated by frictional losses throughout the cavity.

Statistically when the inlet height is 0.4m, the mass flow rate for a 0.2m wide cavity is slightly higher. Considering the errors associated with the measurement it could be that the mass flow rates are similar and not dependent upon inlet height.

Figure 4.12 shows that as the cavity width is increased up to 0.3m and 0.5m the inlet height begins to show an influence on the mass flow rate. More mass flow is produced with high inlet. In such cases the frictional losses inside the cavity are negligible and thus, the pressure loss at the inlet becomes significant. When the inlet is increased, more mass flow is allowed through the inlet due to diminuation of pressure loss and also down flow becomes less.

4.2.3 Type of flow

The nature of the flow was determined using the Raleigh number for natural convection and the Reynolds number for forced convection. For exposed surfaces the flow was turbulent if $GrPr > 10^9$, and for flow in pipes, the flow is turbulent if $Re > 3000$.

Table 4.19 Effect of inlet height on air flow rate for 0.1 wide cavity.

$(T_{sm}-20)$ K		5	10	15	20	30	40
Mass flow	0.1m high inlet	0.036	0.049	0.059	0.065	0.080	0.088
(*kg/sm*)	0.4m high inlet	0.035	0.046	0.056	0.067	0.080	0.088

Table 4.20 Effect of inlet height on air flow rate for 0.2m wide cavity.

$(T_{sm}-20)$ K		5	10	15	20	30	40
Mass flow	0.1m high inlet	0.043	0.060	0.073	0.082	0.099	0.110
(*kg/sm*)	0.4m high inlet	0.045	0.064	0.079	0.094	0.103	0.118

Table 4.21 Effect of inlet height on air flow rate for 0.3 wide cavity.

$(T_{sm}-20)$ K		5	10	15	20	30	40
Mass flow	0.1m high inlet	0.041	0.059	0.071	0.080	0.097	0.109
(*kg/sm*)	0.4m high inlet	0.047	0.067	0.086	0.097	0.107	0.121

Table 4.22 Effect of inlet height on air flow rate for 0.5m wide cavity.

$(T_{sm}-20)$ K		5	10	15	20	30	40
Mass flow	0.1m high inlet	0.040	0.055	0.069	0.080	0.091	0.103
(*kg/sm*)	0.4m high inlet	0.052	0.073	0.093	0.097	0.108	0.124

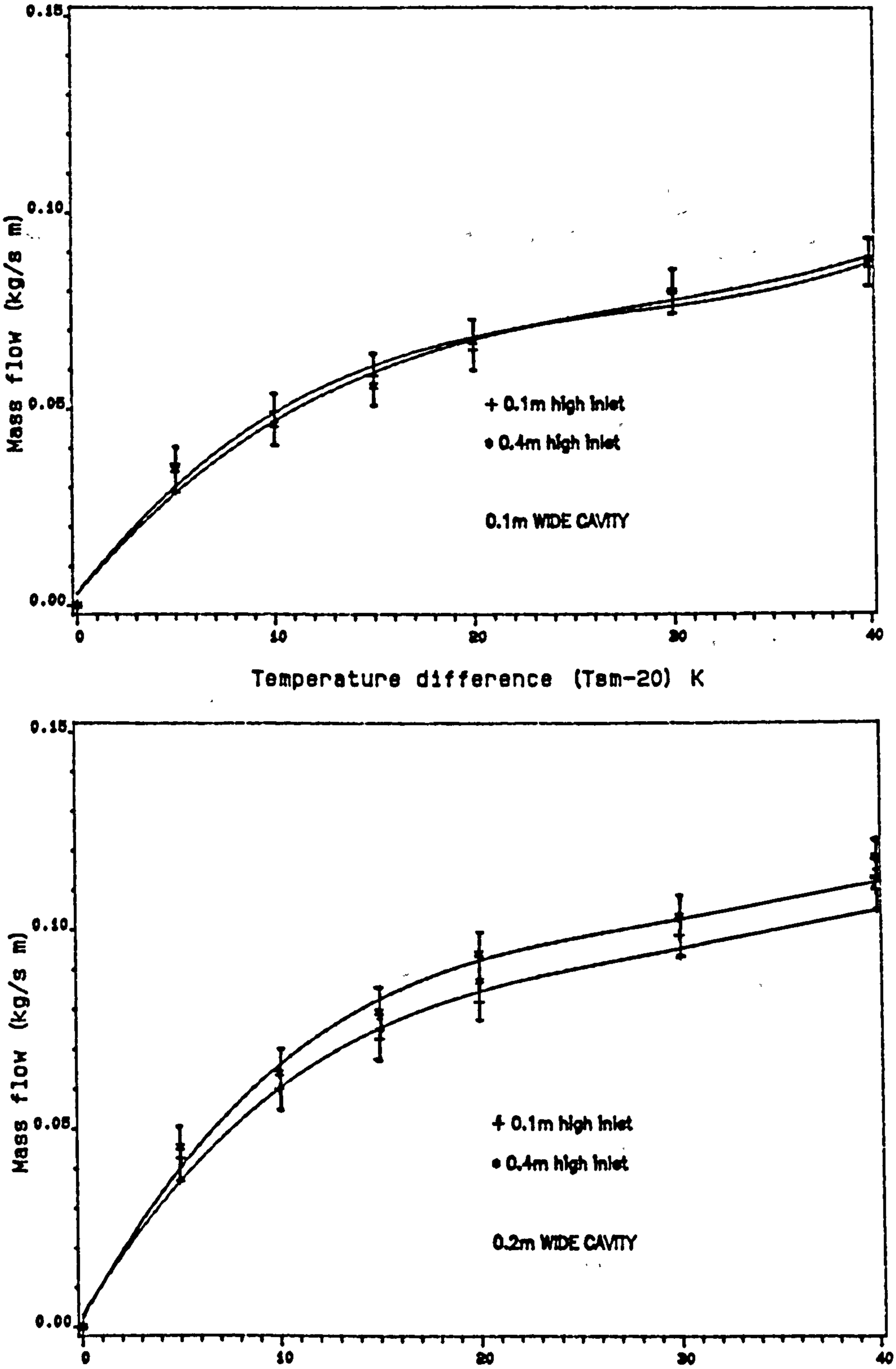

Figure 4.11 Effect of inlet height on air flow rate for 0.1m and 0.2m wide cavities.

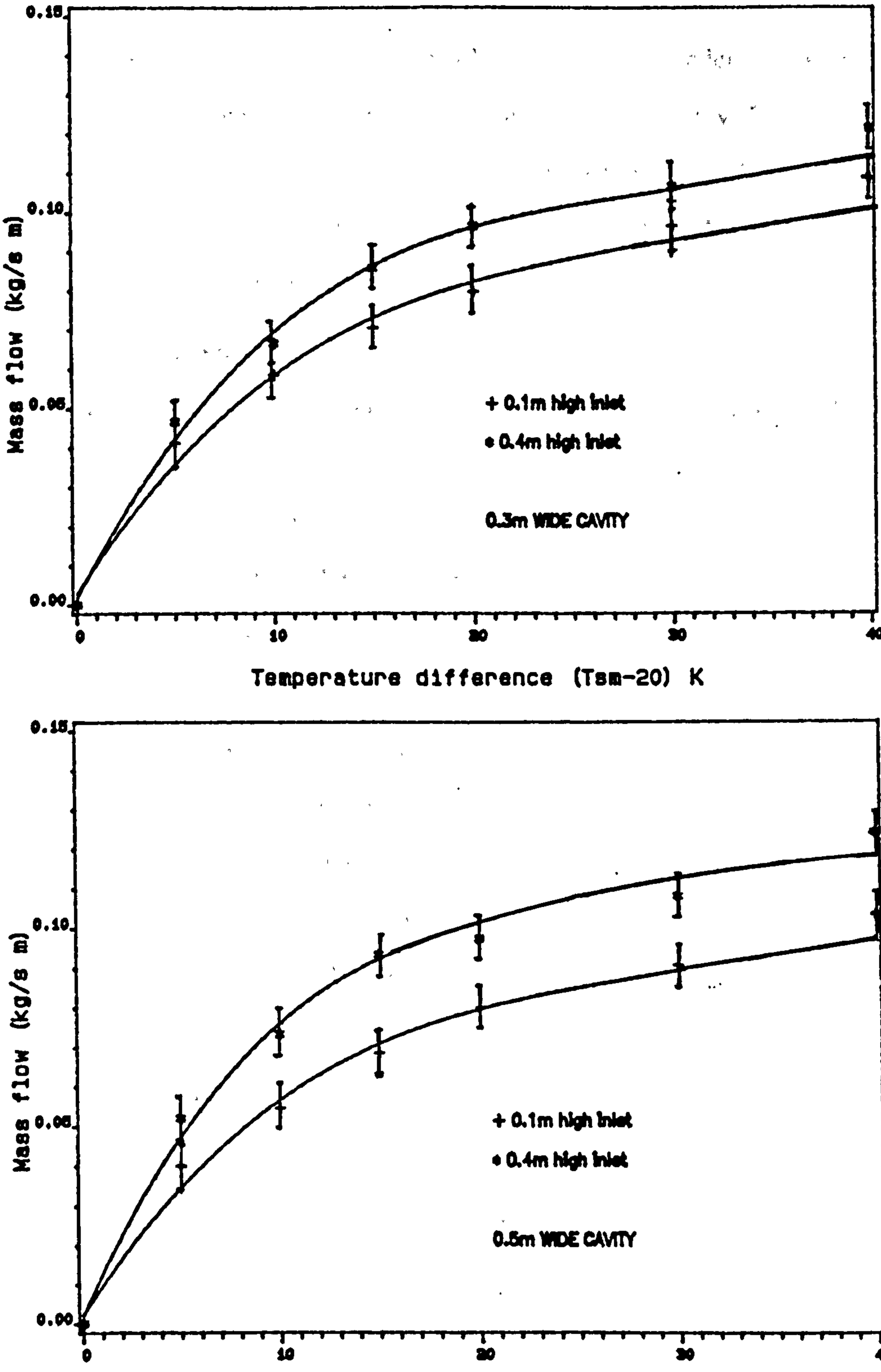

Figure 4.12 Effect of inlet height on air flow rate for 0.3m and 0.5m wide cavity.

For flow between parallel planes, the Reynolds number is dependent upon the "hydraulic diameter" which is proportional to the separation and fluid velocity. Tables 4.23 and 4.24 give the Raleigh and Reynolds numbers based on measurements. These confirm that the flow is turbulent using either criterion. This finding agrees with Akbarzadeh *et al.* (1982) who reported that the flow in a Trombe wall channel was turbulent.

4.2.4 Effect of surface temperature

The effect of surface temperature on the rate of mass flow through a heated cavity is an important parameter. The results obtained by increasing the surface temperatures of the cavity above the ambient air temperature, for 0.1m to 1.0m wide cavities, are given in tables 4.25 to 4.26. Tabulated data are plotted in figure 4.13 from which it can be seen that increasing the surface temperature of the cavity walls more than 15 K above the ambient air temperature ($T_{sm}-20$) has a reduced effect on the the mass flow rate. Data on the rate of change of mass flow in relation to the surface temperatures increase is presented in tables 4.27 and 4.28 and plotted in figure 4.14. This shows that the rate of change in the mass flow is rapid up to a point where the surface temperature increase ($T_{sm}-20$) is about 15K. Beyond this the rate of change is not so dramatic. This indicates that once wall temperatures are 10 to 15 K above the temperature of the entering air, further wall temperature increase gives little additional mass flow.

4.3 Heat Transfer

The performance of a cavity will depend on the amount of stored solar heat. The outside air at T_{ai} enters the inlet at a mass flow rate M, and leaves at T_{out}. The heated surfaces of the cavity heat the air by convection. The rate of heat removal by the moving air is dependent on the temperature difference between it and the surfaces, and the heat transfer coefficient between the cavity surfaces and the moving air. A heat balance on the moving air gives:

$$Mc(T_{out}-T_{ai})=2YZh_c(T_{sm}-T_{ac}) \tag{4.2}$$

Table 4.23 Raleigh and Reynolds numbers for test with 0.1m high inlet.

ΔT	$10^9 GrPr$	D_h	$\overline{v}$	Re
07.8	8.5	0.187	0.42	4600
16.0	17	0.187	0.56	6100
24.5	26	0.187	0.68	7400
32.8	35	0.187	0.77	8400
08.1	8.8	0.353	0.26	5400
16.7	18	0.353	0.35	7200
25.2	27	0.353	0.42	8700
34.0	36	0.353	0.47	9700
08.4	9.1	0.500	0.17	5000
17.2	19	0.500	0.23	6700
26.0	28	0.500	0.27	7900
35.0	38	0.500	0.31	9100

Table 4.24 Raleigh and Reynolds numbers for test with 0.4m high inlet.

ΔT	$10^9 GrPr$	D_h	$\overline{v}$	Re
08.2	13	0.187	0.39	4300
17.0	26	0.187	0.57	6200
25.7	39	0.187	0.73	8000
34.5	53	0.187	0.73	8000
08.4	13	0.353	0.27	5600
17.5	27	0.353	0.40	8300
26.4	41	0.353	0.44	9100
35.5	54	0.353	0.50	10300
08.5	1.3	0.500	0.15	4400
17.7	27	0.500	0.27	7900
27.0	42	0.500	0.30	8800
36.0	55	0.500	0.34	9900

Table 4.25 Effect of surface temperature on mass flow with 0.1m high inlet.

$(T_{sm}-20)$ K		5	10	15	20	30	40
Mass flow (kg/sm)	0.1m wide cavity	0.036	0.049	0.059	0.065	0.080	0.090
	0.2m wide cavity	0.043	0.060	0.073	0.082	0.099	0.110
	0.3m wide cavity	0.041	0.059	0.071	0.080	0.097	0.109
	0.5m wide cavity	0.040	0.055	0.069	0.080	0.091	0.103
	1.0m wide cavity	0.043	0.053	0.061	0.068	0.083	0.091

Table 4.26 Effect of surface temperature on mass flow with 0.4m high inlet.

$(T_{sm}-20)$ K		5	10	15	20	30	40
Mass flow (kg/sm)	0.1m wide cavity	0.035	0.046	0.056	0.067	0.080	0.086
	0.2m wide cavity	0.045	0.064	0.079	0.094	0.103	0.118
	0.3m wide cavity	0.046	0.060	0.086	0.097	0.107	0.121
	0.5m wide cavity	0.052	0.073	0.085	0.097	0.113	0.124
	1.0m wide cavity	0.048	0.066	0.080	0.083	0.096	0.105

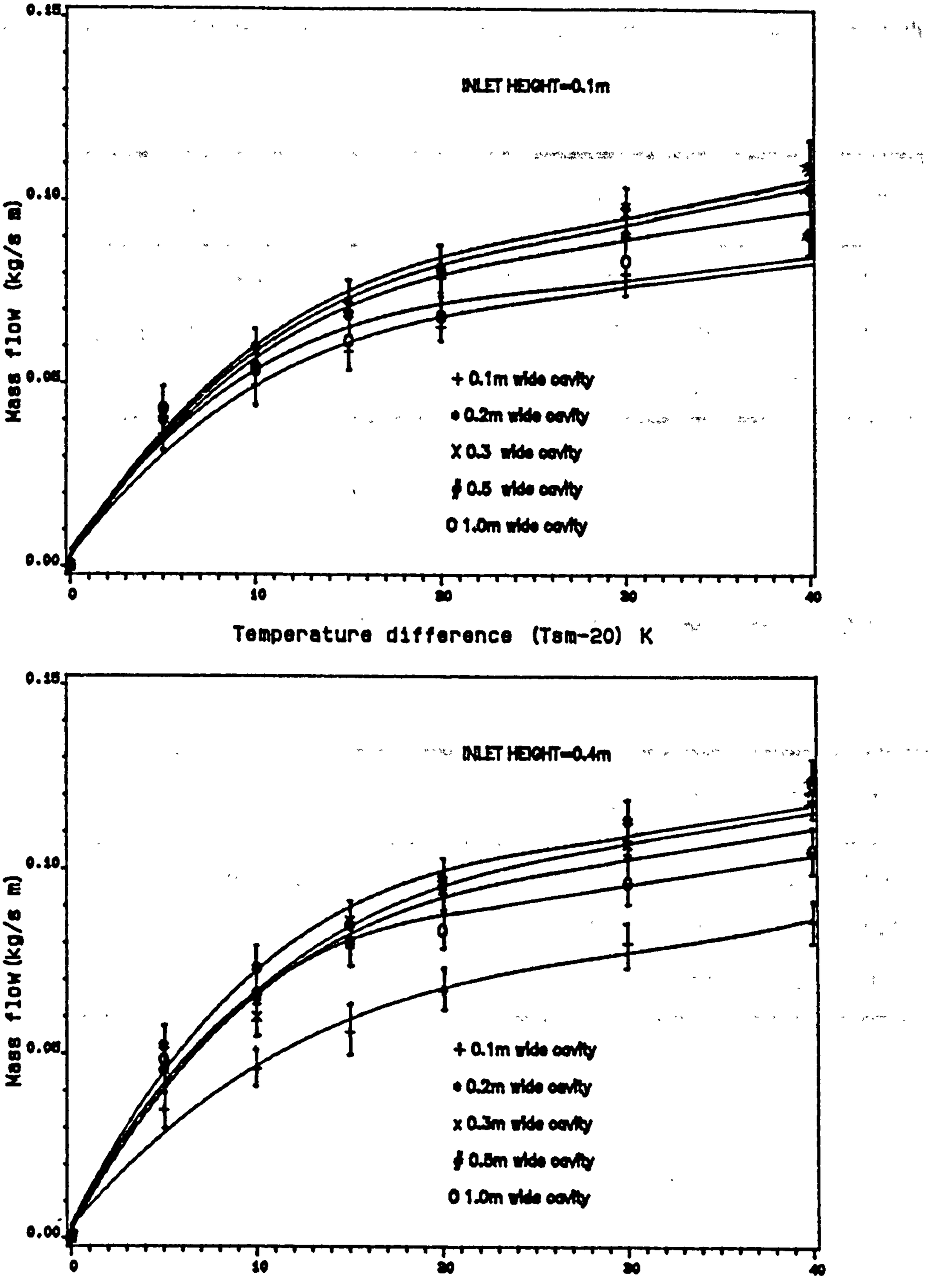

Figure 4.13 Effect of surface temperature on mass flow

Table 4.27 Rate of change of mass flow in relation to surface temperatures with 0.1m high inlet.

$(T_{sm}-20)$ K		5	10	15	20	30	40
Mass flow (kg/sm)	0.1m wide cavity	7.2	2.7	1.9	1.3	1.5	1.0
	0.2m wide cavity	8.5	3.5	2.5	1.9	1.7	1.1
	0.3m wide cavity	8.0	2.9	2.8	2.3	1.1	1.3

Table 4.28 Rate of change of mass flow in relation to surface temperatures with 0.4 high inlet.

$(T_{sm}-20)$ K		5	10	15	20	30	40
Mass flow (kg/sm)	0.1m wide cavity	6.9	2.3	2.0	2.3	1.3	0.6
	0.2m wide cavity	9.1	3.7	3.07	2.93	0.93	1.47
	0.3m wide cavity	10.4	4.3	2.3	2.5	1.6	1.1

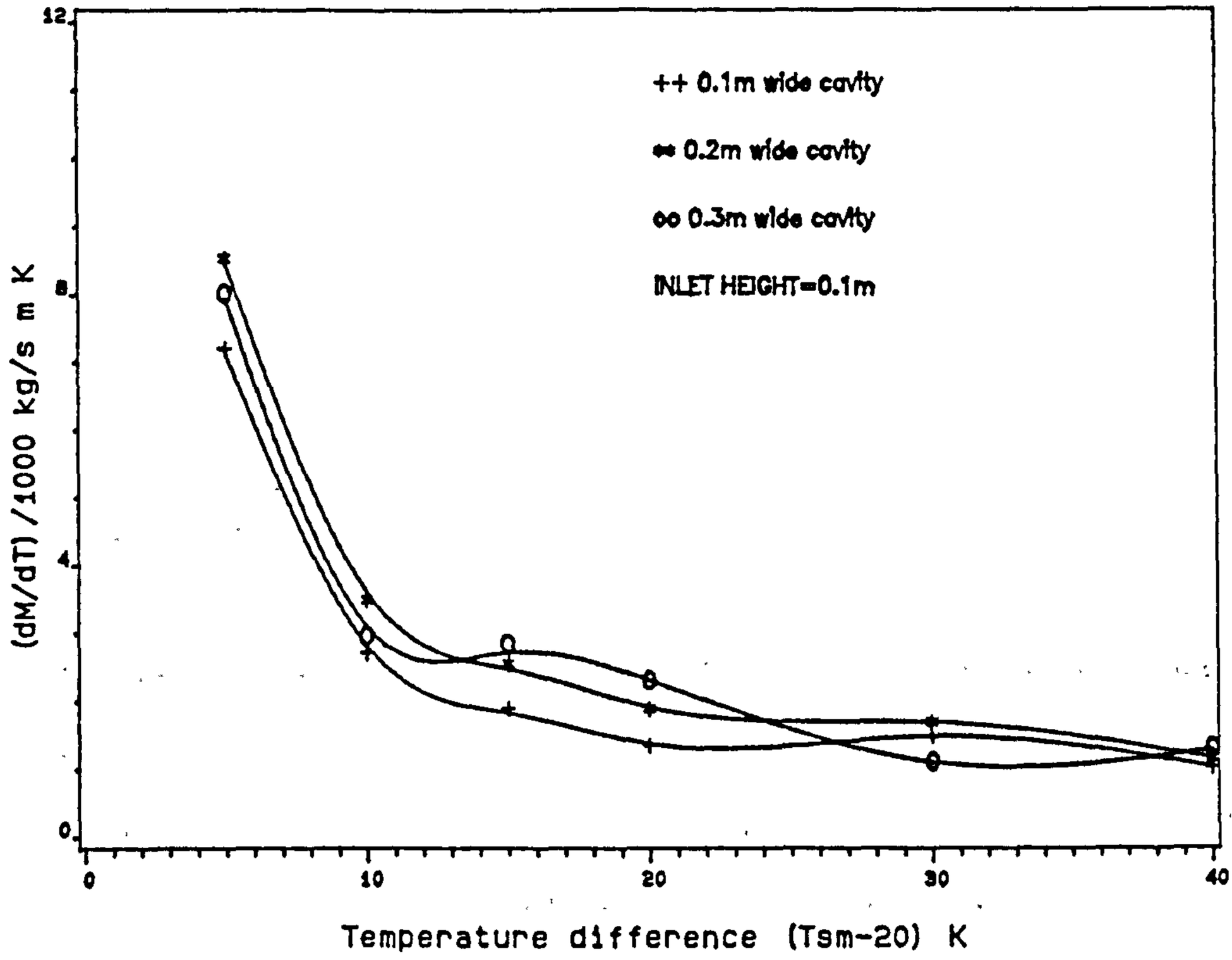

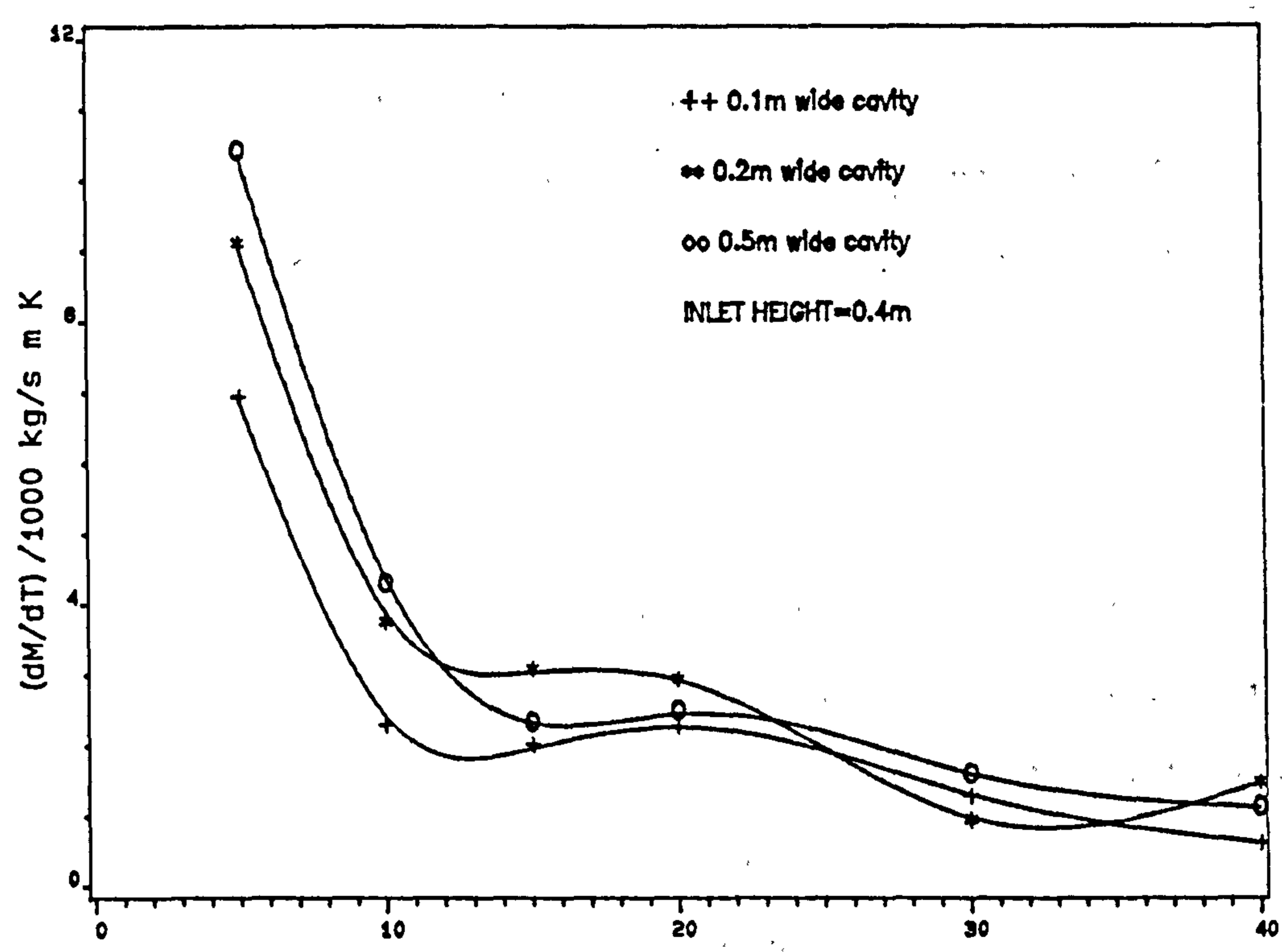

Figure 4.14 Rate of change of mass flow in relation to surface temperatures

from which,

$$h_c = \frac{Mc}{2YZ}\frac{(T_{out} - T_{ai})}{(T_{sm} - T_{ac})} \tag{4.3}$$

where

$$T_{ac} = (T_{ai} + T_{out})/2$$

With measured values for inlet, outlet and surface temperatures, and mass flow rate per unit length of cavity (kg/sm), the average heat transfer coefficient could be determined. Results, calculated for different mass flow rates are given in tables 4.29 and 4.30. The inlet was increased from 0.1m to 0.4m, and the cavity width varied from 0.1m to 0.3m at a 0.1m interval. The 0.5m and 1.0m wide cavity were not considered because of the complexity of the flow. Tabulated results are plotted in figure 4.15 which shows that the convective heat transfer coefficient as a function of the mass flow rate per unit length of cavity (kg/sm). Regression lines were drawn through the data using equation 4.4. The coefficient of correlation was 0.99 with $P<0.05$.

$$h_c = a + bM \tag{4.4}$$

When M approaches zero, a approaches 3, whereas b is a linear function of the cavity widths. Values of a and b for different mass flow rates are given in tables 4.31 and 4.32. The average density of the moving air was about 1.17 kg/m^3. It can be seen that, statistically, the cavity width has a markedly greater effect on b and thus on the heat transfer, for the lesser inlet height. The error bars shows little difference for 0.1m and 0.2m wide cavities.

Tables 4.33 and 4.34 give the results of the air temperature increase along the cavity for different conditions. The inlet height was varied from 0.1m to 0.4m and the surface temperature increased from 10K to 40K above ambient air temperature. The tabulated data

Table 4.29 Convection heat transfer coefficients for cavity with 0.1m high inlet.

Mass flow rate (kg/sm)		0.049	0.065	0.080	0.090
$hc(W/m^2K)$	0.1m wide cavity	6.7	8.2	8.9	9.8
Mass flow rate(kg/sm)		0.060	0.082	0.099	0.110
$hc(W/m^2K)$	0.2m wide cavity	7.0	7.9	9.3	9.7
Mass flow rate (kg/sm)		0.059	0.080	0.095	0.109
$hc(W/m^2K)$	0.3m wide cavity	5.6	6.5	7.4	7.8

Table 4.30 Convection heat transfer coefficients for cavity with 0.4m high inlet.

Mass flow rate (kg/sm)		0.046	0.067	0.080	0.086
$hc(W/m^2K)$	0.1m wide cavity	4.9	5.9	6.6	6.8
Mass flow rate (kg/sm)		0.064	0.094	0.103	0.118
$hc(W/m^2K)$	0.2m wide cavity	6.10	6.7	7.0	7.5
Mass flow rate (kg/sm)		0.053	0.097	0.107	0.121
$hc(W/m^2K)$	0.3m wide cavity	4.5	6.1	6.5	6.7

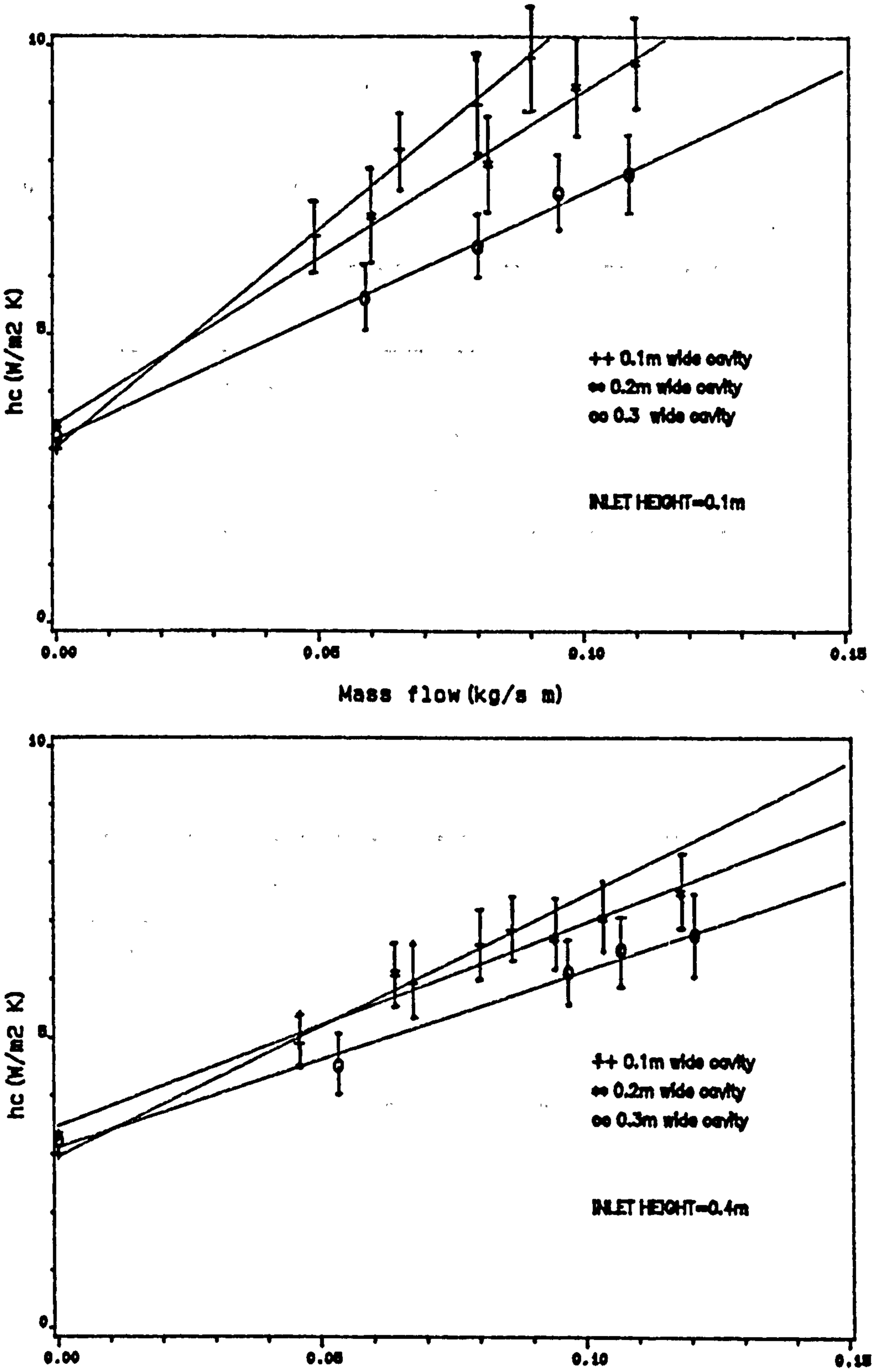

Figure 4.15 Convection heat transfer coefficient

Table 4.31 Values of a and b when the inlet is 0.1m high.

Parameters	a	b
0.1m wide cavity	3.0	75.7
0.2m wide cavity	3.4	57.6
0.3m wide cavity	3.2	42.8

Table 4.32 Values of a and b when the inlet is 0.4m high

Parameters	a	b
0.1m wide cavity	2.9	45.0
0.2m wide cavity	3.4	35.1
0.3m wide cavity	3.1	30.6

Table 4.33 Temperature rise of air in the cavity with 0.1m high inlet.

$(T_{sm}-20)$		10	20	30	40
Temperature rise (K)	0.1m wide cavity	4.3	8.0	11.0	14.3
	0.2m wide cavity	3.8	6.5	9.5	12.0
	0.3m wide cavity	3.2	5.6	8.0	8.0
	0.5m wide cavity	3.0	5.5	7.5	9.6

Table 4.34 Temperature rise of air in the cavity with 0.4m high inlet.

$(T_{sm}-20)$		10	20	30	40
Temperature rise (K)	0.1m wide cavity	3.5	6.0	8.5	11.0
	0.2m wide cavity	3.2	5.0	7.2	9.0
	0.3m wide cavity	2.9	4.5	6.5	8.0
	0.5m wide cavity	2.85	4.0	6.0	7.8

are plotted in figure 4.16. This shows that the temperature rise of the air is increased as the width of the cavity decreases.

The wider the cavity and the higher the inlet, the less the temperature rise. Consequently the buoyancy pressure will decrease. Statistical analysis showed a linear regression through the data, with a coefficient of correlation of 0.999 and $P<0.05$. The regression equation was given by;

$$T_{rise} = a + b(T_{sm} - 20) \tag{4.5}$$

The parameters a and b are given in tables 4.35 and 4.36. The intercept a is not significant and it ought to be zero because there will be no temperature increase if the surfaces are at the same temperatures as the ambient air.

4.4 Error analysis

To give a sound basis to the experimental results, an uncertainty analysis was performed. Some errors are difficult to evaluate and cannot be reduced by increasing the number of measurements, they are caused by factors such as:

-radiation sources,

-poor thermal contact between thermocouples and the surfaces,

-convective currents from the heated thermistor

-dust on the sensors

-calibration of the equipment, ..etc

According to Cronvall (1980b), a measurement error can be regarded as consisting of three components, these are; the instrument errors E_1, the method error E_2 and the read-off error E_3.

The read-off errors in the present measurements were neglected because the reading were taken from digital instruments. The probable average estimate of errors $\overline{E}$ is evaluated from the following equation (Taylor 1982):

$$\overline{E} = (E_1^2 + E_2^2)^{0.5} \tag{4.6}$$

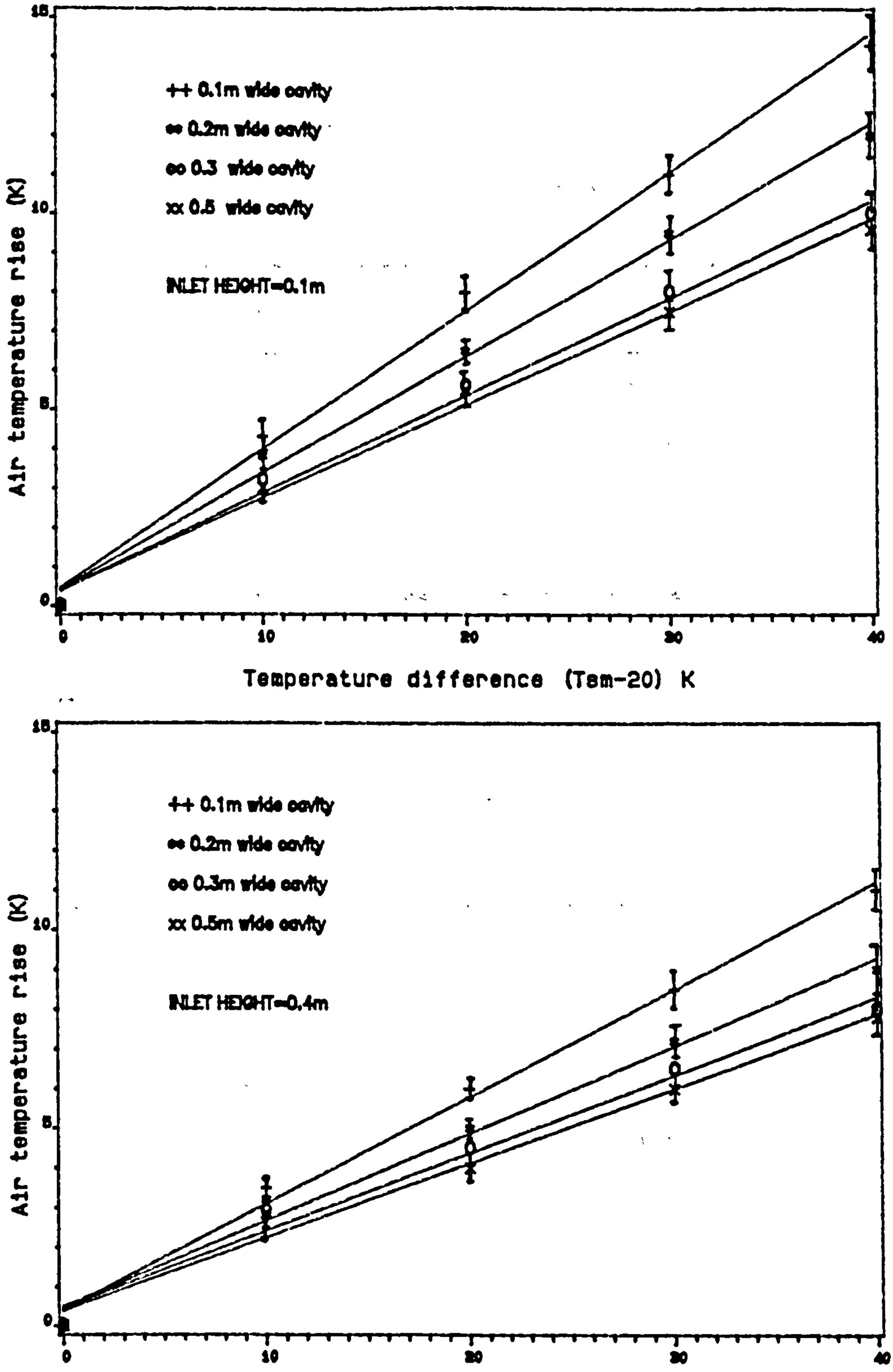

Figure 4.16 Temperature rise of air in the cavity

Table 4.35 Values of a and b when the inlet is 0.1m high.

Parameters	a	b
0.1m wide cavity	0.46	0.35
0.2m wide cavity	0.42	0.30
0.3m wide cavity	0.40	0.24
0.5m wide cavity	0.38	0.24

Table 4.36 Values of a and b when the inlet is 0.4m high

Parameters	a	b
0.1m wide cavity	0.40	0.27
0.2m wide cavity	0.48	0.22
0.3m wide cavity	0.46	0.20
0.5m wide cavity	0.38	0.19

The probable average uncertainties in the measurement parameters are summarised in table 4.37.

Table 4.37 Uncertainties of parameters in the measurements.

$T_{sm}(°C)$	25	30	35	40	50	60
			(±%)			
$v(m/s)$	7	6	5	5	5	5
$T_{ai}(°C)$	2	2	1	2	3	3
$T_{sm}(°C)$	2	2	3	3	4	4
A	1	1	1	1	1	1
$T_{ao}(°C)$	3	3	4	4	4	4
ρ	5	5	4	4	4	4

The uncertainty in the mass flow depends on uncertainties in its parameters such as density, air velocity and the area in which the flow takes place. The total fractional uncertainties in the mass flow is determined in quadratic form as suggested by Taylor (1982) as;

$$\frac{\partial M}{M}=\left\{\left(\frac{\partial v}{v}\right)^2+\left(\frac{\partial A}{A}\right)^2+\left(\frac{\partial \rho}{\rho}\right)^2\right\}^{1/2} \tag{4.7}$$

With a maximum of:

$$\left(\frac{\partial M}{M}\right)_{\max}=\frac{\partial v}{v}+\frac{\partial A}{A}+\frac{\partial \rho}{\rho} \tag{4.8}$$

The uncertainties in the convection heat transfer coefficient depends on the following parameters; M, T_{out}, T_{ai}, T_{sm} and T_{ac} as described by equation 4.3. The total uncertainties for h_c is;

$$\frac{\partial h_c}{h_c}=\left\{\left(\frac{\partial M}{M}\right)^2+\ldots+\left(\frac{\partial T_{ac}}{T_{ac}}\right)^2\right\}^{1/2} \tag{4.9}$$

where

$$\frac{\partial T_{ac}}{T_{ac}} = \left\{ \left(\frac{\partial T_{ao}}{T_{ao}} \right)^2 + \left(\frac{\partial T_{ai}}{T_{ai}} \right)^2 \right\}^{1/2}$$

The uncertainties in the temperature rise come from two parameters; T_{out} and T_{ai}, because $T_{rise} = T_{out} - T_{ai}$. So that the total uncertainties will be given in the following equation;

$$\frac{\partial T_{rise}}{T_{rise}} = \left\{ \left(\frac{\partial T_{out}}{T_{out}} \right)^2 + \left(\frac{\partial T_{ai}}{T_{ai}} \right)^2 \right\}^{1/2} \tag{4.10}$$

The uncertainties in M, h_c and T_{rise} are given in tables 4.38.

It is always difficult in buildings to find similar situation to compare the accuracy of the measurements. Because of many factors, such as the equipment used, the type of the measurements and the configuration of the systems. However, Akbarzadeh *et al.* (1982) carried out an investigation on the performance of a Trombe wall where they used an anemometer for air velocity measurement. They reported that the anemometer used had a typical error of ±10% , this is about double the error calculated for the equipment used in the present study.

4.5 Discussion and conclusion

The air within the hot layers must be replaced by cooler air through the inlet or from down flow through the top opening. If the inlet height is reduced, and the cavity is widened, downward flow becomes significant. If the inlet height is increased and the width of the cavity is decreased, the hot air in the cavity will be replaced by cooler air from the inlet. Consequently, down flow becomes less significant. Upward flow takes place in layers close to the bounding surfaces. Outside these hotter layers, in the centre, the air goes downward only when the cavity is wide.

Table 4.38 Uncertainties in mass flow M.

$T_{sm}(°C)$	25	30	35	40	50	60
			(±%)			
$\frac{\partial M}{M}$	9	8	7	7	6	6
$\left(\frac{\partial M}{M}\right)_{\max}$	13	12	11	11	11	11

Uncertainties in h_c.

$T_{sm}(°C)$	30	40	50	60
		(±%)		
$\frac{\partial h_c}{h_c}$	10	10	10	10
$\left(\frac{\partial h_c}{h_c}\right)_{\max}$	19	20	22	22

Uncertainties in temperature rise T_{rise}.

$T_{sm}(°C)$	30	40	50	60
		(±%)		
$\frac{\partial T_{rise}}{T_{rise}}$	4	4.5	5	5
$\left(\frac{\partial T_{rise}}{T_{rise}}\right)_{\max}$	5	7	7	7

Smoke tests showed that the air flowed upward over the heated surfaces of the cavity in layers about 250mm thick. The thickness of each layer is similar to that of a boundary layer over a vertical flat plate for turbulent flow given by Eckert and Jackson (1954), as:

$$b = 0.565 Gr^{-0.1} Pr^{-8/15} (1 + 0.494 Pr^{2/3})^{0.1} z \qquad (4.11)$$

Considering Pr = 0.7 for air, it is easy to show that:

$$b = 0.11 z^{0.7} (T_c - T_{az})^{-0.1} \qquad (4.12)$$

Where

T_c = cavity mean surface temperature ($°C$)

T_{az} = air temperature at height z above the base of the cavity ($°C$).

The thickness of the boundary layer varies slightly with temperature because of the low exponent. If the temperature difference between the cavity and the air is 20 K, then:

$$b = 0.08 Z^{0.7} \qquad (4.13)$$

At the top of the cavity, where Z = 1.95m, the two boundary layers just touch if the width of the cavity is:

$$2b = 0.26m \qquad (4.14)$$

This consequently is the optimum width for an effective cavity. If the cavity were taller, the optimum cavity width would be greater.

For a 4m high cavity, the optimum width to induce ventilation without down flow would be about 0.4m.

As the inlet height increases the resistance to the air flow is decreased, thus the flow will increase. However increasing the inlet height will result in reducing the internal wall material, consequently heat storage will be less.

As was stated earlier, thermal comfort can be improved if sufficient air movement is allowed over the body. CIBSE (1986) recommends a resultant temperature of 28 °*C* for thermal comfort in hot climates with very low air movement. Nicol (1975), however showed that the resultant temperature can be higher and that 80% of a population feel comfortable with a resultant temperature between 32 and 36°*C* providing the air speed past human body is of the order of 0.25 *m/s*. From the measurements, it was found that for a 3m long by 2m high cavity with a temperature difference between the cavity surfaces and the ambient air of 5K, a mass flow of 0.13 *kg/s* could be achieved giving an average air velocity in the order of 0.18 *m/s* which is not far from the value suggested by Nicol (1975). For still air the resultant temperature would be,

$$T_{res} = 0.5T_{mr} + 0.5T_a \tag{4.15}$$

With an air velocity of 0.18, the resultant temperature will be,

$$T_{res} = 0.43T_{mr} + 0.57T_a \tag{4.16}$$

which shows that the coefficient of the mean radiant temperature is reduced as the air speed increases. If we assume a mean radiant temperature of 37 °*C* and ambient air at 28 °*C*, the resultant temperature will be about 32 °*C*. According to Nicol, this is quiet comfortable.

For a temperature difference in the order of 40 *K* a mass flow rate of 0.28 *kg/s* is achieved, giving an air speed around 0.4m/s, which would improve thermal comfort. For higher cavities, the mass flow will be greater. The height of the cavity in practice is limited to the height of the building.

The observations played an important role in understanding the air flow mechanisms in the room and the cavity. The results showed the significance of a heated cavity in producing air currents. For optimum design, inlet height and cavity width are important parameters. To avoid down flow the width of the cavity should be kept as narrow as possible within the limits specified.

Analysis showed that the mass flow rate is dependent upon the temperature difference between the cavity walls and the ambient air, and that the convection heat transfer coefficient is dependent on the cavity width and the velocity of the air. The temperature increase of the air as it travels along the cavity also was found to be a linear function of temperature difference ($T_{sm} - 20$).

CHAPTER FIVE

THEORETICAL ANALYSIS

5.1 Introduction

A steady state analysis was carried out to give a clearer insight into the experimental results. Boundary layer, temperature of the air in the cavity and mass flow, pressure and life of the cavity are discussed.

In a warmed cavity, the air would be heated by convection from the surrounding surfaces and be supplied from the room to the cavity and then be moved upwards to the outside by buoyancy. Observations showed that this was not always so. If the cavity is narrow, the flow of air will be upward, but then frictional resistance to flow will be significant. If the cavity is wide there will be undesirable down flow in the centre.

5.2 Flow over vertical surfaces

If a vertical surface is heated to a temperature above that of the air around it, the air close to the surface is heated by convection and moves upward by buoyancy. The thickness of the boundary layer b within which this occurs is zero at the lower edge of the surface and increases upward. The thickness of a boundary layer for turbulent natural convection over a vertical plate is given by Eckert & Jackson (1950) as,

$$b = 0.565 Gr^{-0.1} Pr^{-8/15} (1 + 0.494 Pr^{2/3})^{0.1} z \qquad (5.1)$$

for air Pr = 0.7, and thus equation 5.1 becomes,

$$b = 0.11 z^{0.7} (T_c - T_{ar})^{-0.1} \qquad (5.2)$$

Where

T_c = cavity mean surface temperature (°C)

T_{az} = air temperature at height z above the base of the cavity (°C).

The thickness of the boundary layer varies only slightly with temperature because of the low exponent. If the temperature difference between the cavity and the air is 20 K, equation 5.2 simplifies into,

$$b = 0.08z^{0.7} \tag{5.3}$$

If z = 1.95m, b=0.128m.

5.3 Flow between vertical parallel walls

If another vertical surface is placed parallel to the first, the flow of air will take place within two boundary layers (figure 5.1). The upward flow will depend on how far the two surfaces are apart.

If they are close to one another, the boundary layers will interact and produce upward flow. If they are further apart, down flow may occur in the space between them.

5.3.1 Temperature of the air

An attempt was made to exploit an empirical equation for air temperature distribution across a boundary layer given by Eckert and Jackson (1950) to determine the air temperature in the cavity. After consideration this was rejected because it states that air in contact with the vertical surface would be at the same temperature as that of the surface, so that there could be no heat transfer between the flowing air and the surface. The temperature of the air in the cavity may be determined by assuming an elemental strip of air thickness dz within a chimney of height Z, width X and length Y, and the surfaces are at temperatures T_{s1} and T_{s2} (figure 5.2).

Heat transferred by convection from the surfaces of the chimney increases the temperature of the air within the element, so that by a heat balance:

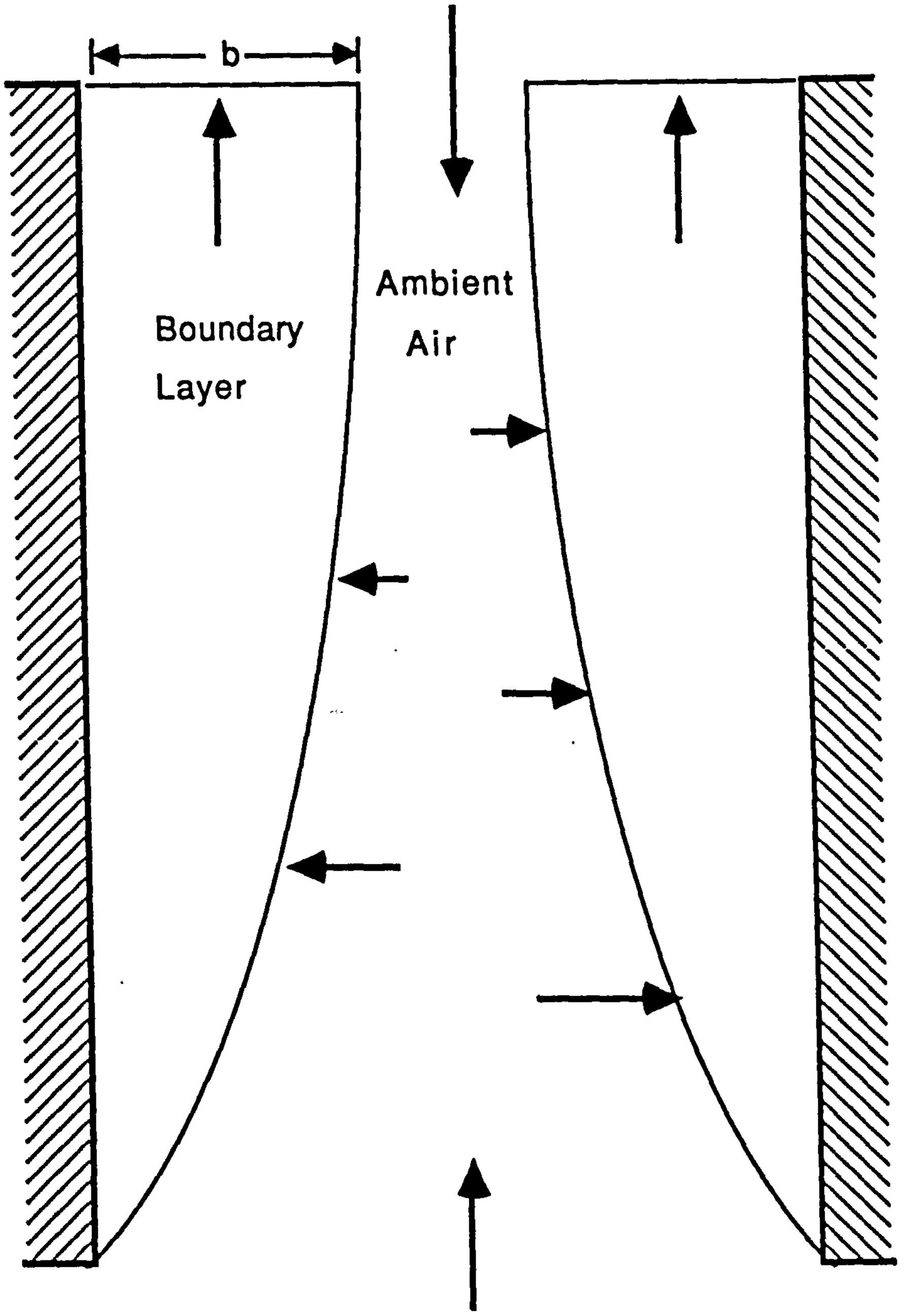

Figure 5.1 Flow of air between two vertical parallel walls

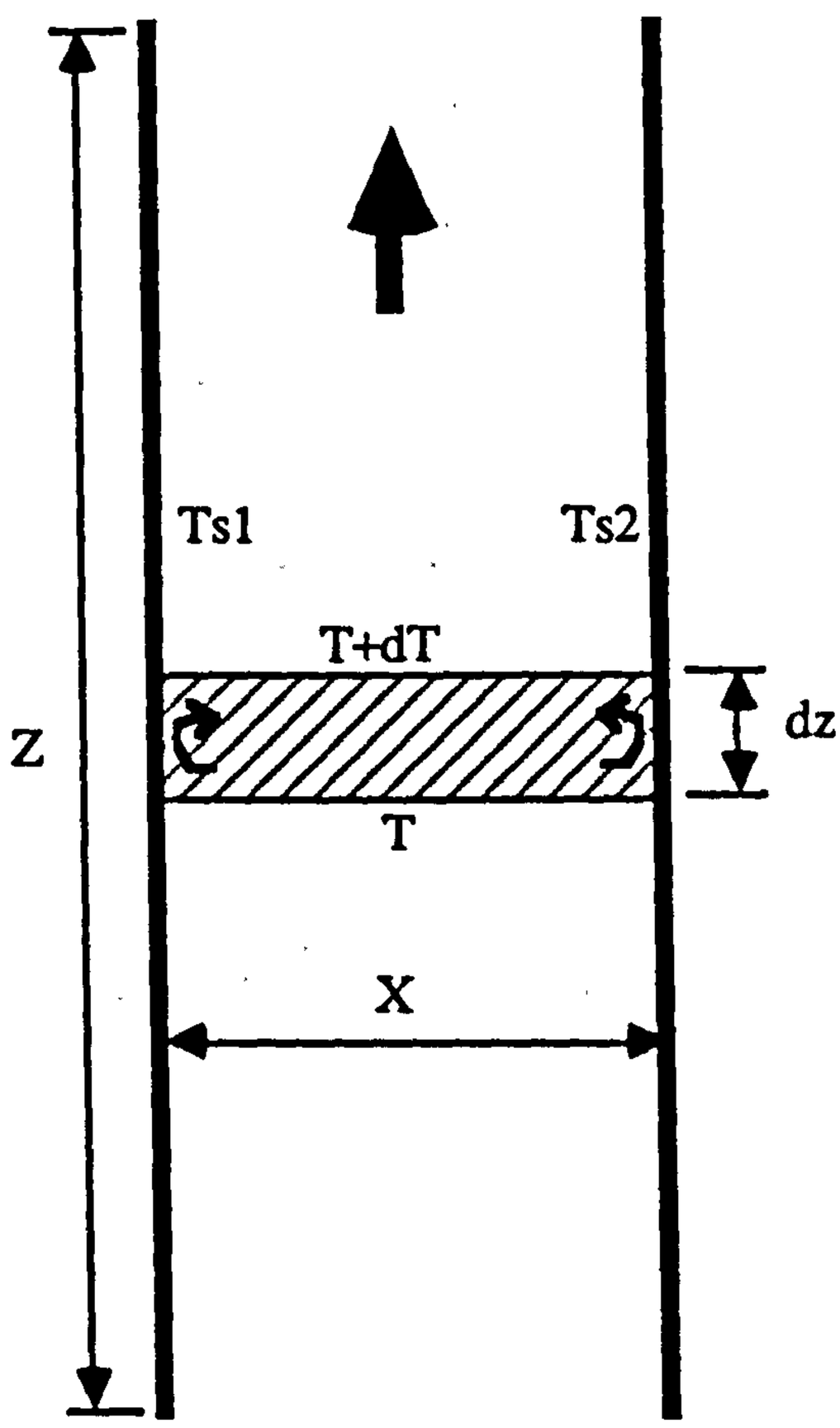

Figure 5.2 Schematic diagram of the heat balance using elemental strip

$$McdT = ((T_{s1} - T) + (T_{s2} - T))Yh_c dz \tag{5.4}$$

from which:

$$McdT = 2(T_{sm} - T)Yh_c dz \tag{5.5}$$

where $T_{sm} = (T_{s1} + T_{s2})/2$

Using the empirical heat transfer coefficient for parallel flow over a flat-plate given by McAdams (1954):

$$h_c = 5.8 + 4.1\bar{v} \tag{5.6}$$

which, in terms of mass flow, becomes:

$$h_c = 5.8 + 4.1\frac{M}{\rho XY} \tag{5.7}$$

we find:

$$dz = \frac{Mc}{2Y(5.8 + 4.1M/\rho XY)}\left(\frac{dT}{T_{sm} - T}\right) \tag{5.8}$$

which can be written as:

$$dz = a\frac{dT}{T_{sm} - T} \tag{5.9}$$

from which it follows that:

$$z = -a\ln(T_{sm} - T) + C \tag{5.10}$$

when $z = 0, T = T_{ai}$, so that $C = a\ln(T_{sm} - T_{ai})$

whence,

$$T = T_{sm} - (T_{sm} - T_{ai}) \exp -z/a \tag{5.11}$$

The outlet air temperature T_{out} for a cavity of height Z is then:

$$T_{out} = T_{sm} - (T_{sm} - T_{ai}) \exp -Z/a \tag{5.12}$$

so that air temperature rise in the cavity is:

$$T_{rise} = T_{out} - T_{ai} = (T_{sm} - T_{ai})(1 - \exp -Z/a) \tag{5.13}$$

Figure 5.3 shows the expected temperature increase of the air travelling up through the cavity, for different inlet heights. It is clear that increasing the width of the cavity will result in a temperature decrease of the air leaving the cavity. Increasing the inlet height will also result in a decrease of the temperature rise. Increasing the temperature difference by 40 K will only give a temperature rise of 15 K, which suggests that not much stored heat is removed from the walls of the cavity. This helps the ventilation to continue longer. Statistical analysis of the data showed a linear first order relationship given by $T_{rise} = a + b(T_{sm} - 20)$ with a coefficient of correlation of 0.99 and P <0.05. The parameters a and b are given in tables 5.1 and 5.2 for each case. Parameter a is not significant, and it ought to be zero, because there will be no temperature increase if the surfaces are at similar temperatures to that of the ambient air. However, the value of a could be neglected by considering the errors associated to the whole equation. Theoretical values of a are slightly higher than experimental. This is partly due to the use of McAdams heat transfer coefficient which is higher especially when the flow approaches zero, and partly due to the uncertainties in the parameters.

The temperature rise given by equation 5.13 has associated errors which depend on the uncertainties of the parameters, T_{sm}, T_{ai}, Z, M and h_c. Different values for the convective

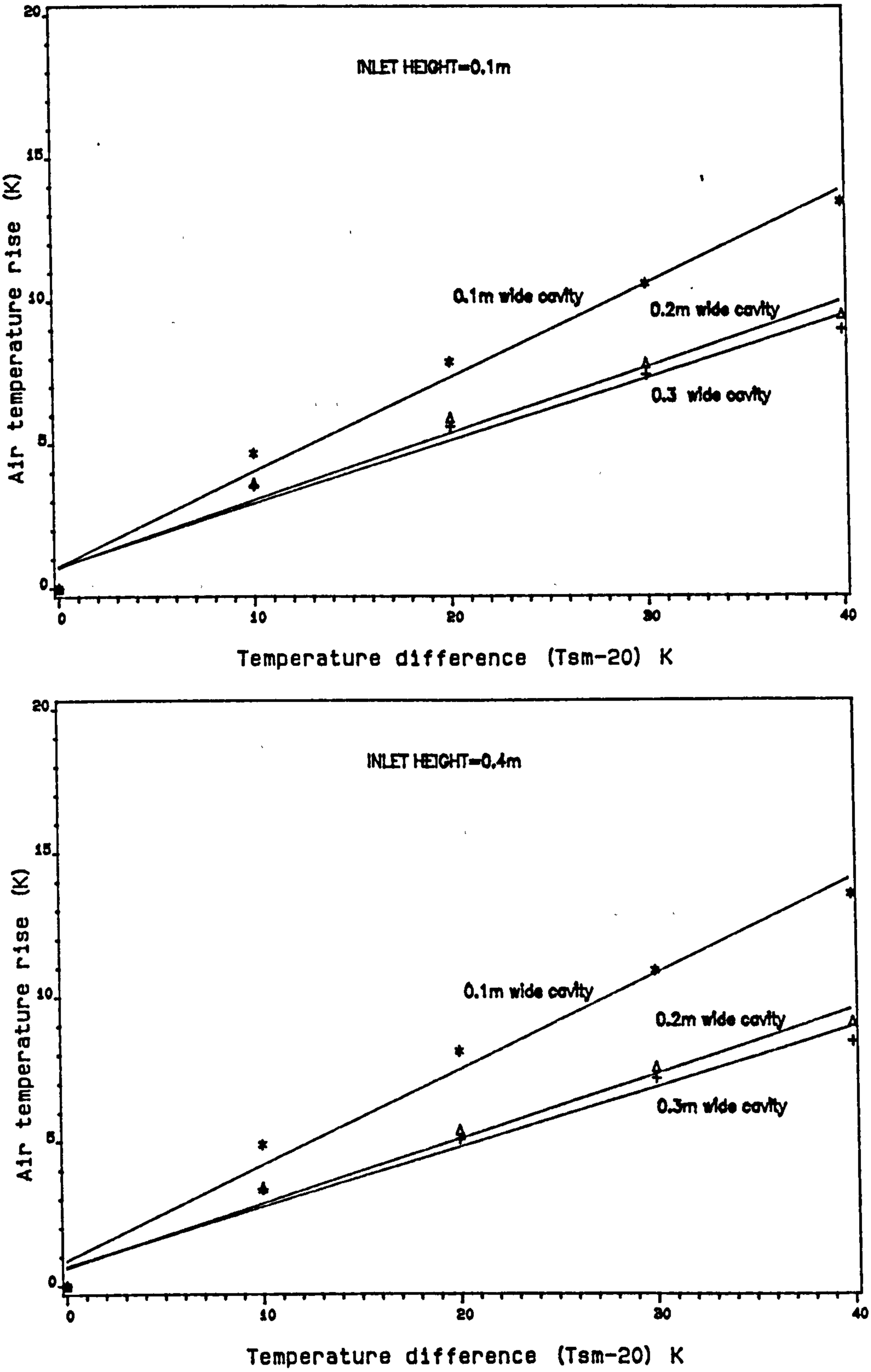

Figure 5.3 Predicted temperature rise of air in the cavity

Table 5.1 Values of a and b when the inlet is 0.1m high.

	a	b
0.1m wide cavity	0.75	0.32
0.2m wide cavity	0.73	0.23
0.3m wide cavity	0.74	0.22

Table 5.2 Values of a and b when the inlet is 0.4m high

	a	b
0.1m wide cavity	0.87	0.33
0.2m wide cavity	0.61	0.22
0.3m wide cavity	0.66	0.20

heat transfer coefficient were reported in the literature. For example Warner and Arpaci (1968) and IHVE Guide (1970) state that for natural convection over a vertical wall h_c has a value of about 3 W/m^2K whereas McAdams (1954) stated that this could be 6 W/m^2K. As be seen, reported uncertainties in h_c can be large, so a value of ±30% has been assumed. The uncertainties in the parameters used are summarised in table 5.3.

Table 5.3 Uncertainties in temperature rise parameters.

Parameter	Uncertainty
T_{sm}	$\pm 1°C$
T_{ai}	$\pm 1°C$
Z	$\pm 2\%$
M	$\pm 8\%$
h_c	$\pm 30\%$

According to Taylor the total uncertainty in equation 5.14 is:

$$\partial T_{rise} = \left\{ \left(\frac{\partial T_{rise}}{\partial T_{sm}} \delta T_{sm} \right)^2 + \left(\frac{\partial T_{rise}}{\partial T_{ai}} \delta T_{ai} \right)^2 + \left(\frac{\partial T_{rise}}{\partial Z} \delta Z \right)^2 + \left(\frac{\partial T_{rise}}{\partial a} \delta a \right)^2 \right\}^{0.5} \qquad (5.14)$$

where

$$\frac{\partial T_{rise}}{\partial T_{sm}} \delta T_{sm} = 1 - \exp -Z/a$$

$$\frac{\partial T_{rise}}{\partial T_{ai}} \delta T_{ai} = -1 + \exp -Z/a$$

$$\frac{\partial T_{rise}}{\partial Z} \delta Z = \left(\frac{1}{a} \right) (T_{sm} - T_{ai}) \exp -Z/a$$

$$\frac{\partial T_{rise}}{\partial a} \delta a = \left(\frac{1}{a^2} \right) (T_{ai} - T_{sm}) \exp -Z/a$$

where

$$\frac{\partial a}{a} = \left\{ \left(\frac{\delta M}{M} \right)^2 + \left(\frac{\delta h_c}{h_c} \right)^2 \right\}^{0.5}$$

Inserting the appropriate values from table 5.3 into the above equations, yields an average uncertainty in temperature rise $\pm 1.5\ K$.

5.3.2 Mass flow rate

More air flows upwards near the walls whereas it is stationary or flows downward in the centre of the cavity. Air flow upwards will be the total of the air entering the boundary layers through the inlet and from the "stationary air" in the middle.

Eckert and Jackson (1950) give the velocity distribution across a boundary layer over a vertical surface by the empirical relation,

$$v_x = C(x/b)^{1/7}(1-x/b)^4 \tag{5.15}$$

which gives zero flow at $x = 0$ and $x = b$ (the boundary layer "thickness"), as required.

where

$$C = 1.85(\gamma/Z)Gr^{0.5}\{1+0.5Pr^{2/3}\}^{-0.5}$$

$$\gamma = 1.5\times10^{-5}$$

using this the mean air velocity $\overline{v}$ is:

$$\overline{v} = (C/b)\int_0^b v_x dx \tag{5.16}$$

if $x/b = S$, then

$$\overline{v} = C\int_0^1 S^{1/7}(1-S)^4 dS \tag{5.17}$$

which leads to:

$$\overline{v} = 0.15C \tag{5.18}$$

The mass flow M in the boundary layer is then given by:

$$M = \rho\overline{v}A_b \tag{5.19}$$

Substituting equation 5.18 gives:

$$M = 0.15\rho C A_b \tag{5.20}$$

where

A_b = is the horizontal cross sectional area of the boundary layer ($A_b = bY$).

and

Y = width of the boundary layer

For two walls separated $2b$, the rate of air flow will be doubled.

Figure 5.4 shows the mass flow against temperature difference for a 2m high cavity using Eckert and Jackson's relationship. The walls are 0.3m apart.

Comparison is made between the mass flow using Eckert and Jackson's relation with the mass flow rate reported by Ryan and Mara (1983) for a heated vent pipe to exhaust smells from pits. Ryan and Mara reported that with a vent pipe of diameter $0.125\ m$, $2\ m$ high, heated to $30\ °C$, ambient air at $20\ °C$, a mass flow of the order of $2.5 \times 10^{-3}\ kg/s$ was produced. They used in the estimation of the mass flow, a heat balance over an elemental strip of the pipe and integration over the length of the pipe. If we assume a cavity size similar to the vent pipe, the Eckert & Jackson equation yields a mass flow rate of the order of $2.6 \times 10^{-3}\ kg/s$ which is nearly the same.

The total uncertainty in the mass flow given by equation 5.19 depends on uncertainties in ρ, $\bar{v}$ and A_b. The total average uncertainty is given by:

$$\frac{\delta M}{M} = \left\{ \left(\frac{\delta \rho}{\rho}\right)^2 + \left(\frac{\delta \bar{v}}{\bar{v}}\right)^2 + \left(\frac{\delta A_b}{A_b}\right)^2 \right\}^{1/2} \tag{5.21}$$

Assuming the following uncertainties $\rho = 5\%$, $\bar{v} = 7\%$ and $A_b = 5\%$ then $\delta M/M$ will be about 10%.

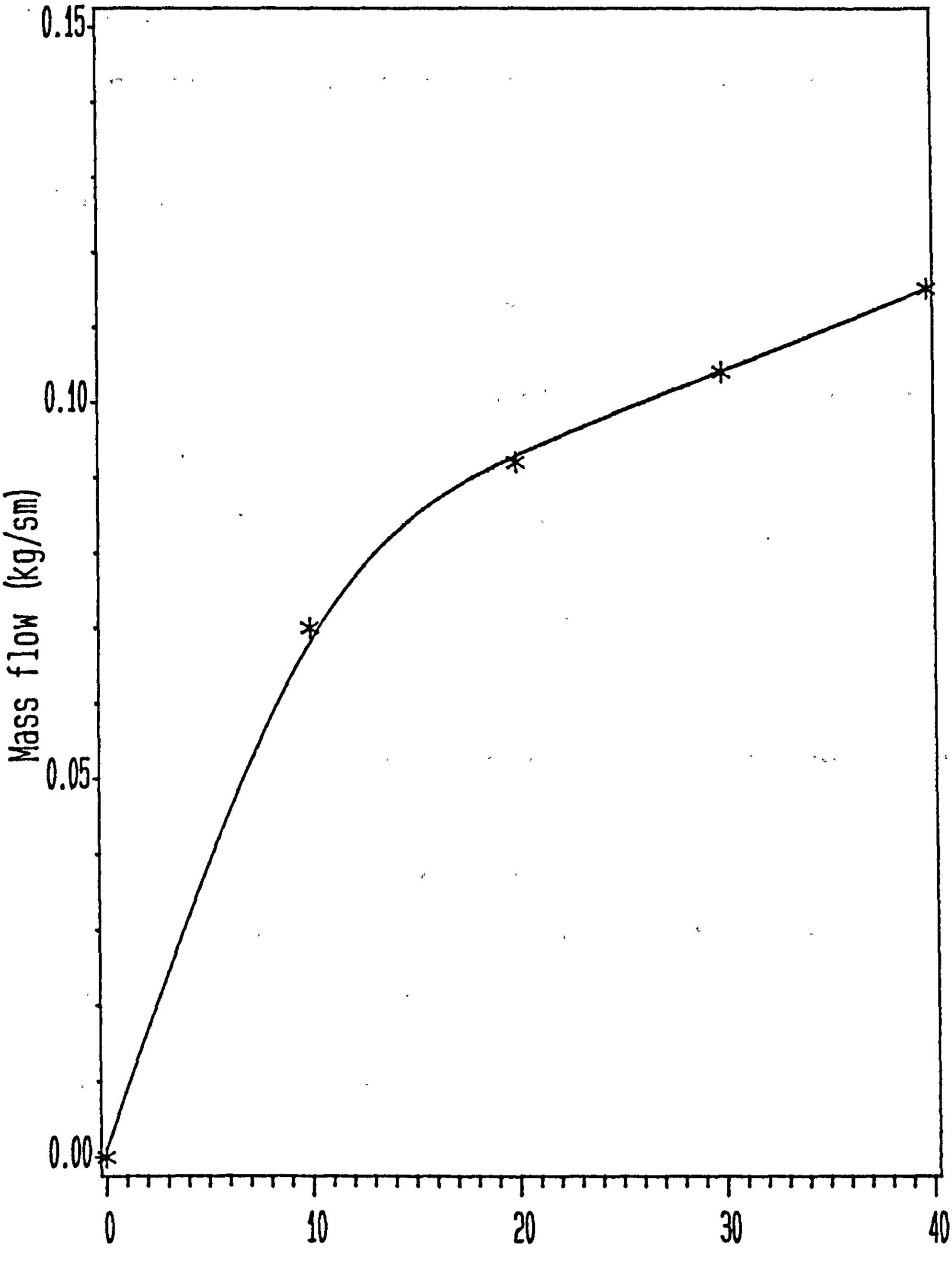

Figure 5.4 Mass flow rate according to Eckert & Jackson

5.4 Pressure changes

The warm air in the cavity rises by buoyancy. The buoyancy pressure is caused by the difference in density between the air in the cavity and that outside and is given for a cavity of height Z by:

$$P_b = gZ(\rho_{ai} - \rho_{ac}) \tag{5.22}$$

The density of air at temperature T is given by its density at a reference temperature usually $0°C$ or $273°K$, where dry air has a density of 1.293 kg/m^3 (CIBSE 1986), $\rho = 1.293 \times 273/(273+T)$, with g=9.81 m/s^2, so that:

$$P_b = 3463Z\frac{T_{ac} - T_{ai}}{(T_{ai}+273)(T_{ac}+273)} \tag{5.23}$$

As air flows through a room and into a cavity, it is subject to pressure losses. The main resistances to flow are at the cavity inlet, exit and possibly within the cavity, with little pressure loss in the room being ventilated.

The temperature changes of the air entering the room are slight to that the air density throughout the system may be taken as constant. The pressure losses thus are as follows:

The pressure loss at the exit may be taken as one velocity head as given by the CIBSE Guide (1986).

$$P_e = \rho v_e^2/2 \tag{5.24}$$

The pressure loss within the cavity due to friction is:

$$P_f = 4fZ\rho v^2/2D_h \tag{5.25}$$

where

D_h = hydraulic diameter (twice the separation for a long cavity)

The friction factor f for turbulent flow depends upon the Reynolds number and the relative roughness (K_s/D_h), where K_s is the linear measure of the roughness of the internal surface, which for concrete K_s varies from 0.3 to 3mm with an average of 1.6mm. For two parallel concrete surfaces 1.5m long separated by a 0.1, 0.2 and 0.3m air layer, the relative roughness will be between 0.003 and 0.008. For Reynolds numbers between 4000 and 10000, using the Moody diagram, a mean friction factor of 0.011 is obtained.

The pressure loss at the inlet of the cavity may be expressed in terms of an unknown number, K, of velocity heads at the entry as:

$$P_i = K\rho v_i^2/2 \tag{5.26}$$

Figures 5.5, 5.6 and 5.7 show pressure losses at various places. It can be seen from figure 5.5 that the pressure loss inside the cavity due to friction is low but not negligible (for the cavity width of 0.1m) whereas it is negligible when the width of the cavity is 0.2m or 0.3m (figures 5.6 and 5.7).

Pressure loss coefficient K, for bends of rectangular section are rare in the literature. Most of the standard books presents values of loss coefficients for different type of bends for pipes of circular cross section. However, Kronvall (1980a) gave an equation for estimation of a right angle bend coefficient for a rectangular cross section, which will be used for comparison.

The nature of the flow of air from the room into the boundary layers inside the cavity is complicated and was not investigated, but K can be estimated from experimental values as follows:

The buoyancy pressure balances pressure losses through the system which are those at the cavity entry, exit and in the cavity,

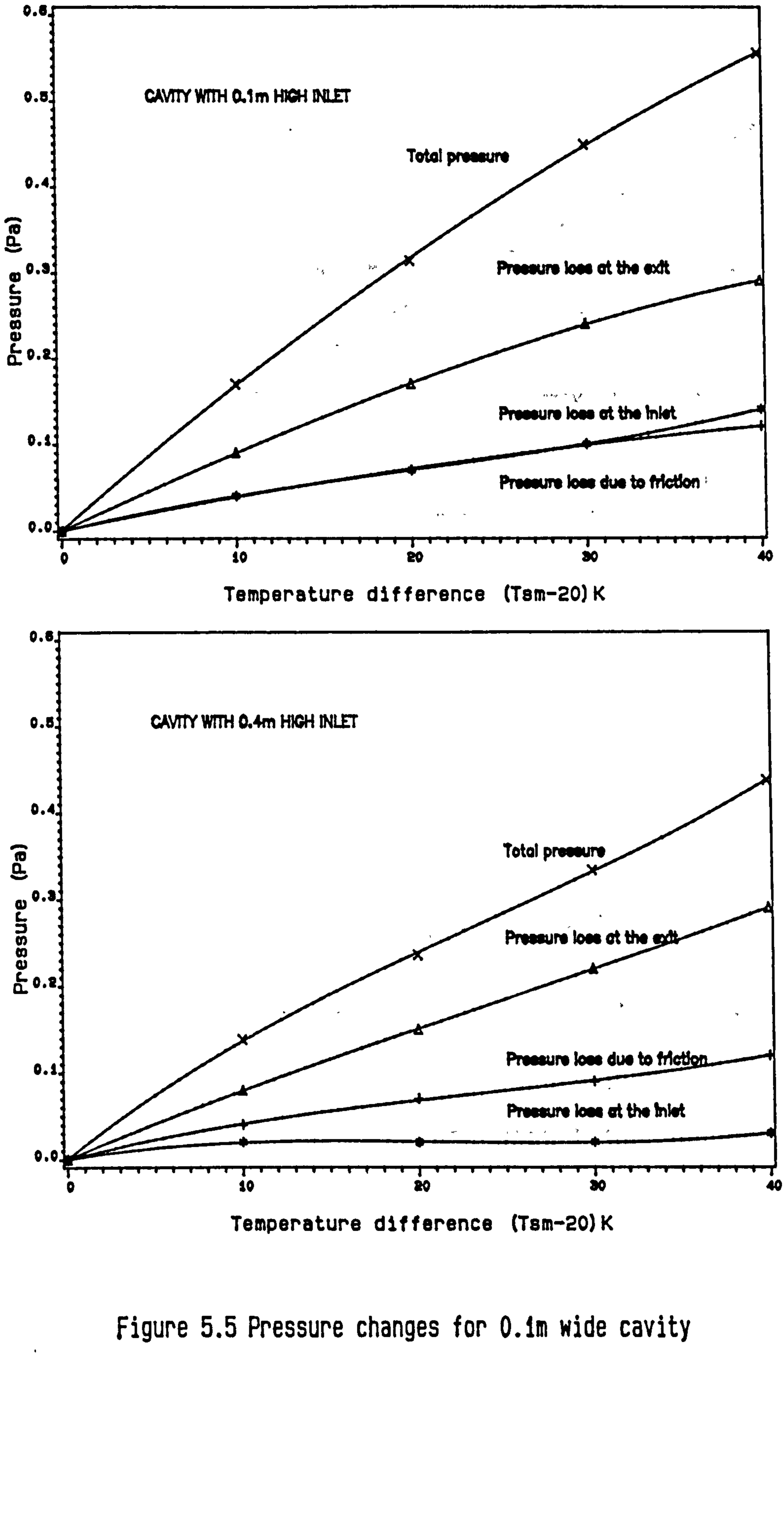

Figure 5.5 Pressure changes for 0.1m wide cavity

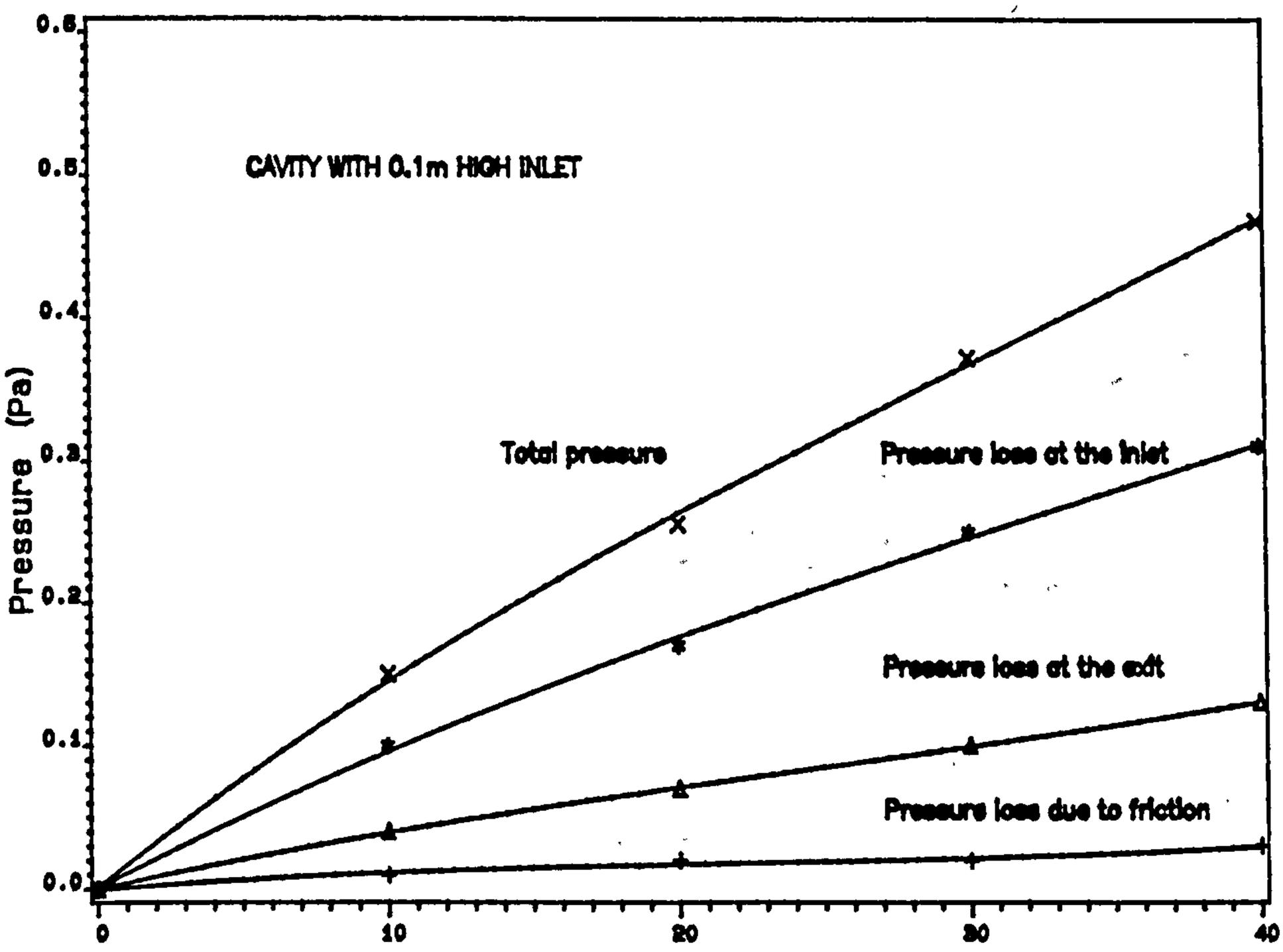

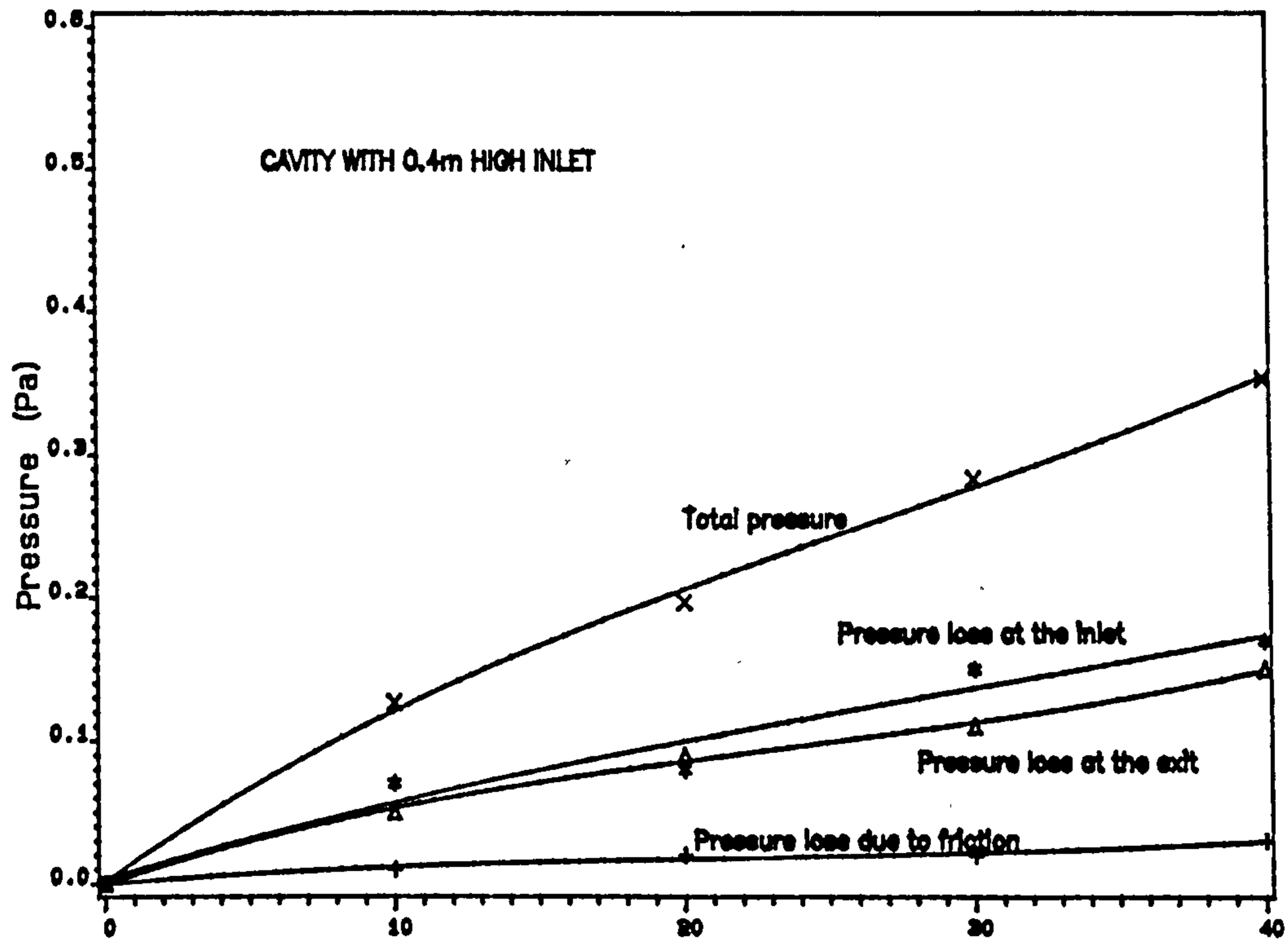

Figure 5.6 Pressure changes for 0.2m wide cavity

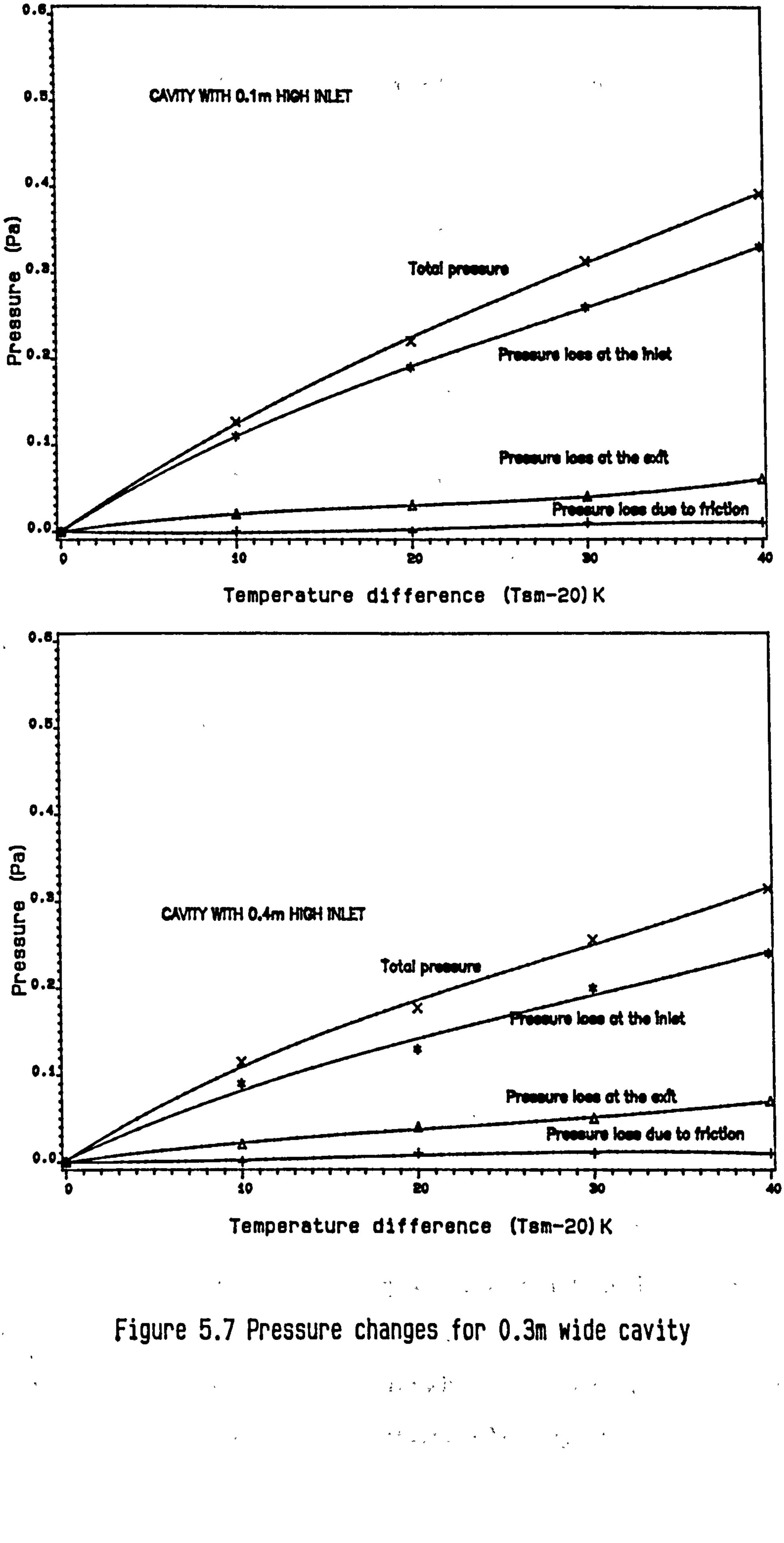

Figure 5.7 Pressure changes for 0.3m wide cavity

Buoyancy pressure = Total pressure loss

so that:

$$P_b = P_i + P_f + P_e \tag{5.27}$$

which gives:

$$P_i = P_b - (P_e + P_f) \tag{5.28}$$

Substituting equations 5.24, 5.25 and 5.26 into 5.28 yields:

$$K\rho v_i^2/2 = P_b - (\rho v_e^2/2 + 4fZ\rho v_c^2/2D_h) \tag{5.29}$$

where

v_e = velocity at exit (m/s)

v_c = velocity inside cavity (m/s)

by converting velocity into mass flow using the continuity equation,

$$v = M/\rho A \tag{5.30}$$

and rearranging for K yields,

$$K = \frac{2\rho A_i^2}{M^2} P_b - \frac{A_i^2}{A_c^2}(1 + 4fZ/D_h) \tag{5.31}$$

Table 5.4 and 5.5 show K for different conditions. The difference in K for the 0.1m and the 0.4m high inlet, suggests that the types of flow are different in the two cases.

In order to compare values with those of Kronvall (1980a), two situations are considered. The first is when the inlet is 0.1m with a 0.1m wide cavity, 1.5m long cavity. The second when the inlet height is increased to 0.4m high. Kronvall (1980a) suggested

Table 5.4 K with 0.1m high inlet.

$T_{sm}(°C)$	30	40	50	60
Cavity width (m)	K			
0.1	0.4	0.4	0.4	0.5
0.2	0.6	0.5	0.5	0.5
0.3	0.7	0.6	0.6	0.6

The table shows that for the 0.1m high inlet cavity, K is about a half, with a suggestion that it rises a little with cavity width.

Table 5.5 K with 0.4m high inlet.

$T_{sm}(°C)$	30	40	50	60
Cavity width (m)	K			
0.1	5.0	2.8	1.8	2.2
0.2	5.4	3.4	4.7	4.0
0.3	7.7	5.1	6.7	5.5

This table shows that K rises with cavity width and decreases with rising wall temperature. The use of a mean of 4 to 5 will not lead to important errors.

that $K = 180fC1$, where K is the coefficient of the bend, f is the friction factor which in here taken as 0.009, and C1 is a coefficient which depends on inlet and outlet configurations.

In the first case $K = 180 \times 0.009 \times 0.8$, about 1.3. Compared against a current value of about 0.4 (table 5.4).

For the second case $K = 180 \times 0.009 \times 2$ or about 3.2. Compared with 5.0 (table 5.5).

The difference between values may be due to differences in configurations of the system. However, for both, K increased when the inlet height is increased.

5.5 Cavity "life"

An order of magnitude estimate of how long a cavity may be expected to move air was made.

The time taken for the heat in the walls to dissipate into the cavity would be about the ratio of their heat content to the mean rate of heat gain of the air flowing through it.

The "life" of the cavity in hours is thus:

$$t_c \sim \frac{2YZW_t\rho_c C_c(T_{sm} - T_i)}{3600Mc(T_o - T_i)} \qquad (5.32)$$

where

ρ_c = density of cavity walls $2100 kg/m^3$

t_c = time in hours

W_t = thickness of the wall of the cavity (m)

T_i = inlet air temperature $°C$

c = specific heat capacity of the air, $1000\ J/kgK$

C_c = specific heat capacity of the walls, around $900 J/kgK$

T_o = outlet air temperature $°C$

For a 2m high cavity, 1.5m wide with 0.2m thick walls at 40 °*C*, with air entering at 30 °*C* and leaving at 34 °*C* with a mass flow of 0.07 *kg/s*, the life of this cavity may be:

$$t_c = \frac{2 \times 2 \times 0.2 \times 2200 \times 900(40-30)}{3600 \times 0.07 \times 1000(34-30)} \quad \text{or} \quad \text{about} \quad 17\text{h}$$

which is much longer than required.

The "life" of the cavity can be extended by making it higher and giving it thicker walls, although this would lead to a decline of its mean temperature, thus reducing the air flow. An adequate "life" calculation is complicated, but is taken further in chapter seven where a dynamic model using the "finite differences" technique is presented.

5.6 Applications

To improve the effect of the cavity ventilation the air moved could be cooled on entering a room by making it flow over a wet surface. If, as a result of evaporation of water, the moisture content of the air is raised by N *kg* of water vapour per *kg* of dry air, and if all the required latent heat comes from the air, the temperature of the air will fall by (L N/c) *K*. Where c is the specific heat capacity of the air, L the latent heat of vaporisation of water, taken as $2.26 \times 10^6 J/kg$ of evaporated water. This becomes (2260 N) *K*, so that if the moisture content rises by 0.001kg (about 5% in the case of the air at 30 °*C*, and 70% relative humidity) the temperature will fall by about two degrees.

A sun-warmed cavity could be used for the drying of agricultural products. A grain silo, for example, could be built as a "solar chimney" by which an improved draught is caused to dry the grain.

The sun-warmed cavity was originally envisaged for use in a single storey house and was controlled by a damper at the top as shown in figures 5.7. However, it could also be used in multistory buildings as suggested in figure 5.8.

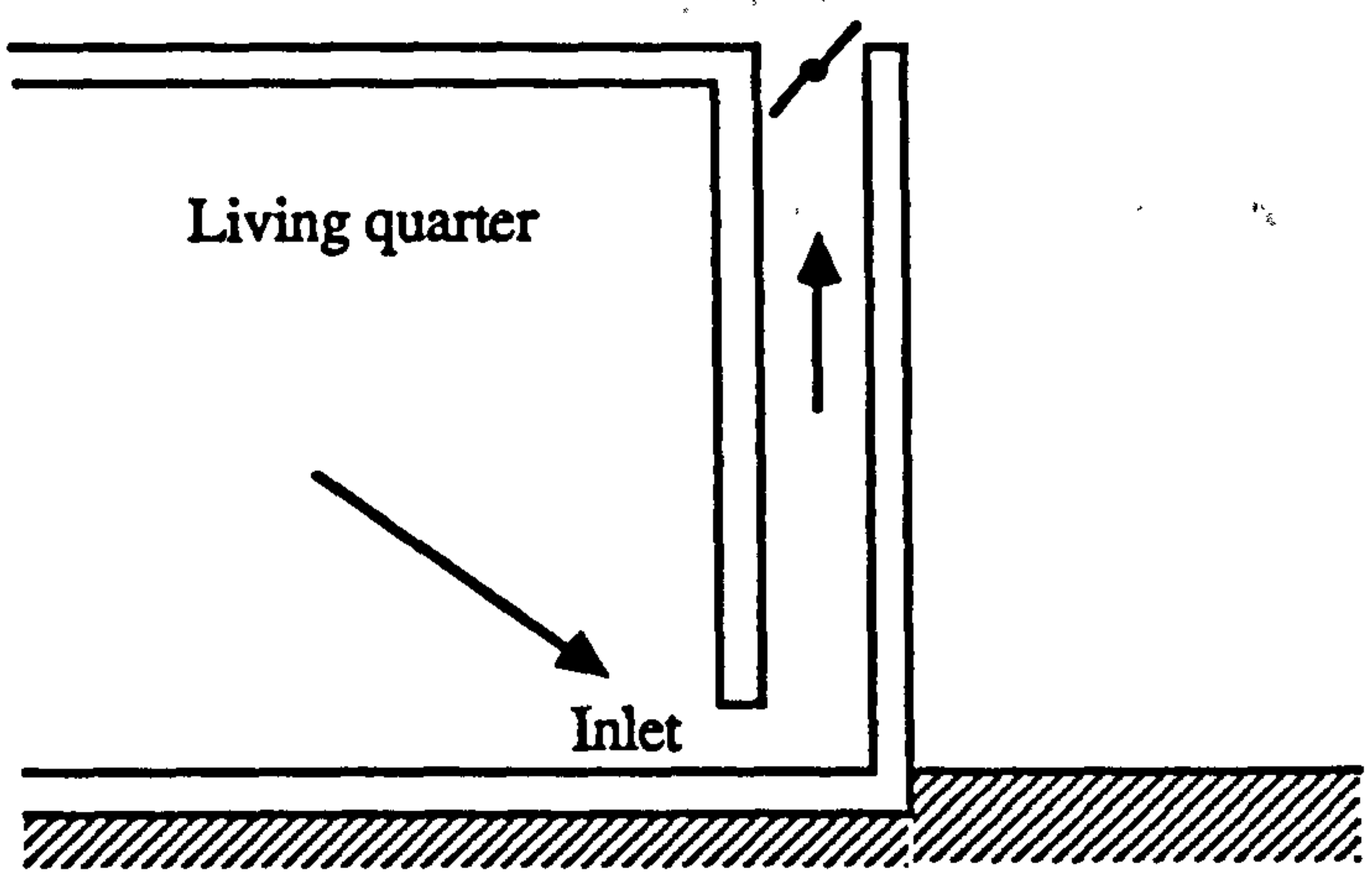

Figure 5.7 Sun-warmed cavity with single storey house

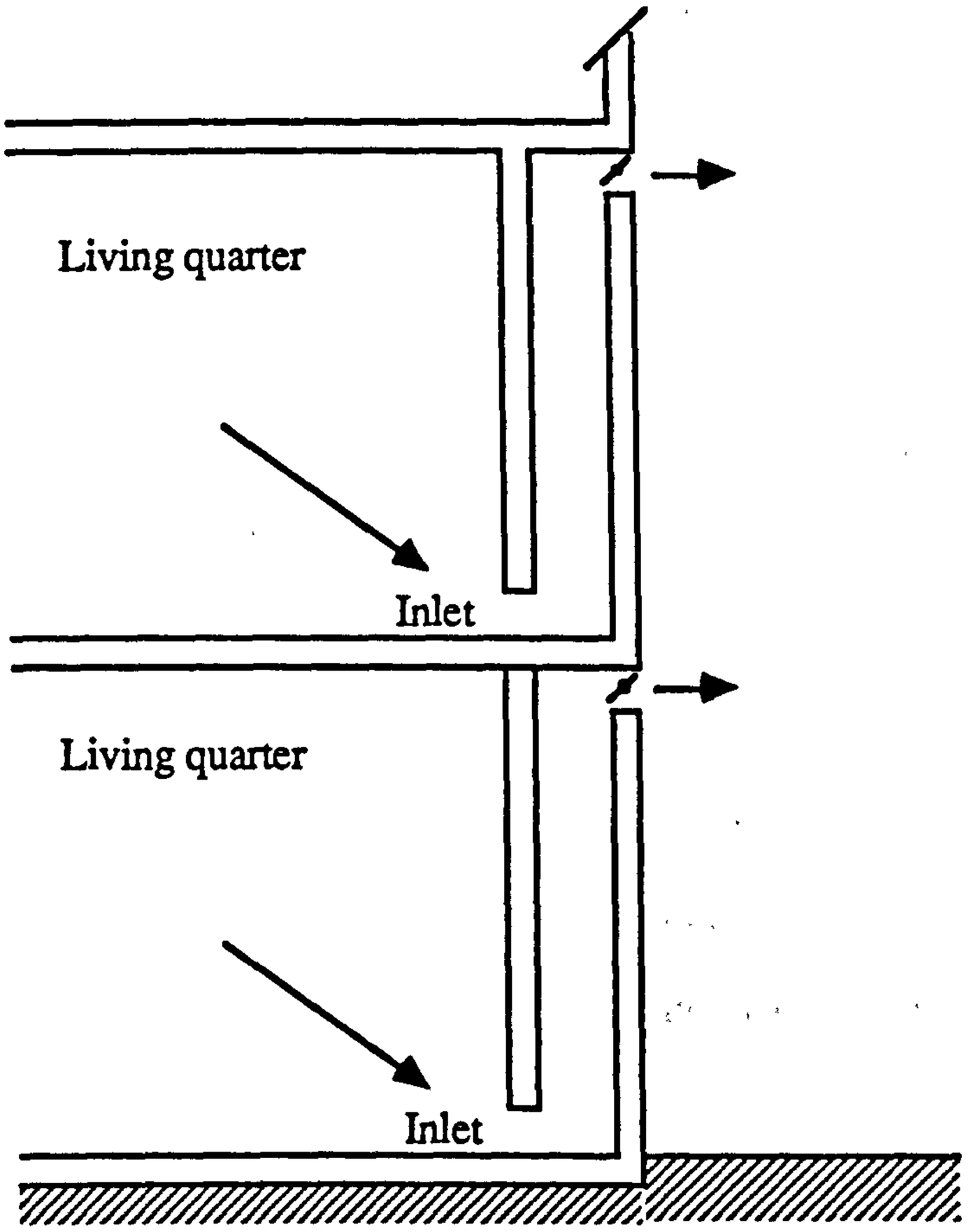

Figure 5.8 Sun-warmed cavity with multi-storey buildings

CHAPTER SIX

COMPARISON BETWEEN OBSERVATIONS AND ANALYSIS

6.1 Introduction

This chapter discusses the comparison between observations and analysis. Attention is given to the following points:

-air flow mechanisms and air flow patterns, mainly focus on the thickness of the boundary layer which was an important indicator of optimum cavity width.

-the rise of air temperature along the cavity and its relationship to the temperature difference between the surfaces of the cavity and the ambient air ($T_{sm} - 20°C$).

-the mass flow, the measured values were compared with those predicted by Eckert and Jackson's relationship for velocity.

-the other parameter which is also given attention is the convection heat transfer coefficient in the cavity. The measured values of the convection heat transfer coefficient are compared with those predicted by McAdams.

6.2 Air flow mechanisms

Observations showed that the flow of air in the cavity takes place within layers near the heated surfaces. The air was supplied to these layers from the room through an inlet at the bottom of the cavity and from the outside by downward flow through the top near the center, if the cavity is wide enough.

These layers may be thought of as boundary layers resulting from the flow of air over heated vertical plates. The thickness of each air layer, observed at the top of the cavity using smoke, was found in most tests to be close to 0.125m. This agrees with values predicted using the boundary layer relationship of Eckert and Jackson (1950), equation 5.1.

$$b = 0.565 Gr^{-0.1} Pr^{-8/15} (1 + 0.5 Pr^{2/3})^{0.1} z \qquad (5.1)$$

which was simplified earlier into $b = 0.08 z^{0.7}$. With height z=1.95m, we find b=0.128m. Observations showed that the thickness of each boundary layer at the top of the cavity varied slightly with the temperature difference between the surface of the cavity and the ambient air. With higher temperature differences, the layer was thicker. Eckert and Jackson's equation (6.1) indicates that with an increase in temperature difference the thickness of this layer decreases, because of the negative exponent in the Grashof number. However, the low exponent of Grashof number makes this disagreement insignificant.

6.3 Rise of air temperature

Figures 6.1, 6.2 and 6.3 compare measured and predicted temperature rises of the air in the cavity for different cavity widths. Data are linearly related suggesting that the air temperature, as it travels along the cavity, is a linear function of temperature difference $(T_{sm} - 20)$ with an equation of the form of $T_{rise} = a + b(T_{sm} - 20)$, where a is the intercept which for this case is nearly zero within the limit of uncertainties, and b depends on cavity configuration.

6.4 Mass flow

Figure 6.4 compares the measured and predicted mass flows. The measured mass flows were plotted for a cavity 0.3m wide with inlet 0.1m and 0.4m high. Values shown by the dotted lines are those predicted by Eckert and Jackson's equation for velocity for two combined vertical parallel surfaces (given in chapter five). Statistically, the curves have a similar trend. Their regression equations may be of the form, $M = a + bX + cX^2 + dX^3$, where X is the temperature difference between the surfaces of the cavity and the ambient air $(T_{sm} - 20)$. The regression lines show that the measured results for a cavity with an inlet 0.1m high gives lower values than those predicted, probably because of the increase of pressure loss with the narrow inlet, whereas the results from a

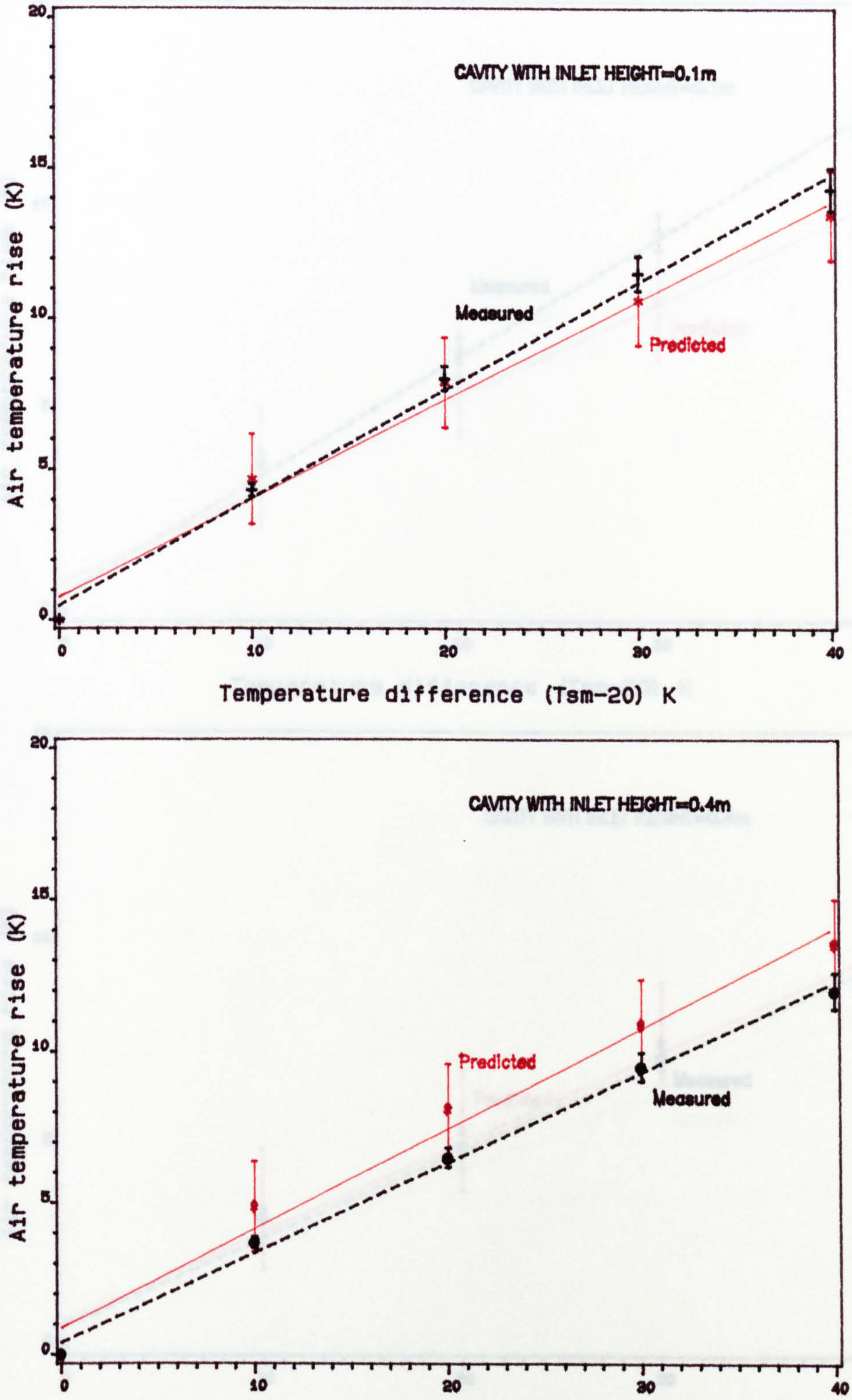

Figure 6.1 Comparison between predicted and measured results for air temperature rise for 0.1m wide cavity

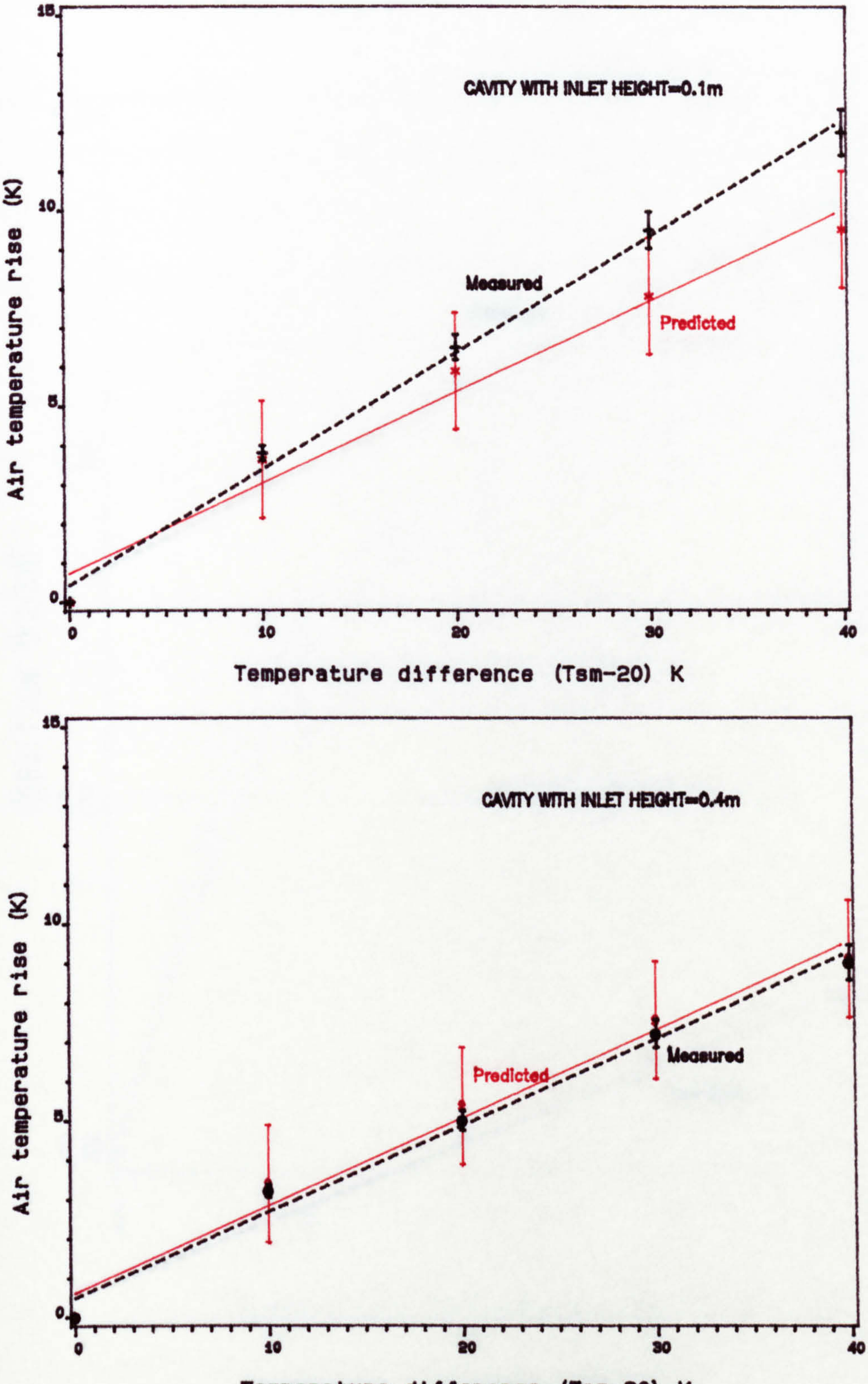

Figure 6.2 Comparison between predicted and measured results for air temperature rise for 0.2m wide cavity

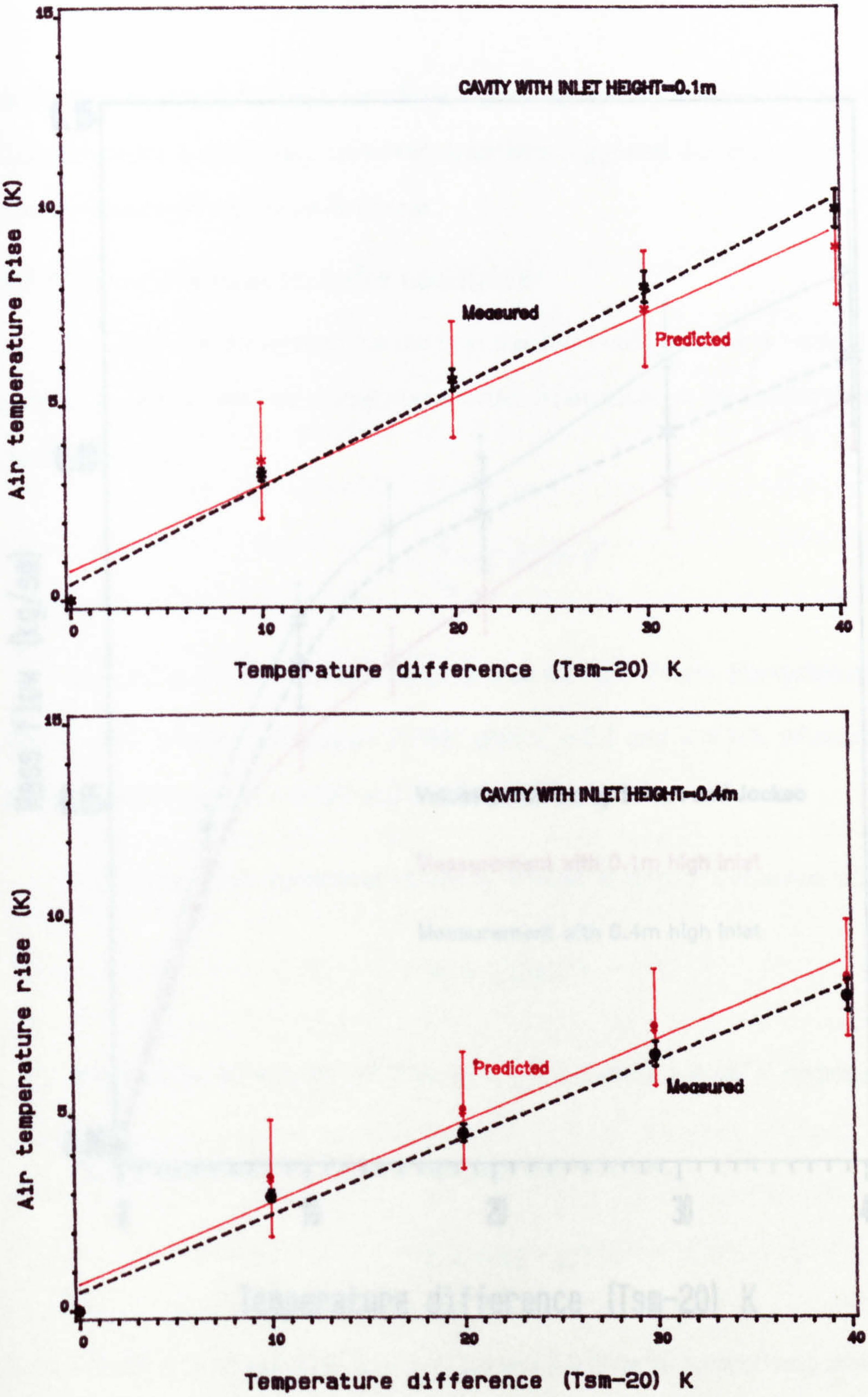

Figure 6.3 Comparison between predicted and measured results for air temperature rise for 0.3m wide cavity

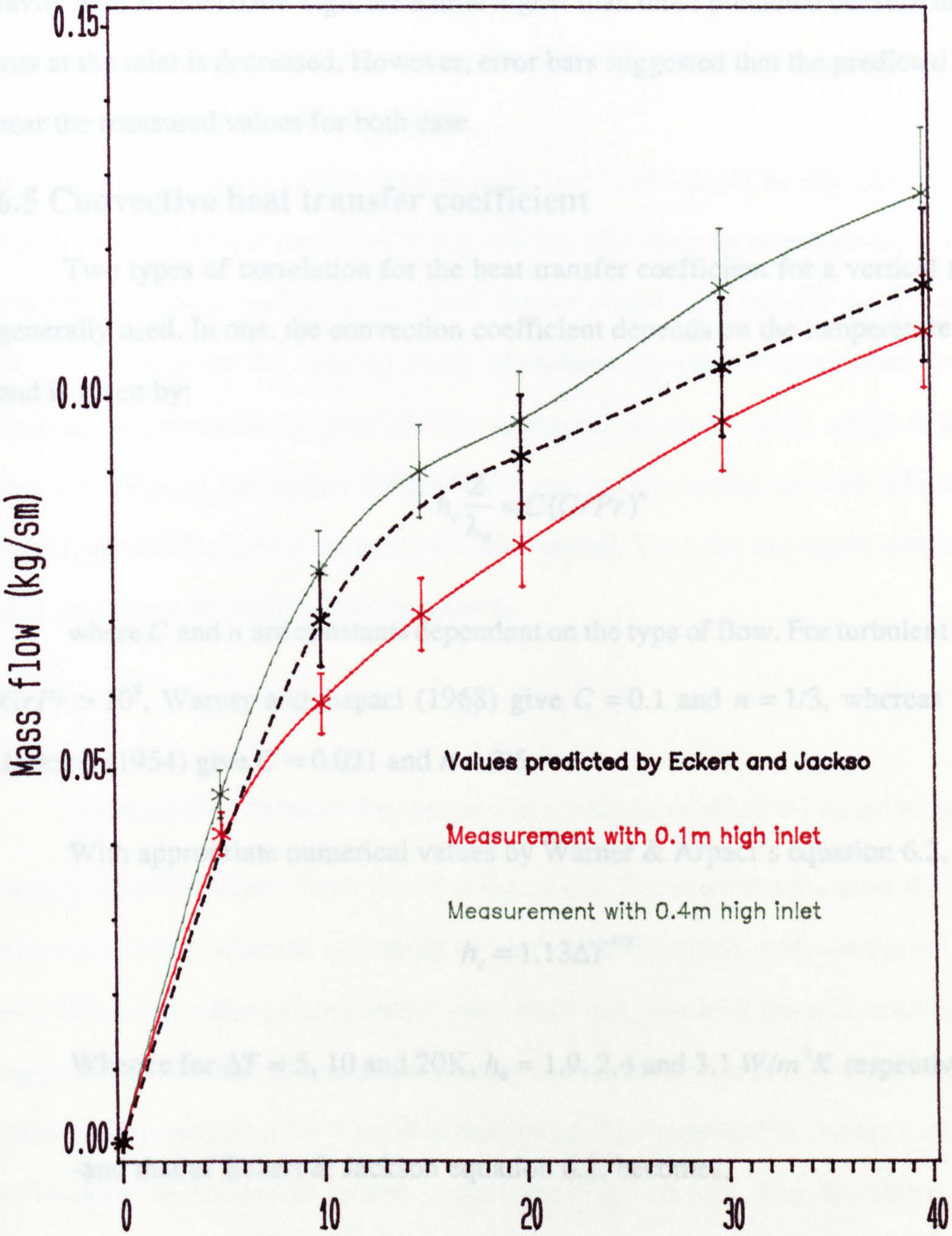

Figure 6.4 Comparison between predicted and measured mass flows for 0.3m wide cavity.

cavity with an inlet 0.4m high, are a little higher than those predicted because the pressure loss at the inlet is decreased. However, error bars suggested that the predicted values are near the measured values for both case.

6.5 Convective heat transfer coefficient

Two types of correlation for the heat transfer coefficient for a vertical surface are generally used. In one, the convection coefficient depends on the temperature difference and is given by:

$$h_c \frac{Z}{\lambda_a} = C(GrPr)^n \tag{6.2}$$

where C and n are constants dependent on the type of flow. For turbulent flow, when $GrPr > 10^9$, Warner and Arpaci (1968) give $C = 0.1$ and $n = 1/3$, whereas Eckert and Jackson (1954) give $C = 0.021$ and $n = 2/5$.

With appropriate numerical values by Warner & Arpaci's equation 6.2, becomes,

$$h_c = 1.13\Delta T^{1/3} \tag{6.3}$$

Whence for ΔT = 5, 10 and 20K, h_c = 1.9, 2.4 and 3.1 W/m^2K respectively.

-and that of Eckert & Jackson equation 6.2, becomes,

$$h_c = 0.8Z^{0.2}\Delta T^{0.4} \tag{6.4}$$

for ΔT = 5, 10 and 20K, h_c = 1.7, 2.3 and 3.0 W/m^2K respectively which agree with the values given by Warner and Arpaci.

The IHVE Guide (1970) suggested that $h_c = 3W/m^2K$ for a vertical wall.

It can be seen from the above convection heat transfer coefficients that they do not depend on velocity, and all give values near $3W/m^2K$, known to be applicable for natural convection in "still air" (Waters 1977).

For moving air the convection heat transfer coefficient might be expected to depend on the air velocity, as was observed. Wong (1976), who gives an extensive collection of heat transfer data, gives no relation in which the convective heat transfer coefficient depends on the velocity of the moving fluid. McAdams reported a convection heat transfer coefficient correlation for parallel flow dependant on air velocity, which was originally found by Nusselt and Jurges (1922) from experiments carried out with a heated vertical plate mounted flush with the wall of a wind tunnel. They did not report whether the flow was laminar or turbulent. Their relation is,

$$h_c = 5.8 + 4.1\overline{v} \tag{6.5}$$

A comparison between the observed heat transfer coefficients h_c and those calculated according to McAdams is presented in figure 6.5. The observations show that h_c depends on cavity width, whereas according to McAdams it depends only on the velocity of the air. When the velocity approaches zero (still air), the heat transfer coefficient should approach the natural convection value known to be near $3W/m^2K$ as observed here, whereas McAdams gives about 5.8 W/m^2K at zero speed. The measured values are a linear function of velocity, which can be written in the form of $h_c = a + bv$, W/m^2K, where a is about 3 W/m^2K, and b is a parameter which depends on cavity width and inlet height. The values of b are defined statistically with a coefficient of correlation of 0.99 with $P<0.05$, and they are summarised in table 6.1.

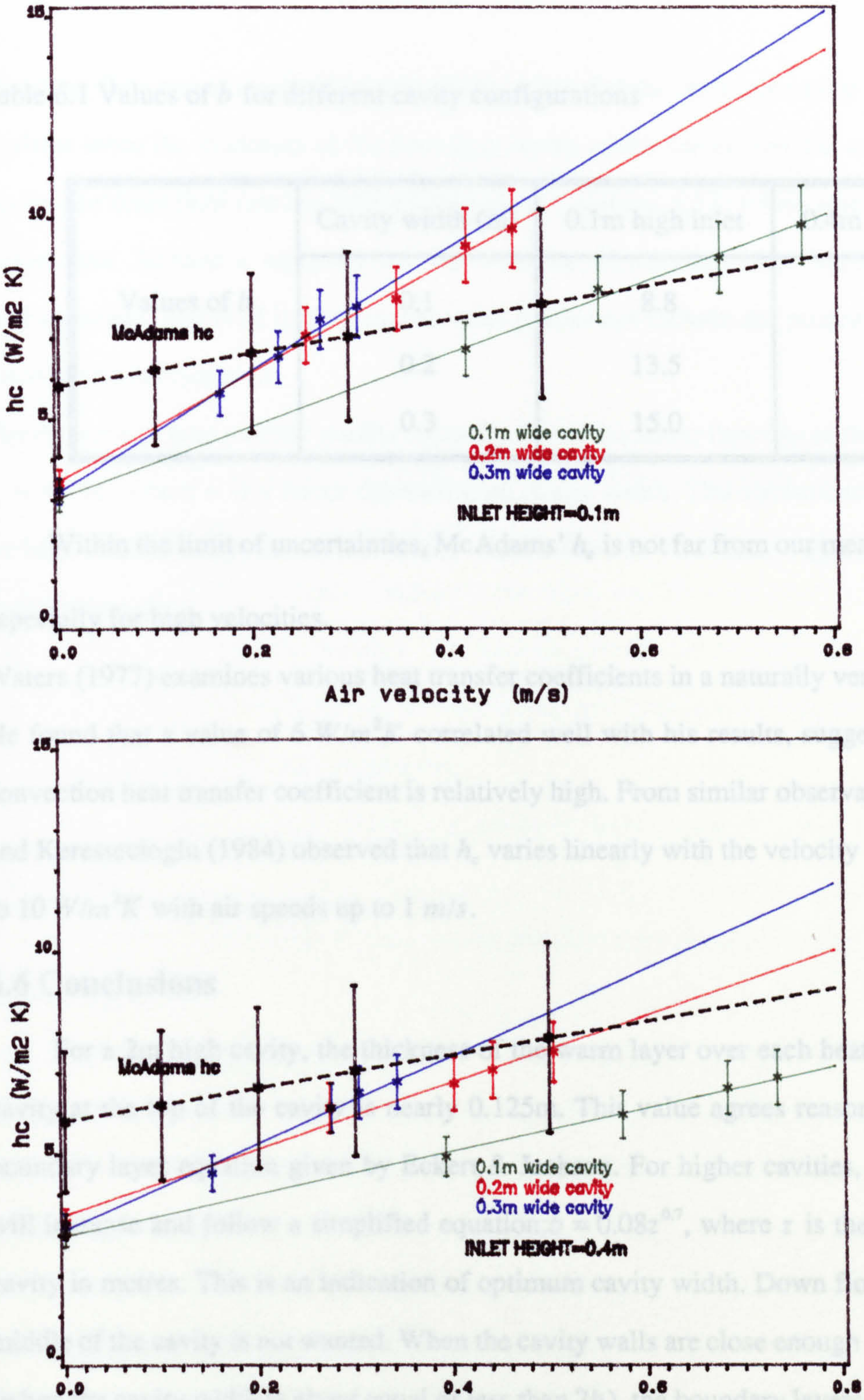

Figure 6.5 Comparison between observed hc and those predicted by McAdams

Table 6.1 Values of b for different cavity configurations

	Cavity width (m)	0.1m high inlet	0.4m high inlet
Values of b	0.1	8.8	5.3
	0.2	13.5	8.2
	0.3	15.0	10.7

Within the limit of uncertainties, McAdams' h_c is not far from our measured values, especially for high velocities.

Waters (1977) examines various heat transfer coefficients in a naturally ventilated room. He found that a value of 6 W/m^2K correlated well with his results, suggesting that the convection heat transfer coefficient is relatively high. From similar observation, Chandra and Keresteciogl u (1984) observed that h_c varies linearly with the velocity and can be up to 10 W/m^2K with air speeds up to 1 m/s.

6.6 Conclusions

For a 2m high cavity, the thickness of the warm layer over each heated face of the cavity at the top of the cavity is nearly 0.125m. This value agrees reasonably with the boundary layer equation given by Eckert & Jackson. For higher cavities, this thickness will increase and follow a simplified equation:$b = 0.08z^{0.7}$, where z is the height of the cavity in metres. This is an indication of optimum cavity width. Down flow through the middle of the cavity is not wanted. When the cavity walls are close enough to one another (when the cavity width is about equal or less than $2b$), the boundary layers just touch and thus the air flow will be fully upwards.

The temperature of the air flowing up the cavity increases linearly with the temperature difference $(T_{sm} - 20)$, but slowly. Heating the surfaces to 40 K above the ambient air will raise the air temperature about 15 K.

The mass flow rate is a cubic function of $(T_{sm} - 20)$. For the optimum cavity width, which is about twice the thickness of the boundary layers which forms over the surfaces of the cavity, the mass flow rate can be predicted using equation (5.17) which was derived from Eckert and Jackson's equation for the velocity distribution over vertical surfaces. Unfortunately, this is of limited use because it does not include the pressure loss due to the system configuration.

The convection heat transfer coefficient in the cavity is a linear function of the air velocity, $h_c = 3 + bv$, where b is a factor dependent on cavity width. The convection heat transfer for high velocities approaches McAdams' values. For low velocities, it approaches natural convection values.

CHAPTER SEVEN

DYNAMIC MODEL FOR A SUN-WARMED CAVITY

7.1 Introduction

There are various ways of calculating the unsteady heat transfer in buildings. They are the Harmonic Method, the Response Factor Method and Numerical Methods. In the present study, an implicit finite difference technique is used because it has more advantages than other existing dynamic methods. The implicit method can be used when the boundary conditions are time dependent with a complicated configuration. It is stable with any time or space increment, and easy to program.

The other existing dynamic modelling methods have limitations and disadvantages, forexample:

-the explicit finite difference method has the disadvantage of not being stable for any time or space increment.

-the harmonic method assumes the climatic data are periodic which in reality they are not. The other restriction is that the boundary conditions are assumed constant and time invariant. Linear approximations have to be used for the convective and radiative boundary conditions.

-the response factor method is complicated from the point of view of computation and it cannot deal easily with multidimensional heat flow.

More details on dynamic models are given in chapter two.

The dynamic model developed in the current study was based on a numerical solution of the Fourier's equation for transient heat flow in the building fabric. Heat balance equations were used in conjunction with the boundary conditions for which a computer program was written.

The climatic data for El-Oued described in chapter one were used in the model. The external wall thickness of the cavity "external leaf" was 0.05m, 0.10m, 0.15m and 0.20m. The choice of azimuth is subject to many considerations, including topography, sources of noise and wind direction. Attention in this study is given to solar radiation and its heating effect on the performance of the cavity facing different directions.
Calculations were made for azimuths East, South and West. Cavity ventilation was assumed from 2000, 2200, and 2400h to 1000h and from 2000h to 0800h.

7.2 The model and assumptions

The model considered here is shown in figure 7.1. It is a cubic room (3m x 3m x 3m) with concrete walls 0.30m thick, roof and floor 0.20m thick, and a 3m high cavity with an external leaf of variable outer thickness. The air cavity was 0.20m wide. For simplicity, the calculations were performed assuming homogeneous materials and their assumed properties are presented in table 7.1.

Table 7.1 Material properties used in the dynamic model.

	Walls	Roof	Floor	Air
Thermal Conductivity (W/mK)	1.1	0.2	1.1	0.027
Density (kg/m^3)	2100	500	2000	1.2
Specific heat capacity (J/kgK)	900	840	840	1000

The temperature of the ground at a depth of 0.60m was considered constant, at the monthly average outside air temperature.

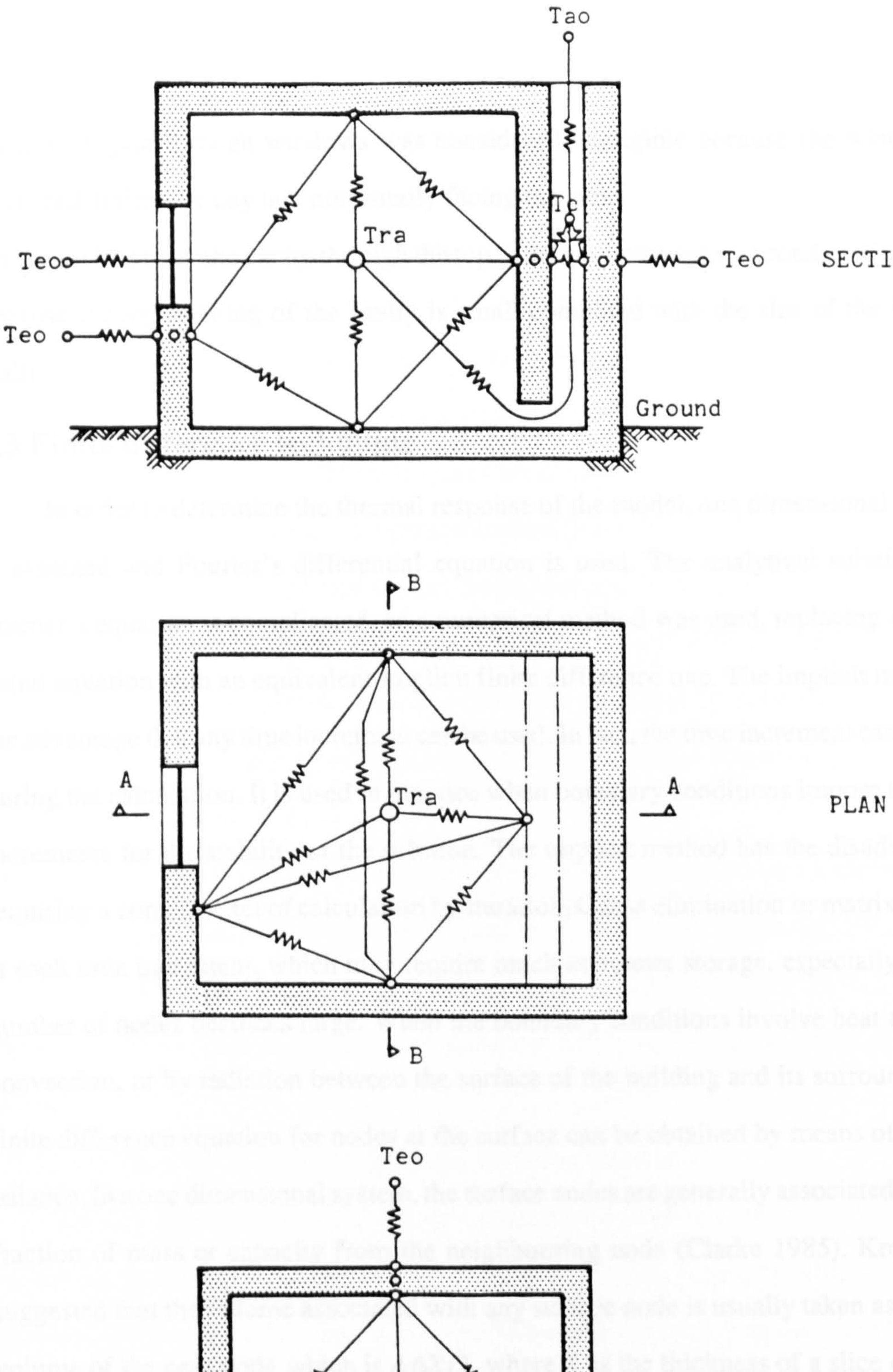

Figure 7.1 Nodal network for the dynamic model

Solar heat gain through windows was considered negligible because the windows are shuttered during the day and not usually facing the sun.

Radiation loss from the cavity through the top to the environment was condiered negligible because the top opening of the cavity is small compared with the size of the bounding walls.

7.3 Finite difference technique

In order to determine the thermal response of the model, one dimensional heat flow is assumed and Fourier's differential equation is used. The analytical solution of the Fourier's equation is complicated, so a numerical method was used, replacing the differential equation with an equivalent implicit finite difference one. The implicit method has the advantage that any time increment can be used. In fact, the time increment can be varied during the calculation. It is used in practice when boundary conditions impose small time increments for the stability of the solution. The implicit method has the disadvantage of requiring a complete set of calculation by iteration, Gauss elimination or matrix inversion at each time increment, which may require much computer storage, especially when the number of nodes becomes large. When the boundary conditions involve heat transfer by convection, or by radiation between the surface of the building and its surroundings, the finite difference equation for nodes at the surface can be obtained by means of an energy balance. In a one dimensional system, the surface nodes are generally associated with some fraction of mass or capacity from the neighbouring node (Clarke 1985). Kreith (1973) suggested that the volume associated with any surface node is usually taken as half of the volume of the next node which is $A\,\Delta X/2$, where X is the thickness of a slice of the wall. The final result of an implicit method is a set of equations for the future temperature of each node in terms of the present temperature of that node and the future temperatures at neighbouring nodes. There will be as many equations as there are unknown future temperatures, once this set of equations is solved the resulting future temperature becomes the initial temperature for the next time increment. The implicit method will be stable with

any time increment. Its accuracy depends on using the right time step and right space increments. The larger the number of nodes and the smaller the time step, the more computer time is used. Nevertheless, Clarke (1985) suggested that in building applications three nodes per homogeneous element and a time step of an hour are consistent with acceptable accuracy. This conclusion was reached based on a theoretical study using a finite difference approximation. He compared the temperature variation and heat flow at the internal and external boundary surfaces of a wall divided into three nodes with a similar wall divided into fifteen nodes, he reported no significant difference. In the present model, three nodes are used for each slab such as walls, roof and floor. The temperature variation for each single node is evaluated by energy balances. The basis of the heat balance equations is that the algebraic sum of the rate of heat transfer to a node by convection, conduction and radiation must equal the rate of increase of heat content of that node for a given time as discussed in chapter two.

The conditions under which the model was run to give realistic answers were bounded by the climatic conditions of a hot climate. These were; outside air temperature which ranges 15 $^{\circ}C$ to 45 $^{\circ}C$ and surface temperatures variations between 5 $^{\circ}C$ and 75 $^{\circ}C$.

There are four boundary conditions for each case in the present model which are discussed below.

7.3.1 Heat balance at nodes inside solid building elements

The first boundary condition is obtained from a heat balance within the walls and the bounding surfaces. It is modelled using Fourier's one dimensional heat conduction equation, where the rate of temperature increase is proportional to the rate of change of temperature gradient, given by:

$$\frac{\partial T}{\partial t} = \frac{\lambda}{\rho c}\frac{\partial^2 T}{\partial x^2} \qquad (7.1)$$

This equation can be solved numerically, as suggested by Kreith (1973), by dividing the wall into layers of thickness ΔX called nodes, and making a heat balance for each. In this study the wall was divided into three layers. The heat balance for a node in the middle of the wall is as follows:

$$\frac{T_{so}^{t+1}-T_{wm}^{t+1}}{R_{so,wm}}+\frac{T_{si}^{t+1}-T_{wm}^{t+1}}{R_{si,wm}}=\frac{(\rho cV)_{wm}}{\Delta T}(T_{wm}^{t+1}-T_{wm}^{t}) \qquad (7.2)$$

The thermal resistance of a slab of homogeneous material is calculated by dividing its thickness by its thermal conductivity and its area, thus:

$$R=\frac{dx}{A\lambda} \qquad (7.3)$$

where

dx = thickness of the layer

A = area of the layer

$R_{so,wm}$ = thermal resistance between outside surface node and the node in the middle of the wall (m^2K/W)

$R_{si,wm}$ = thermal resistance between inside surface node and the node in the middle of the wall (m^2K/W)

7.3.2 Heat balance at the external surface nodes

The second boundary condition is obtained from the heat balance equation for the outside surfaces of the model. The external wall exchanges heat with surrounding surfaces by radiation, with the outside air by convection, and into the wall by conduction. The heat balance for a node exposed to the outside environment according to Kreith (1973) is given by:

$$\frac{T_{eo}^{t+1}-T_{so}^{t+1}}{R_{eo,so}}+\frac{T_{wm}^{t+1}-T_{so}^{t+1}}{R_{wm,so}}=\frac{(\rho cV)_{so}}{\Delta T}(T_{so}^{t+1}-T_{so}^{t}) \qquad (7.4)$$

It is common practice in building energy simulation to represent the external environmental thermal conditions by a single temperature known as the "sol-air temperature" as defined in the CIBSE Guide (1986). The surrounding surfaces are then assumed at outside air temperature. The sol-air temperature is given by:

$$T_{eo} = T_{ao} + R_{eo,so}(\alpha I_{tvd} - EI_l) \tag{7.5}$$

where

$$R_{eo,so} = \frac{1}{(Eh_r + h_c)} \tag{7.6}$$

and

$R_{eo,so}$ = combined outside surface resistance (m^2K/W)

α = surface absorptivity

I_l = long-wave radiation loss (W/m^2)

I_{tvd} = total solar radiation (W/m^2)

V_{so} = volume of a layer (m^3)

7.3.3 Heat balance at the internal surface nodes

The third boundary condition is obtained from heat balances at any of the inside surfaces of the room and the cavity, where the heat is exchanged by convection with the inside air, by radiation with other surrounding surfaces and by conduction with the walls. The convection heat transfer coefficient used in the room was the one suggested by Alamdari & Hammond (1983). The radiation heat transfer coefficient between the surfaces described in chapter two was used. In the cavity, various convection coefficients were used including the one suggested by the IHVE Guide (1970), but using the model there was no significant difference in the resulting temperatures. For the radiation heat exchanges in a room or cavity, the room and the cavity are divided into p surfaces. The heat balance at each of the bounding surfaces is:

$$\frac{T_{wm}^{t+1}-T_{si}^{t+1}}{R_{wm,si}}+\frac{T_{ai}^{t+1}-T_{si}^{t+1}}{R_{ai,si}}+\sum_{p=1}^{p=n}\frac{T_{p}^{t+1}-T_{si}^{t+1}}{R_{p,si}}=\frac{(\rho cV)_{si}}{\Delta T}(T_{si}^{t+1}-T_{si}^{t}) \qquad (7.7)$$

where

$\sum_{p=1}^{p=n}$ is for the radiation part between the surfaces,

$R_{ai,si}$ = convective thermal resistance between air node and inside surface node (m^2K/W),

$R_{p,si}$ = radiation thermal resistance between inside surface nodes (m^2K/W).

7.3.4 Heat balance for room air and cavity air

The fourth boundary condition is obtained from a heat balance on the room air and the cavity air, where the heat exchange with the air nodes, in the room and in the cavity, takes place by convection with the surrounding surfaces and by ventilation conductance with the outside air.

a) Heat balance equation for the room air based on Kreith (1973) principle is given by:

$$\sum_{m=1}^{m=n}\frac{T_{m}^{t+1}-T_{ar}^{t+1}}{R_{m,ar}}+((T_{ao}^{t+1}-T_{ar}^{t+1})+(T_{ac}^{t+1}-T_{ar}^{t+1}))C_{v}=\frac{(\rho cV)_{ar}}{\Delta T}(T_{ar}^{t+1}-T_{ar}^{t}) \qquad (7.8)$$

where

$R_{m,ar}$ = thermal resistance by convection between the inside surface nodes of the room and the air in the room (m^2K/W),

C_v = ventilation conductance (the reciprocal of the ventilation resistance) given by:

$$C_{v}=\rho cV_{f} \qquad (7.9)$$

and

V_f = volume flow (m^3/s)

The volume flow rate is equal to the mass flow rate, M, divided by the air density, ρ.

The mass flow rate, M, produced by the temperature difference is determined from equation 5.11 from the steady state analysis (see chapter five) and is given by:

$$M = \frac{11.6YZ/c}{\ln\{(T_{sm} - T_{ai})/(T_{sm} - T_{out})\} - 8.2YZ/\rho XYc} \tag{7.10}$$

b) The heat balance for the air node inside the cavity is:

$$\sum_{p=1}^{p=n} \frac{T_p^{t+1} - T_{ac}^{t+1}}{R_{p,ac}} + ((T_{ao}^{t+1} - T_{ac}^{t+1}) + (T_{ar}^{t+1} - T_{ac}^{t+1}))C_v = \frac{(\rho c V)_{ac}}{\Delta T}(T_{ac}^{t+1} - T_{ac}^{t}) \tag{7.11}$$

A computer program was written whereby the temperature distribution at all nodes and the air flow rate produced by the cavity were calculated. The hourly climatic data were read by the program and interpolated for any time increment by a subroutine. For simplicity of computation, the heat balance equations were written in the matrix form of $AX = B$., where X denotes unknown future temperatures. The matrix gives a system of linear equations with 23 unknowns. The unknown temperatures were calculated for each time interval using a NAG library subroutine F04ARF. The first run of the program was made by a starting temperature distribution for each node, calculated by steady state conditions. It was soon realised that this was not necessary because whatever the value of the starting temperature there was stability. The radiation and convection heat transfer coefficients were calculated using several function routines. A time increment of 15 minutes was used. The calculations were repeated for one week after which stable temperatures were obtained.

Figure 7.2 is a flowchart of the program written for the dynamic model. The listing of the computer program for the dynamic model is given in Appendix 6.

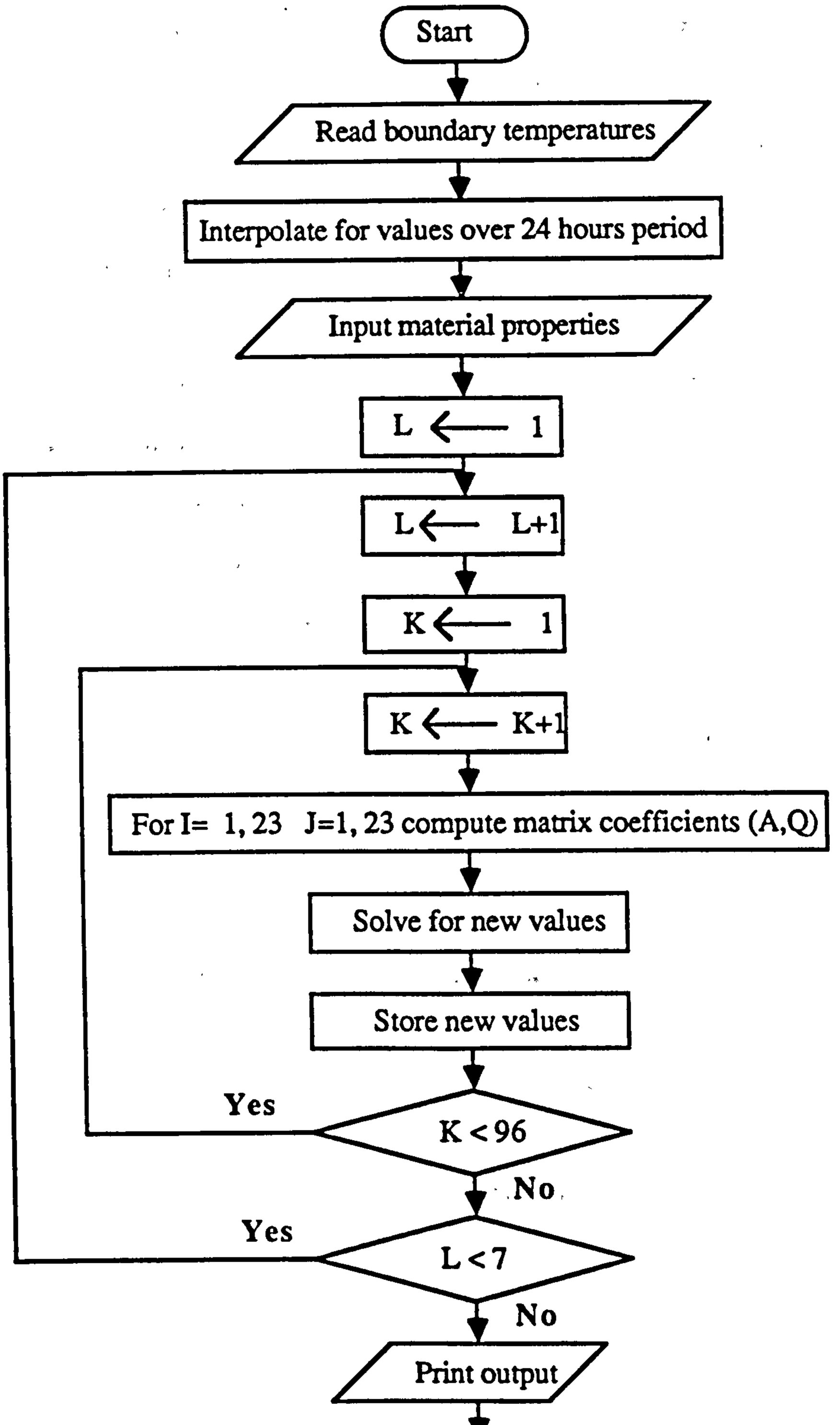

Figure 7.2 Flowchart of the computer program for the dynamic model

7.4 Results and discussion

The dynamic model enabled the response of the cavity with in a building under climatic changes with variable boundary conditions to be studied. It was simplified to one dimensional heat flow equations with a single node for each surface, for the room and the cavity air. It would probably have been more accurate if two dimensional heat transfer had been used with more nodes throughout the cavity. This would have been more complicated and have required greater computer storage and running time. The model was simplified further by not considering the effect of intermittent heat inputs from lighting and occupants.

7.4.1 Magnitude of mass flow rate

The aim of the sun warmed cavity is to move as much air as possible. Rates of mass flow were calculated by the above model and results are plotted in figures 7.3 to 7.6 which show the mass flow rate of air per unit cavity length of a typical cavity (3m high, 0.20m wide and 3m long) facing east, south or west with variable external leaf thickness. The maximum rate of ventilation occurs about 2000h when the dampers of the cavity are open. Maximum ventilation rates are given in table 7.2. This shows that, for a west cavity, as the leaf thickness is increased the mass flow decreased because the thickness of the walls are increased and their mean mean temperature decreases. The peak ventilation decreases sharply a short time after the opening of the dampers to an average of $0.035 kg/sm$. This continues throughout the night until 0800h when its rate decreases again. At 1000h the dampers are closed and thus the flow becomes zero.

Table 7.2 The peak mass flow rates for a typical cavity.

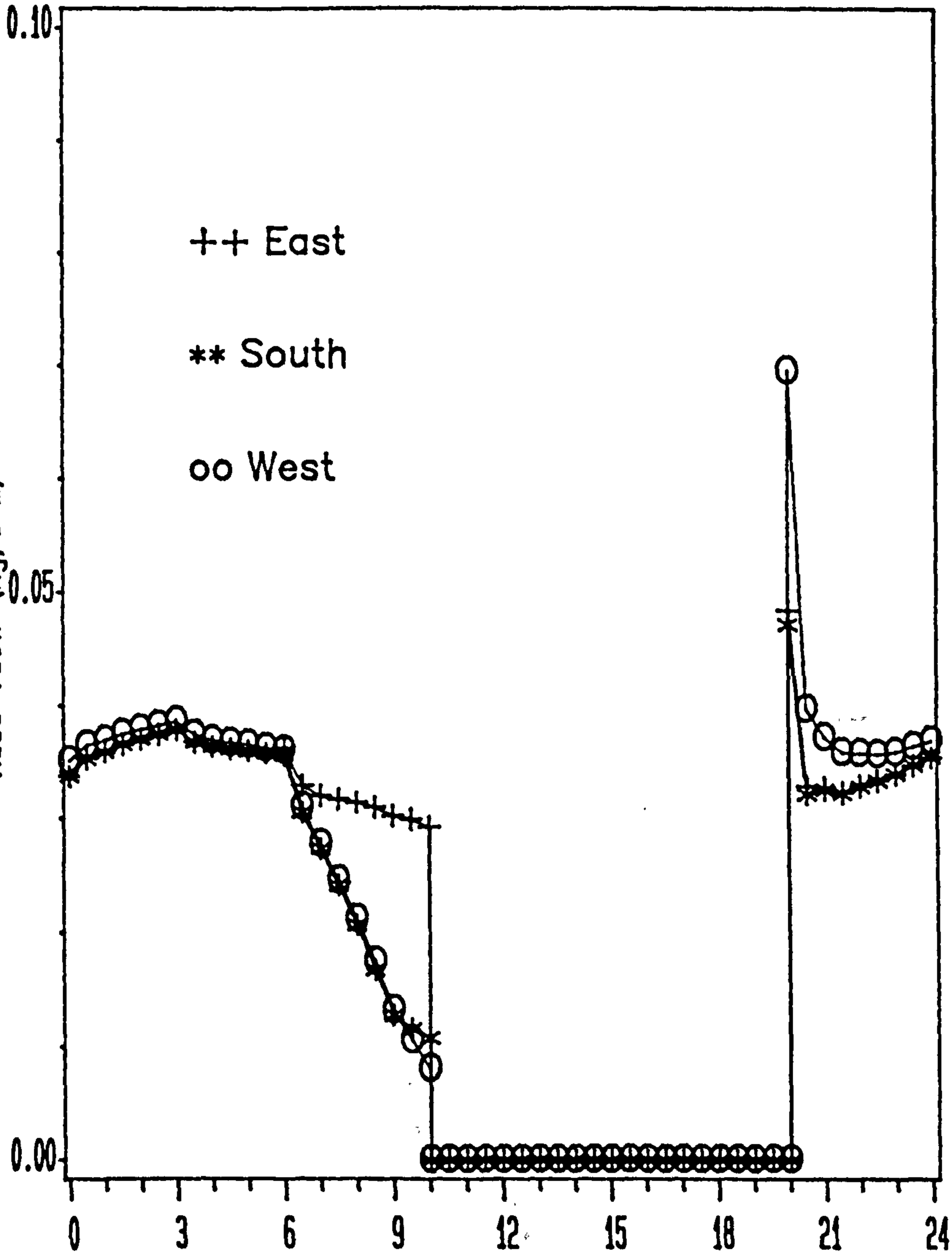

Figure 7.3 Mass flow per unit length with 0.05m thick external wall of the cavity

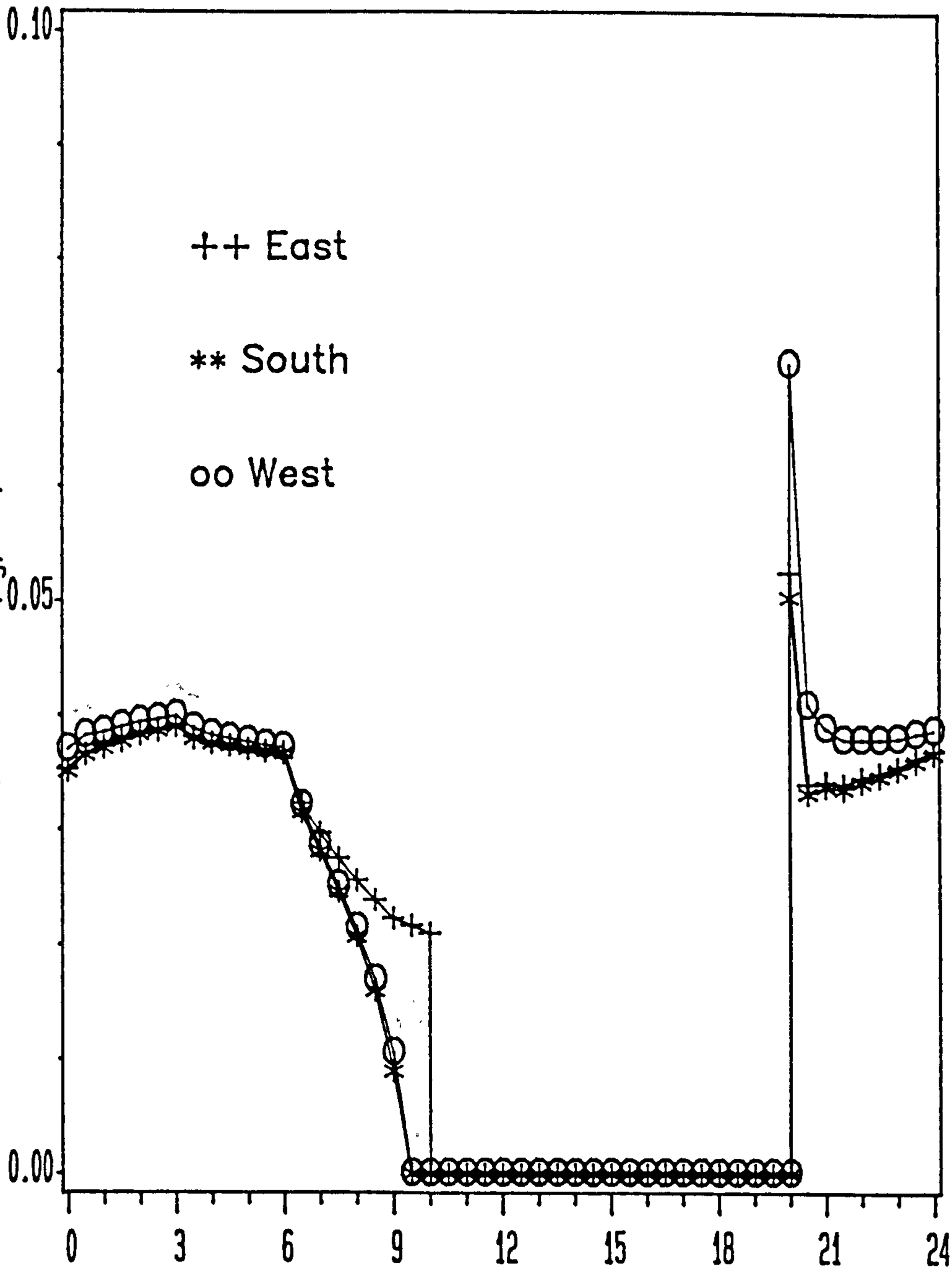

Figure 7.4 Mass flow per unit length with 0.10m thick external wall of the cavity

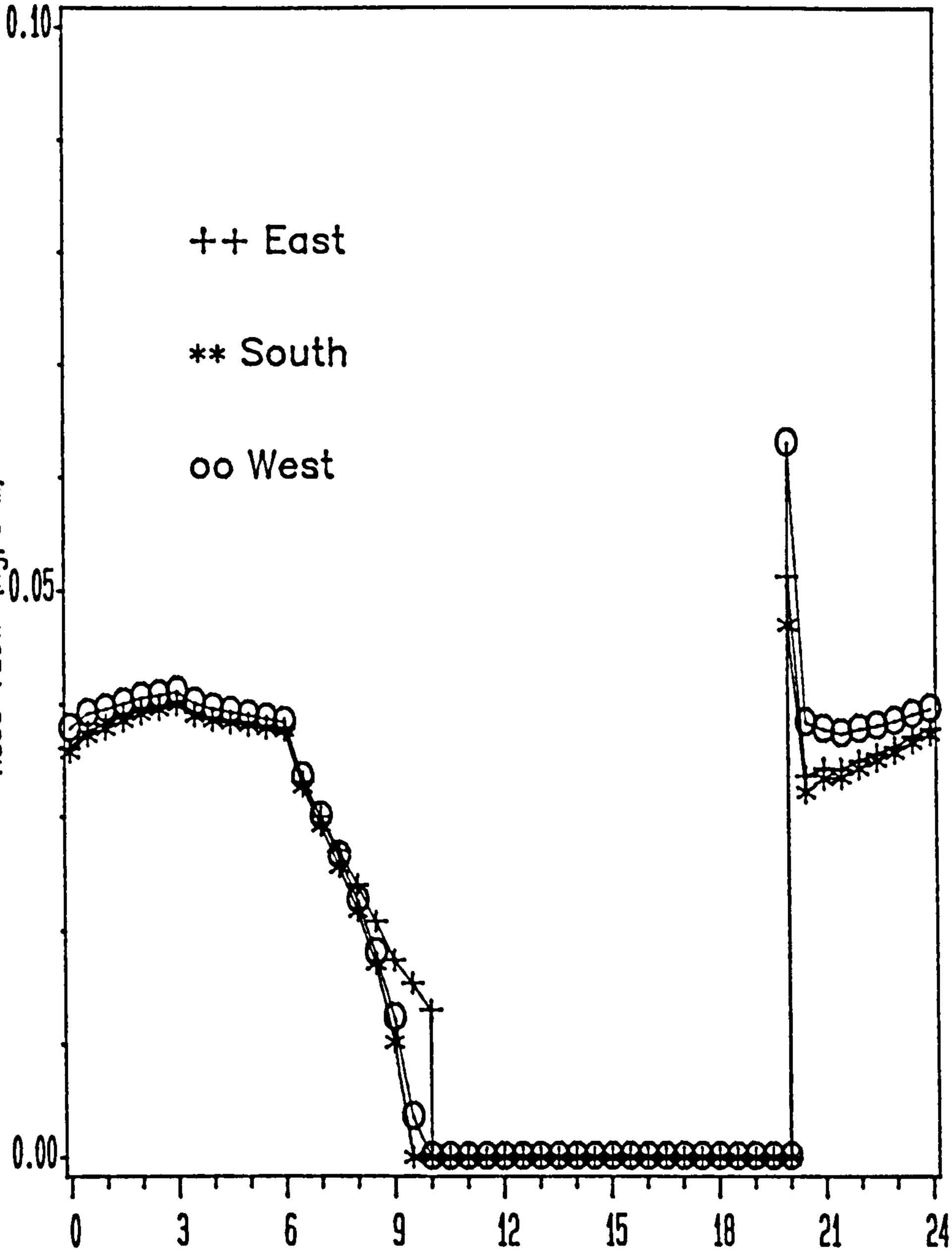

Figure 7.5 Mass flow per unit length for 0.15m thick external wall of the cavity

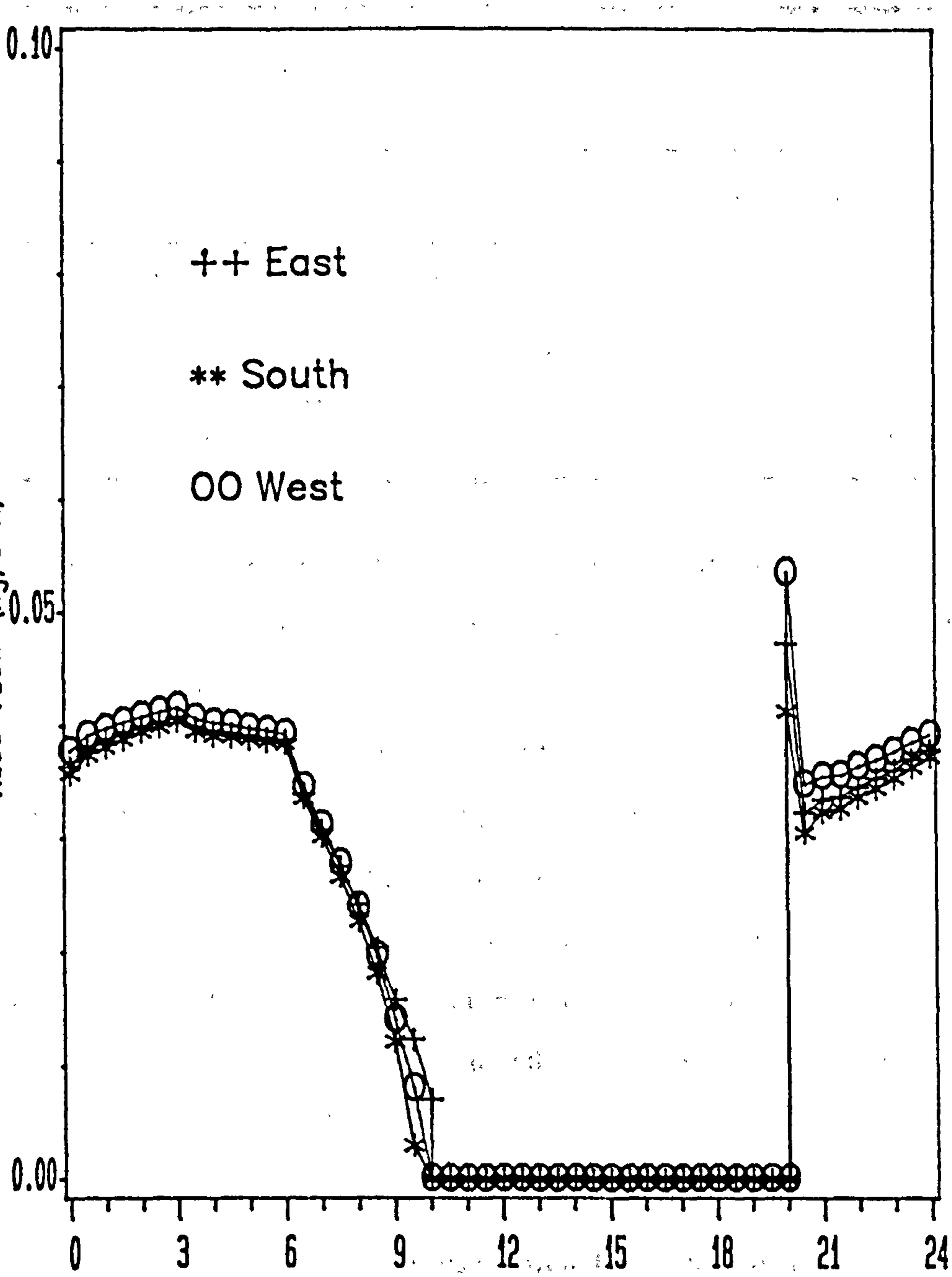

Figure 7.6 Mass flow per unit length for 0.20m thick external wall of the cavity

External leaf thickness (m)	0.05	0.10	0.15	0.20
Cavity orientation	Maximum mass flow rate (kg/sm)			
East	0.048	0.052	0.051	0.047
South	0.047	0.050	0.047	0.041
West	0.069	0.071	0.063	0.053

In order to compare the mass flows obtained from the dynamic model and the experiment, typical values were taken. From the model, considering a time of 2000h the mean surface temperature of the cavity was 44 °C and the outside temperature of the air was at 34 °C, with a temperature difference of 10 K. This gave a mass flow rate of 0.07 kg/ms. From experimental work, considering similar temperatures, the mass flow was 0.06 kg/ms. The two values can be seen to agree closely.

Considering a second example. From the dynamic model at 0650h, a temperature difference of 5 K was predicted between the surfaces of the cavity and the outside air. This gave a mass flow of 0.032 kg/ms. From measured data at the same temperature difference a mass flow of 0.043 kg/ms was obtained.

7.4.2 Optimum azimuth

The azimuth at which a sun-warmed cavity would give the best performance has to be known. The south might be thought "the best azimuth" for a sun-warmed cavity or solar chimney, but not so in low latitudes. Figures 7.3 to 7.6 show the comparison of the rates of mass flows in cavities with azimuths East, South and West for a latitude 33 °N. From the figures it is clear that a cavity facing west produces higher mass flow in the evening (from 2000h to 2400h).

The fact that the west azimuth is preferably best comes from the fact that at low latitudes such as 33.3 °*N*, the total solar radiation received on a west wall is much more than the other azimuths as shown in table 7.3.

Table 7.3 Irradiance on facades at latitude 33.3 °*N*

Azimuth	Total irradiance MJ/m^2day	Insolation (h)	Peak (W/m^2)	Time of peak (h)
S	14	7	546	1200
SW	18	7	723	1500
W	21	7	866	1600
NW	17	7	701	1700

Facades facing eastward have been ignored, because if the air movement required by the sun-warmed cavity is to be in the evening or at night, which is desirable, then solar energy collected in the afternoon has to be stored for a shorter time. This also reduces possible heat losses. The table shows that in July at latitude 33.3 °*C*, the most insolation is not received on the south and not even on the south west, but on the west. Even the north west receives more than the south. This is because when the sun is in the south, its elevation is high, with a low horizontal component.

7.4.3 Optimum leaf thickness

In hot climates buildings usually have walls from 0.3m to 0.5m thick. In the application of a sun-warmed cavity, the internal leaf has generally a fixed thickness between 0.2m and 0.3m. In this study the outer leaf is made variable. If the outer leaf be thicker, more heat can be stored, but this would result in the decline of the cavity mean air temperature. If the leaf is made thinner, less heat can be stored and the cavity life would be shorter. Consequently there must be an optimum performance thickness. Figures 7.7 to 7.9 compare the mass flow rates of air produced by a cavity of various external leaf thicknesses with different azimuths.

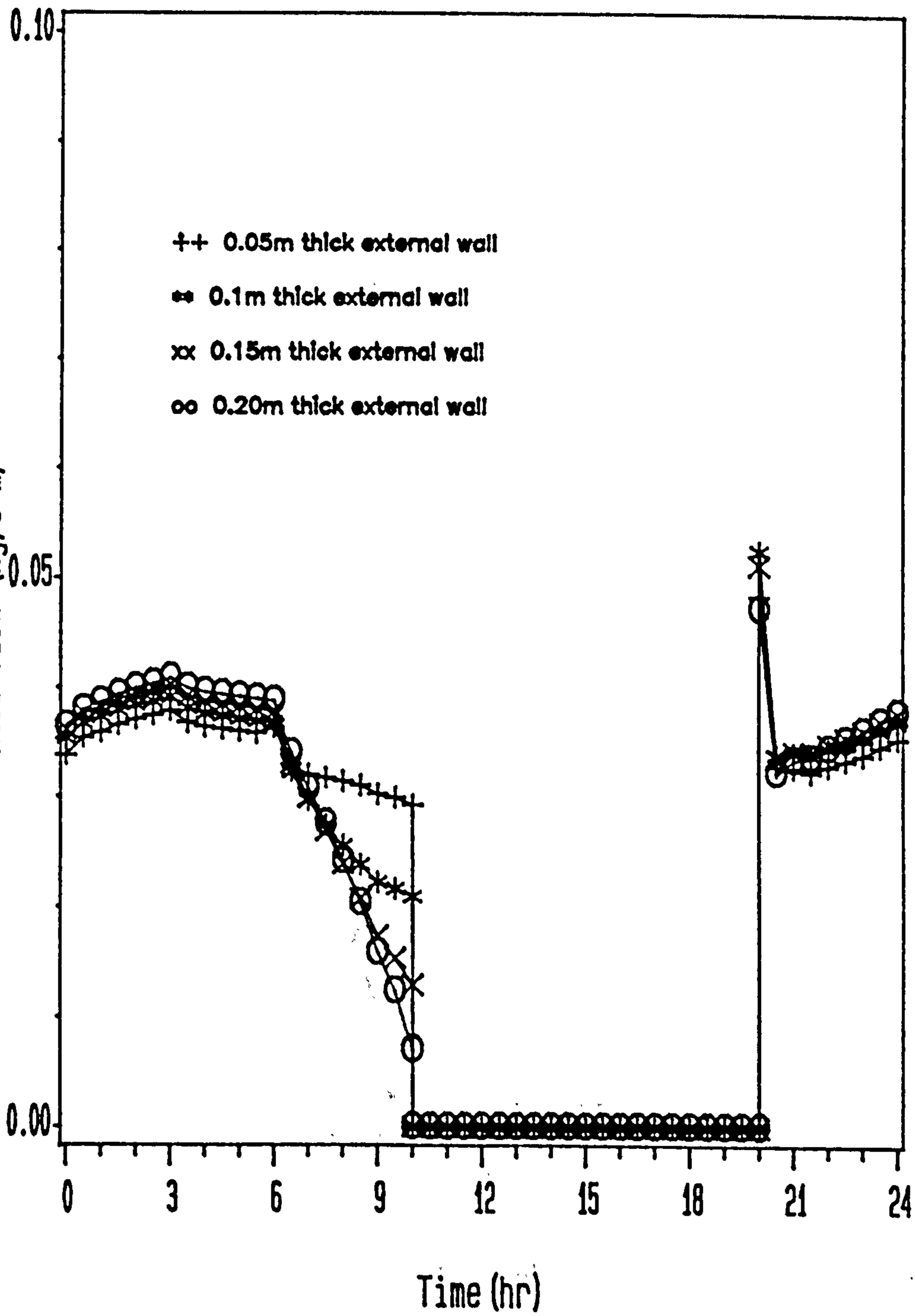

Figure 7.7 Mass flow per unit length produced by an east facing cavity

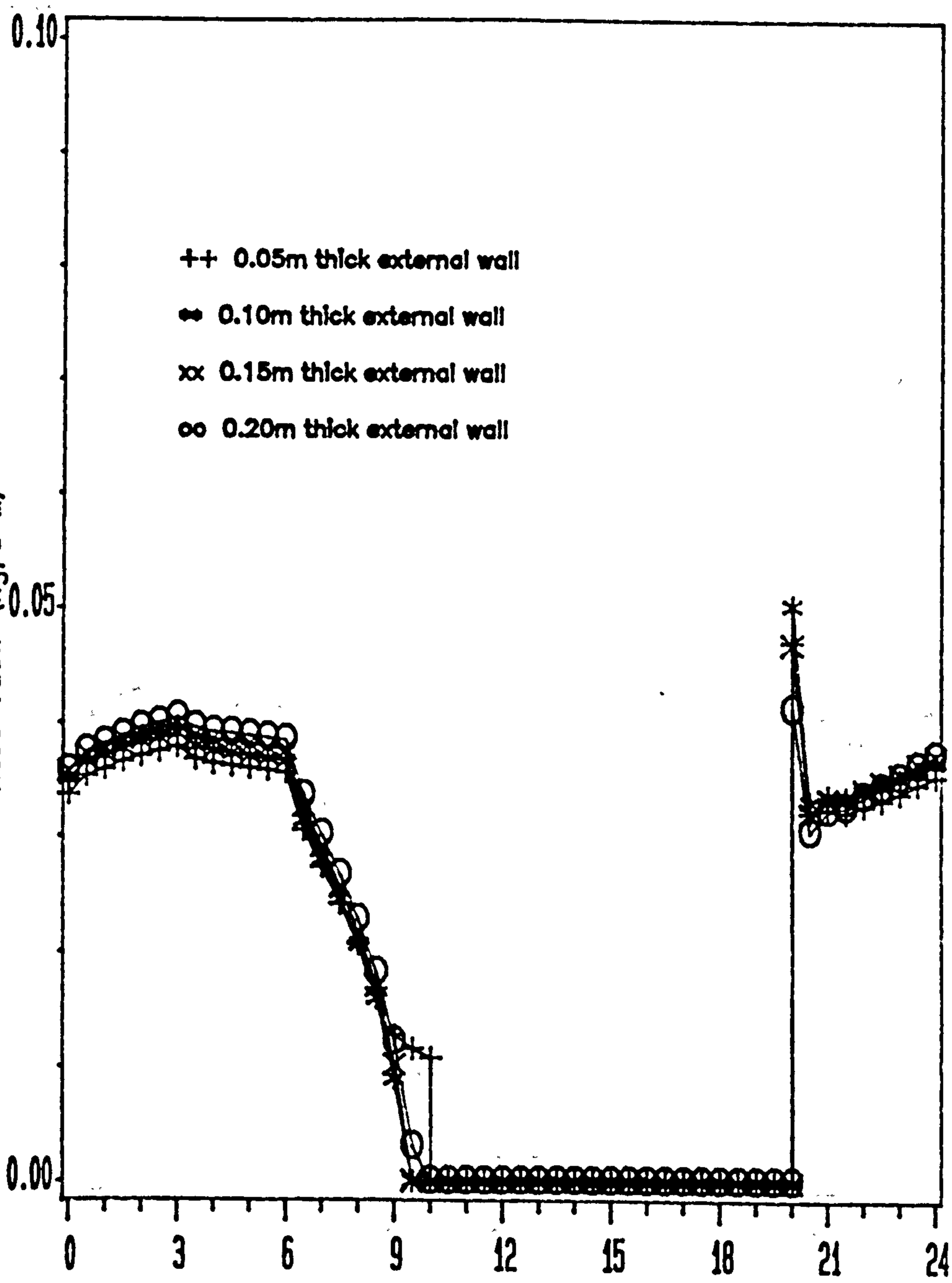

Figure 7.8 Mass flow per unit length produced by a south facing cavity

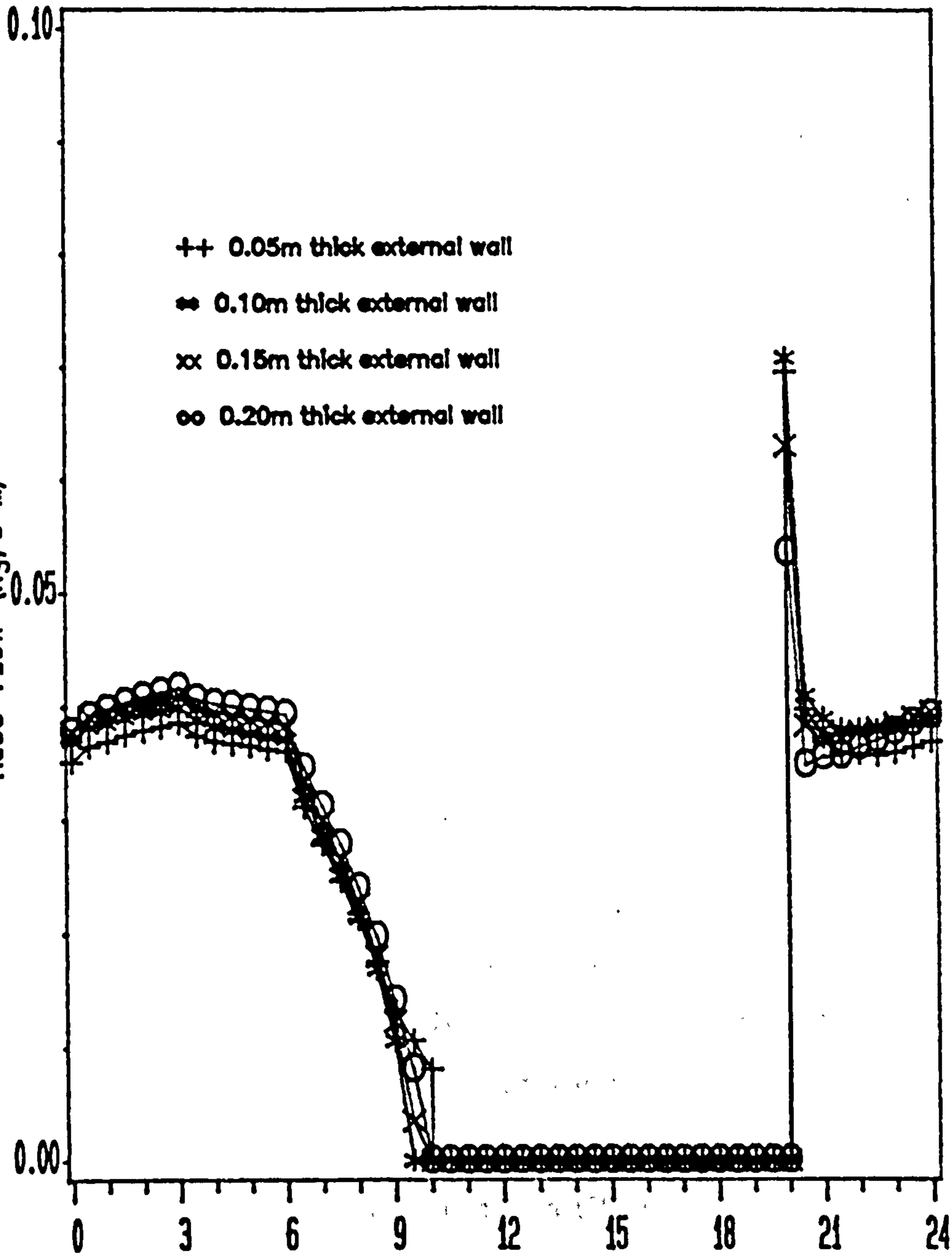

Figure 7.9 Mass flow per unit length produced by a west facing cavity

Although the differences between the results are not significant, there is an indication that the thicker the external leaf of the cavity, the higher the rate of mass flow from 2400h until 0900h will be in the evening up to 2400h, when the damper is open, the trend of the results is different. A 0.20m thick leaf gives low ventilation whereas a 0.10m thick cavity leaf gives a slightly better value. This indicates that the optimum thickness of the outer leaf of a cavity lies between 0.10m to 0.15m.

Economically, reducing the amount of material used is desirable, consequently a 0.10m leaf on the outside of the cavity may be the best.

7.4.4 Cooling effect

In order to assess the cooling in a typical room with a typical cavity, room air temperatures were calculated when

-the dampers are closed all day with low ventilation,

-and when air flow in the cavity is permitted in the evening, because the dampers are open.

Figure 7.10 shows the room air temperatures for the two cases. The corresponding sol-air and outside air temperatures are also shown. It can be seen that the room air temperature reduced by about $5K$ in the latter circumstance.

Comparison with other models is very limited because of lack of data in the literature for similar cases. However, Yagoubi and Golneshan (1986) studied the effect of cross ventilation at night on room air temperature using a wind tower in a hot climate. The ventilation was allowed from 2300h to 600h. They showed that with a rate of 12 air changes per hour, the room temperature is reduced by an average of $2K$ during the day, with a maximum reduction of about $4K$. This is not far from our values.

The sensation of cooling depends on several factors such as air temperature, mean radiant temperature, air movement and humidity. The "resultant temperature" is used here as an

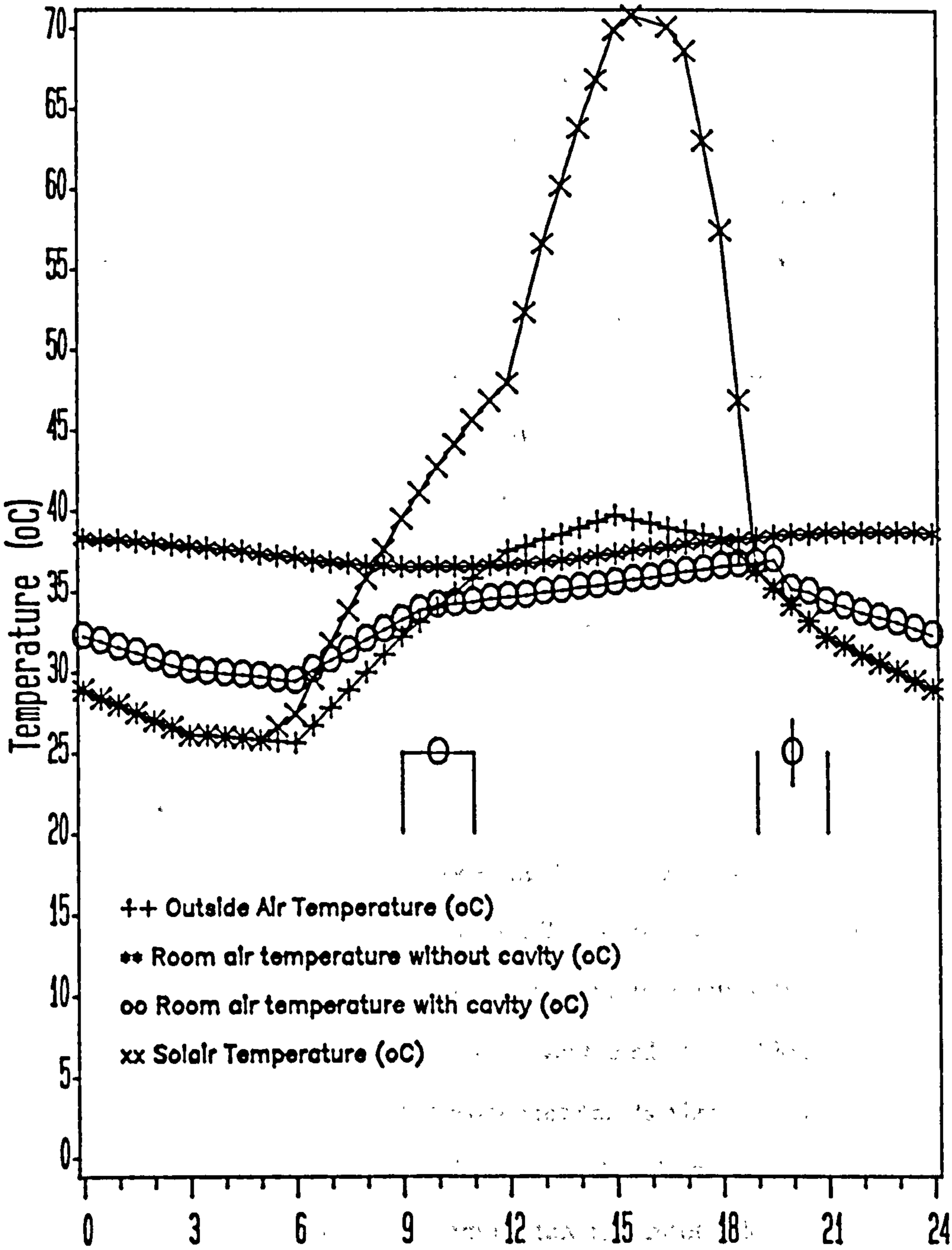

Figure 7.10 Room air temperature with west facing cavity

order of magnitude to estimate comfort in a room with a sun-warmed cavity.

The CIBSE Guide suggests a desirable resultant temperature of 28 °*C* for comfort in summers for hot climates where the relative humidity is 40 %, but Nicol (1975) has shown that a comfort or a resultant temperature of 36 °*C* can be tolerated if enough air movement be allowed, with an air velocity up to 0.25 *m/s*. The dynamic model showed that an average mass flow rate of 0.035 *kg/s* is achieved for a 1m long heated cavity, 0.2m wide is achieved. For a 3m long cavity, this would be three times greater, about 0.1 *kg/s*. If we assume that the air travels mainly in stream lines through the room into the cavity, as shown experimentally in chapter four, this would result in an air speed of 0.15 m/s. When the cavity is open, the mass flow is at its highest value of 0.071x3 *kg/s* giving an air velocity of 0.3m/s. Without the cavity, the dynamic model showed a high resultant temperature between 36 and 39 °*C*. With the cavity the resultant temperature decreased to the range of 32 to 36 °*C*, an improvement of 3 to 4 *K*.

7.4.5 Best time to open dampers

In order to know the best time for opening the dampers of a sun-warmed cavity for ventilation, different times were selected. Figure 7.11 shows how the room air temperature changes when the damper is opened at different times. Ventilation from 2000h to 1000h gives a lower room air temperature than when ventilated from 2200h to 1000h or from 2400h to 1000h. There is no difference between the results when the ventilation is allowed from 2000h to 0800h. This suggests that for improved cooling, ventilation at night should be prolonged for as long as the outside temperature is comfortable.

The results presented here are based on climatic data for El-Oued where the outside air temperature at night is high. In most hot climates, where the outside air temperature at night is lower, cooling with ventilation will be more effective.

7.5 Conclusions

The dynamic model showed that:

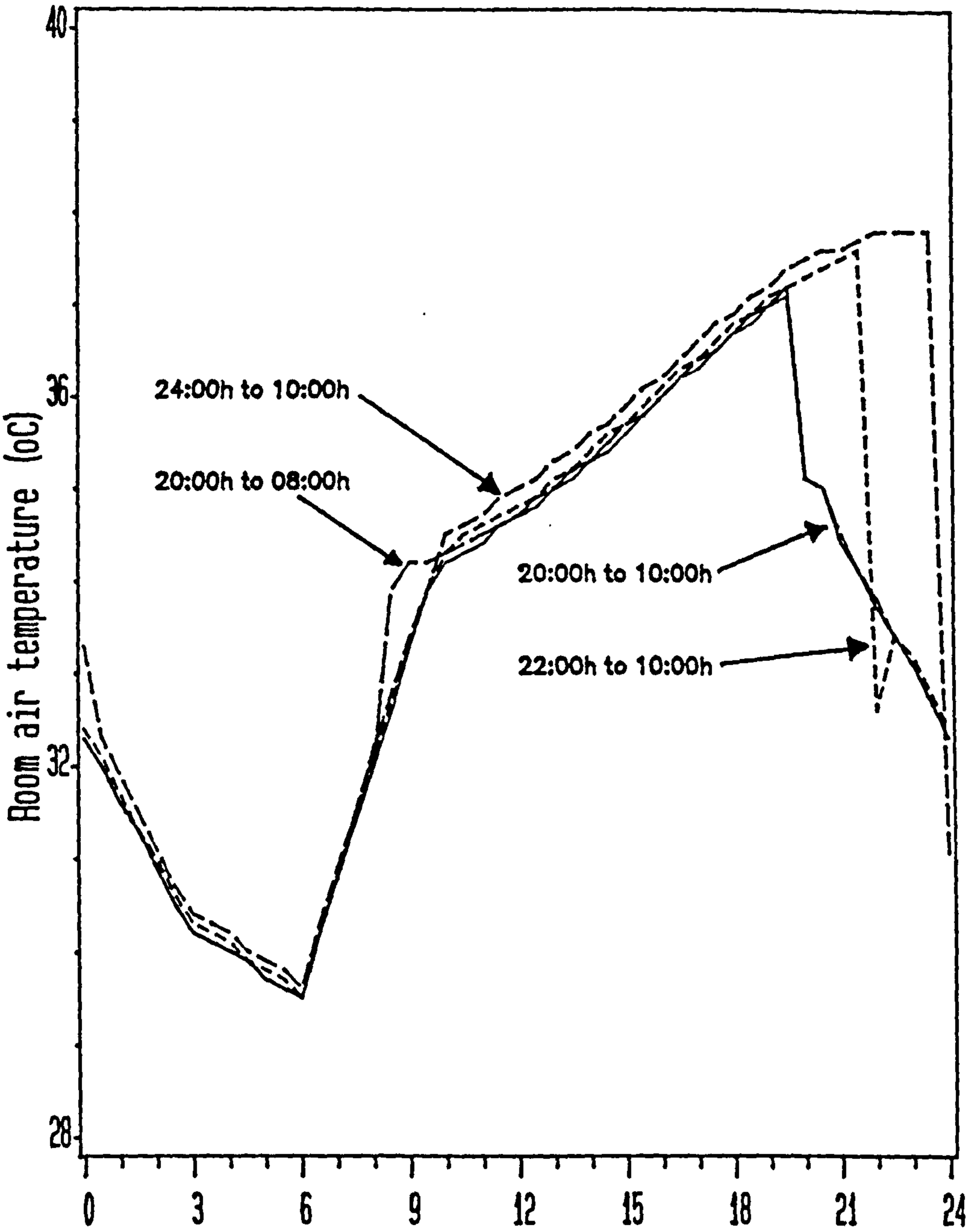

Figure 7.11 Effect of opening times of damper on room air temperature

A sun-warmed cavity can improve ventilation at night giving higher air velocities. The air movement produced will help to improve thermal comfort inside buildings.

The ventilation reduces the resultant temperature from the range of 36-38 °C to the lower range of 32-34 °C and thus improves thermal comfort.

Cooling is more effective if the ventilation is prolonged at night, especially between 2000h and 1000h.

The optimum outer leaf thickness of a cavity is from 0.10m to 0.15m.

The west is the best azimuth for a sun-warmed cavity at low latitudes.

CHAPTER EIGHT

CONCLUSIONS AND SUGGESTIONS FOR FURTHER WORK

8.1 Conclusions

This study suggests that thermal comfort can be improved by using a sun-warmed cavity to promote ventilation during the night.

The experimental work played an important role in finding the rate of ventilation provided by a heated cavity and in identifying the optimum dimensions for an effective cavity. It was shown that a warm layer developed over each heated surface and when these layers interacted the air flow was almost entirely upwards through the cavity which was desirable. When the layers were discrete with no overlapping, there was down flow in the central section which decreased the rate of air flow through the room. For a 2m high cavity and an inlet height of 0.1m, the optimum cavity width was about 0.2m. With higher cavities the optimum width would be wider.

Smoke was used to trace the upward and downward air flows in the cavity and to determine the boundary layer thickness. It also enabled the air flow patterns in the room to the cavity to be traced. The smoke showed that the air flows mainly in a stream line manner through the room into the cavity and that there is no reverse flow from the cavity into the room.

The experimental results also showed that for a temperature difference of $5\,K$ between the cavity surface and incoming air, a mass flow rate of about $0.043\ kg/ms$ could be achieved. This values would be three times greater if the cavity were 3m long. The air velocity achieved by this mass flow rate is in the order of $0.18\ m/s$ up the cavity. Such a velocity would reduce the resultant temperature to a comfortable region. For example,

with a mean radiant temperature of 37 $°C$ and ambient air at 28 $°C$, at an air velocity of 0.18m/s the resultant temperature would be about 32 $°C$ which, according to authorative literature is quiet comfortable for people acclimatised to a hot climate.

The dynamic model that was used enabled the response of the whole system under changing climatic conditions to be studied. Although it was simple, it allowed some design parameters to be determined which could not be established by the experimental technique such as; the optimum azimuth, the best thickness for the external wall of the cavity and the amount of air flow under unsteady conditions.

The model showed that, just north of the equator, west was the best aspect for a sun-warmed cavity. At such a location longer periods of horizontal solar radiation are received on east and west walls than on the south. Near the equator the sun's elevation is high, so that facing south its horizontal component is relatively small for most of the time. Therefore, if a sun-warmed cavity or "solar chimney" is to be used to induce evening ventilation in buildings in low latitudes, its best location is on a west wall. Such positioning also reduces the length of heat storage time required before the cavity is opened.

Results from the dynamic model also showed that the optimum thickness of the outer leaf is between 0.1m and 0.15m. If the outer leaf of the cavity is thicker more heat can be stored, but this would result in the decline of the cavity mean air temperature. If thinner less heat can be stored and the cavity life would be shorter.

The model predicted that for a typical room in a hot climate, with a cavity facing west, a maximum ventilation rate of 0.07 kg/s could be obtained with a 1m long and 3m high cavity. An average value would be 0.035 kg/s over the time the cavity was opened, this being equivalent to 4 air change per hour and an air speed across the room of 0.15m/s. If the cavity were extended the full length of a wall, whilst operational, the flow rate would be three times greater with an average of 12 air changes per hour. This would induce air speed across the room of about 0.17m/s. Without the sun-warmed cavity, the resultant

temperature in the room would be in the range of 36-38 °C. With the cavity increasing the air speed across the room the resultant temperature would be reduced to between 32 and 36 °C which is comfortable.

When building a sun-warmed cavity on a dwelling in a hot climate, maximum ventilation will be achieved by following appropriate guide-lines such as:

a) orienting the cavity westward at low latitudes near the equator.

b) constructing long cavities so that more heat is stored. However, this may occasionally be an uneconomic use of materials and be impracticable.

c) optimising the width of the cavity to its height by the following relationship $W_{optimum} = (Z/10)$.

d) extending the inlet along the length of the cavity to maximise air entry.

e) constructing the outer (wall) 0.1m to 0.15m thick.

In the study, it was shown that a sun-warmed cavity can be a useful means of improving thermal comfort in a room. However, there may be some disadvantages such as:

-in multistory buildings, the warm air within the cavity might be prevented from rising by stack effect due to opposing wind conditions.

-the cavity may permit entry of dust and insects.

-maintenance difficulties.

-additional cost building the cavity.

-increasing floor area.

8.2 Suggestions for further work

During this study it became apparent that further areas require investigating. The following work is suggested:

-On site construction of a solar warmed cavity to establish how practical the design is and how effective it is under actual climatic conditions and other parameters that might affect its performance such as the effect of wind and occupancy.

-More analysis and observations of the air flow mechanisms at the bottom of the cavity. It is not clear how air flows when it turns at right angles at the entry to the cavity and what paths it follows. Such knowledge will assist in the design of more efficient entry details.

-The sun-warmed cavity can be used for purposes other than ventilation. One application is to make the air flow over wet surfaces to make it cooler. This however increases its relative humidity. It is not clear how efficient such a process is and consequently requires further study. Another application for the use of the sun-warmed cavity is the drying of agricultural products. Drying such, using high solar radiation only without sufficient air movement tends to over-dry them. It is of interest to study the practicability of such a design to reduce the problem.

REFERENCES

Akbarzadeh, A., Charters, W.W.S. and Lesslie, D.A. 1982. Thermo-circulation characteristics of Trombe wall passive test cell. *Solar energy*, vol. 28, No. 6, pp. 461-468.

Alamdari, F. and Hammond, G. P. 1983. Improved data correlations for buoyancy-driven convection in rooms. *BSER & T*, vol. 4, no. 3, pp. 106-12.

ASHRAE. 1985. Handbook of Fundamentals. *American Society of Heating Refrigerating and Air-conditioning Engineers*. Atlanta, GA, U.S.A.

Bahadori, M.N. 1978. Passive cooling systems in Iranian architecture. *Scientific American*, vol. 238, pp. 144-154.

Bahadori, M.N. 1979. *Natural cooling in hot arid regions*. Solar Energy in Buildings, A. A. Sayigh, editor, Academic Press, New York, pp. 198-225.

Bahadori, M.N. 1981. Pressure coefficients to evaluate air flow patterns in wind towers. *Proc. Int. Passive and Hybrid Cooling Conf.*, vol. I, Miami beach, Fla. International Solar Energy Society, pp. 206-210.

Bahadori, M.N. 1985. An improved design of wind towers for natural ventilation and passive cooling. *Solar Energy*, vol. 35, No. 2, pp. 119-129.

Balcomb, J.D., Hedstorm, J.C. and MacFarland, R.D. 1977. *Passive solar heating of buildings*, Los Alamos Scientific Laboratory Rep. LA-UR 77-1162.

Batchelor G.K. 1954. Heat transfer by free convection across a closed cavity between vertical boundaries at different temperatures. *Quarterly of applied mathematics*, vol. 12, No. 3, pp. 209-233.

Bedford, T. 1936. *The warmth factor in comfort at work*. Medical Research Council, Industrial Health Research Board, Report No. 76.

B.R.E. 1973. *British Research Establishement.* Digest No. 60, 2nd Series, pp. 1-7.

B.R.E. 1978. *British Research Establishement.* Digest No. 210, pp. 1-7.

British Standard 1974. B.S. 4937 part 5. International thermocouple reference tables.

Chandra, S. and Keresteciogiu, A.A. 1984. Heat transfer in naturally ventilated rooms: data from full-scale measurements. *ASHRAE Transactions*, part 1b, pp. 211-225.

CIBSE 1986. *CIBSE Guide Volume A.* Chartered Institution of Building Services Engineer, London.

Clarke, J. A. 1978. The effect of space and time steps in finite difference computations of building energy flow. *ABACUS Occasional paper*, Glasgow: University of Strathclyde.

Clarke, J. A. 1985. *Energy simulation in building design.* Adam Higher Ltd. Bristol and Boston.

Colwell, R.G. and Welty, J.R. 1973. An experimental study of natural convection with low Prandtl number fluids in vertical channel with uniform wall heat flux. *ASME paper, 14th Heat transfer conference*, held Atlantia, GA, USA, pp. 1-8.

Davies, M.G. 1974. Presentation of environmental temperature in a room. *Building Services Engineering*, vol. 41 pp. 246-249.

Davies, M.G. 1978. On the basis of environmental temperature. *Building Science*, vol. 13 pp. 29-46.

Daws, L.F. 1966. Heat transfer and condensation in domestic boiler chimneys. *National Building Studies*, Research Paper No.40, HMSO, London.

deGraaf, J.G.A. and van der Held, E.F.M. 1953. The relation between the heat transfer and the convection phenomena in enclosed plane layers. *Applied Scientific Research*, second A, vol. 3, pp. 393.

Eckert, E.R.G. and Jackson, T.W. 1950. *NACA Tech. Note*, 2207.

Eckert, E.R.G. and Carlson, W.O. 1961. *Int. J. Heat Mass Transfer, vol 2, p. 106.*

Elenbaas, W. 1948. Dissipation of heat by free convection. Part I and II, *Philips Research Report 3*, N. V. Philips' Gloeilampen Fabrieken, Eindhoben, Netherlands, pp. 338-360 and 450-465.

Emery, E. and Chu, N.C. 1965. Heat transfers across vertical layers. *Trans. Am. Soc. Mech. Engrs*, vol. 87, pp. 110-116.

Evans, M. 1980. *Housing climate and comfort.* The Architectural Press, London Halsted press division John Wiley and Sons, New York.

Fanger, P.O. 1979. *Thermal comfort.*

Fox, L.L. and Whittaker, D. 1957. Ventilation due to open fires. *J. Inst. Heat. Vent. Engrs*, vol. 25, pp. 123-134.

Golany, G. 1980. *Housing in Arid Lands, Design and Planning.* The Architectural Press Ltd, London.

Gupta, C.L., Spencer, J.W. and Muncey R.W.R. 1970. A conceptual survey of computer-oriented thermal calculation methods. *Proc. Second Int. Symp. on Use of Computers for Environmental Enging Related to Buildings, Paris.* Building Science series 39, 4.

Haisley, R.J. 1981. Solar chimney theory: Basic precepts. *Proc. Of the Int. Passive and Hybrid Cooling Conference*, Miami Beach, Fla. pp. 211-215.

Holm, D. 1983. *Energy conservation in hot climates.* The Architectural Press: London.

Holwell, J. R. 1982. *Radiation Configuration Factors.* McGraw-Hill Book Company. New York.

I.H.V.E. 1970. Guide Book A Design Data. *Institution of Heating and Ventilating Engineers*. London.

Jakob, M. (1946). Free heat convection through enclosed plane gas layers. *Trans. ASME*, vol. 68, p. 180.

Jakob, M. 1949. *Heat transfer*. Jhon Wiley & Sons, Inc., New York.

Klauss, A.K., Tull R.H., Roots, L.M. and Pfafflin, J.R. 1970. History of the Changing Concepts in Ventilation Requirements. *ASHRAE Journal*, vol. 12, No 6, pp. 51-55.

Kronvall, J. 1980(a). *Air flows in building components*. Division of Building Technology, Lund Institute of Technology, Lund Sweden.

Kronvall, J. 1980(b). *Airtightness- measurements and measurement methods*. Swedish Council for Building Research, Stockholm, Sweden.

Liddament, M.W. 1986. *Air infiltration calculation techniques - An application guide*. Air Infiltration and Ventilation Centre, Bracknell, U.K.

Loudon, A.G. 1970. Summertime temperature in building without air conditioning. *Journal of Institution of Heating and Ventilating Engineers*, vol. 37 pp. 280-292.

Koenigsberger, O.H., Ingersoll, T.G., Mayhew, A., and Szokolay, S.V. 1974. *Manual of tropical housing and building; Climatic design*. Longman group Ltd, London.

Kreith, F. 1973. *Principles of Heat transfer*. Intext Educational Publishers, New York.

Kusuda, T. 1976. Computer programs for heating and cooling loads in buildings. Building Environment Division National Bureau of Standard Washington D.C. U.S.A.

MacGregor, R.K. and Emery, A.F. 1969. Free convection through vertical plane layers-Moderate and high Prandtl number fluids. *Journal of Heat Transfer*, vol. 91 pp. 391-403.

Markus, T.A. and Morris, E.N. 1980. *Building, Climate and Energy*. Pitman Publishing Ltd, London.

McAdams, W.H. 1954. *Heat transmission*. McGraw-Hill Publishing Co. Ltd. New York.

Missenard, A. 1933. Etude physiologique et technique de la ventilation. Librairie de l'Enseignement Technique, Paris.

Mitalas, G.P. 1965. An assessment of common assumption in estimating cooling loads and space temperatures. *ASHRAE Transactions*, vol. 71(2) p. 72.

Stephenson, D.G. and Mitalas, G.P. 1967(a). Cooling load calculations by thermal response factor. *ASHRAE Transactions*, vol. 73 (III) pp. 1.1-1.7.

Mitalas, G.P. and Stephenson, D.G. 1967(b). Room thermal response factors. *ASHRAE Transactions*, vol. 73 (III) pp. 2.1-2.10.

Mohsen, M.A. 1979. Solar radiation and courtyard house forms. I. A mathematical model. *Building and Environment*, vol. 14, pp. 75-82.

Nicol, J.F. 1975. An analysis of some observations of thermal comfort in Roorkee India and Baghdad Iraq. *Building Research Establishment*, Garston Watford U.K.

Nusselt, W. and Jurges, W. 1922. Die Kuhlung einer ebenen Wand durch einen Luftstrom. *Gesundh Ingenieur.*

O.N.M, Office National de la Meteorologie, B.P. 153 Dar-El-Beida, Alger.

Olgyay, V. 1963. *Design with climate - Bioclimatic approach to architectural regionalism.* Princeton University Press, Princeton, New Jersey.

Orlouski, H. 1979. Thermal chimneys and natural ventilation. Earth covered buildings: *Technical notes.*

Oscar, F. and Kell, J.R. 1979. *Heating and Air Conditioning of Buildings*. The architectural Press, London.

Page, D.E.W and Cheyney, B.S 1981. Flues and Chimneys. *Dom. Heat. Air Condit.*, vol.14, pp. 2-6.

Pratt, R.G.and Karaki, S. 1979. Natural convection between vertical plates with external losses - Application to Trombe walls. *Proc. 3rd National Passive Solar Conferences*, San Jose, CA, US, pp. 61-66.

Rohsenow, W.M. and Choi H.Y. 1961. *Heat mass and momentum transfer*. Prenctice-Hall International, London, 1961.

Ryan, B.A. and Mara, D. 1983. TAG technical note No.6, The World Bank, Washington.

Schmitt, L.B. and Engdahl, R.B. 1948. Performance of residential chimneys. *Heating Piping and Air-Conditioning*, vol. 20(11),PP. 111-118.

Tredgold, T. 1836. *The principle of warming and ventilation public buildings*. M. Taylor. London.

Taytlor, J.R. 1982. *An introduction to error analysis*. U.S.A., Oxford University Press.

van Straaten, J.F. 1967. *Thermal performance of buildings*. Elsevier.

Warner C. Y. and Arpaci V. S. 1968. An experimental investigation of turbulent natural convection in air at low pressure along a vertical heated flat plate. *Int. J. Heat Mass Transfer*, vol.11, pp. 397-406.

Waters, J.R. 1977. *The derivation and experimental verification of a computer aided thermal design method for buildings*. PhD Thesis, Lanchaster Polytechnic.

Webb, C.G. 1964. Thermal discomfort in a tropical environment. *Nature*, 202, 1193-1194.

Winslow, C.E.A., Gagge, A.P. and Herrington, L.P. 1939. The influence of air movement upon heat losses from the clothed human body. *J. Physiol*, 127: 505-518.

Wong, H.Y. 1977. *Hand book of essential formulae and data on Heat transfer for engineers*. Longman Group Ltd London.

Yaglou, C.P. and Whitheridge, W.N. 1937. Ventilation requirements. *ASHVE Transactions*, Part 2, vol. 43, pp. 423-436.

Yagoubi, M.A. and Golneshan, A.A. (1986). Passive cooling of an underground room (Sardab). *Iranean Journal of Science & Technology*. vol. 10, No. 1&2, Shiraz, Iran.

Zambrano, W. and Alvarado, S. 1984. Design construction and testing of a chimney that reduces dangerous temperatures in a radiative convective solar dryer. *Solar Energy*, vol. 32, No 5, pp. 581-584.

APPENDIX 1

Climatic data for El-Oued (33.3 °N) from 1971 to 1981

Table A1.1 Monthly mean hourly outside air temperature °C

	Hours							
	0	3	6	9	12	15	18	21
Jan.	7.59	6.90	5.98	9.37	14.33	16.07	12.17	9.28
Feb.	10.36	9.00	8.07	12.10	16.92	18.43	15.27	11.94
Mar.	12.40	10.90	9.81	15.47	19.86	21.22	18.64	14.51
Apr.	15.94	14.08	13.32	19.39	23.49	25.07	23.02	18.42
Mai.	20.82	18.84	18.60	24.50	28.89	30.67	29.09	23.95
Jun.	26.09	23.47	22.00	29.36	34.42	36.78	35.11	29.45
Jul.	28.89	26.14	25.58	32.25	37.54	39.65	38.27	32.07
Aug.	28.22	25.78	24.49	31.96	36.63	38.63	36.76	30.97
Sep.	24.51	22.61	21.47	27.76	32.32	33.87	31.14	26.60
Oct.	17.84	16.16	15.01	21.23	25.72	26.03	22.39	19.65
Nov.	11.41	10.15	9.06	14.40	19.12	20.12	15.78	12.86
Dec.	8.08	6.98	6.17	10.07	15.38	16.55	11.92	9.33

Table A1.2 Monthly mean hourly relative humidity %

	Hours							
Month	0	3	6	9	12	15	18	21
Jan.	74.98	78.55	81.96	69.93	51.01	45.91	61.97	70.99
Feb.	66.33	70.89	74.44	57.89	43.18	41.31	51.84	58.02
Mar.	59.74	64.73	68.46	48.04	35.09	30.75	40.39	51.81
Apr.	53.62	59.03	63.16	42.66	32.29	27.59	32.66	43.92
Mai.	46.13	55.14	57.22	38.44	28.20	24.13	27.02	37.56
Jun.	40.96	49.65	52.45	34.06	24.46	19.95	21.90	32.46
Jul.	36.09	46.34	50.76	32.28	22.31	18.41	20.18	29.01
Aug.	39.38	48.88	53.83	34.38	24.19	19.64	22.69	32.82
Sep.	51.42	60.71	66.67	44.64	33.16	27.78	33.41	43.35
Oct.	59.99	66.02	70.65	50.33	37.69	33.53	44.33	53.41
Nov.	71.84	76.77	79.36	60.33	45.01	41.35	55.09	65.70
Dec.	77.01	80.21	82.24	68.00	49.93	46.88	65.44	72.68

Table A1.3 Monthly mean hourly air speed *m/s*

	Hours							
	0	3	6	9	12	15	18	21
Jan.	2.68	2.83	2.69	3.29	4.29	4.10	2.00	2.27
Feb.	3.32	3.30	3.26	4.43	5.44	5.21	2.69	2.87
Mar.	3.55	3.48	3.44	5.11	5.53	5.53	3.46	3.26
Apr.	4.36	4.22	4.26	6.05	6.15	6.30	4.83	4.23
Mai.	4.25	4.31	4.24	5.71	5.49	5.24	4.24	3.81
Jun.	4.88	4.72	4.81	6.03	5.53	5.20	4.62	4.57
Jul.	4.14	4.07	4.16	5.56	5.01	4.26	3.30	3.01
Aug.	3.73	3.72	3.59	5.14	4.60	3.96	2.97	2.69
Sep.	3.27	3.34	3.06	4.94	4.45	4.04	2.57	2.82
Oct.	2.61	2.56	2.45	4.16	4.54	4.20	2.22	2.30
Nov.	2.22	2.16	2.14	3.12	3.77	3.53	1.74	1.97
Dec.	2.37	2.38	2.42	2.93	3.97	3.74	2.01	2.13

Table A1.4 Monthly mean temperature of the air °C

	Minimum	Maximum	Mean	21st of the month
Jan.	5.1	16.7	10.9	10.8
Feb.	7.2	19.2	13.2	12.7
Mar.	9.2	22.0	15.6	16.0
Apr.	12.6	25.9	19.2	19.2
Mai.	18.8	29.9	24.3	25.0
Jun.	22.0	37.5	29.7	29.9
Jul.	24.5	40.3	32.5	33.0
Aug.	24.1	39.3	31.7	31.3
Sep.	21.0	34.6	27.8	27.8
Oct.	14.5	27.5	21.0	21.0
Nov.	8.5	20.9	14.7	14.6
Dec.	5.4	17.2	11.3	11.2
Yearly mean	14.4	27.6	21.0	21.0

Table A1.5 Monthly mean relative humidity and hours of insolation

	Relative humidity %			Hours of insolation
	Minimum	Maximum	Mean	Hours
Jan.	42.7	87.2	64.9	7.3
Feb.	37.4	80.0	58.7	7.9
Mar.	27.3	74.7	51.0	8.5
Apr.	24.4	68.6	46.5	8.9
Mai.	21.3	63.9	42.6	10.4
Jun.	17.7	56.8	37.2	11.0
Jul.	16.5	55.1	35.8	12.0
Aug.	18.1	57.5	37.8	11.2
Sep.	25.6	70.1	47.8	9.7
Oct.	30.9	74.8	52.8	8.7
Nov.	38.0	84.3	61.1	8.1
Dec.	43.6	87.6	65.6	7.5
Yearly mean	28.6	71.7	50.1	9.3

Table A1.6 Monthly air speed and atmospheric pressure

	Mean air speed (m/s)	Atmospheric Pressure (Pa)
Jan.	3.0	101170
Feb.	3.8	100910
Mar.	4.1	100710
Apr.	5.0	100550
Mai.	4.7	100500
Jun.	5.0	100440
Jul.	4.2	100540
Aug.	3.8	90510
Sep.	3.5	100730
Oct.	3.1	100880
Nov.	2.6	101160
Dec.	2.7	101270

Table A1.7 Percentage of yearly wind speeds from 1975 to 1984

Wind speed (m/s)	Orientations							
	N	NE	E	SE	S	SW	W	NW
1-5	9.2	7.7	9.8	3.0	8.8	8.8	7.8	5.6
6-10	12.7	3.6	5.2	1.4	2.4	2.1	2.7	2.7
11-15	10.2	0.2	0.4	0.0	0.2	0.2	0.3	0.3
>15	10.0	0.0	0.0	0.0	0.0	0.0	0.0	0.0
Calm	15%							

APPENDIX 2

Calibration of the AVM 502 probe

Table A2.1 Temperature calibration

Thermometer (°C)	Temperature measured by the AVM (°C)	Corresponding voltage (*volts*)
2.8	2.0	0.2
15.1	14.6	1.46
19.2	19.4	1.94
27.0	27.3	2.73
32.0	32.4	3.24
49.0	48.0	4.8

Table A2.2 Velocity calibration

Velocity reference (*m/s*)	Velocity measured by the AVM (*m/s*)	Corresponding voltage (*volts*)
5.0	5.20	6.00
4.0	4.10	5.47
3.0	3.00	4.88
2.0	1.98	4.09
1.0	0.98	3.00
0.9	0.85	2.84
0.8	0.75	2.67
0.7	0.66	2.48
0.6	0.57	2.28
0.5	0.50	2.06
0.4	0.40	1.79
0.3	0.30	1.48
0.2	0.19	1.07

APPENDIX 3

PASSIVE SOLAR INDUCED VENTILATION

8th Miami Int. Conference on
Alternative Energy Sources,
1987, Miami Beach.

A Bouchair, D Fitzgerald and J A Tinker
Department of Civil Engineering
University of Leeds
Leeds LS2 9JT
England

ABSTRACT

Cooling ventilation within a building may be promoted by exploiting the buoyancy of hot air within a sun-warmed cavity or 'solar chimney' added to a building on the sunward side. The chimney may be constructed from brick, concrete or any other building material of high thermal capacity.
Heat stored within the walls forming the cavity eventually transfers to the air within and promotes movement of the air by stack effect.
The cavity is closed at the top and bottom by a damper. These, when opened, allow the hot air contained within to rise, drawing cooler outside air into the building to promote cooling ventilation. This process continues until the energy stored within the fabric of the walls is exhausted.
Observations confirm that air movement may be improved to a satisfactory standard by the method proposed. The work is continuing.

1. INTRODUCTION

Building practice in hot climates generally incorporates some form of space cooling. Especially popular is evaporative cooling using fountains or water sprinkled upon blinds and floors. Air movement is also used as a mode of cooling, and is promoted using courtyard spaces and wind towers. Basements are frequently occupied during the daytime because of their coolness [1,2,3].

It is known that in some areas of the world such as Algeria, outside air is so hot during the day that cooling by natural ventilation provides little benefit until the evening. A solar warmed cavity or 'chimney' constructed from stone, concrete or any other suitable high thermal capacity material added to a building on the sunward side will help promote such ventilation. The 'chimney' is sealed at the top and bottom throughout the day during which time it is passively heated. In the evening the dampers are opened. The warm air within the chimney rises by stack effect which in turn encourages the now cool outside air into the building to promote cooling by ventilation. The process is continuous, relying upon the thermal energy stored by the thermal capacity of the chimney walls. The advantages of the technique is that air can be encouraged to move more than "naturally" without the use of electricity which, in low-cost housing, is often not available.

Experimental investigations on the performance of several 'chimney' configurations have been undertaken. The effect of chimney width on the rate of air movement has been studied and results were compared against theoretically derived values.

2. THEORETICAL MODEL

A mathematical model has been developed to study and predict the rate of air flow caused by the buoyancy pressure within a solar chimney. The results from this have been compared with experimental data. We are concerned with air flow and heat flow.

2.1 Air Flow

Driving pressure: The buoyancy pressure that encourages air to rise up a chimney is caused by the difference in density between the air in the chimney and that outside. It may be expressed by the general equation for stack effect as follows:

$$P_b = g\ Z\ (\rho o - \rho i) \qquad (1)$$

where:

P_b = buoyancy pressure difference (Pa)
g = gravitational acceleration (9.81m/s^2)
Z = height of the solar chimney (m)
ρo = density of outside air (kg/m^3)
ρi = density of air within the chimney (kg/m^3)

ρo and ρi are given by:

$$\rho o = Pat/287\ (To+273) \qquad (2)$$
$$\rho i = Pat/287\ (Ti+273) \qquad (3)$$

where:

Pat = atmospheric pressure at the locality (Pa)
To = temperature of the outside air (^{0}C)
Ti = temperature of the air within the chimney (^{0}C)

Because densities are dependent on atmospheric pressure it is important to note that if we have a very tall chimney where air at the inlet is subjected to high pressure and that at the outlet to a lower pressure then this will cause air to flow without the use of solar heat.

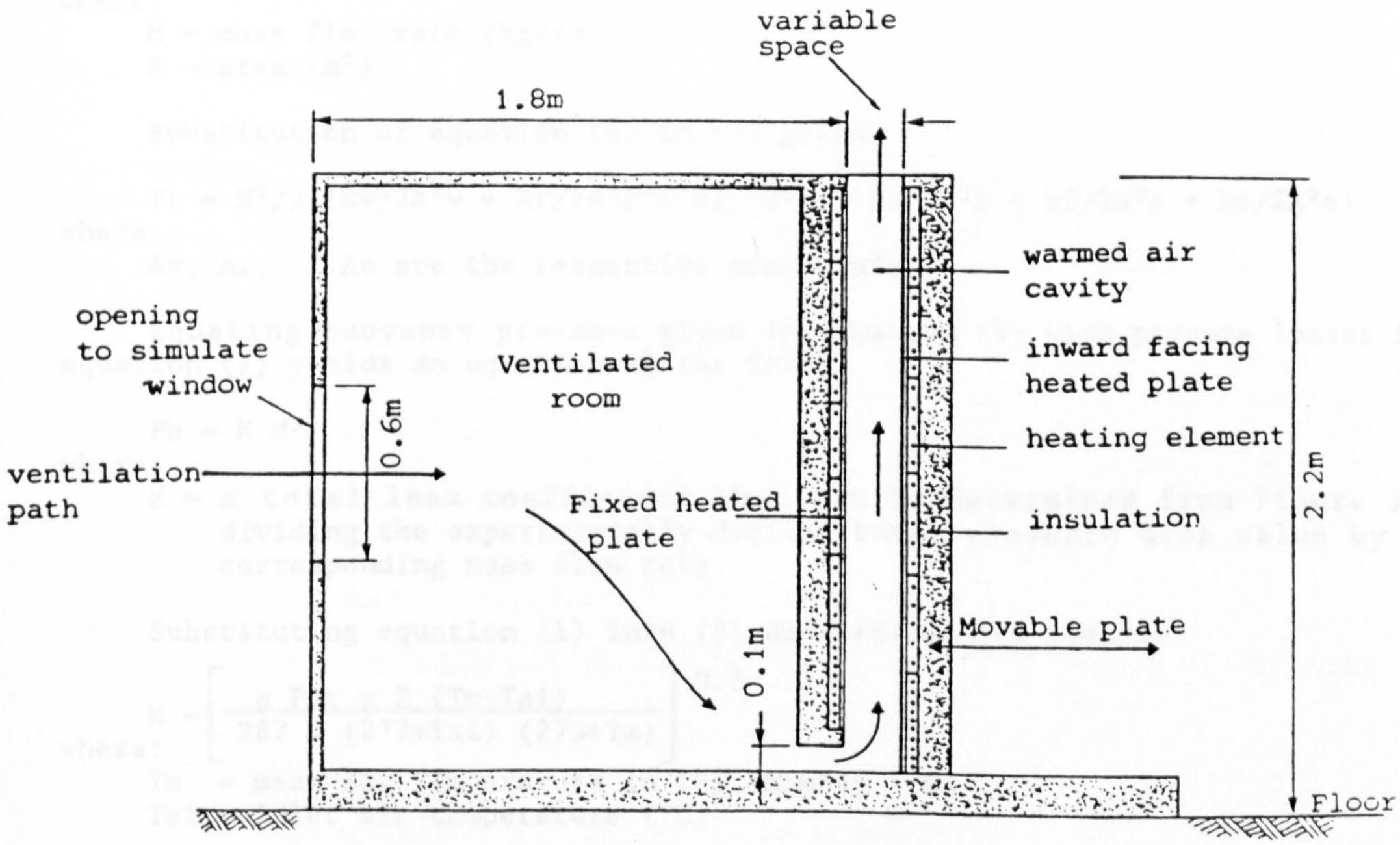

Fig 1 Vertical section through experimental rig

Pressure losses: As air flows through a sytem it is subjected to pressure losses due to contractions, expansions, bends, friction etc. Assuming a constant air density throughout the system then the total pressure loss in a typical configuration as shown in Figure 1, may be expressed as:

$$Pt = Pw + Pr + Pi + Pb + Pf + Pe \quad (4)$$

where

Pt = the total pressure drop (Pa)
Pw = pressure drop at the window of the room (Pa)
Pr = pressure drop across the room due to sudden expansion (Pa)
Pi = pressure drop at the inlet (Pa)
Pb = pressure drop due to the bend (Pa)
Pf = pressure drop due to friction (Pa)
Pe = pressure drop at the exit (Pa)

Pressure losses may be expressed in terms of velocity pressures by general equation of the form:

$$\text{Pressure loss} = k\ \rho V^2/2$$

where:

k = pressure loss coefficient
ρ = density (kg/m^3)
V = air speed (m/s)

Hence equation (4) becomes:

$$Pt = kw\ \rho V^2w/2 + kr\ \rho(Vw-Vr)^2/2 + ki\ \rho V^2i/2 + kb\ \rho V^2b/2 + kf\ \rho V^2f/2 + ke\ \rho V^2e/2 \quad (5)$$

where:

kw, kr, ...ke are loss coefficients whose values depend on such variables as configuration and roughness.

Vw, Vr, ...Ve are the air velocities (m/s).

Equation (5) may be simplified by converting velocities to mass flow rates as follows:

$$M = \rho\ V\ A = \text{CONSTANT} \quad (6)$$

where:

M = mass flow rate (kg/s)
A = area (m^2)

Substitution of equation (6) in (5) gives:

$$Pt = M^2/\rho\ (kw/2A^2w + kr/2A^2r + ki/2A^2i + kb/2A^2b + kf/2A^2e + ke/2A^2e) \quad (7)$$

where:

Aw, Ar, ...Ae are the respective areas (m^2)

Equating buoyancy pressure given in equation (1) with prssure losses from equation (7) yields an equation of the form:

$$Pb = K\ M^2 \quad (8)$$

where:

K = a total loss coefficient that can be determined from Figure 2 by dividing the experimentally derived total pressure drop value by the corresponding mass flow rate.

Substituting equation (1) into (8) and rearranging yields:

$$M = \left[\frac{\rho\ Pat\ g\ Z\ (Tm-Tai)}{287\ K\ (273+Tai)\ (273+Tm)}\right]^{0.5} \quad (9)$$

where:

Tm = mean air temperature in the chimney (°C)
Tai = inlet air temperature (°C)

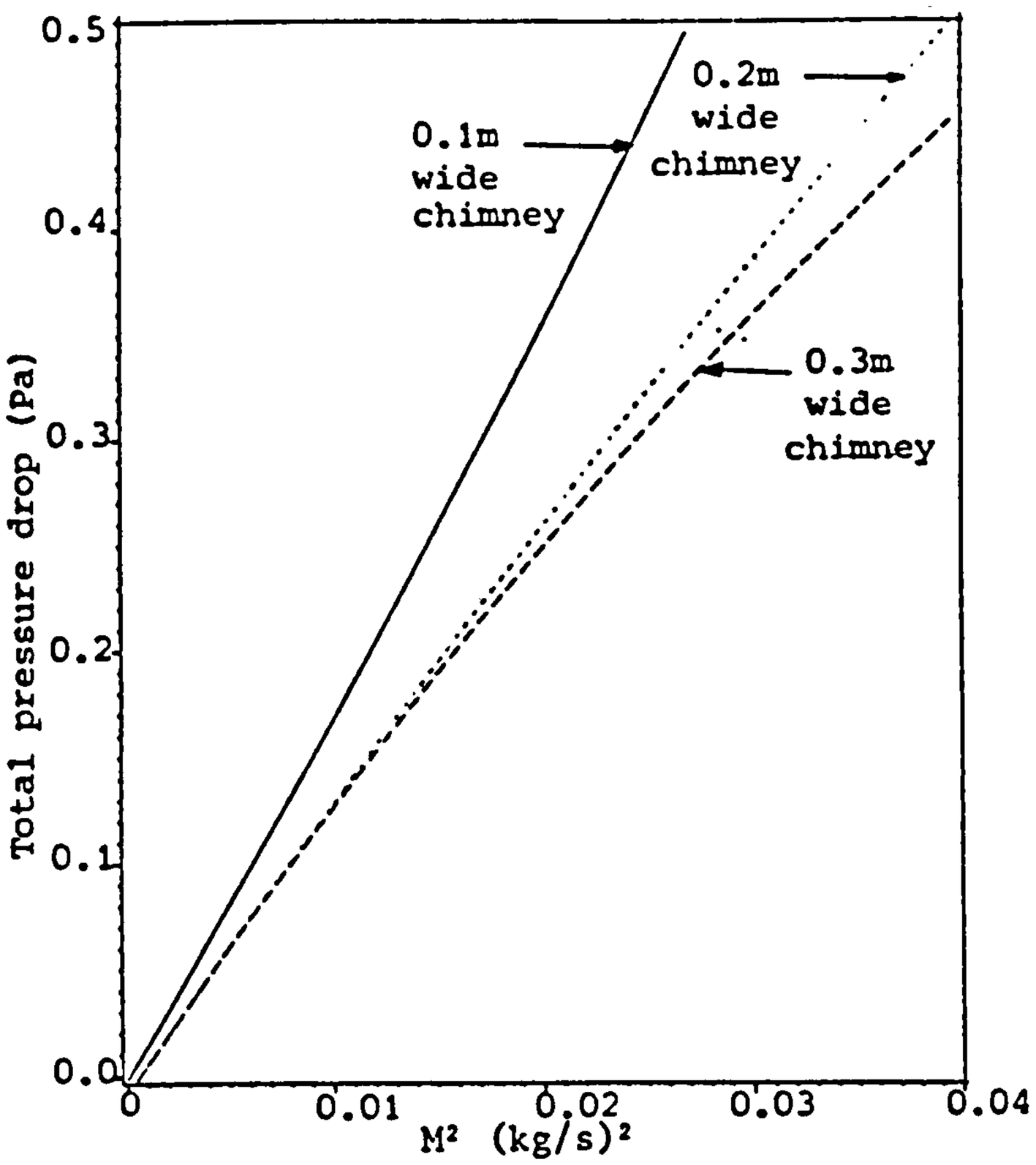

(For a chimney 1.5m long and 2m high)

Fig 2 Total pressure drop as a function of (mass flow rate)²

2.2 Heat Transfer

Modelling the process of heat transfer within the cavity of a solar chimney is complex. Problems arise when deciding whether the air flow is turbulent or laminar, or whether it is significantly affected by the roughness of the surfaces and the configuration of the system. In the model, heat transfer to the air was assumed to take place by turbulent natural convection from two vertical parallel plates.

Heat transfer coefficient: Reliable data on natural convection heat transfer coefficients was unavailable. Preliminary values were obtained from equations published by Warner [4] and McAdams [5] where the heat transfer coefficient hc depends on the temperature difference between mean surface temperature and air temperature inside the chimney. The coefficient comes from:

$$Nu = (hc\ Z/Ka) = C(Gr\ Pr)^{1/3} \qquad (10)$$

where:

C = constant which may take different values (0.1 according to Warner [4] and 0.13 according to McAdams [5])
Ka = thermal conductivity of the air (W/m K)
Nu = Nusselt number
Gr = Grashof number
Pr = Prandtl number for air which is about 0.7

It has been found experimentally that C may approach 0.3; this is approximately 3 times larger than the values found by others and may be attributable to the complexity of the system, roughness of the surfaces and the inlet and outlet configurations.

Mean air temperature inside chimney: In order to evaluate the mass flow rate from equation (9), the mean air temperature inside the chimney Tm, must be known. This may be determined by assuming an elemental strip of air dz within a chimney of height Z, width X and length Y (Figure 3).

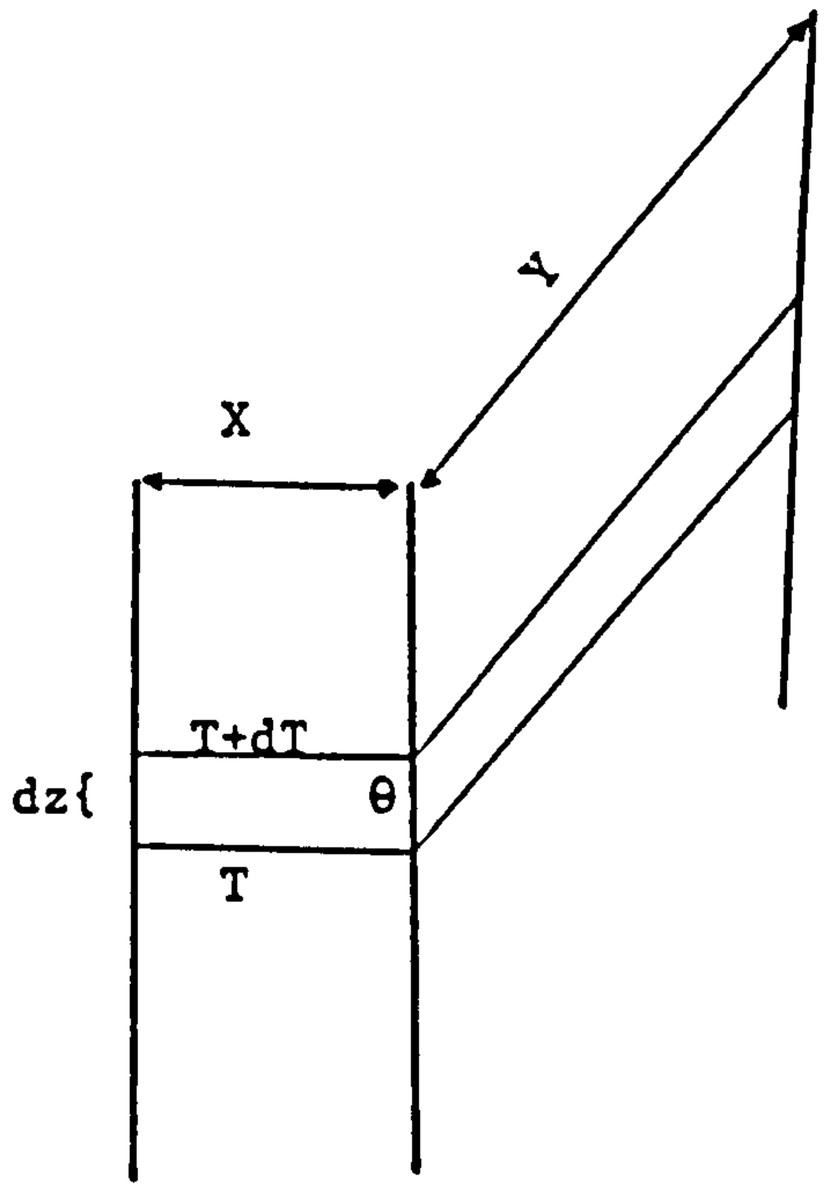

Fig 3 Schematic diagram of the elemental strip

A heat balance over the slice thickness dz of the chimney gives:

$$M\ C_p\ dT = 2(x+y)dz(\theta - T)hc$$

where:

M - mass flow (kg/sec)
C_p - specific heat capacity (J/kg K)
dT - temperature increase of air within the element (K)
θ - mean surface temperature of the element (^{0}C)
hc - confection heat transfer coefficient (W/m^2 ^{0}K)
T - mean air temperature of the element (^{0}C)

which (with room air temperature TAI) integrates to:

$$T - TAI = (\theta - TAI)\ (1-\exp(-az)) \quad (12)$$

whre:

$$a = 2(x+y)hc/M\ C_p \quad (13)$$

z - positional height up the chimney (m)

and the mean temperature Tm, of the rising air

$$Tm = \left(\frac{1}{Z}\right) \int_0^Z T \quad (14)$$

$$= \theta - (\theta - TAI)\ (1-\exp(-aZ))/aZ \quad (15)$$

It is in fact readily shown that T-TAI remains slightly small, so that the amount of heat removed from the chimney when air is flowing within it is small. This means that the chimney, as a means of causing air to flow, will work for a long time.

Boundary layer: In reality, heat transfer and air flow occur simultaneously within the boundary layers close to the wall surfaces. The thickness of the layer adjacent to a vertical wall in turbulent flow depends on the wall height and temperature difference between the surface and the air. The thickness of a boundary layer may be obtained from work published by Rohsenow et al.[6]:

$$Xb = 0.56(Gr)^{-0.1}Pr^{-8/15}[1+0.5\ Pr^{2/3}]^{0.1}Z \qquad (16)$$

where:

Xb = thickness of the boundary layer (m)

As Pr = 0.7, with little variation for air, equation (16) simplifies to

$Xb = 0.66\ Z\ Gr^{-0.1}$ giving

$$Xb = 0.08Z^{0.7}\ m$$

with a numerical value for the parameter of the Grashof number. If Z = 1.9m the optimum chimney width of 2Xb = 0.25m, indicating that if the chimney is over 0.25m wide, its centre contains air not taking part in the heat transfer and flow processes.

3. EXPERIMENTAL INVESTIGATION

3.1 Experimental Model

The experimental investigation was carried out under steady state conditions in a laboratory considered to be large enough to simulate a free atmospheric environment. The measuring section of the 'chimney' comprised two parallel walls. One, fixed in position on the room side, was 1.9m high by 1.5m wide, and one, movable, was 2.0m high by 1.5m wide. The area of the air inlet of the cavity remained constant at 0.1m high by 1.40m wide. The area of the room window was 0.5m wide by 0.6m high (see Figure 1). The walls forming the cavity were made of thin aluminium sheet textured with a layer of sand to provide a roughness similar to building materials such as bricks or concrete. The walls of the cavity were heated electrically and designed as isothermal surfaces. Their temperature was controlled.

The air speed through the window of the room and at the inlet and outlet of the chimney was measured using a calibrated thermistor anemometer accurate to (± 5%). The accuracy of such thermistors may be affected by radiation coming from the wall surfaces and surrounding sources of light. Such sources make the thermistor assume a higher temperature. To isolate the probe from the influence of any radiation source it was enclosed in an aluminium shield.

The surface temperatures of the 'chimney' were measured using calibrated copper-constantan thermocouples and air flow patterns were traced by injecting smoke into the air stream.

3.2 Experimental Results

The mass flow performance of the solar chimney was measured at widths varying from 0.1 to 0.5m. Results obtained are plotted in Figure 4 as a function of the temperature difference between the mean surface temperature of the chimney and the inlet air temperature.

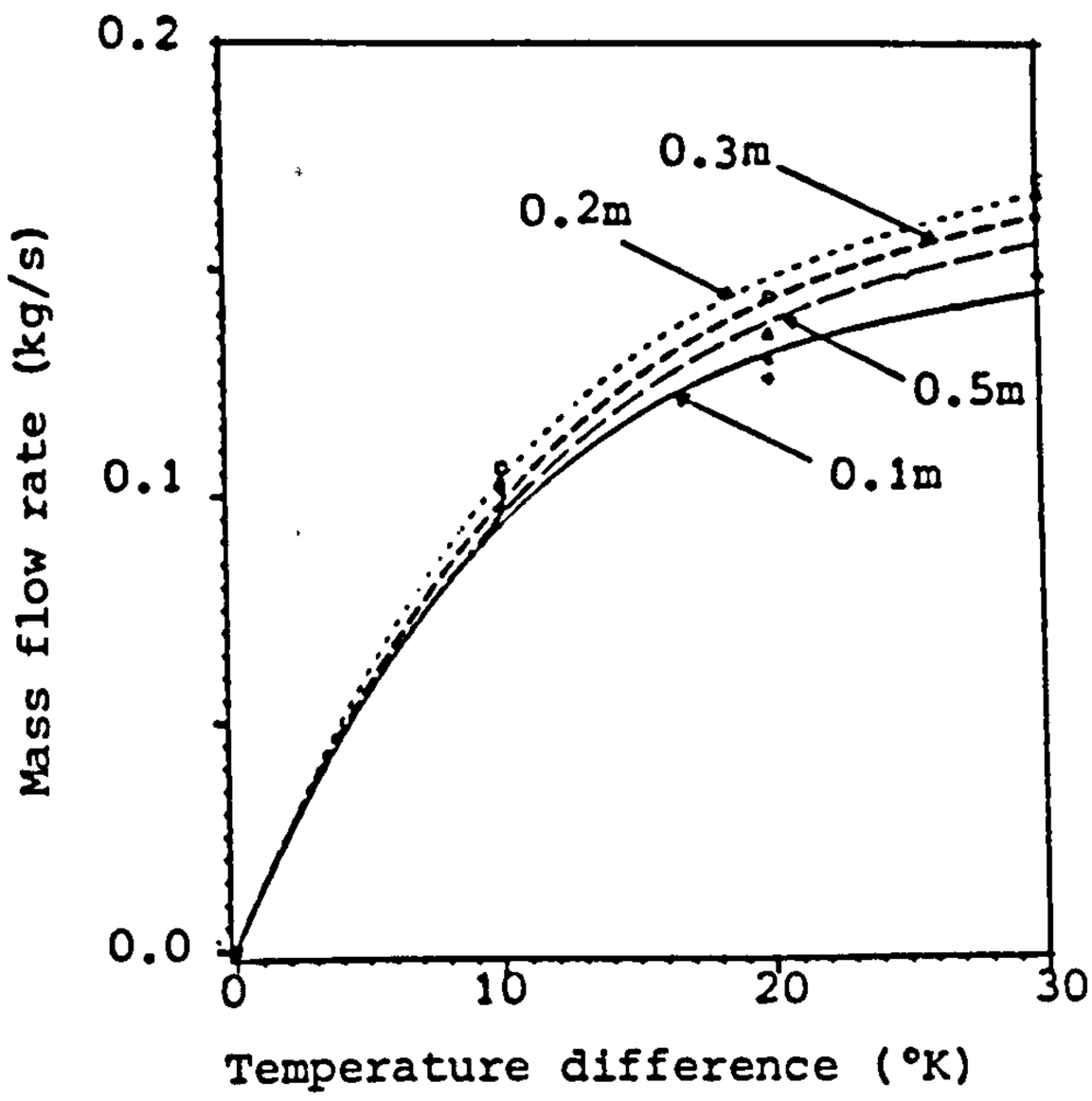

Fig 4 Variation of the mass flow rate with chimney width

Measurements obtained from the 0.1m and 0.2m wide cavity were compared against values predicted by the model (Figure 5).

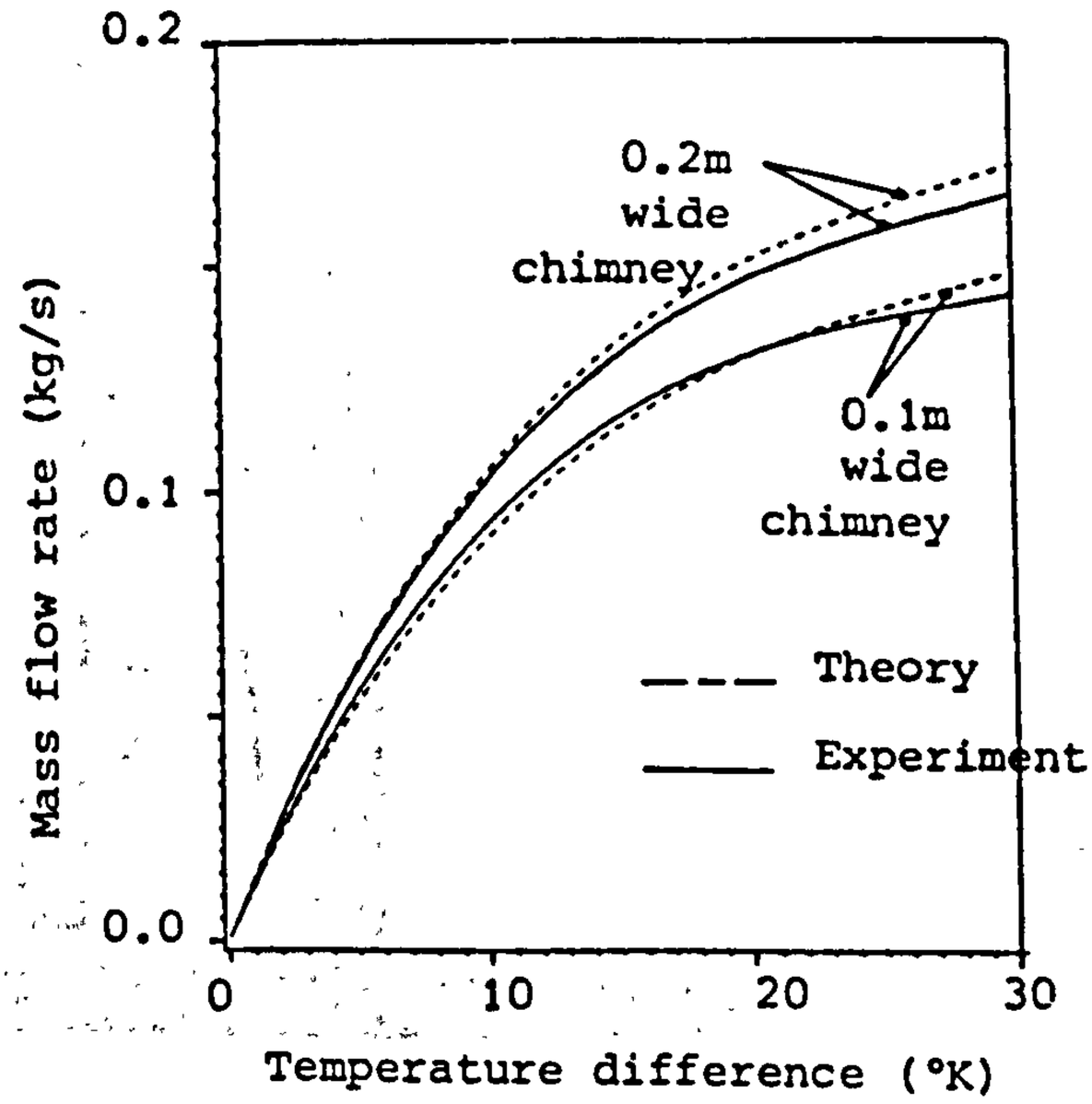

Fig 5 Comparison between experimental results and theoretical model

For the purpose of clarity other chimney widths have been omitted. As can be seen, results correlate reasonably well. The use of smoke as a tracer showed that in a 0.5m wide chimney the air flow was upwards on its faces and downward in the centre. Most of the air rising over the outward-facing plate was supplied from the downdraught in the centre of the chimney (see Figure 6).

With a 0.3m wide chimney, the flow was mostly upward, although the velocity in the central section was slower than over the surfaces. The total mass flow was greater than that obtained with the wider cavity. In a 0.2m wide chimney, the flow was slightly greater than in a 0.3m wide chimney, and was totally upwards. As the chimney width was narrowed to 0.1m wide the flow reduced. This was partly due to the increased pressure drop along the height.

Varying the mean air temperature in the chimney also affected the mass flow rate as can be seen in Figure 7.

Raising the air temperature from approximately 22 °C to 26 °C increased the mass flow by more than 50%. Unfortunately, to raise the air temperature by such a modest amount requires the surface temperature of the chimney to be increased 30K, as can be seen in Figure 8, where the mean air temperature in the chimney is plotted as a function of surface temperature.

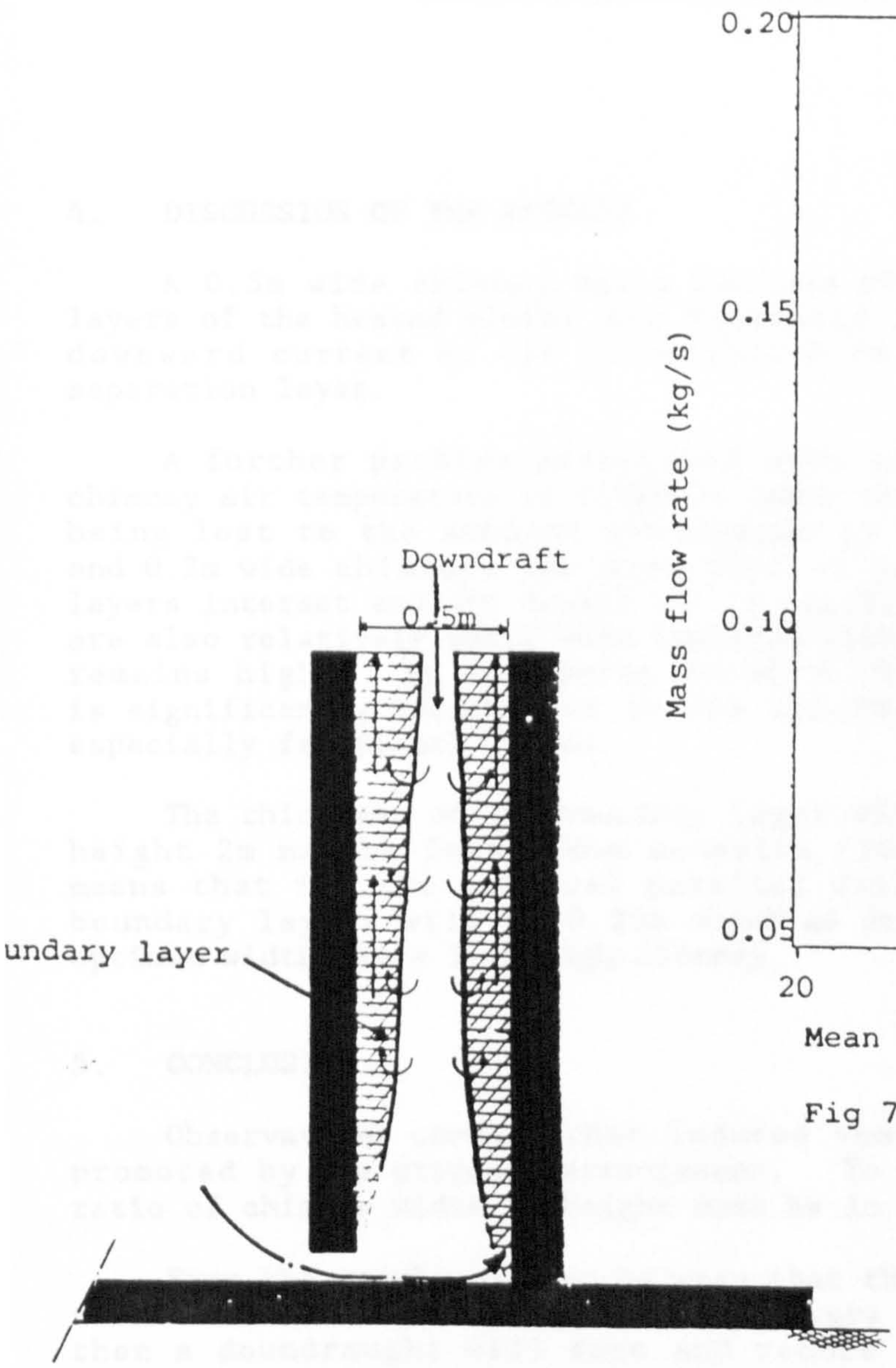

Fig 6 Convection paths within the chimney

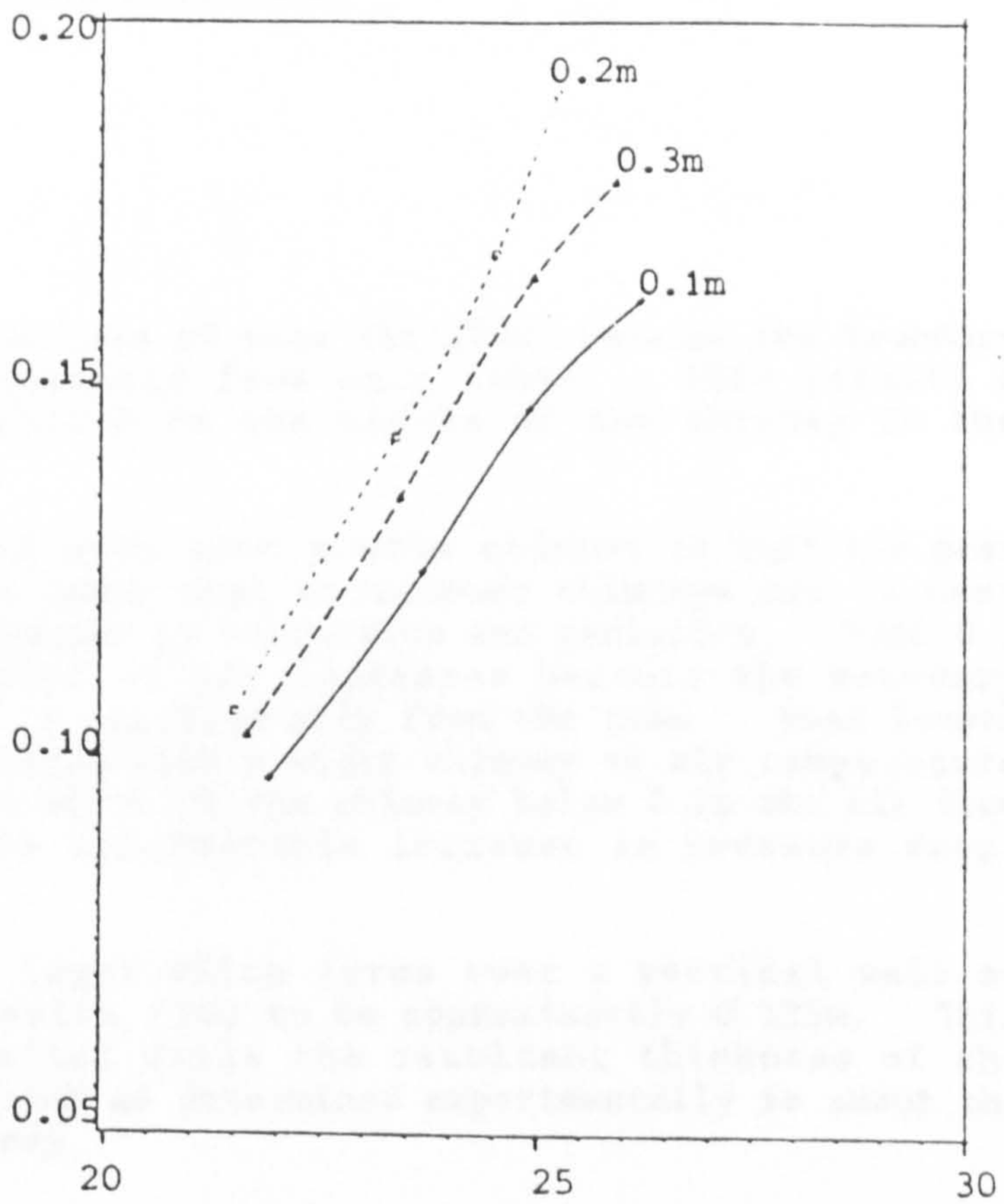

Fig 7 Mass flow rate plotted as a function of mean air temperature in chimney

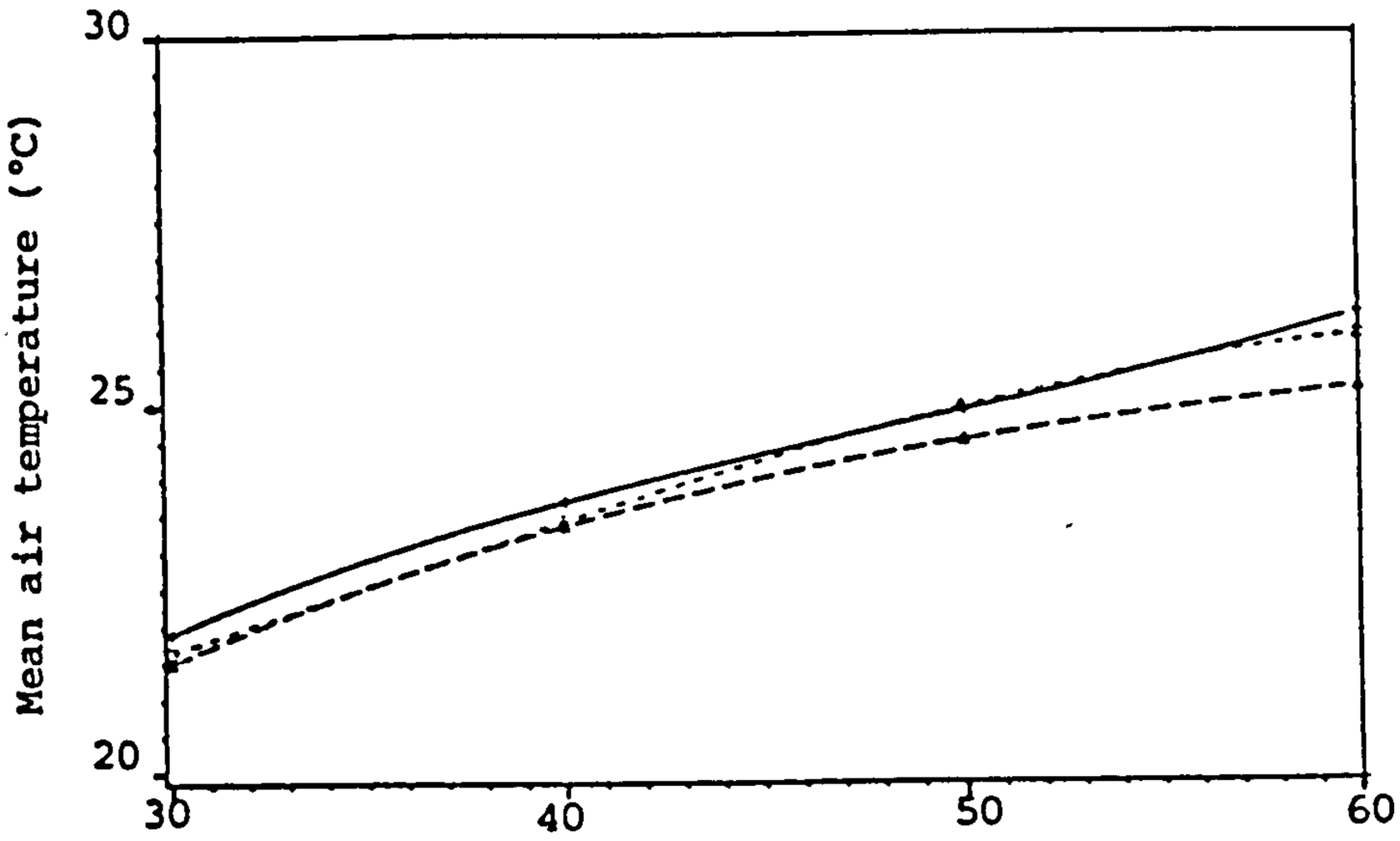

Fig 8 Mean air temperature in chimney as a function of surface temperature

4. DISCUSSION OF THE RESULTS

A 0.5m wide chimney has a low rate of mass air flow, because the boundary layers of the heated plates are separated from each other. This permits a downward current of air to establish in the middle of the chimney in the separation layer.

A further problem associated with such a wide chimney is that the mean chimney air temperature is slightly lower than in narrower chimneys due to heat being lost to the ambient environment by convection and radiation. With 0.3 and 0.2m wide chimneys the mass flow of air increases because the boundary layers interact and the upward air is supplied only from the room. Heat losses are also relatively small when compared with a wider chimney so air temperature remains high. By decreasing the width of the chimney below 0.1m the air flow is significantly reduced due to the considerable increase in pressure drop, especially frictional losses.

The thickness of the boundary layer which forms over a vertical wall of height 2m may be found from equation (16) to be approximately 0.125m. This means that for two vertical parallel walls the resultant thickness of the boundary layers will be 0.25m which as determined experimentally is about the optimum width for a 1.9m high chimney.

5. CONCLUSION

Observations confirm that induced ventilation within a building can be promoted by the proposed arrangement. To get optimum ventilative cooling, the ratio of chimney width to height must be in the correct proportions.

From the results it can be seen that the cavity width should not exceed the thickness of the sum of the boundary layers of the warmed walls. If it does, then a downdraught will form and reduce the rate of air movement through the room. Excessive heat losses also occur which reduce the effective stack

effect. If the cavity width is reduced too much then the frictional pressure losses increase and the mass flow is again reduced. Observation shows that for a cavity 1.9m high, the optimum width is somewhere between 0.2m and 0.3m.

The work has investigated a simple way of using the sun to move air for any purpose. Realising that a reliable way has been developed, work is now progressing to cool the incoming room air by a technique based on the evaporation of water.

6. REFERENCES

1. Allan, K., 'Design primer for hot climates', The Architectural Press Ltd., London, 1980.

2. Golany, G., 'Housing in Arid Lands, Design and Planning', The Architectural Press Ltd., London, 1980.

3. Bahadori, M.N., 'An improved design of wind tower for natural ventilation and passive cooling', Solar Energy, Vol.35, No.2, pp.119-129, 1985.

4. Warner, C.Y. and Arpaci, V.S., 'An experimental investigation of turbulent natural convection in air at low pressure along a vertical heated flat plate', Int. J. Heat Mass Transfer, Vol.11, pp.397-406, 1968.

5. McAdams, W.H., Heat Transmission, McGraw-Hill, New York, 1954.

6. Rohsenow, W.M., and Choi, H.Y., 'Heat, Mass and Momentum Transfer', Prentice-Hall, International, London, 1961.

APPENDIX 4

Energy and Buildings, *12* (1988) 135 - 140

The Optimum Azimuth for a Solar Chimney in Hot Climates

A. BOUCHAIR and D. FITZGERALD

Civil Engineering Department, University of Leeds, Leeds LS2 9JT (U.K.)

(Received April 24, 1987; accepted July 21, 1987; revised paper received April 22, 1988)

ABSTRACT

In a solar-heated chimney, used to promote air movement within a building, stored heat is the main source for warming air within the chimney. This creates a buoyancy pressure which draws air through the building. It is therefore important to study the effect of the orientation upon the amount of heat that can be collected by the chimney for better performance. A theoretical study was conducted using a finite difference technique which showed that the amount of heat that can be collected by a solar chimney is strongly dependent upon its azimuth.

1. INTRODUCTION

The cooling of dwellings is one of the major aims in hot climates. Several methods are encountered in traditional buildings, one of which is the use of air movement; wind towers and courtyard spaces are particularly common. Unfortunately, the air outside is sometimes so hot that ventilation is of no benefit until the evening. An arrangement as illustrated in Fig. 1 has been investigated [1, 2]. This could be used to promote evening ventilation, at which time the outside air is cool. This relies upon the collection within the fabric of a solar chimney of sufficient heat to induce cooling draughts through the building. Walls on the sunny side warm the air within the chimney which, when opened at the top and bottom, induces ventilation.

This work was aimed at determining the orientation at which the solar-heated chimney would give the best performance. Heat storage within a solar chimney at different azimuths for latitude 33°N was calculated for summer conditions, using a one-dimensional finite difference approximation.

2. ANALYSIS

2.1. Determination of solar radiation

Solar radiation reaches the outside wall of the chimney in three ways: radiation direct from the sun, diffused from the sky and reflected from the ground and surroundings, such as building surfaces. The intensity of solar radiation depends mainly on the latitude, the altitude above sea-level and sky clarity. The total solar radiation intensities on the outer wall of the solar chimney were determined, based on the radiation data published by CIBSE [3], as follows:

$$I_{tvd} = I_{Dvd} + 0.5(I_{dhd} + k_r I_{thd}) \quad (1)$$

where the ground reflection factor k_r has a value of 0.5 for hot arid climates and 0.2 for other climates.

$$I_{Dvd} = k_{af} k_D I_{Dvb} \quad (2)$$

The altitude correction factor, k_{af}, may be assumed as unity for altitudes between 0 and 300 m above sea-level. It can be calculated for other values from

$$k_{af} = 1.02 + 10^{-5}[2 + 5\ \mathrm{cosec}(h)]H \quad (3)$$

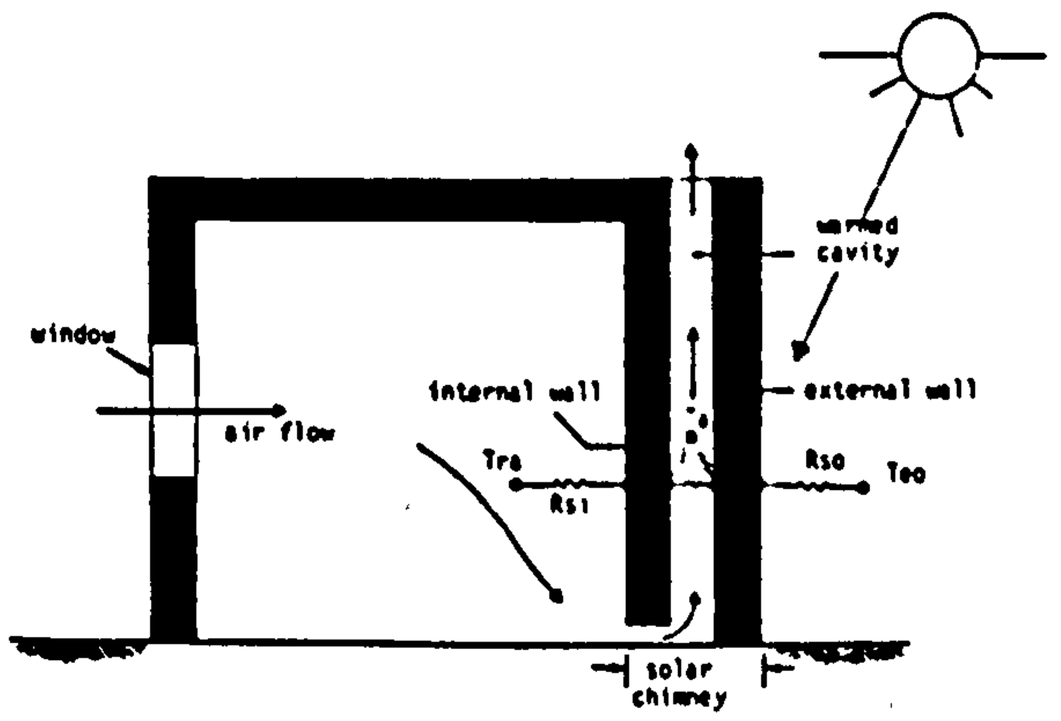

Fig. 1. Section through the room and 'solar chimney'.

0378-7788/88/$3.50

and the direct radiation factor value k_D is 1.1 for hot arid climates.

$$I_{dhd} = k_{af} k_d I_{dhb} \quad (4)$$

The diffuse radiation factor k_d has a value of 0.9 for arid climates.

$$I_{thd} = k_{af}(k_D I_{Dbb} + k_d I_{dhb}) \quad (5)$$

Equation (1) may be simplified, by substituting eqns. (2), (3), (4) and (5) into it and inserting the correction factors with their values, to the following form:

$$I_{tvd} = k_{af}(1.1 I_{Dvb} + 0.675 I_{dhb} + 0.275 I_{Dhb}) \quad (6)$$

It is apparent from Fig. 2, for latitude 33°N in summer that the peak total intensity received by a southern wall is 550 W/m^2 at noon, whereas a western wall at 16:00 receives 885 W/m^2.

2.2. Determination of the solair temperature

The determination of hourly solair temperature is important, because the heat transferred into the solar chimney depends upon the difference between the solair temperature and the outside surface temperature of the chimney. This may be obtained from the following equation:

$$T_{eo} = T_{ao} + R_{so}(\alpha I_{tvd} - E I_e) \quad (7)$$

where the outside air temperature, T_{ao}, is obtained from the climatic data of El-Oued [4]. The outside total thermal resistance R_{so} is a combination of convective and radiative thermal resistances. From Fig. 3, the highest solair temperature for latitude 33°N on a west-facing wall is 77 °C and for a south-facing one is 55 °C.

2.3. Heat transfer

The walls of the solar chimney are designed to collect as much solar energy as possible. They can be built from any high thermal capacity building material. In this investigation, we have assumed a material with density 2000 kg/m^3, thermal conductivity 1.1 W/mK and specific heat capacity 900 J/kgK. The outer wall of the solar chimney is 0.1 m thick and the inner wall is 0.2 m thick.

The outside wall of the solar chimney receives solar radiation from the sky and the surroundings and has convective heat exchange with the ambient air. The outside total thermal surface resistance is taken as

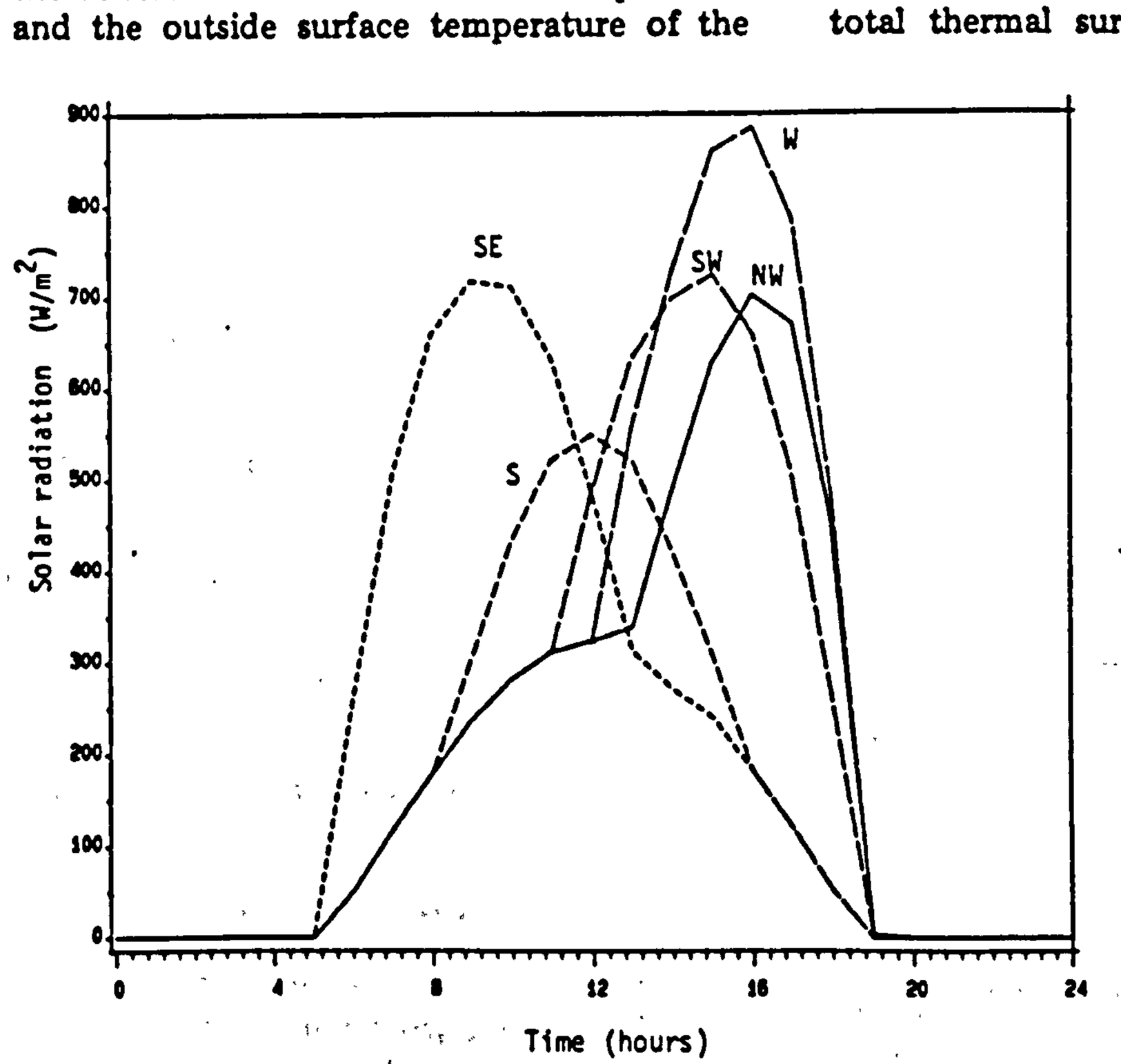

Fig. 2. Daily intensities of solar radiation received by vertical walls facing SE, S, SW, W, and NW at latitude 33°N.

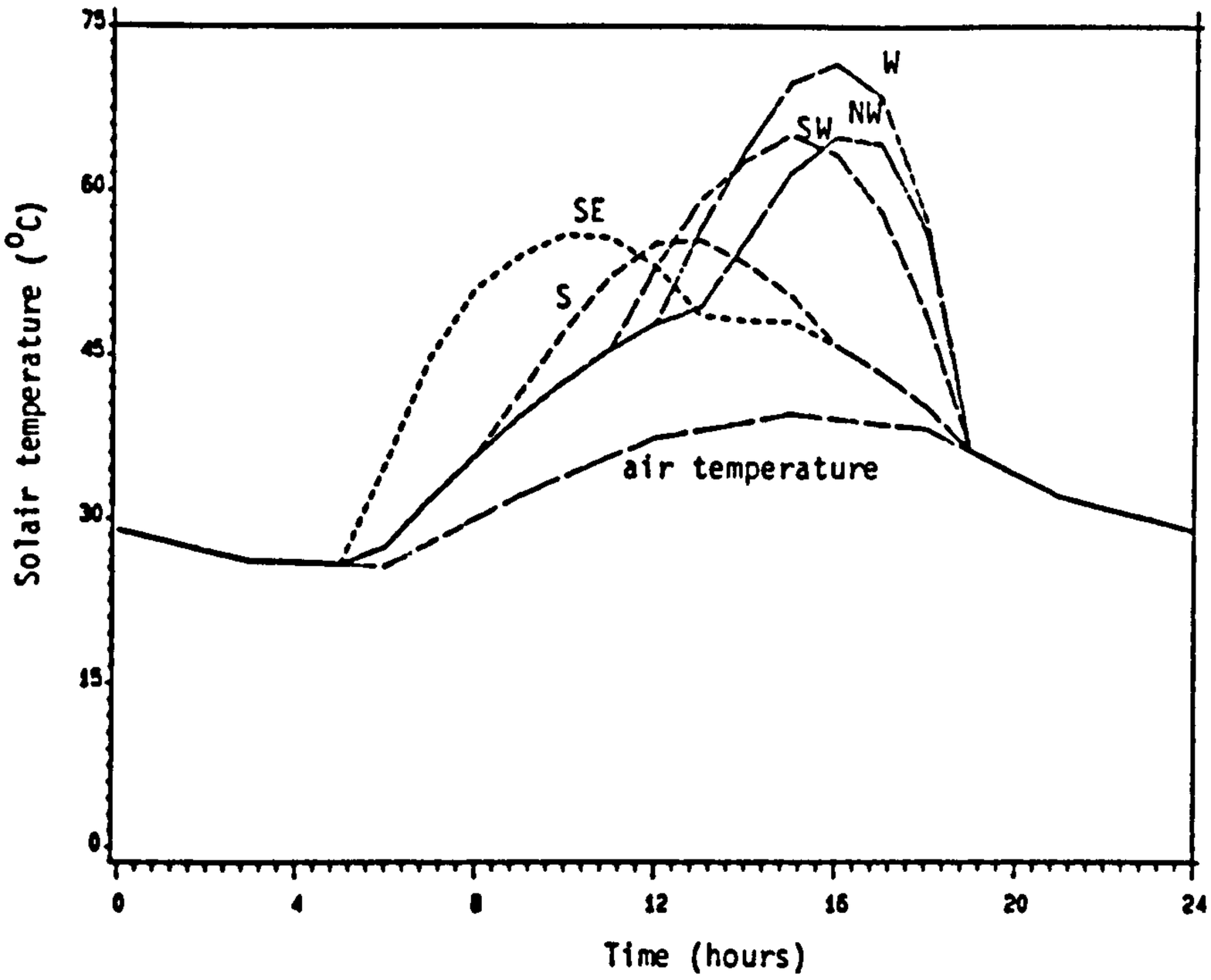

Fig. 3. Daily solair temperatures on vertical walls facing SE, S, SW, W and NW at latitude 33°N.

0.05 m^2K/W. On the inner side of the room, the walls are assumed to be exposed to air at constant temperature and to be surrounded by surfaces at a mean radiant temperature equal to the air temperature. The convective heat loss up the chimney is considered small compared with radiative heat exchange between the two walls. These assumptions are made in order to simplify the analysis and are acceptable since the purpose of this study is to compare the magnitudes of heat storage within the walls of the chimney at different azimuths. The inside thermal surface resistance of the room is taken as 0.123 m^2K/W. The transient temperature is obtained by dividing the walls into slices.

Assuming a one-dimensional heat flow through the walls, a heat balance equation may be established as follows:

Heat entering a node (n)

— Heat leaving that node

= Heat stored in it in a given time

which leads to:

$$T_{(n,\,t+1)} = \text{fact}_1\, T_{(n-1,\,t)} + \text{fact}_2\, T_{(n,\,t)} + \text{fact}_3\, T_{(n+1,\,t)} \tag{8}$$

where fact_1, fact_2 and fact_3 are coefficients whose values are given as follows:

$$\text{fact}_1 = \frac{C_{(n-1,\,n)}\,dt}{\rho\,\delta x\,c_p} \tag{9}$$

$$\text{fact}_2 = 1 - \frac{[C_{(n-1,\,n)} + C_{(n,\,n+1)}]\,dt}{\rho\,\delta x\,c_p} \tag{10}$$

$$\text{fact}_3 = \frac{C_{(n,\,n+1)}\,dt}{\rho\,\delta x\,c_p} \tag{11}$$

The stability and accuracy of the numerical solution depends upon the time and the distance increment, which should be chosen so that the time step

$$dt \leqslant \frac{\rho\,\delta x\,C_p}{C_{(n-1,\,n)} + C_{(n,\,n+1)}} \tag{12}$$

For surface nodes the thickness of the slice is taken as half the actual slice.

The heat transfer within the chimney occurs by convection and radiation. The convective heat transfer coefficient may be obtained from the equation for a vertical flat plate given by Arpaci [5] as follows:

$$h_c = 0.1(GrPr)^{1/3}K_a/Z \tag{13}$$

where Gr and Pr are the Grashof and Prandtl numbers.

The radiation heat transfer coefficient, h_r, between two parallel walls is

$$h_r = 5.8C_{F_{12}} \tag{14}$$

where $C_{F_{12}}$ is a configuration factor which depends on the emissivity, the areas and the relative view (or 'shape') factor F_{12} of the two surfaces.

$$C_{F_{12}} = \left[\frac{1}{E_1} - 1 + \frac{A_1}{A_2}\left(\frac{1}{E_2} - 1\right) + \frac{1}{F_{12}}\right]^{-1} \quad (15)$$

where the subscripts 1 and 2 refer to the first and second walls. F_{12} is the relative view factor obtained from O'Callaghan [6] and Wong [7] for example.

2.4. Determination of heat storage

The total stored heat within the walls of the solar chimney can be obtained by calculating the heat stored in each slice over a given time, dt, and then taking the total of all slices as follows:

$$H_{s(n)} = \rho c_p \, \delta x \, A(\bar{T}_{(n)} - T_r) \quad (16)$$

where

$$\bar{T}_{(n)} = (T_{(n-1,\,n)} + T_{(n,\,n+1)})/2 \quad (17)$$

so that the whole stored heat is

$$H_T = \sum_1^n H_{s(n)} \quad (18)$$

Figure 4 shows the energy stored by the solar chimney as a function of time in July for latitude 33°, and Fig. 5 shows the maximum energy plotted against azimuths. From Figs. 4 and 5, the energy content of a west-facing chimney is greater than that obtained with one facing south. It is interesting to note that the peak energy content is reached at about 20:00 when the outside air is approaching a comfortable temperature.

3. CONCLUSION

The heat storage of a solar chimney was found to be strongly dependent upon the orientation. It was found that a west-facing solar-heated chimney receives more energy than one facing south at latitude 33°. This is because the more one goes south, the more solar radiation is received on east and west walls and less on the south. So if a solar-heated chimney is to be used to induce evening ventilation in a building in low latitudes, it should go on a west wall.

LIST OF SYMBOLS

a	surface absorptivity
A	area (m^2)
$C_{(n-1,\,n)}$	thermal conductance between the nodes, $(n-1)$ and n (W/m^{2}K)

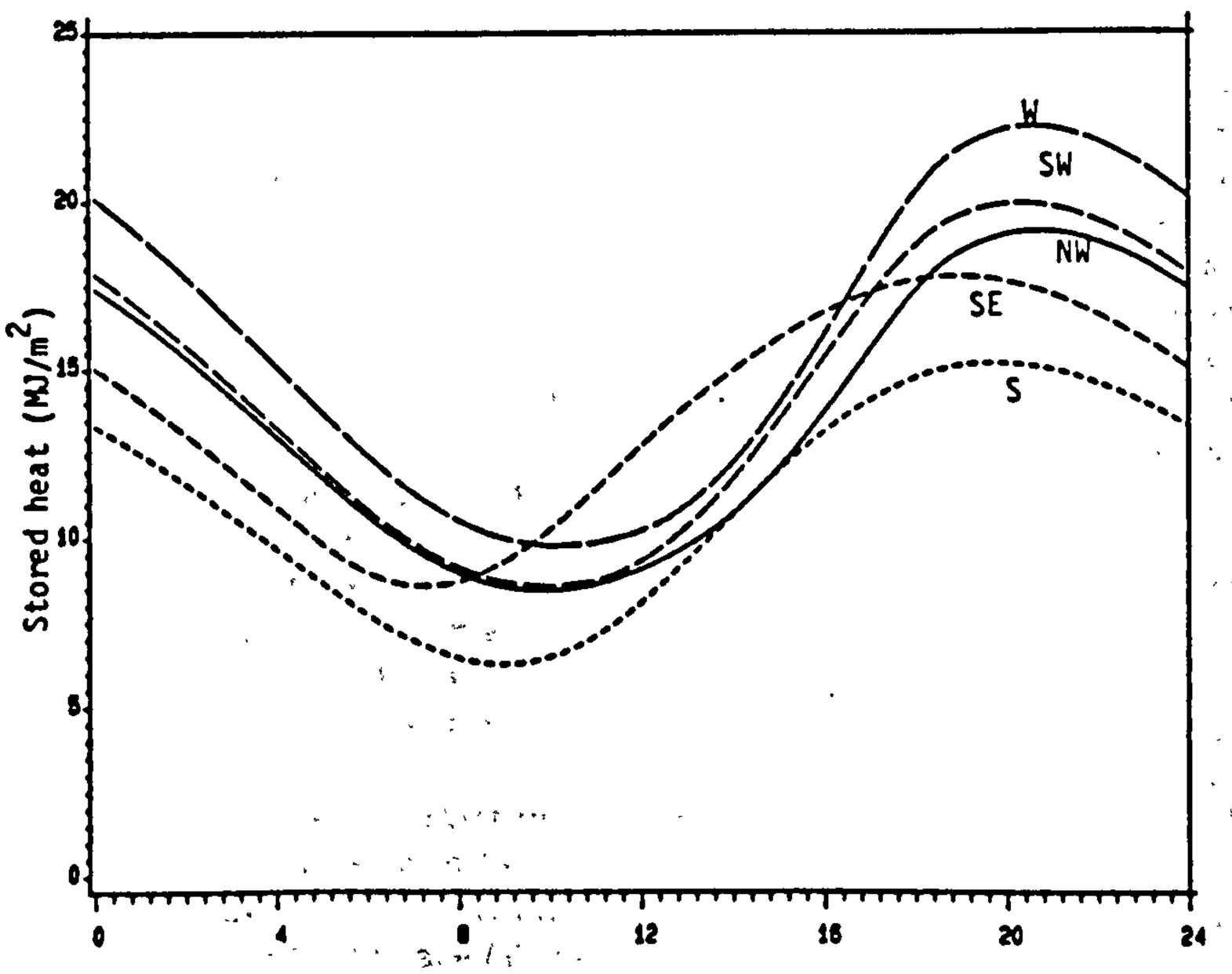

Fig. 4. Heat stored within a chimney against time with respect to T_r = 30 °C.

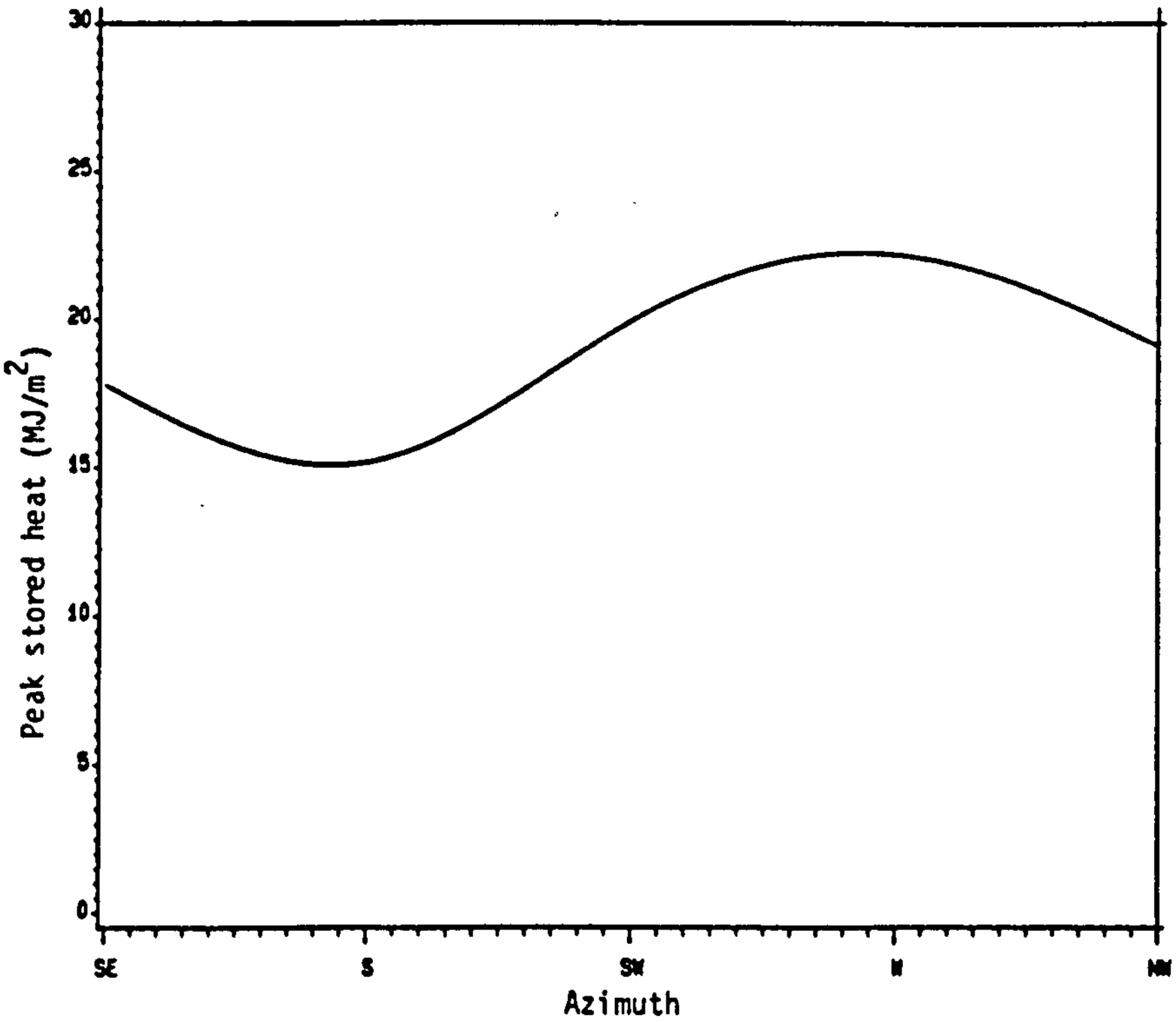

Fig. 5. Peak stored heat against azimuth for latitude 33°N.

c_p specific heat capacity of the node n (J/kg K)
dt time increment (s)
E surface emissivity (0.9 for ordinary building material)
h solar altitude (degrees)
h_c surface convection coefficient inside the cavity (W/m^2K)
H altitude above sea-level (m)
$H_{s(n)}$ heat stored within a single slice of a wall (MJ/m^2)
H_T total stored heat in the chimney (MJ/m^2)
I_{dhb} basic diffuse irradiance on a horizontal surface (W/m^2)
I_{dhd} design diffuse irradiance on a horizontal surface (W/m^2)
I_{Dhb} basic direct irradiance on a horizontal surface (W/m^2)
I_{Dvb} basic direct irradiance on a vertical surface (W/m^2)
I_{Dvd} design direct irradiance on a vertical surface (W/m^2)
I_e longwave radiation loss from black surfaces (W/m^2)
I_{thd} design total irradiance on a horizontal surface (W/m^2)
I_{tvd} design total irradiance on a vertical surface (W/m^2)
K_a thermal conductivity of the air (W/m K)
k_D direct radiation coefficient (1.1 for arid climates)
k_{af} altitude correction factor
k_d diffuse radiation coefficient (0.9 for arid climates)
k_r ground reflection factor (0.5 for arid places)
R_{si} total inside surface thermal resistance on the room side (m^2K/W)
R_{so} total outside surface thermal resistance (m^2K/W)
T_{eo} solair temperature (°C)
$T_{(n,\,t+1)}$ future temperature of the node n predicted from the known temperatures (°C)
T_a air temperature within the chimney (°C)
T_{ra} room air temperature (°C)
T_r reference temperature (30 °C)
Z height (m)
δx distance increment (m)
ρ density of the material of the node n (kg/m^3)

REFERENCES

1 A. Bouchair, D. Fitzgerald and J. A. Tinker, Passive solar induced ventilation, *Proc. 8th Int. Conference on Alternative Energy Sources, Miami Beach, Florida, U.S.A., 1987*, to be published by Hemisphere Publ. Corp., New York.

2 A. Bouchair, D. Fitzgerald and J. A. Tinker, Moving air using stored solar energy, *Proc. 13th National Passive Solar Conference, 1988, Cambridge, MA*, ASES, pp. 33 - 38.

3 *CIBSE Guide*, Chartered Institution of Building Service Engineers, London, 1986.

4 Climatic data from the Algerian Meteorological Office in Algiers.

5 C. Y. Warner and V. S. Arpaci, An experimental investigation of turbulent natural convection in air at low pressure along a vertical heated flat plate, *Int. J. Heat Mass Transfer, 11* (1968) 397 - 406.

6 P. W. O'Callaghan, *Building for Energy Conservation*, Pergamon Press, Oxford, 1978.

7 H. Y. Wong, *Handbook of Essential Formulae and Data on Heat Transfer for Engineers*, Longman, London, 1977.

APPENDIX 5

Solar' 88

Proc. 1988 Ann. Meeting of

the U.S. Solar Energy Soc. Inc.

Cambridge Massachusets.

MOVING AIR, USING STORED SOLAR ENERGY

Ammar Bouchair B.Arch.
D.Fitzgerald M.A. B.Sc. Ph.D. C.Eng.
J.Tinker B.Sc. M.Sc. Ph.D.

Civil Engineering Department
The University of Leeds LS2 9JT
England

ABSTRACT

Air may be moved without a fan, making use of buoyancy forces from a solar chimney, added on the sunward side of a building. On a sunny day the chimney collects enough solar energy to move air all day, so that, apart from ventilation, the air may be used for other needs such as cooling or drying. The analysis of the fluid flow in the chimney is considered, but needs more study.

1. INTRODUCTION

If, anywhere in the Western world we want to move air, on any scale, it is most likely we use a fan, driven by an electric motor. Electricity is available , and if not, generating it is easy. Not so in the Developing World.

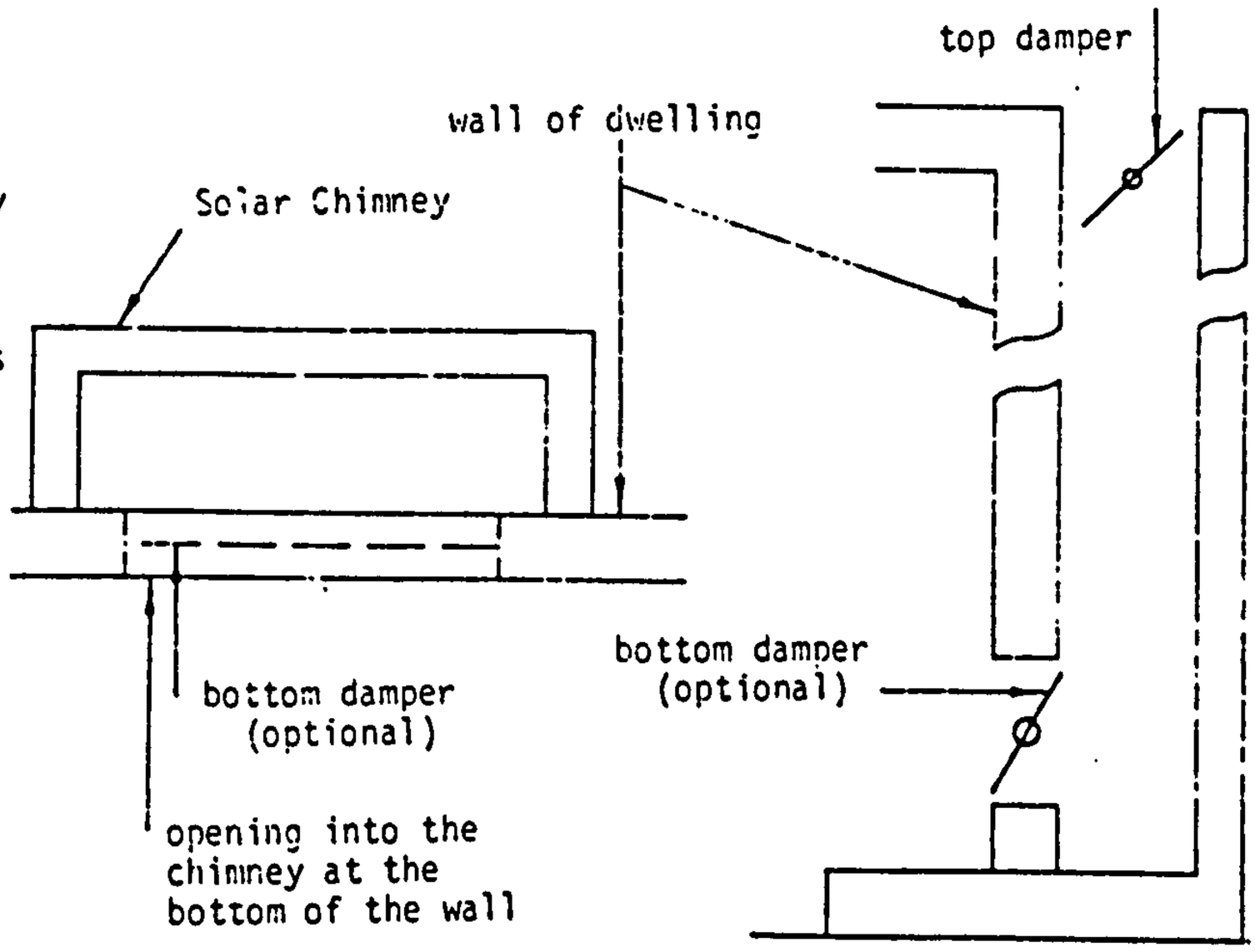

Fig. 1 Plan and section of the Solar Chimney

For a particular need, we have developed a way of moving air using stored solar energy, which is of much wider application than the need which created our idea. In some hot countries, including parts of Algeria, home of one of us, the temperature of the air outside during the day is so high that it cannot be used for ventilation, and the windows are kept shut, until the air is a little cooler in the late afternoon or early evening, when windows are opened. The "solar chimney" described below was first intended to increase this ventilation, but its uses are much wider.

2. THE SOLAR CHIMNEY

Figure 1 is a plan and section of a solar chimney added on the sunward side of the building to be ventilated. During the day, when the sun strikes the outside of the chimney, the damper at the top of the chimney, and that at the bottom (if fitted) are closed, and little or no air flows up the chimney. The chimney, and the part of the facade within it, get very hot during the day, and the air within it will also become hot. On a clear day 50°C or more will be reached. When the windows are opened for ventilation, the dampers will also be opened, and the air imprisoned within it will flow upward by buoyancy, drawing warm air into the chimney from the house, replaced by cooler air from outside. The air now in the chimney will become warmer by convection with the inside surfaces of the chimney, and also flow up it by buoyancy, cooling the chimney slightly. The temperature of the flowing air changes but little, so that it does not consume much of the solar energy stored in the chimney. Once started, the ventilation will continue throughout the evening and night, and into the next day if required. The first purpose of the solar chimney was to help in ventilation, but on its way into the chimney, the air could serve other purposes, such as drying, or it could pass over wet surfaces or water, and thus cool by evaporation, to name but two

possibilities.

3. THE AZIMUTH OF THE CHIMNEY

The South is obviously the best azimuth, or is it? We are concerned not with the maximumtotal insolation in a day, but with the maximum on a vertical surface. Table 1 applies to latitude 35°, and the month of July, as then air temperatures in Southern Algeria are very high, and a solar chimney to help ventilation would be very valuable. The first column shows the total solar energy, direct and diffuse, on a facade in the directions shown. Although the sun shines for 13 hours on a day in July at latitude 35°, the facades shown receive only seven hours of sun, which arrives during those seven hours at the mean rates given. The table also gives peak insolations, and when the peaks occur. The table shows that in July at latitude 35°, the most insolation is not received on the South, and not even on the South West, but on the West. The horizontal receives very much more than any of the facades, because in summer, at latitude 35°, the sun is high!

For the benefit of people not familiar with the sun at low latitudes, Table 2 applies to Southern England, latitude 52°N, helpful in the very improbable event of someone wanting to build a solar chimney there.In the South of England the sun is much lower in July than it is in Algeria, so peak insolations are higher. The means are lower, but the totals received are higher, because the time of sunshine on each facade is about twice as long as in Algeria. For Southern England, the South West is the best azimuth, marginally, the South and West receiving nearly as much. These data are given in the polar diagram of Figure 2, for the latitudes of Algeria, 35°N, and Southern England 52°N.

TABLE 1 INSOLATION ON FACADES S, SW, W, AND NW AT LATITUDE 35°

Azim.	MJ/m²day	hours insol.	mean W/m²	Peak W/m²	Time of peak(hours)
S	6.2	7	230	285	12
SW	10.6	7	420	500	15.5
W	12.3	7	490	680	16
NW	8.9	7	350	505	17
hor.	29.4	13	545	1005	12

TABLE 2 INSOLATION ON FACADES S, SW, W, AND NW AT LATITUDE 52°

Azim.	MJ/m²/day	hours insol.	mean W/m²	Peak W/m²	Time of peak(hours)
S	18.6	15	340	550	12
SW	19.9	15	360	580	14.5
W	19.4	15	360	580	16
NW	15.1	15	280	410	17
hor.	29.8	15	550	815	12

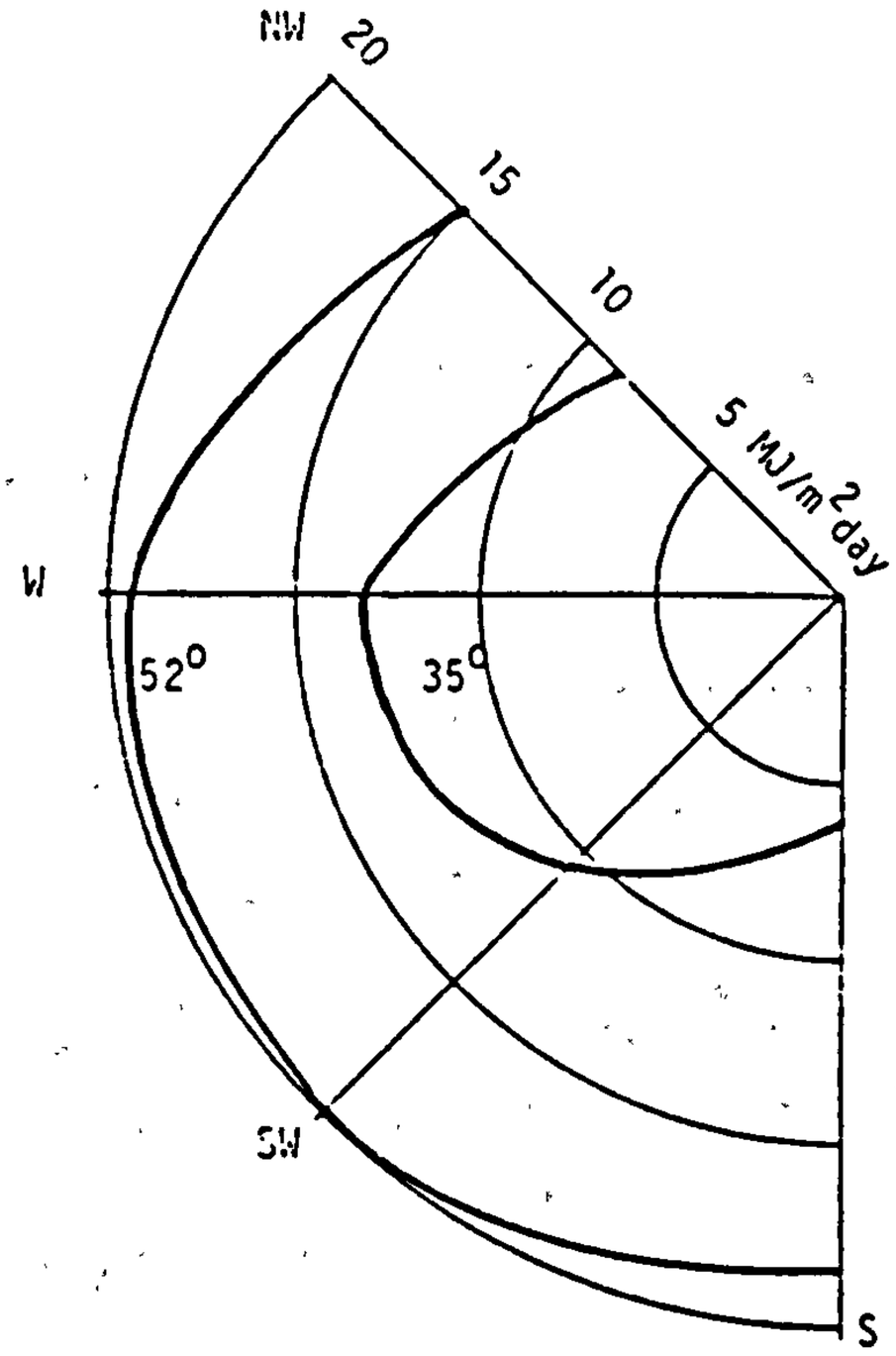

Fig. 2 Solar Energy received per day in July, as function of the azimuth of a vertical surface at latitudes 35° and 52°

Facades facing East have been ignored in these tables, because if the air movement caused by the chimney is to be in the evening or at night, which seems likely, solar energy collected in the afternoon has to be stored for a shorter time, so that losses will be less.

4. DETERMINING CHIMNEY "LIFE"

An order-of-magnitude estimate of how long a chimney may be expected to move air follows:

Heat content of chimney, in relation to that of the air entering it is

$$2YZD\ dc\ cc(Tc - \theta i)\ J$$

and the rate of heat gain of the air entering it is

$$vXY\ da\ ca(\theta o - \theta i)\ W$$

Here Z is the height of the chimney, and Y is its width, and X is the distance between its two surfaces; dc and cc are the density and specific heat capacity of the material of the chimney, da and ca are the density and specific heat capacity of air, Tc is the temperature of the surfaces of the chimney, and θi and θo are the temperatures of the air entering and leaving the chimney, and v is the speed of the air.

An order-of-magnitude "life" of the chimney as mover of air is the ratio of the two quantities given, a time. Using conservative numerical values, this is

$$\frac{2\times2\times0.2\times2200\times900(40-30)}{0.1\times0.25\times1.2\times1000\times6\times3600}$$

or some 24 hours. This is at least twice as long as it might be neededas an aid forventilation, as the chimney will still contain stored solar energy from the day before, when it gains more. It is easy to see that the "life" of a chimney to be used as a means of moving air can be extended by making it higher, and giving it thicker walls, although this would result in the decline of its mean temperature. We are engaged on a detailed analysis of the life of a solar chimney used for air movement in general.

5. THE EXPERIMENTAL CHIMNEY

As the thermal capacity of any practical chimney is large in relation to the thermal changes taking place within it, it is not necessary to represent its thermal capacity in laboratory equipment to test its performance. The chimney we built is 1.95m high, 1.5m long, and of variable width, as finding the best width was an important aim of the measurements. The two main inner faces of the chimney were of aluminium sheet, given a 'rough' surface with sand and adhesive. Each face was heated by horizontal electric heaters, well insulated, to prevent heat entering the 'room', or being lost 'outside'. The heaters were separated by horizontal partitions, to discourage vertical air movement behind the heated surfaces, to help keep the temperature of the chimney surfaces nearly constant. These temperatures were of course controlled.

Temperatures were measured with copper-constantan thermocouples, calibrated to British Standard 1826(1961). When used to measure surface temperatures, such as those of the inner surfaces of the chimney, the couples were carefully attached to the surfaces, and the wires run along them, to avoid heat conduction along them. When used to measure air temperatures, they were always screened from thermal radiation, with polished aluminium foil.

The speed of air movement was measured with a heated thermistor anemometer, claiming an accuracy of some 5%; its lower scale started indicating at about 0.005 m/s. The anemometer was used to carry out a mass balance on the moving air, when the chimney was working. In one set of measurements, when the two surfaces of the chimney were separated by 500mm, the air mass flow found for the air entering the 'room' being ventilated agreed well with that obtained across the opening between the room and the bottom of the chimney. A mass balance at the top of the chimney suggested that less air was entering the chimney that was leaving it. This curious result came from the assumption that all air flows observed were flowing upward, as seemed reasonable (and desirable!). Remembering that the heated thermistor anemometer gives air speeds, but not the direction of air movement, it was easy to show that the air in the centre of the chimney was moving downward. This is clearly shown by Figure 3, in which smoke, near the centre of the chimney is moving downward.

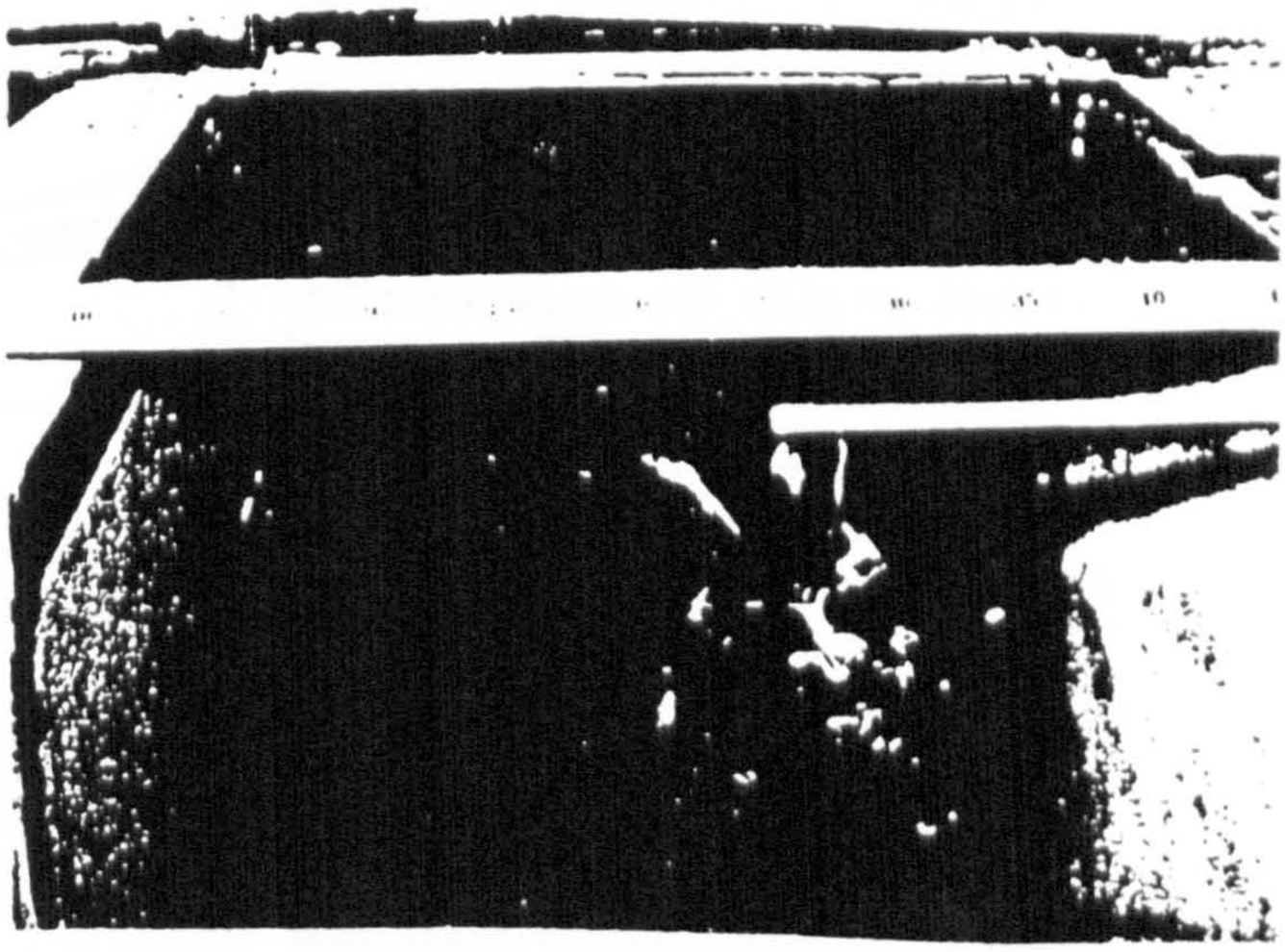

Fig. 3 Smoke shows downward moving air in the centre of a 500mm wide chimney.

6. OBSERVATIONS

Figure 4 shows the rate of air flow up the chimney for chimneys up to 50°C in temperature, with the air entering at 20°C, for chimneys up to 500mm wide. The highest flow was found for a width of 200mm, a little less for 300mm , and less still for 500mm. It appears that the upward flow of air takes place as two separate flows on the two sides of the chimney, each side being covered by a 'boundary layer', within which the flow takes place, and that if the two sides of the chimney are far enough apart, the two boundary layers are independent. Observations suggest that each boundary layer is over 100mm thick, and that at a width of 200mm the two boundary layers are not, as far as their thickness is concerned, fully developed and that the lesser flow for a wider chimney (300mm) is accounted for by interference between the boundary layers, or, in case of the 500mm chimney, by flow downward.

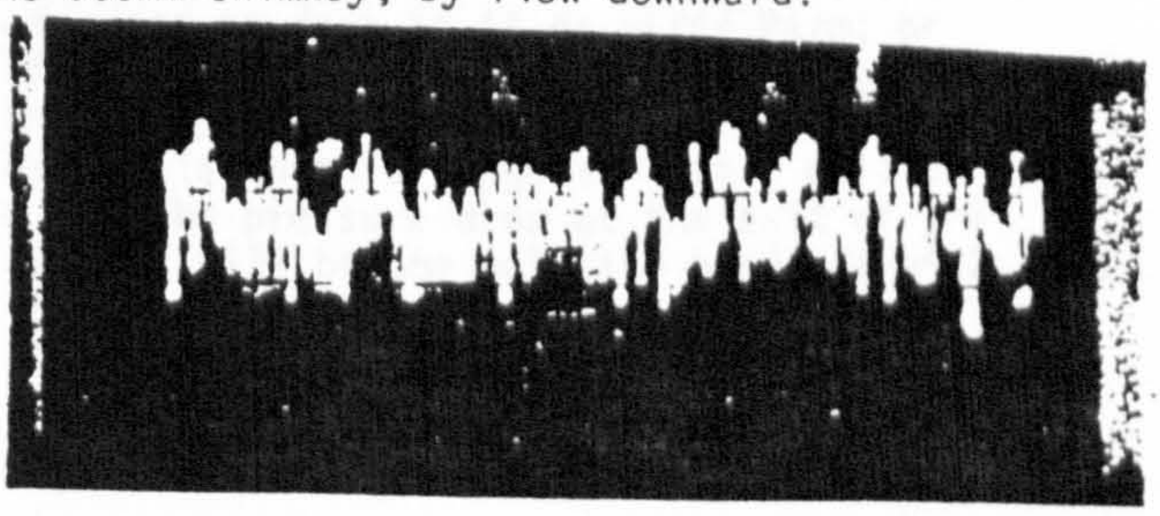

Fig. 5 Air speed against time shows that the air flow is turbulent

Figure 5 shows the variation of air flow in

about 20 seconds, when the mean air speed was about 0.4 m/s. The variations shown are about + 0.1 m/s, and the Reynolds' number then is about 11000.

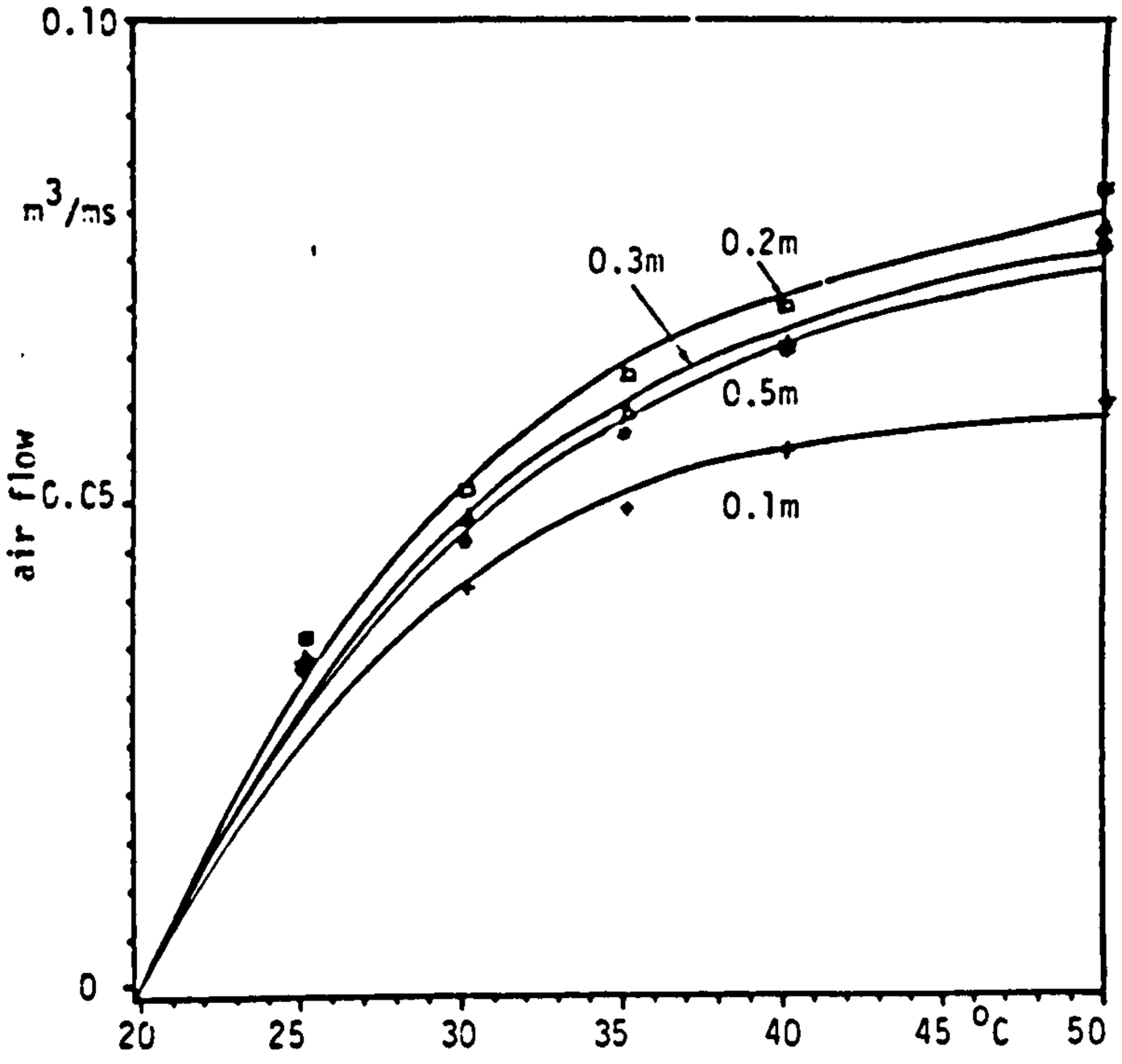

Fig. 4 Air flow up the chimney, as function of its internal surface temperature, for several widths of chimney, the air entering at 20°C

7. ANALYSIS

According to Rohsenow and Choi (1) the thickness of the boundary layer is given by

$b/z = 0.565Gr^{-0.1}Pr^{-8/15}(1 + 0.494Pr^{2/3})^{0.1}$

from which it is easily shown that

$b = 0.11z^{0.7}(Tc - \theta)^{-0.1}$, and if the height of the chimney be taken as $z = 1.95m$, then

$b = 0.177(Tc - \theta)^{-0.1}$ where θ is the air temperature at height z above the base of the chimney. If we take $Tc = 50°C$, and let θ be 20, 30 and 40°C, we find that $b = 126$, 131 and 141 mm, so that the best width of the chimney need vary but little with the expected temperatures. If we put $Tc - \theta = 50 - 30 = 20K$, we find $b = 0.082z^{0.7}$, so that at the top of the chimney, when $z = 1.95m$, the two boundary layers just touch if the width of the chimney is $2x0.082x1.95^{0.7} = 0.164x1.60 = 0.262m$ or 262mm. Halfway up the chimney the boundary layers will be separated by

$2(131 - 0.082x0.98^{0.7}x10^3) = 100mm$, this space containing notionally still air, or, more likely, air which is also moving upward, and entering the boundary layer as it rises. This is discussed below. Figure 6 shows how the thickness of the boundary layer changes with height, for a chimney at 50°C, 1.95m high, with air entering it at 20°C. Note that the two scales are different. The line stops short of bottom, because it clearly cannot apply there, because the air entering has to turn through a right angle, and then separate into two, if not three flows. This is clearly a region of confusion. Studies continue.

Rohsenow and Choi (loc. cit.) quote relations by Eckert and Jackson giving the temperature and velocity distributions to be expected in the boundary layer; reference to the original (2) paper gives less confidence in the numerical portions of the relations, and we decided to reject the temperature relation, because it stated that air in contact with the warm vertical surface would be at the temperature of that surface. If this were so, there would of course be no heat transfer between the flowing air and the surface. We replaced the temperature relation by an authoritative relevant heat transfer coefficient (3), and used these relations to predict the temperature rise of the flowing air. The predicted rises were a small fraction of those found, suggesting that the resulting buoyancy pressures would be very small. These disagreements, even though our Grashof numbers were small compared with those of Eckert and Jackson, but well within the range for which they claimed that their relations were applicable, suggest that more analysis of event within the boundary layer is required.

7. CHANGES IN PRESSURE

In the application of the solar chimney as described, the main resistances to flow are at the entry and exit, with little pressure drop in the room being ventilated and within the chimney.

Within the chimney the flow is turbulent, and assuming a hydraulic diameter of 2X, the rate of pressure drop is $4f\ da\ v^2/4X$ Pa/m, or $Zf\ da\ v^2/X$ Pa, where f is the friction factor. With a Reynolds' number of some thousands, the Re/f relationship suggests that f will be about 0.01. The pressure drop at the exit of the chimney will be one velocity head, $da\ v^2/2$, and the ratio of this to the pressure drop within the chimney will be $X/2Zf = 0.3/(2x1.95x0.01)$ or 7.7, confirming that the pressure drop within the chimney can be ignored.

The buoyancy pressure drawing air through the chimney is proportional to the density difference between that of the air entering it, and

that within the chimney, given by

PB = gZ(dai - (dai + dao)/2) = gZ(dai - dao)/2

where da is the air density, i and o mean air entering and leaving. In general, density da = d(ref)273/(273 + θ), which is Charles' Law. If the reference air is saturated with moisture at 0°C, da(ref)=1.29kg/m^3, whence

da = 352/(273+θ)

so that

$$PB = \frac{176gZ(\theta o-\theta i)}{300x300}$$

where the denominator is the two absolute air temperatures, which vary but little. With Z = 1.95m we find

PB=0.037(θo-θi) Pa

For a chimney 0.3m wide, with its surfaces at 30,50°C, and air entering at 20°C, we find air speeds of 0.048,0.077/0.3=0.16,0.26 m/s. The corresponding air densities within the chimney are 352/(273 + 24.3 ,29.8) = 1.185,1.163 kg/m^3, so that the velocity heads are 1.185x0.16^2/2 = 0.015 Pa and 1.163x0.26^2/2 = 0.039 Pa, and these are the pressure drops at the top of the chimney, and the corresponding buoyancy pressures are 0.037x4.3,9.8=0.16,0.36Pa The pressure drop within the chimney was shown negligible, so that that at the chimney entry will be 0.16 - 0.015 = 0.145 Pa, and 0.36 - 0.039 = 0.321 Pa; these are conveniently expressed as velocity heads, using the velocities of entry at the 0.1m opening, so that the velocity head will be nine times that within the chimney, 0.015,0.039x9 = 0.135, 0.315 Pa, so that the pressure drop on entry, in terms of velocity heads there are 0.145/0.135 = 1.1 and 0.321/0.351 = 0.9, comfortably giving a mean of one velocity head, a reasonable value.

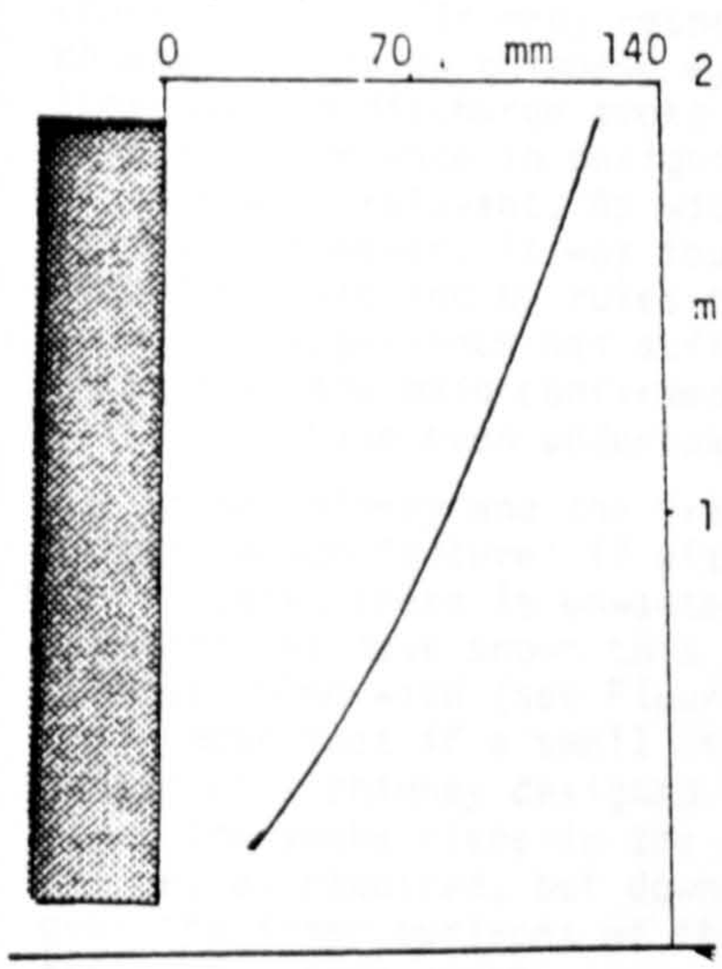

Fig. 6 Thickness of Boundary Layer against height

The same calculation repeated, when the entry at the bottom of the 300mm chimney was 400mm gives the pressure loss on entry into the chimney as 6.7, say 7 velocity heads. This shows very clearly that the nature of the air flow is very different when the air is turning through a right angle, and somewhat decreasing its mean velocity, compared with when its velocity is increased three fold. Detailed observations were difficult, and were not pursued.

3. OTHER APPLICATIONS

We have shown that the solar chimney can be used for other than ventilation, because the energy collected from a day's sun can easily be made much more than is needed for its original purpose, encouraging ventilation in the evening.

The air moved by the solar chimney could be cooled, by making it flow over a wet surface. If, as a result of evaporation of water, the moisture content of the air is raised by j kg of water vapour per kg of dry air, and if all the required latent heat comes from the air, the temperature of the air will fall by Lj/ca K where L is the latent heat of vapourisation of water, 2.26 x 10^6 J/kg of evaporated water, 2260j K, so that if the moisture content rise by 0.001, about 5% in the case of air at 30°C and 70% relative humidity, the temperature will fall by about two degrees, so that the air will be at about 2θ°C and near 85% relative humidity. Figure 7 comes from a diagram in the Fundamentals volume of the A.S.H.R.A.E. Handbook (4), helpful in deciding to what extent it is worthwhile achieving the cooling of air by raising its relative humidity. The "degree of wettedness" is a measure of comfort, and the general

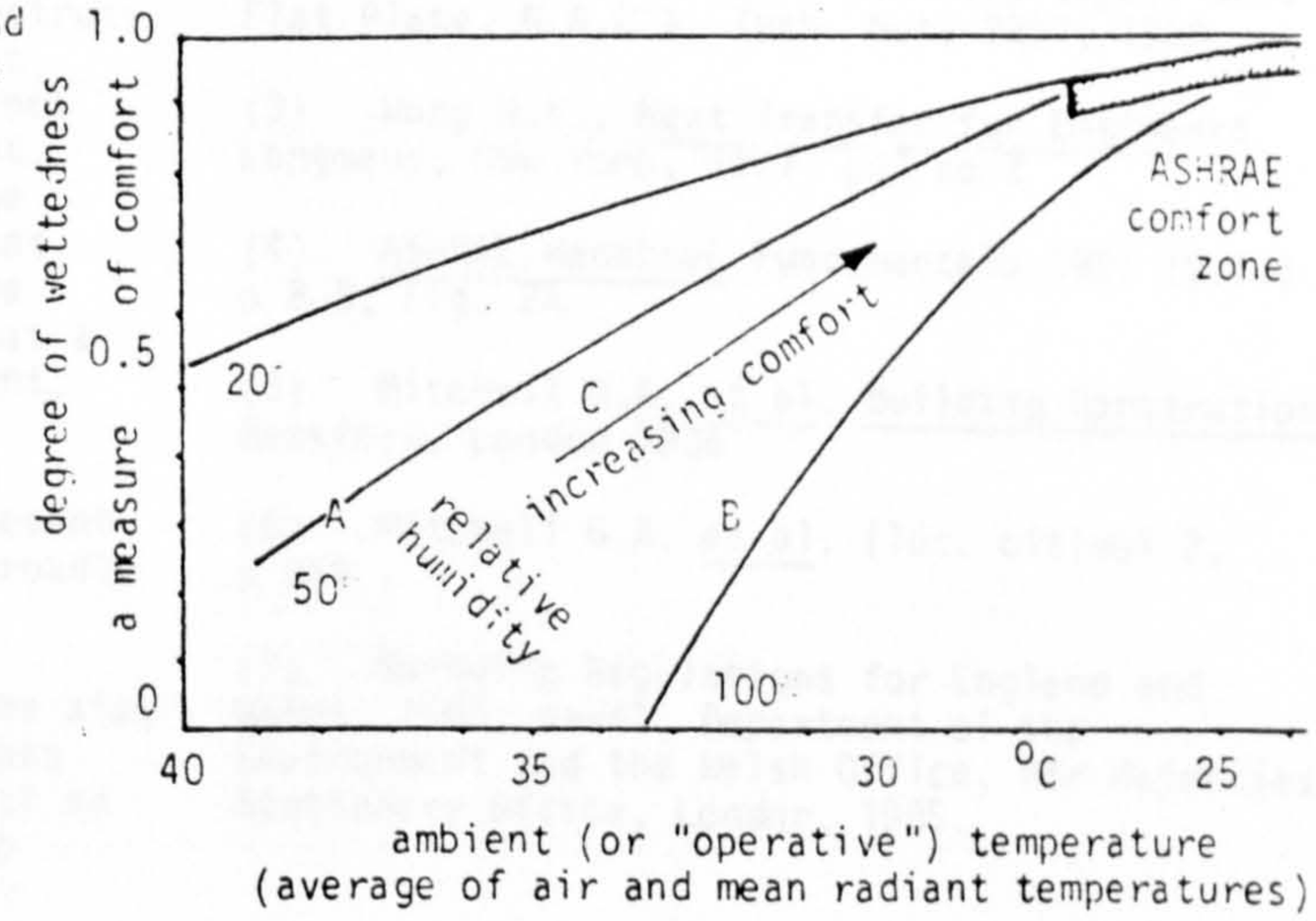

Fig. 7 A measure of comfort against "temperature"

aim of treatment of air must be to raise its "state point" in figure 7, toward the comfort zone of the A.S.H.R.A.E. Handbook, in the top right of the figure. Thus, for example, if the air is initially at A, increasing its r.h. and cooling it by 6K, to reach B, does not improve comfort, but cooling it by only 4K, with rather less increase of relative humidity to C does improve comfort. Work on the relation between temperature and relative humidity of air flowing over wet surfaces is being done in our Department, in view of the fact that one use of our solar chimney could be a combination of encouraging evening ventilation, and making this air cooler.

9. COMPARISON WITH TRADITIONAL CHIMNEYS

Our solar chimney and the traditional chimney differ in that the heat needed to cause an upward flow does not come from a fire at the bottom, but from the sunwarmed walls of the chimney itself. In many respects a solar chimney resembles chimneys such as have been long used to discharge smoke from open fires, so that experience in designing traditional flues may be relevant. As with most traditional building, however, it was found that until recently designing by rules-of-thumb derived from long experience has sufficed, and that this is in the main confirmed by such investigations as have been undertaken.

Our solar chimney and the traditional chimney have a common feature: if either is too big for its purpose, there is unwanted downward air movement. We have shown this with a solar chimney 500mm wide (see Figure 3), and it is well known that if a small fire is lit at the bottom of a chimney designed for a much larger fire, the smoke rises-in the centre of the chimney as required, but downdraught is found over the inner surfaces of the chimney, remote from the rising smoke.

The standard British text on building construction by Mitchell (5) advises that domestic flues should be 230mm square, with walls not less than 230mm, to limit the loss of heat. They should be as high as possible, and be carried sufficiently above roofs to prevent down-draught. Theoretically they should be straight, but experience has shown (6) that a bend in the flue helps to stop down-draught. Pargetting (internal rendering) helps movement of air by reducing friction. The statutory "Building Regulations"(7) at present in force in England and Wales are based broadly on the same requirements.

Mitchell makes some recommendations for the size of fireplace openings, but surprisingly does not record the common experience, that with an open fire, too high an opening may lead to down-draught.

10. ACKNOWLEDGEMENT

One of us is grateful to the Department of Higher Education of Algeria for financial support.

11. NOMENCLATURE

b	boundary layer thickness	m
ca	air specific heat capacity 1000	J/kgK
cc	chimney wall specific heat capacity	J/kgK
D	thickness of chimney walls	m
da	density of air	kg/m^3
dc	density of chimney walls	kg/m^3
f	friction factor	-
j	change in air moisture content	kgwv/kgair
L	latent heat of evaporation of water 2.26×10^6	J/kg
PB	buoyancy pressure	Pa
Ta	temperature of the air outside	°C
Tc	temperature of the inside surfaces of the chimney	°C
V	air volume flow	m^3/ms
v	air velocity	m/s
x	distance from the internal surface of the chimney	m
X	separation of the two internal surfaces of the chimney	m
Y	chimney width along its surfaces	m
Z	total height of the chimney	m
z	height in the chimney $0 \leq z \leq Z$	m
θ	temperature of the air within the chimney	°C
θi	temperature of the air at z=0	°C
θo	temperature of the air at z=Z	°C

12. REFERENCES

(1) Rohsenow W.M., Choi H.Y., Heat, Mass and Momentum Transfer, Prentice Hall, London 1951 pp 202/4

(2) Eckert E.R.G., Jackson T.W., Analysis of Turbulent Free-Convection Boundary Layers on a Flat Plate, N.A.C.A. Tech. Note 2207, 1950

(3) Wong H.Y., Heat Transfer for Engineers Longmans, New York, 1977 pbl no 2

(4) ASHRAE Handbook Fundamentals 1985 (S.I.) p 8.8, Fig. 2A

(5) Mitchell G.A. et al. Building Constrution Batsford, London 1936

(6) Mitchell G.A. et al. (loc. cit)vol 2, p 359

(7) Building Regulations for England and Wales, 1985, partl, Department of the Environment and the Welsh Office, Her Majesties Stationery Office, London, 1985.

APPENDIX 6

```
C.....
C.....
C     PROGRAM FINITEI IMPLICITE FINITE DIFFERENCES TO CALCULATE
C     TEMPERATURES AND AIR FLOW IN ROOM AND CAVITY
C.....
C.....
      PROGRAM FINITEI
      IMPLICIT REAL*8 (A-H,O-Z)
      REAL*8 INC,MEAN,KT,HC,HR,HRC
      INTEGER B
      LOGICAL CLOSED
      PARAMETER (NA=96 )
      DIMENSION A(23,23),T(23),P(23),Q(23),CV(0:NA),FM(0:NA),
     *T1(0:NA),T2(0:NA),T3(0:NA),T4(0:NA),
     *T5(0:NA),T6(0:NA),T7(0:NA),X(23),
     *TT(0:NA,0:24),TIME(0:NA),AC(0:NA),
     *Y1(0:24),Y2(0:24),Y3(0:24),Y4(0:24),
     *Y5(0:24),Y6(0:24),
     *XX(0:24),DTT(NA),DY1(NA),DY2(NA),
     *DY3(NA),DY4(NA),DY5(NA),DY6(NA),
     *PENTE1(25),PENTE2(25),PENTE3(25),PENTE4(25),
     *PENTE5(25),PENTE7(25),HR(23),CPP(23),
     *WKSPC(100),Q1(23),DX(23),KT(23),TRES(0:NA)
      CALL SETTIM

C.....
C     READ INPUT DATA:
C     XX(I) = TIME FOR 24 HOURS
C     Y1, T2 = T4 ARE THE SOLAIR TEMPERATURES ON THE WALLS
C     Y5 = THE SOLAIR TEMPERATURE ON THE ROOF SIDE
C     Y6 = THE OUTSIDE AIR TEMPERATURE
C     Y7 = THE GROUND TEMPERATURE
C.....
      READ(8,*)(XX(I),I=0,24)
      READ(8,*)(Y1(J),J=0,24)
      READ(8,*)(Y2(J),J=0,24)
      READ(8,*)(Y3(J),J=0,24)
      READ(8,*)(Y4(J),J=0,24)
      READ(8,*)(Y5(J),J=0,24)
      READ(8,*)(Y6(J),J=0,24)
      SUM=0.
      DO 10 J=0,24
10    SUM=SUM+Y6(J)
      AVG=SUM/25
      CPU0=CPUTIM(XXXX)
      DT=15*60
      INC=DT/3600.
      B=1/INC
      DO 20 KK=0,24*B
20    T7(KK)=AVG
```

```
      DO 30 I=1,23
30    T(I)=30.
C.....................................................................
C     INTERPOLATION OVER 24 HOURS AT EACH 5 MINUTES
C.....................................................................
C     INTERPOLATE THE TIME
C.....................
      TIME(0)=XX(0)
      DO 40 J=1,24
         DO 40 N=1,B
            KK=B*(J-1)+N
            DTT(N)=N*INC
40    TIME(KK)=XX(J-1)+DTT(N)
C     INTERPOLATE THE TEMPERATURES
C.....................................
      CALL INT(T1,Y1,XX,INC,B)
      CALL INT(T2,Y2,XX,INC,B)
      CALL INT(T3,Y3,XX,INC,B)
      CALL INT(T4,Y4,XX,INC,B)
      CALL INT(T5,Y5,XX,INC,B)
      CALL INT(T6,Y6,XX,INC,B)
      WRITE(9,*)'TIME STEP = ',DT,'SECONDS'
C.....................................................................
C      INPUT DATA ON MATERIAL PROPERTIES
C      KT = THE THERMAL CONDUCTIVITY OF CONCRETE
C      HC = THE CONVECTION HEAT TRANSFER COEFFICIENT
C      DX = THE THICKNESS OF EACH SLICE
C.....................................................................
C     EXTERNAL WALL OF THE CHIMNEY
C.....................................
      DO 50 I=1,3
         DX(I)=0.10/2
         KT(I)=1.35
         CPP(I)=1000
         P(I)=2100
         Q(I)=P(I)*CPP(I)/DT
50    CONTINUE
      PRINT*,'OUTER WALL THICKNESS = ',DX(1)*2
      WRITE(9,230)DX(1)*2
      WRITE(9,240)P(1)
      WRITE(9,250)KT(1)
C.....................................................................
C     CHIMNEY AIR NODE
C.....................
      DX(4)=0.2
C.....................................................................
C     INTERNAL WALL OF THE CHIMNEY
C.....................................
      DO 60 I=5,7
         DX(I)=0.20/2
         KT(I)=1.35
         P(I)=2100
         CPP(I)=900
         Q(I)=P(I)*CPP(I)/DT
60    CONTINUE
```

```
      WRITE(9,260)DX(5)*2
      WRITE(9,240)P(5)
      WRITE(9,250)KT(5)
C.....................................................................
C     ROOM WALLS
C.................
      DO 70 I=8,16
         DX(I)=0.3/2
         KT(I)=1.13
         P(I)=2100
         CPP(I)=900
         Q(I)=P(I)*CPP(I)/DT
70    CONTINUE
      WRITE(9,270)DX(8)*2
      WRITE(9,240)P(8)
      WRITE(9,250)KT(8)
C.....................................................................
C     ROOF
C.........
      DO 80 I=17,19
         DX(I)=0.2/2
         KT(I)=0.16
         P(I)=500
         CPP(I)=840
*     KT(I)=1.13
*     P(I)=2000
         Q(I)=P(I)*CPP(I)/DT
80    CONTINUE
      WRITE(9,280)DX(17)*2
      WRITE(9,240)P(17)
      WRITE(9,250)KT(17)
C.....................................................................
C     FLOOR
C..........
      DO 90 I=20,22
         DX(I)=0.2/2
         KT(I)=1.13
         P(I)=2000
         CPP(I)=1000
         Q(I)=P(I)*CPP(I)/DT
90    CONTINUE
      DXG=0.2/2+0.3
      WRITE(9,290)DX(20)*2
      WRITE(9,240)P(20)
      WRITE(9,250)KT(20)
C.....................................................................
C    ROOM AIR NODE
C................
      DX(23)=3.
C.....................................................................
C    RADIATION COEFFICIENT
C.......................
      DO 100 I=1,23
100   HR(I)=1.2
      CP=1000
```

```
      AR=3.*3.
      Y=3.
      Z=3.
      AK=30
      PAT=100325
      NB=8*B
      NC=20*B
      CQ=3600/(1200*AR*3)
      CC=1.2*PAT*9.8*Z
      PRINT*,'ENTER 1 FOR OPEN, 0 FOR CLOSED'
      READ(5,*)IANS
      CLOSED=IANS.NE.1
C.....
C       INSERT THE ELEMENTS OF THE MATRIX A(I,J) AND Q1(I)
C       A(I,J) IS THE LEFT HANDSIDE AND Q1(I) IS THE RIGHT HANDSIDE
C       NA = 24*B
C       THE CHIMNEY IS CLOSED FROM 10AM TO 19PM
C       IT IS OPENED 20PM TO 10 AM
C       CV MASS FLOW RATE
C       AC ROOM AIR CHANGE PER HOUR
C.....
      DO 150 L=1,7
         DO 140 KK=0,NA
            IF(KK.GT.NB.AND.KK.LT.NC)THEN
               CV(KK)=0.
            ELSEIF(T(4)-T6(KK).LT.0)THEN
               CV(KK)=0.
            ELSE
               CV(KK)=CP*(CC*(T(4)-T6(KK))/(287*AK*(273+T6(KK))
     *         *(273+T(4))))**0.5
*              PRINT*,T(4),KK,L
               IF(CLOSED) CV(KK)=0.
               FM(KK)=CV(KK)/(3.*1000.)
               AC(KK)=CV(KK)*CQ
            ENDIF
C.....
            DO 110 IN=1,23
               DO 110 IM=1,23
                  A(IN,IM)=0.
                  Q1(IN)=0.
110         CONTINUE
            DO 120 I=1,23
            DO 120 J=1,23
               IF(I.EQ.1)THEN
                  A(I,1)=-(20.+KT(I)/DX(I)+Q(I)*DX(I)/2)
                  A(I,2)=KT(I)/DX(I)
                  Q1(I)=-(T(I)*Q(I)*DX(I)/2+T1(KK)*20.)
               ELSEIF(I.EQ.2) THEN
                  A(I,1)=KT(I)/DX(I)
                  A(I,2)=-(2*KT(I)/DX(I)+Q(I)*DX(I))
                  A(I,3)=KT(I)/DX(I)
                  Q1(I)=-(T(I)*Q(I)*DX(I))
               ELSEIF(I.EQ.3)THEN
                  A(I,2)=KT(I)/DX(I)
                  A(I,3)=-(KT(I)/DX(I)+HC(T(3),T(4),Z,1)+HRC(T(3)
```

```
*                 ,T(5),Z)+Q(I)*DX(I)/2)
                  A(I,4)=HC(T(3),T(4),Z,1)
                  A(I,5)=HRC(T(3),T(5),Z)
                  Q1(I)=-T(I)*Q(I)*DX(I)/2
                ELSEIF(I.EQ.4)THEN
                  A(I,3)=HC(T(4),T(3),Z,1)*AR
                  A(I,4)=-(HC(T(4),T(3),Z,1)*AR+HC(T(4),T(5),Z,1)
*                 *AR+2*CV(KK)+1.2*CP*DX(I)*AR/DT)
                  A(I,5)=HC(T(4),T(5),Z,1)*AR
                  A(I,23)=CV(KK)
                  Q1(I)=-(T(I)*1.2*CP*DX(I)*AR/DT+T6(KK)*CV(KK))
                ELSEIF(I.EQ.5)THEN
                  A(I,3)=HRC(T(3),T(5),Z)
                  A(I,4)=HC(T(5),T(4),Z,1)
                  A(I,5)=-(HRC(T(3),T(5),Z)+HC(T(5),T(4),Z,1)+KT(I)
*                 /DX(I)+Q(I)*DX(I)/2)
                  A(I,6)=KT(I)/DX(I)
                  Q1(I)=-T(I)*Q(I)*DX(I)/2
                ELSEIF(I.EQ.6)THEN
                  A(I,5)=KT(I)/DX(I)
                  A(I,6)=-(2*KT(I)/DX(I)+Q(I)*DX(I))
                  A(I,7)=KT(I)/DX(I)
                  Q1(I)=-T(I)*Q(I)*DX(I)
                ELSEIF(I.EQ.7)THEN
                  A(I,6)=KT(I)/DX(I)
                  A(I,7)=-(KT(I)/DX(I)+5*HR(I)+HC(T(7),T(23),Z,2)
*                 +Q(I)*DX(I)/2)
                  A(I,8)=HR(I)
                  A(I,11)=HR(I)
                  A(I,14)=HR(I)
                  A(I,17)=HR(I)
                  A(I,20)=HR(I)
                  A(I,23)=HC(T(7),T(23),Z,2)
                  Q1(I)=-T(I)*Q(I)*DX(I)/2
                ELSEIF(I.EQ.8.OR.I.EQ.11.OR.I.EQ.14)THEN
                  A(I,I)=-(KT(I)/DX(I)+5*HR(I)+HC(T(I),T(23),Z,2)
*                 +Q(I)*DX(I)/2)
                  A(8,7)=HR(I)
                  A(8,9)=KT(I)/DX(I)
                  A(8,11)=HR(I)
                  A(8,14)=HR(I)
                  A(8,17)=HR(I)
                  A(8,20)=HR(I)
                  A(8,23)=HC(T(8),T(23),Z,2)
                  Q1(8)=-T(8)*Q(I)*DX(8)/2
                  A(11,7)=HR(11)
                  A(11,8)=HR(11)
                  A(11,12)=KT(11)/DX(11)
                  A(11,14)=HR(11)
                  A(11,17)=HR(11)
                  A(11,20)=HR(11)
                  A(11,23)=HC(T(11),T(23),Z,2)
                  Q1(11)=-T(11)*Q(I)*DX(11)/2
                  A(14,7)=HR(14)
                  A(14,8)=HR(14)
```

```
      A(14,11)=HR(14)
      A(14,15)=KT(14)/DX(14)
      A(14,17)=HR(14)
      A(14,20)=HR(14)
      A(14,23)=HC(T(14),T(23),Z,2)
      Q1(14)=-T(14)*Q(I)*DX(14)/2
    ELSEIF(I.EQ.9.OR.I.EQ.12.OR.I.EQ.15)THEN
      A(I,I)=-(2*KT(I)/DX(I)+Q(I)*DX(I))
      A(I,I-1)=KT(I)/DX(I)
      A(I,I+1)=KT(I)/DX(I)
      Q1(9)=-T(9)*Q(I)*DX(9)
      Q1(12)=-T(12)*Q(I)*DX(12)
      Q1(15)=-T(15)*Q(I)*DX(15)
    ELSEIF(I.EQ.10.OR.I.EQ.13.OR.I.EQ.16)THEN
      A(I,I)=-(KT(I)/DX(I)+20.+Q(I)*DX(I)/2)
      A(I,I-1)=KT(I)/DX(I)
      Q1(10)=-(T(10)*Q(I)*DX(10)/2+T2(KK)*20.)
      Q1(13)=-(T(13)*Q(I)*DX(13)/2+T3(KK)*20.)
      Q1(16)=-(T(16)*Q(I)*DX(16)/2+T4(KK)*20.)
    ELSEIF(I.EQ.17)THEN
      A(I,7)=HR(I)
      A(I,8)=HR(I)
      A(I,11)=HR(I)
      A(I,14)=HR(I)
      A(I,17)=-(KT(I)/DX(I)+5*HR(I)+HC(T(17),T(23),Z,3)
     +Q(I)*DX(I)/2)
      A(I,18)=KT(I)/DX(I)
      A(I,20)=HR(I)
      A(I,23)=HC(T(17),T(23),Z,3)
      Q1(I)=-T(I)*Q(I)*DX(I)/2
    ELSEIF(I.EQ.18)THEN
      A(I,17)=KT(I)/DX(I)
      A(I,18)=-(2*KT(I)/DX(I)+Q(I)*DX(I))
      A(I,19)=KT(I)/DX(I)
      Q1(I)=-T(I)*Q(I)*DX(I)
    ELSEIF(I.EQ.19)THEN
      A(I,18)=KT(I)/DX(I)
      A(I,19)=-(KT(I)/DX(I)+25+Q(I)*DX(I)/2)
      Q1(I)=-(T(I)*Q(I)*DX(I)/2+T5(KK)*25.)
    ELSEIF(I.EQ.20) THEN
      A(I,7)=HR(I)
      A(I,8)=HR(I)
      A(I,11)=HR(I)
      A(I,14)=HR(I)
      A(I,17)=HR(I)
      A(I,20)=-(KT(I)/DX(I)+5*HR(I)+HC(T(20),T(23),Z,4)
     +Q(I)*DX(I)/2)
      A(I,21)=KT(I)/DX(I)
      A(I,23)=HC(T(20),T(23),Z,4)
      Q1(I)=-T(I)*Q(I)*DX(I)/2
    ELSEIF(I.EQ.21) THEN
      A(I,20)=KT(I)/DX(I)
      A(I,21)=-(2*KT(I)/DX(I)+Q(I)*DX(I))
      A(I,22)=KT(I)/DX(I)
      Q1(I)=-T(I)*Q(I)*DX(I)
```

```
      ELSEIF(I.EQ.22) THEN
          A(I,21)=KT(I)/DX(I)
          A(I,22)=-(KT(I)/DX(I)+4.8+Q(I)*DXG/2)
          Q1(I)=-(T(I)*Q(I)*DXG/2+T7(KK)*4.8)
      ELSEIF(I.EQ.23)THEN
          A(I,20)=HC(T(20),T(23),Z,4)*AR
          A(I,7)=HC(T(7),T(23),Z,2)*AR
          A(I,8)=HC(T(8),T(23),Z,2)*AR
          A(I,11)=HC(T(11),T(23),Z,2)*AR
          A(I,14)=HC(T(14),T(23),Z,2)*AR
          A(I,17)=HC(T(17),T(23),Z,3)*AR
          A(I,4)=CV(KK)
          A(I,23)=-(HC(T(7),T(23),Z,2)*AR+HC(T(8),T(23),Z,2)
     *          *AR+HC(T(11),T(23),Z,2)*AR+HC(T(14),T(23),Z,2)
     *          *AR+HC(T(17),T(23),Z,3)*AR+HC(T(20),T(23),Z,4)
     *          *AR+2*CV(KK)+DX(I)*AR*1.2*CP/DT)
          Q1(I)=-(T(I)*1.2*CP*DX(I)*AR/DT+T6(KK)*CV(KK))
        ENDIF
120     CONTINUE
C.....................................................................
C     SOLVE THE MATRIX BY A NAG LIBRARY SUBROUTINE F04ARF FOR
C     EACH TIME STEP
C.....................................................................
        CALL F04ARF(A,23,Q1,23,X,WKSPC,IFAIL)
        IF(IFAIL.NE.0)THEN
          WRITE(9,*)'NO SOLUTION'
        ELSE
          DO 130 I=1,23
            T(I)=X(I)
            TT(KK,I)=X(I)
130       CONTINUE
        ENDIF
140   CONTINUE
C.....................................................................
C     WRITE THE OUTPUT
C.....................
150   CONTINUE
      DO 160 KK=0,NA,B/2
160   WRITE(9,220)TIME(KK),(TT(KK,J),J=1,23),T6(KK),FM(KK),AC(KK)
     *,TT(KK,4)-T6(KK),HC(TT(KK,3),TT(KK,4),Z,1),HC(TT(KK,4),TT(KK,5)
     *,Z,1)
220   FORMAT(F5.1,2X,23(F4.1,1X),/,F4.1,1X,F6.4,1X,F5.1,1X,F4.1,
     *1X,'HC1',1X,F4.2,1X,'HC2',1X,F4.2)
      CPU1=CPUTIM(XXXX)
      PRINT*,CPU1-CPU0
C.....................................................................
C     WRITE CAVITY AIR TEMPERATURE
C.....................................
C      DO 160 KK=0,96,B/2
C160   WRITE(10,290)TIME(KK),TT(KK,4)
C.....................................................................
C     WRITE OUTSIDE AIR TEMPERATURE
C.....................................
      DO 170 KK=0,96,B/2
170   WRITE(10,310)TIME(KK),T6(KK)
```

```
310   FORMAT('TAO',F5.1,2X,F5.1)
C.....................................................................
C     WRITE ROOM AIR TEMPERATURE WITH CLOSED DAMPER
C.....................................................................
      IF(CLOSED)THEN
         DO 180 KK=0,NA,8/2
180      WRITE(10,320)TIME(KK),TT(KK,23)
320   FORMAT('TRAC',F5.1,2X,F5.1)
      ELSE
C.....................................................................
C     WRITE ROOM AIR TEMPERATURE WITH OPENED DAMPER
C.....................................................................
         DO 190 KK=0,NA,8/2
190      WRITE(10,330)TIME(KK),TT(KK,23)
330   FORMAT('TRAO',F5.1,2X,F5.1)
      ENDIF
C.....................................................................
C     WRITE SOLAIR TEMPERATURE
C.....................................................................
      DO 200 KK=0,NA,8/2
200   WRITE(10,340)TIME(KK),T1(KK)
340   FORMAT('TEO',F5.1,2X,F5.1)
C.....................................................................
C     WRITE MASS FLOW PER UNIT LENGTH
C.....................................................................
      DO 210   KK=0,NA,8/2
210   WRITE(11,350)TIME(KK),FM(KK)
350   FORMAT('A',F5.1,2X,F6.4)
C.....................................................................
C     CALCULATE RESULTANT TEMPERATURE
C.....................................................................
      DO 211   KK=0,NA,8/2
211   TRES(KK)=(((TT(KK,7)+TT(KK,8)+TT(KK,11)+TT(KK,14)+TT(KK,17)+TT(KK,
     *20))/6.)+TT(KK,23)*(10.*FM(KK)/(1.17*0.2))**0.5)/(1.+(10.*FM(KK)/
     *(1.17*0.2))**0.5)
      DO 212   KK=0,NA,8/2
212   WRITE(12,351)TIME(KK),TRES(KK)
351   FORMAT('TRES',F5.1,2X,F5.1)
C.....................................................................
C     WRITE MATERIAL PROPERTIES
C.....................................................................
230   FORMAT('THICKNESS OF OUTER WALL OF CAVITY = ',F6.3)
240   FORMAT('DENSITY = ',F6.1)
250   FORMAT('THERMAL CONDUCTIVITY = ',F6.3)
260   FORMAT('THICKNESS OF INNER WALL OF CAVITY= ',F6.3)
270   FORMAT('THICKNESS OF ROOM WALLS = ',F6.3)
280   FORMAT('THICKNESS OF ROOF = ',F6.3)
290   FORMAT('THICKNESS OF FLOOR = ',F6.3)
      END
C*********************************
C****** END OF THE PROGRAM ******
C*********************************


C.....................................................................
```

```
C       FUNCTION TO CALCULATE THE CONVECTION COEFFICIENT
C.....................................................................
C     1 = CAVITY WALLS  2 = ROOM WALLS  3 = ROOF  4 = FLOOR
C.....................................................................
      FUNCTION HC(TS,TA,Z,IL)
      IMPLICIT REAL *8 (A-H,O-Z)
C.........................
C          CAVITY WALLS
C.........................
      IF(IL.EQ.1)THEN
         AT=ABS(TS-TA)
         HC=(((1.5*((AT/Z)**0.25))**6.0+(1.23*(AT**0.33))**6.0)
     *             **(1.0/6.0))
C.....................................
C     ROOM WALLS
C.....................................
      ELSEIF(IL.EQ.2)THEN
         AT=ABS(TS-TA)
         HC=  (((1.5*((AT/Z)**0.25))**6.0+(1.23*(AT**0.33))**6.0)
     *             **(1.0/6.0))
C.....................................
C     HORIZONTAL SURFACES HEAT FLOW UPWARDS
C.....................................
      ELSEIF(IL.EQ.3.AND.TA-TS.GT.0.0.OR.IL.EQ.4.AND.TA-TS.LT.0.0)THEN
         AT=ABS(TS-TA)
         HC=((1.4*((AT/Z)**0.25))**6.0+(1.63*(AT**0.33))**6.0)
     *          **(1.0/6.0)
C.....................................
C     HORIZONTAL SURFACES HEAT FLOW DOWNWARDS
C.....................................
      ELSE
         AT=ABS(TS-TA)
         HC=0.6*((AT/Z)**0.2)
      ENDIF
      IF(AT.EQ.0)HC=0
      RETURN
      END
C.....................................................................
C     FUNCTION TO CALCULATE RADIATION COEFFICIENT FOR CAVITY
C     F12 = THE VIEW FACTOR BETWEEN ANY TWO PARALLEL
C     SURFACES 1 & 2 BASED ON EQUATION FROM INTRODUCTION TO HEAT TRANSFE
C     BY: D.P.DEWITT & F.P.INCROPERA
C.....................................................................
      FUNCTION HRC(TH1,TH2,Z)
      IMPLICIT REAL *8 (A-H,O-Z)
      DATA PI/3.1415926/
      BOLTZ=5.67E-8
      THX=273.0+TH1
      THY=273.0+TH2
      XL=3.
      W=0.2
      E1=0.9
      E2=0.9
      XH=XL/W
      YH=Z/W
```

```
      XXH=1.0+XH**2.0
      YYH=1.0+YH**2.0
      F12=(2./(3.14*XH*YH))*(LOG(SQRT((XXH*YYH)/(XXH+YH**2.0)))
     *+XH*SQRT(YYH)*ATAN(XH/SQRT(YYH))+YH*SQRT(XXH)*ATAN(YH/SQRT(XXH))
     *-XH*ATAN(XH)-YH*ATAN(YH))
      E12=1./((1-E1)/E1+1/F12+(1-E2)/E2)
      HRC=E12*(THX+THY)*(THX**2.0+THY**2.0)*BOLTZ
      RETURN
      END

C.....
C       SUBROOTINE TO INTERPOLATE THE TEMPERATURES
C.....
      SUBROUTINE INT(TS,YS,XXS,INC,B)
      IMPLICIT REAL *8(A-H,O-Z)
      PARAMETER (NA=96)
      REAL *8 INC
      INTEGER B
      DIMENSION TS(0:NA),YS(0:24),XXS(0:24),DTTS(NA),PENTES(25),
     *DYS(NA),TIMES(0:NA)
      TIMES(0)=XXS(0)
      TS(0)=YS(0)
      DO 10 J=1,24
         PENTES(J)=(YS(J)-YS(J-1))/(XXS(J)-XXS(J-1))
         DO 10 N=1,B
            KK=B*(J-1)+N
            DTTS(N)=N*INC
            DYS(N)=DTTS(N)*PENTES(J)
C           TIMES(KK)=XXS(J-1)+DTTS(N)
            TS(KK)=YS(J-1)+DYS(N)
10    CONTINUE
      RETURN
      END
```